21912

National Library of Canada | Bibliothèque nationale du Canada

CANADIAN THESES ON MICROFICHE | THÈSES CANADIENNES SUR MICROFICHE

NAME OF AUTHOR/NOM DE L'AUTEUR JANKO MISIC

TITLE OF THESIS/TITRE DE LA THÈSE SOLID AND HOLLOW PRESTRESSED CONCRETE BEAMS UNDER COMBINED LOADING

UNIVERSITY/UNIVERSITÉ University of Alberta

DEGREE FOR WHICH THESIS WAS PRESENTED/ GRADE POUR LEQUEL CETTE THÈSE FUT PRÉSENTÉE Ph.D

YEAR THIS DEGREE CONFERRED/ANNÉE D'OBTENTION DE CE DEGRÉ 1974

NAME OF SUPERVISOR/NOM DU DIRECTEUR DE THÈSE Dr. Joseph Wanacaur

Permission is hereby granted to the NATIONAL LIBRARY OF CANADA to microfilm this thesis and to lend or sell copies of the film.

The author reserves other publication rights, and neither the thesis nor extensive extracts from it may be printed or otherwise reproduced without the author's written permission.

L'autorisation est, par la présente, accordée à la BIBLIOTHÈQUE NATIONALE DU CANADA de microfilmer cette thèse et de prêter ou de vendre des exemplaires du film.

L'auteur se réserve les autres droits de publication; ni la thèse ni de longs extraits de celle-ci ne doivent être imprimés ou autrement reproduits sans l'autorisation écrite de l'auteur.

DATED/DATÉ Sept 30 SIGNED/SIGNÉ J Misic

PERMANENT ADDRESS/RÉSIDENCE FIXÉ 408 Michener Park
Edmonton

NL-91 (10-73)

THE UNIVERSITY OF ALBERTA

SOLID AND HOLLOW RECTANGULAR PRESTRESSED CONCRETE BEAMS UNDER COMBINED LOADING

by

© JANKO MISIC

A THESIS
SUBMITTED TO THE FACULTY OF GRADUATE STUDIES AND RESEARCH
IN PARTIAL FULFILMENT OF THE REQUIREMENTS FOR
THE DEGREE OF DOCTOR OF PHILOSOPHY IN CIVIL ENGINEERING

EDMONTON, ALBERTA

FALL 1974

THE UNIVERSITY OF ALBERTA

FACULTY OF GRADUATE STUDIES AND RESEARCH

The undersigned certify that they have read, and recommend to the Faculty of Graduate Studies and Research, for acceptance, a thesis entitled SOLID AND HOLLOW RECTANGULAR PRESTRESSED CONCRETE BEAMS UNDER COMBINED LOADING submitted by JANKO MISIC in partial fulfilment of the requirements for the degree of Doctor of Philosophy in Civil Engineering.

.....
Supervisor

.....

.....

.....

.....

.....
External Examiner

Date July 15 1974.

ABSTRACT

Tests on eighty-four solid and hollow prestressed concrete beams under various ratios of torsion, bending and shear are reported in this investigation. All beams had nominally the same length of 10' - 9" and were divided into three series according their cross-sections:

(i) Series A*, 6 x 12 inches (52 beams)

(ii) Series B, 8 x 12 inches (20 beams)

(iii) Series C, 12 x 12 inches (12 beams)

Primary variables in Series A included eccentricity of prestress, amount of transverse steel, and torsion, bending and shear ratios, while in Series B and C the effect of a longitudinal opening was studied in conjunction with different loading ratios.

Available theories for cracking analysis of beams were examined and two procedures are proposed. One is based on the biaxial stress criteria and includes such effects as stirrup contribution and partial plastification at cracking, and the other utilizes an equivalent elliptical cross-section for solid and hollow sections. Some shortcomings of the commonly used theories for the ultimate analysis are pointed out and a new iterative method based on a biaxial strain

---

* *Twenty beams of Series A were tested and reported by Mr. E.B. Jacobsen (see list of references) in his M.Sc. study. Since these beams constitute an integral part of Series A they are also included here in chapters on cracking and ultimate analysis.*

criteria is presented. Comparison of theoretical and experimental results was made and a very good correlation was observed.

Original contributions contained herein are: (i) utilization of a biaxial stress criteria in the cracking analysis, (ii) use of the equivalent elliptical cross-sections for predictions of cracking strength and precracking stiffness for solid and hollow beams, and (iii) utilization of a biaxial strain criteria in the ultimate strength analysis.

ACKNOWLEDGEMENTS

This investigation was made possible through the financial assistance provided by the National Research Council of Canada. The testing facilities were provided at the Structural Engineering Laboratory of the University of Alberta. The Associated Engineering Services Ltd. Scholarship and the National Research Council of Canada Postgraduate Scholarship have been awarded to the author during his postgraduate study.

The investigation was guided by Dr. J. Warwaruk, Professor in the department of Civil Engineering. His assistance in planning the investigation, constructive criticism and helpful comments during the preparation of the manuscript are gratefully acknowledged.

Discussions with Dr. J.G. MacGregor, Professor in Civil Engineering and Dr. J.B. Haddow, Professor in Mechanical Engineering are sincerely appreciated.

Helpful discussions with former and present fellow graduate students, Dr. D.L.N. Rao, Mr. B. Slight, Mr. R. Linder and Dr. S. Hamada are acknowledged with thanks. The technical staff of the laboratory under supervision of Messrs. H. Panse and L. Burden helped in the test program.

Miss Julie Melville typed the manuscript with great care and her cooperation is appreciated.

My wife, Milica, deserves special mention for her patience during many hours when postgraduate study took precedence over family attentions.

TABLE OF CONTENTS

	Page
Abstract	iii
Acknowledgements	v
Table of Contents	vi
List of Tables	ix
List of Figures	x
List of Symbols	xiii
CHAPTER I - INTRODUCTION	1
1.1 General Remarks	1
1.2 Object and Scope	2
CHAPTER II - CURRENT STATE OF KNOWLEDGE	3
2.1 Introduction	3
2.2 Cracking Strength	5
2.3 Ultimate Strength	8
CHAPTER III - EXPERIMENTAL PROGRAM	11
3.1 Test Specimens	11
3.2 Fabrication of Specimens	16
3.3 Instrumentation of Specimens	21
3.3.1 Reinforcement Strains	21
3.3.2 Angle of Twist	28
3.3.3 Deflections	29

Page

3.4 Test Equipment 29

3.5 Tesing Procedure 31

CHAPTER IV - PRESENTATION AND DISCUSSION OF TEST RESULTS 37

4.1 General 37

4.2 Principal Test Results 39

4.3 Precracking Behavior and Cracking Strength 47

4.4 Development of Cracks, Postcracking Behavior, and Ultimate Strength 53

4.5 Interaction of Torsion, Bending and Shear at Ultimate 57

CHAPTER V - CRACKING STRENGTH, THEORIES AND COMPARISONS 64

5.1 Introduction 64

5.2 Available Theories 67

5.2.1 Elastic Analysis 67

5.2.2 Plastic Analysis 72

5.2.3 Skew Bending Theory 74

5.2.4 Statistical and Numerical Procedures 77

5.3 Proposed Theories 79

5.3.1 Elasto-Plastic Analysis 79

5.3.1.1 General Remarks and Assumptions 79

5.3.1.2 Biaxial Stress Failure Criteria 82

5.3.1.3 Contribution of Stirrups 87

5.3.2 Analysis Based on an Equivalent Elliptical Cross-Section 91

5.3.2.1 General 91

5.3.2.2 Hollow Cross-Section 94

Page

5.3.2.3 Solid Cross-Section 96

5.4 Comparative Study 97

5.5 Precracking Stiffness 106

CHAPTER VI - ULTIMATE STRENGTH - THEORY, EXPERIMENTA AND COMPARISON 113

6.1 Introduction 113

6.2 Remarks on the Skew Bending Theory 115

6.3 Proposed Analysis 125

6.3.1 General Remarks 125

6.3.2 Torsion to Bending Ratio, ψ_β 125

6.3.3 Failure Criteria and Stress-Strain Characteristics of Concrete 128

6.3.4 Assumptions of the Analysis 133

6.3.5 Bending and Torsion Transfer on β-Plane 135

6.3.6 Summary of the Proposed Analysis 143

6.3.7 Concluding Remarks on the Proposed Analysis 148

6.4 Comparison of Experimental and Theoretical Results 149

CHAPTER VII - SUMMARY AND CONCLUSIONS 159

7.1 Summary 159

7.2 Conclusions 159

REFERENCES 164

APPENDIX A - TEST RESULTS FOR SERIES B AND C 171

APPENDIX B - STRAIN GAUGE READINGS 188

APPENDIX C - PHOTOGRAPHS OF TESTED BEAMS 220

APPENDIX D - COMPUTER PROGRAM 237

LIST OF TABLES

Table		Page
3.1	Sieve analysis of sand	12
3.2	Sieve analysis of coarse aggregate	12
4.1	Parameters considered in this study	38
4.2	Series A, group identification	38
4.3	Test results	40
5.1	Torsional constants for rectangular cross-section	71
5.2	Cracking torques for solid cross-sections by different theories	98
5.3	Summary of T_{test}/T_{theory} values for solid x-section	105
5.4	Cracking torques of hollow beams	105
5.5	Torsional stiffness of solid cross-section	109
5.6	Torsional stiffness of hollow cross-section	110
6.1	Ultimate strength, comparison of experimental and theoretical results, Series A	151
6.2	Ultimate strength, comparison of experimental and theoretical results, Series B	155
6.3	Ultimate strength, comparison of experimental and theoretical results, Series C	157
6.4	Average test/theory values	158
A-1 to A-32	Test results, observed data for beams of Series B and C	171
B-1 to B-59	Strain gauge readings for Series B and C	188

LIST OF FIGURES

Figure		Page
3.1	Beam series identification	13
3.2	Cross-sectional properties and group identification	14
3.3	Portion of stress-strain diagram for transverse steel (stirrups)	15
3.4	Idealized stress-strain curve and manufacturer's data for 1/2" dia. strand	17
3.5	Idealized stress-strain curve and manufacturer's data for 3/4" dia. strand	18
3.6	Reinforcement cage for a hollow beam	20
3.7	Elevation view and instrumentation of BS group of beams	22
3.8	Elevation view and instrumentation of BlS group of beams	23
3.9	Elevation view and instrumentation of BH group of beams	24
3.10	Elevation view and instrumentation of CS group of beams	25
3.11	Elevation view and instrumentation of CH group of beams	26
3.12	Equipment arrangement viewed from north side	30
3.13	Fixed head	32
3.14	Twisting head	33
3.15	Detailed view of test setup for combined loading	34
3.16	Torsional loading equipment	35

Figure		Page
4.1	Torque-twist curves, Series B	48
4.2	Torque-twist curves, Series C	49
4.3	Moment-deflection curves, Series B	51
4.4	Moment-deflection curves, Series C	52
4.5	Typical crack pattern of a beam under combined loading	54
4.6	Interaction between torsion and bending at ultimate, Series A	59
4.7	Interaction between torsion and bending at ultimate, Series B and C	60
4.8	Interaction between torsion and shear at ultimate, Series A	61
4.9	Interaction between torsion and shear at ultimate, Series B and C	62
5.1	Influence of structural shapes on the ratio of warping to Saint-Venant torsion	66
5.2	Stress components under combined loading	68
5.3	Comparison of torsional coefficient by different theories	75
5.4	Shearing stress distribution in a rectangular cross-section subjected to torque	81
5.5	Membrane analogy for square and slender cross-section	81
5.6	Strength of concrete under combined tension and compression	85
5.7	Stirrup strains before cracking	88
5.8	Cracking strength-contribution of stirrups	93
5.9	Equivalent elliptical cross-sections for solid and hollow rectangle	93

Figure		Page
5.10	Precracking torsional stiffness, solid cross-sections	111
5.11	Precracking torsional stiffness, hollow cross-sections	112
6.1	Three approaches to the problem of combined loading	114
6.2	Failure modes according to skew bending theory	116
6.3	Mode 1 - free body diagram	119
6.4	Crack opening under combined loading	123
6.5	Crack opening under combined loading (Beam B1S-6a)	124
6.6	Torsion to bending ratio on β-plane	126
6.7	Relationship between ψ, ψ_β and β	129
6.8	Biaxial strain of concrete	130
6.9	Stress-strain characteristics of concrete	132
6.10	Relationship between inclination of spiral crack θ and angle of uncracked zone β	137
6.11	Bending on the inclined β-plane	139
6.12	Mechanism of torsion transfer on β-plane	139
6.13	Schematical concept of proposed procedure	145
6.14	Typical iteration paths for different modes	146
6.15	Alternate procedure	147
C-1 to C-32	Photographs of crack patterns at failure for beams of B and C series	220
D-1	General flow diagram and subroutine identification	242

LIST OF SYMBOLS

Most of the symbols are defined in the text where they first appear; however, commonly used symbols are listed here for convenient reference. Nomenclature used in the computer program is listed in Appendix D.

Dimensions and Section Properties

a	depth of neutral axis measured from the compression face of the beam
b	width of a rectangular section
b_h	width of a void in a rectangular cross-section
b'	centerline width of a closed stirrup
e	eccentricity of prestress force with respect to centroid of cross-section
h	height of a rectangular cross-section
h_h	height of a void in a rectangular cross-section
h'	centerline height of a closed stirrup
I	moment of inertia of an uncracked beam
I_h	moment of inertia of an uncracked hollow beam
Q	statical moment of the cross-section
s	longitudinal spacing of transverse reinforcement

Material Properties

E_c	modulus of elasticity of concrete
E_p	modulus of elasticity of prestressing steel

E_t	modulus of elasticity of transverse reinforcement
ε_u	ultimate strain in concrete in pure bending
f'_c	compressive strength of concrete cylinder
f_{py}	yield stress of prestressing steel
f_r	modulus of rupture of concrete
f'_t	tensile strength of concrete
f_{sp}	split cylinder tensile strength of concrete
f_{ty}	yield stress of stirrup
G_c	shear modulus of concrete

Forces and Moments

C, T	compressive and tensile force
M	bending moment
M_{cr}	bending moment at cracking
M_u	ultimate bending moment in combined loading
M_{uo}	ultimate shear-bending or pure bending moment
M_β	bending moment on β-plane
T	twisting moment (torque)
T_β	twisting moment (torque) on β-plane
T_{cr}	cracking torque
T_{ec}	cracking torque based on elastic concept of concrete behavior
T_{pc}	cracking torque based on plastic concept of concrete behavior
T_{sb}	cracking torque based on skew bending theory

T_u	ultimate torque in combined loading
T_{up}	ultimate torque of plain concrete members
T_{uo}	ultimate strength in pure torsion
V	shear force
V_c	shear force taken by concrete compression zone
V_{cr}	shear force at cracking
V_u	ultimate shear in combined loading
V_β	shear force on inclined β-plane

Stresses and Strains

ε_c	compressive strain of concrete in a biaxial state of strain
ε_{ce}	strain in concrete due to effective prestress
ε_ℓ	strain in longitudinal direction
ε_t	tensile strain of concrete in a biaxial state of strain
ε_{sa}	increase in strain in prestressing steel between initial and ultimate loading
ε_{se}	strain in prestressing strand due to effective prestress
ε_{th}	strain in horizontal leg of stirrup
ε_{tr}	strain in transverse steel
ε_{tv}	strain in vertical leg of stirrup
ε_β	strain perpendicular to β-plane
σ_B	stress at bottom face of section due to prestress
$\sigma_{max,min}$	principal stresses of concrete in a two-dimensional state

σ_p	average stress due to prestress
σ_s	stress in a middle of side face of section due to prestress
σ_T	stress at top face of section due to prestress
ϕ_{cr}	angle of twist at cracking
ϕ_u	angle of twist at ultimate
τ_c	shear stress due to V_c
τ_t	torsional shear stress
τ_v	flexural shear stress
τ_x, τ_y	torsional shear stress in two perpendicular directions

Miscellaneous

c_h	a constant defined by Equation 5.41
k	a constant defined in the text
k_s	torsion constant according to statistical procedure
m	ratio of volume of longitudinal steel to volume of transverse reinforcement
α, γ	torsion factors in St. Venant theory
α_{ep}	torsion constant according to elasto-plastic theory
β	inclination of the compression zone to the longitudinal axis of the beam
β_{ep}	torsion constant according to elasto-plastic theory
δ	loading ratio defined as $2T/bV$
ψ	loading ratio defined as T/M
ψ_β	loading ratio defined as T_β/M_β
θ	inclination of the tensile crack to the longitudinal axis of the beam

CHAPTER I

INTRODUCTION

1.1 General Remarks

With the trend in recent years towards more sophisticated use of concrete in bridge girders and in edge beams of shells and slabs interest in research on torsion in prestressed concrete has significantly increased. Continuous refinements of design specifications with reduced factors of safety require an explicit recognition and understanding of torsional effects; in the past large safety factors for flexure and shear indirectly accounted for "secondary" effects, including torsion.

Considerable progress in research in this area resulted in the provisions of ACI 318-71[1]* for design of reinforced concrete members subjected to torsion. At the time it was felt that a similar recommendation for the design of prestressed concrete could not be included, because of inadequate research and test data. It is intended that the experimental data and theoretical findings presented in this report will complement other current research programs being carried out elsewhere and in this way assist towards the formulation of design procedures.

---

* Numbers refer to entries in the list of references.

1.2 Object and Scope

The primary objectives of this investigation were: (i) to observe the behavior, the cracking and ultimate strengths of solid and hollow prestressed concrete beams subjected to combined loading, (ii) to examine commonly used theories for cracking and ultimate strength, and the assumptions on which these theories are founded, and, (iii) to develop analyses for predicting the cracking and ultimate strength of solid and hollow prestressed concrete beams.

The experimental portion of this investigation consisted of tests on eighty-four solid and hollow prestressed concrete beams under various ratios of torsion, bending and shear. The main variables included magnitude and eccentricity of prestress, amount of transverse steel, torsion to bending ratio, torsion to shear ratio and size of longitudinal opening. The experimental data obtained in this study includes cracking strength, ultimate strength, strains in the prestressing steel and transverse reinforcement, torque-twist and load-deflection characteristics, and crack patterns.

Using the analysis developed in this study, theoretical capacities at cracking and ultimate have been compared with test values. Expressions for the initial torsional stiffness of solid and hollow beams have been developed and compared with test results.

CHAPTER II

CURRENT STATE OF KNOWLEDGE

2.1 Introduction

Research on torsion in structural concrete has an interesting history dating back to 1929 when E. Rausch[18] presented the truss analogy for torsion in reinforced concrete members. According to this analogy transverse reinforcement acts as tension members while cracked concrete provides the compression struts. Another break-through in research activities in this area came in 1958 when N.N. Lessig[51, 52] proposed the skew bending theory, where equilibrium conditions based on the observed failure mode are considered. More recently investigators such as Lampert[49], Hsu[36], and Collins[11], introduced the equivalent thin tube theory where a solid beam is treated as a rectangular thin walled tube. This approach is based on the space truss model first developed by Lampert[49] and is essentially a generalization of the original truss theory.

The fundamentals of general torsion theory (which dates back to the eighteenth century, when Coulomb found the solution for a cylindrical bar of circular cross-section) are available in most textbooks on strength of materials[61], theory of elasticity[69, 72], or theory of plasticity [59], and consequently will not be presented here. Research on torsion in structural concrete has been active mainly in the last two decades and is currently carried out in over thirty institutions

throughout the world, resulting in numerous publications. An extensive literature review dealing with torsion in structural concrete has been presented by Zia[82], Johnston and Zia[40], Woodhead and McMullen[75] and Rao and Warwaruk[65]. Only research that has a close relevance to the material presented in this report is reviewed here. In the introductory sections of Chapters 5 and 6, where cracking and ultimate analyses are presented, reference is made also to the most pertinent publications dealing with these two areas.

It is not surprizing that research on torsion in prestressed concrete members gained momentum only after the problem was better defined and understood for plain and reinforced concrete. For that reason many authors, when conducting their literature review, approached the problem by dividing the whole area into (i) plain concrete, (ii) reinforced concrete, and (iii) prestressed concrete. Others preferred to make a distinction between (i) pure torsion, (ii) torsion and bending, and (iii) torsion bending and shear. Both treatments are justified since the problem of combined loading was historically approached in both these manners. However, it should be mentioned that all these cases represent special cases of a fully reinforced and prestressed beam under combined torsion, bending and shear. Such a beam exhibits two distinct behavioral regions; one between initial load and the cracking load and another between cracking and ultimate. For that reason available theories for cracking analysis are discussed first and then theories for ultimate analysis are reviewed.

2.2 Cracking Strength

The major concern of a torsional cracking analysis is the determination of a stress distribution and a failure criteria. Several theories have been used in the past regarding torsional shear stress distribution at cracking. Three common approaches are those from the Elastic theory[69], the Plastic theory[59], and the Skew bending approach[31].

In the elastic theory a material is assumed to be perfectly elastic and failure occurs when the limiting stress is reached at the maximum shearing stress location. On the other hand, the plastic theory assumes perfectly plastic behavior implying that the shear stresses due to torsion are constant over the whole cross-section. According to both theories, shearing stress can be expressed as follows:

$$\tau = \frac{T}{kb^2h} \qquad (2.1)$$

where k is the torsion constant and is a function of the cross-sectional aspect ratio. For the same cross-section this factor is always larger for plastic theory as compared to elastic theory.

Torsional shearing stresses determined by Equation 2.1 must be superimposed on the stresses caused by prestress, bending, and flexural shear. To such a generalized state of stress a failure criteria is applied. Unfortunately, no agreement exists among researchers as to which failure criteria should be used for concrete at cracking.

For the case of combined loading, generally the maximum stress criteria has proved to be more popular. However, the tensile strength of concrete must be known, regardless of the adopted failure criteria; it can be determined from the uniaxial tensile test or the splitting tensile test. The disadvantage of the former is that it is difficult to perform, while in the latter case a pure tensile state of stress cannot be attained; tensile stress is always associated with a compressive stress amounting to approximately 0.25 f'_c.

It should be noted that Equation 2.1 is applicable only to solid rectangular cross-sections. For cross-sections with re-entrant corners such as T, L, U, I or hollow box sections a numerical solution of the following partial differential equation is required:

$$\frac{\partial^2 F_{(x,y)}}{\partial^2 x} + \frac{\partial^2 F_{(x,y)}}{\partial^2 y} = -2K_T\phi \qquad (2.2)$$

where $F_{(x,y)}$ denotes the stress function in cartesian coordinates, K_T the torsional rigidity, and ϕ the angle of twist per unit length.

Based on experimental observations, Hsu[31] concluded that the stress distribution due to torsion at cracking can be interpreted as a skew bending phenomenon. This approach has been extended by Gangarao and Zia[24] to include bending and torsion and by Henry and Zia[29] to include the general case of combined bending, torsion, and shear. While it was observed that this approach gives good correlation with

test results for beams with aspect ratios close to 2:1, it was not satisfactory for beams having a square or nearly square cross-section.

Swamy[68] conducted tests on twenty prestressed beams without web reinforcement. He concluded that both maximum stress criterion and maximum strain criterion do not give satisfactory results for the entire range of torsion to bending ratios. Johnston and Zia[40] applied elastic theory using a finite difference technique for the determination of the torsional shear stresses in prestressed hollow beams subjected to combined loading. They based tensile strength of concrete on the splitting test for the reason that the biaxial state of stress in the splitting tensile test is similar to the state of stress resulting from combined loading. The same beams were analysed by the skew bending approach; comparison shows that the elastic theory correlates better with test results than the skew bending approach. Subsequently, Woodhead and McMullen [75] analysed 177 rectangular prestressed beams using elastic theory with f_t equal $7\sqrt{f'_c}$. Since the main values of experimental to theoretical ratios ranged from 1.035 to 1.330 they pointed out that their conservative predictions resulted from some plastic action at cracking and contribution of web reinforcement to the cracking strength. In a recent study, Rao and Warwaruk[66] investigated the cracking strength and precracking behavior of prestressed I-beams under combined loading. Forty-one beams were analysed according to both plastic theory with f_t equal to $6\sqrt{f'_c}$ and elastic theory, where a finite element technique was employed, with f_t equal to $7.5\sqrt{f'_c}$. It is interesting to note that the

average test to theory ratios according to both theories were the same, that is 1.26. Although it may appear somewhat surprising that the plastic theory also underestimates cracking capacity this probably resulted from the smaller value of f_t adopted in this theory as compared to elastic theory.

2.3 Ultimate Strength

Three approaches are most commonly used for the determination of ultimate strength of reinforced or prestressed concrete beams under combined loading; truss analogy[18], skew bending theory[51], and space truss theory[47]. All three approaches are applicable only to underreinforced members. While it is relatively easy to establish limits of longitudinal reinforcement in a member subjected to bending only, no clear theoretical definition has been given in the literature as to what amount of web and longitudinal reinforcement would correspond to "balanced condition" for a member subjected to combined torsion, bending and shear. It has been recognized that a reinforced or prestressed beam without web reinforcement fails at first cracking if subjected to pure torsion or combined loading; this implies that the analysis for cracking torque would also apply for the determination of ultimate capacities. Researchers also agree that the relative amounts of web and longitudinal reinforcement and initial prestress not only contribute to the ultimate strength but may significantly influence the postcracking behavior.

A very limited number of investigations dealing with the problem of combined loading in hollow beams have been published. Hsu[35] reported tests on four reinforced hollow, and corresponding solid beams subjected to pure torsion. Capacities were similar for similarly reinforced solid and hollow beams implying that the beam core did not contribute to the ultimate strength. Swamy[68] applied a skew bending analysis to twenty hollow prestressed beams subjected to combined bending and torsion. Probably the most complete experimental and theoretical investigation has been done by Johnston and Zia[40] who reported tests on thirty-seven eccentrically prestressed hollow beams under various ratios of torsion, bending and shear. As mentioned earlier, an elastic analysis in conjunction with a finite difference technique was used for the cracking analysis, while the ultimate analysis was based on the skew bending approach.

Of the three theories mentioned above the Skew bending theory has been mostly used in the past, equally for reinforced and prestressed concrete. Most recent works on rectangular prestressed concrete beams under combined loading include those by Gangarao and Zia[24], Henry and Zia[29], Johnston and Zia[40], and Woodhead and McMullen[75]. Rao and Warwaruk[65] used this theory to predict ultimate capacities of prestressed I-beams under combined loading. It should be mentioned, however, that certain assumptions of this theory have been questioned. As compared to the truss analogy, skew bending theory results in a more complex solution. Recently, Elfgren[18] showed that no significant dif-

ference exists between these two theories if both are based on the same assumptions and simplifications.

The space truss theory is the most recent appraoch and has been introduced by Lampert[47]. Although some of its assumptions are controversial[11, 36] it appears that this approach provides a sound tool for the study of beam behavior at postcracking stages. Using this approach, Collins[11] found that complete torque-twist curves can be predicted in a symmetrically reinforced beam subjected to torsion only.

CHAPTER III

EXPERIMENTAL PROGRAM

3.1 Test Specimens

The results of tests made on eighty four beams, divided in three series according to their overall cross-sectional dimensions as shown in Figure 3.1, are reported in this investigation. Each of the three series is further divided into groups having the following variables: eccentricity of prestressing force, amounts of longitudinal and transverse steel and whether the beam is of solid or hollow cross-section. Figure 3.2 illustrates the group identification. The nominal compressive strength of concrete was 5000 psi with the same concrete mix for all beams. The following mix proportions were used:

1. Cement (type III) 150 lbs
2. Sand 310 lbs
3. Coarse aggregate 500 lbs
4. Water 85 lbs/batch

This mix yielded seven cubic feet of concrete with a slump of approximately 3 inches. The sieve analysis of sand and coarse aggregate is given in Tables 3.1 and 3.2, respectively.

The details of the stress-strain characteristics for the transverse steel are given in Figure 3.3. Representative samples of the #2 plain bars and the #3 deformed bars were subjected to a tension

TABLE 3.1 SIEVE ANALYSIS OF SAND

Sieve Size	Weight Retained (gms.)	% Retained	Cumulative % Retained	A.S.T.M. Standard
# 4	17.5	3.0	3.0	0 - 5
# 8	85.2	14.7	17.7	
# 16	54.6	9.5	27.2	20 - 55
# 30	60.0	10.3	37.5	
# 20	208.4	35.8	73.3	70 - 90
# 100	122.9	21.1	94.4	90 - 98
Pan	17.8	3.1	-	
Silt	14.4	2.5	-	
Total	580.8	100.0	253.1	
Fineness Modulus = 2.53				

TABLE 3.2 SIEVE ANALYSIS OF COARSE AGGREGATE

Sieve Size	Weight Retained (lbs.)	% Retained	Cumulative % Retained
3/4"	0.30	1.1	1.1
3/8"	15.63	58.4	59.5
# 4	10.03	37.5	97.0
Pan	0.80	3.0	100.0
Total	26.76	100.0	

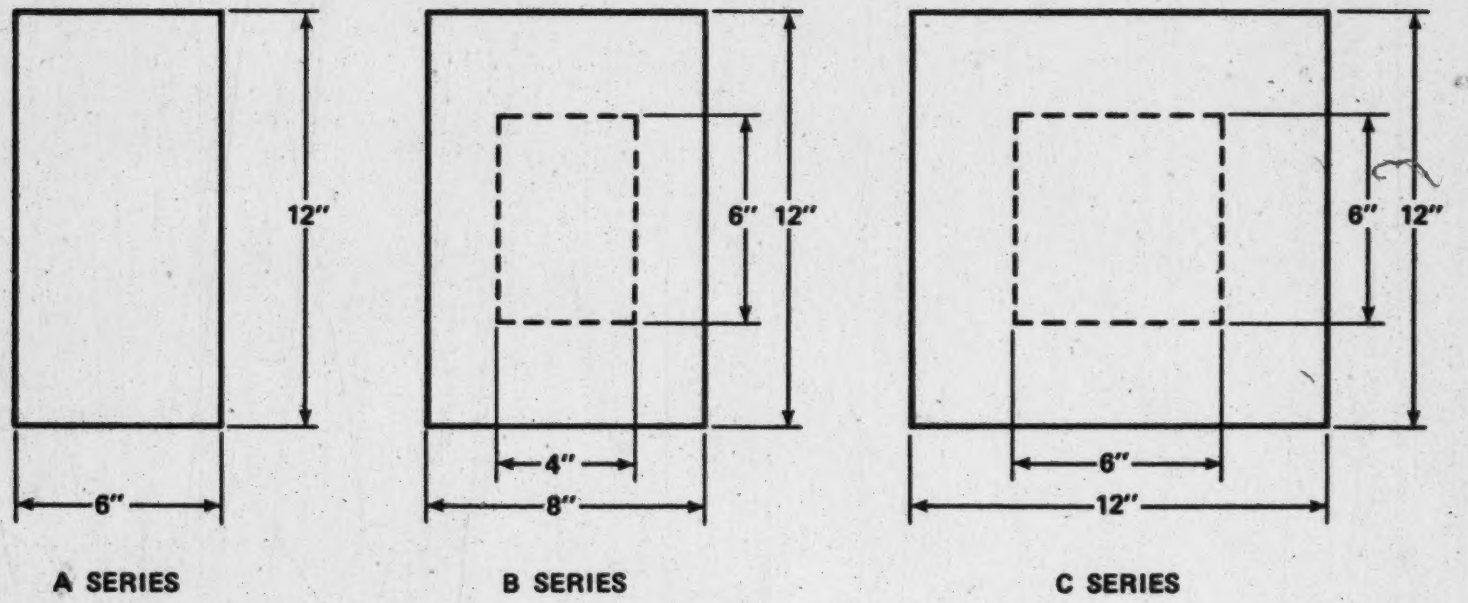

FIG. 3.1 BEAM SERIES IDENTIFICATION

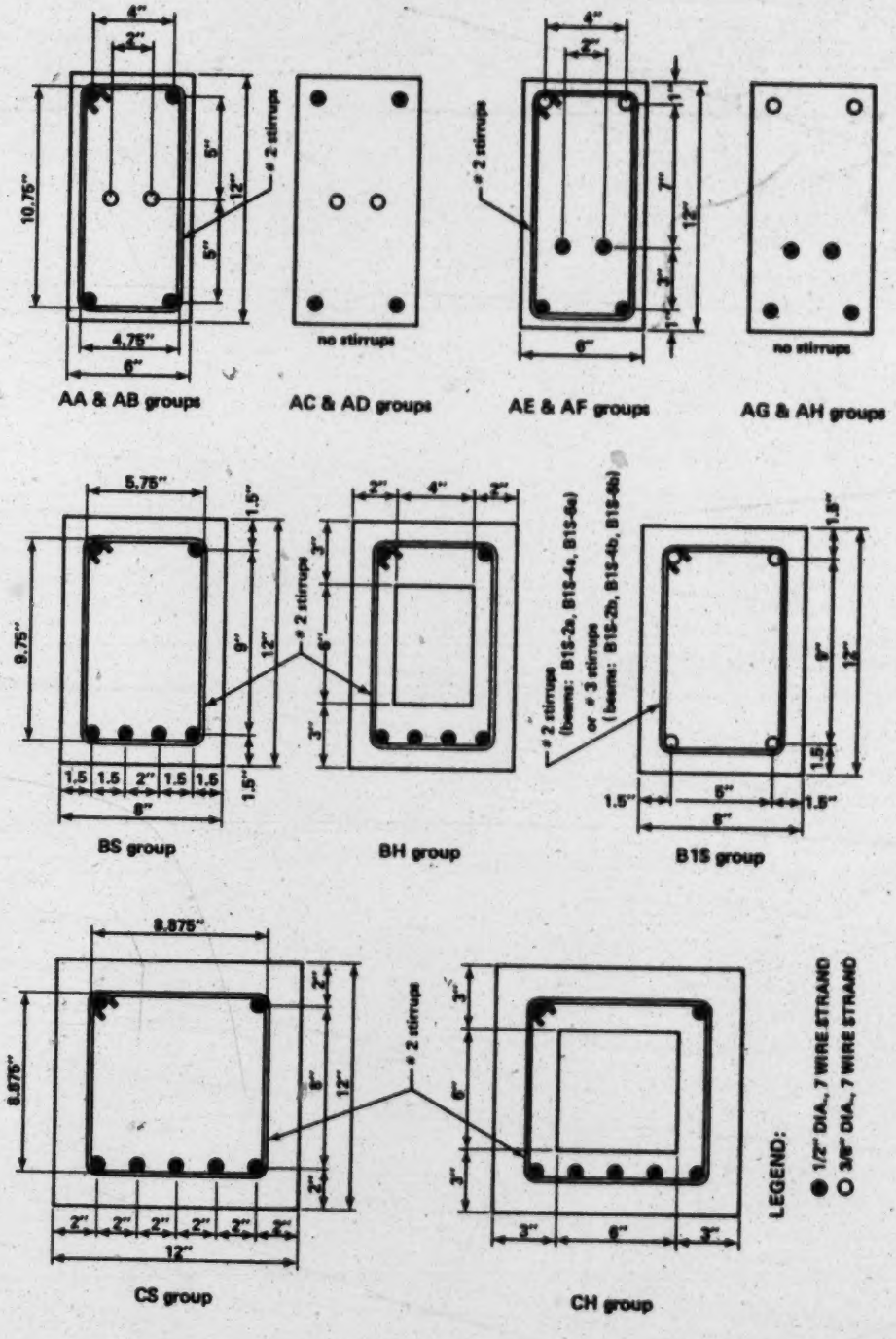

FIG. 3.2 CROSS-SECTIONAL PROPERTIES AND GROUP IDENTIFICATION

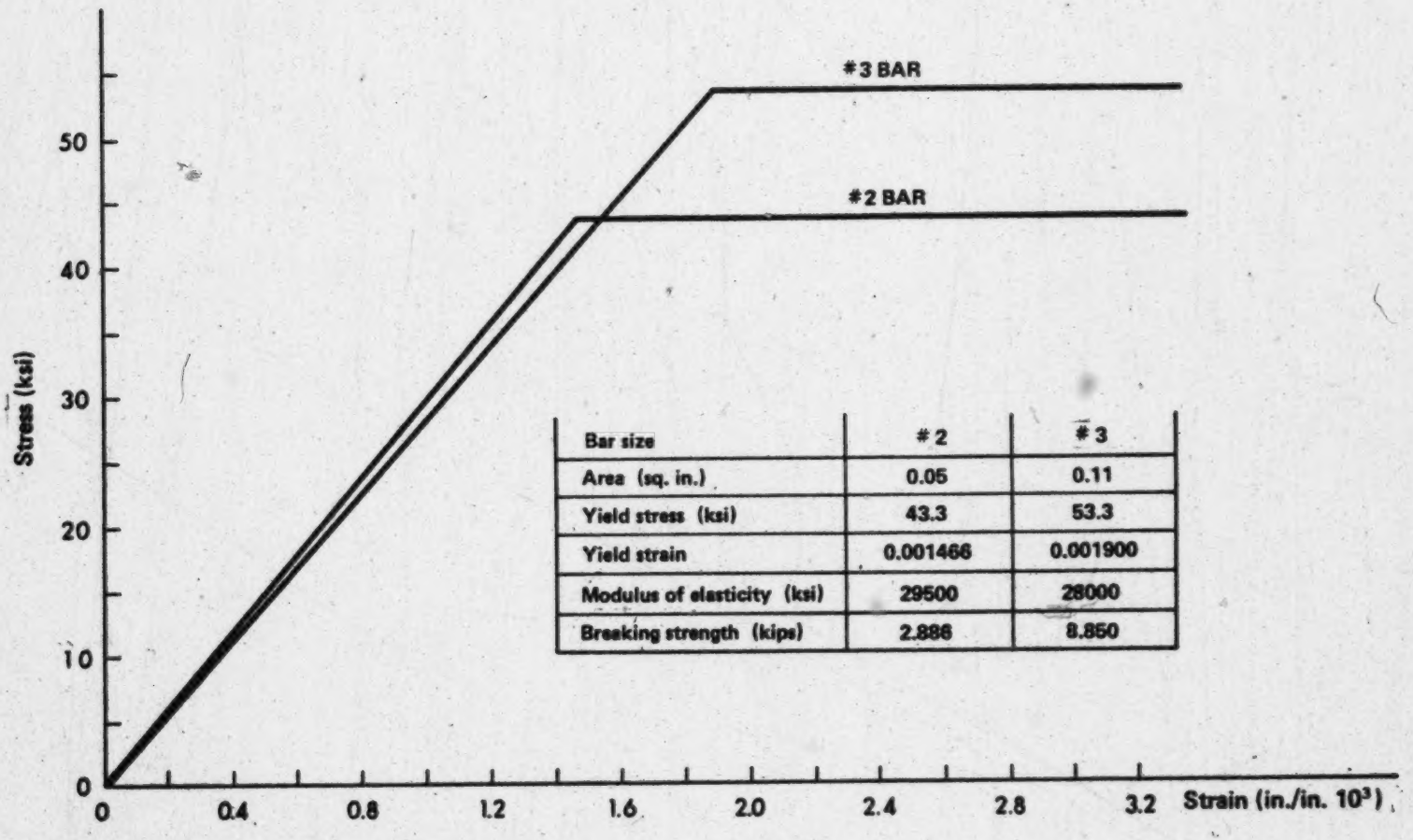

Bar size	# 2	# 3
Area (sq. in.)	0.05	0.11
Yield stress (ksi)	43.3	53.3
Yield strain	0.001466	0.001900
Modulus of elasticity (ksi)	29500	28000
Breaking strength (kips)	2.886	8.850

FIG. 3.3 PORTION OF STRESS - STRAIN DIAGRAM FOR TRANSVERSE STEEL (STIRRUPS)

test in order to obtain their stress-strain curves. Only the initial portions of stress-strain curves are shown in Figure 3.3 since the strain hardening region was not utilized. The prestressing cables for the test specimens were 3/8 and 1/2 inches in diameter, both being seven wire strand with a guaranteed minimum yield strength of 250 ksi. Data supplied by the manufacturer was used to prepare the idealized stress-strain curves for prestressing cables as shown in Figures 3.4 and 3.5. Equations representing the stress-strain relationship for the prestressing strands are used in the theoretical analysis of this investigation.

3.2 Fabrication of Specimens

Prior to the fabrication of the beams prestressing cables were cut and placed between two concrete bulkheads, which were fastened to the laboratory floor by eight large high strength bolts. At both bulkheads wedge grip and anchorages were installed on the ends of the cables. One end served as a point of force application and at the other load cells provided data needed for the determination of prestressing force. When the cables were aligned, each strand was individually stressed using a Simplex center-hole hydraulic jack operated by an electric pump. Although an attempt was made to stress the cables to the designated level of prestress, small variations in anchorage losses made this virtually impossible. After prestressing, the transverse reinforcement was positioned and fixed by wiring the

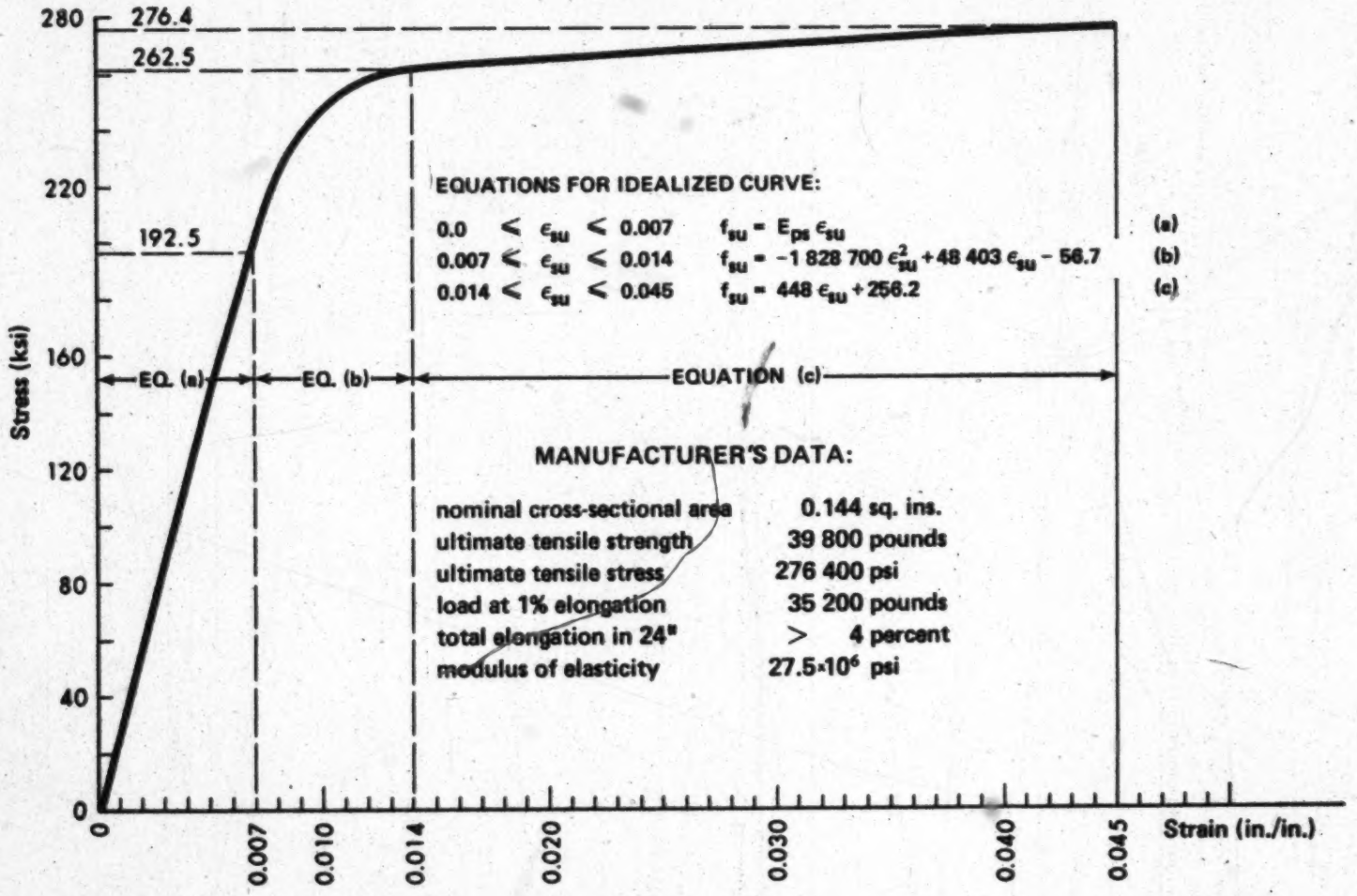

FIG. 3.4 IDEALIZED STRESS - STRAIN CURVE AND MANUFACTURER'S DATA FOR ½" DIA. STRAND

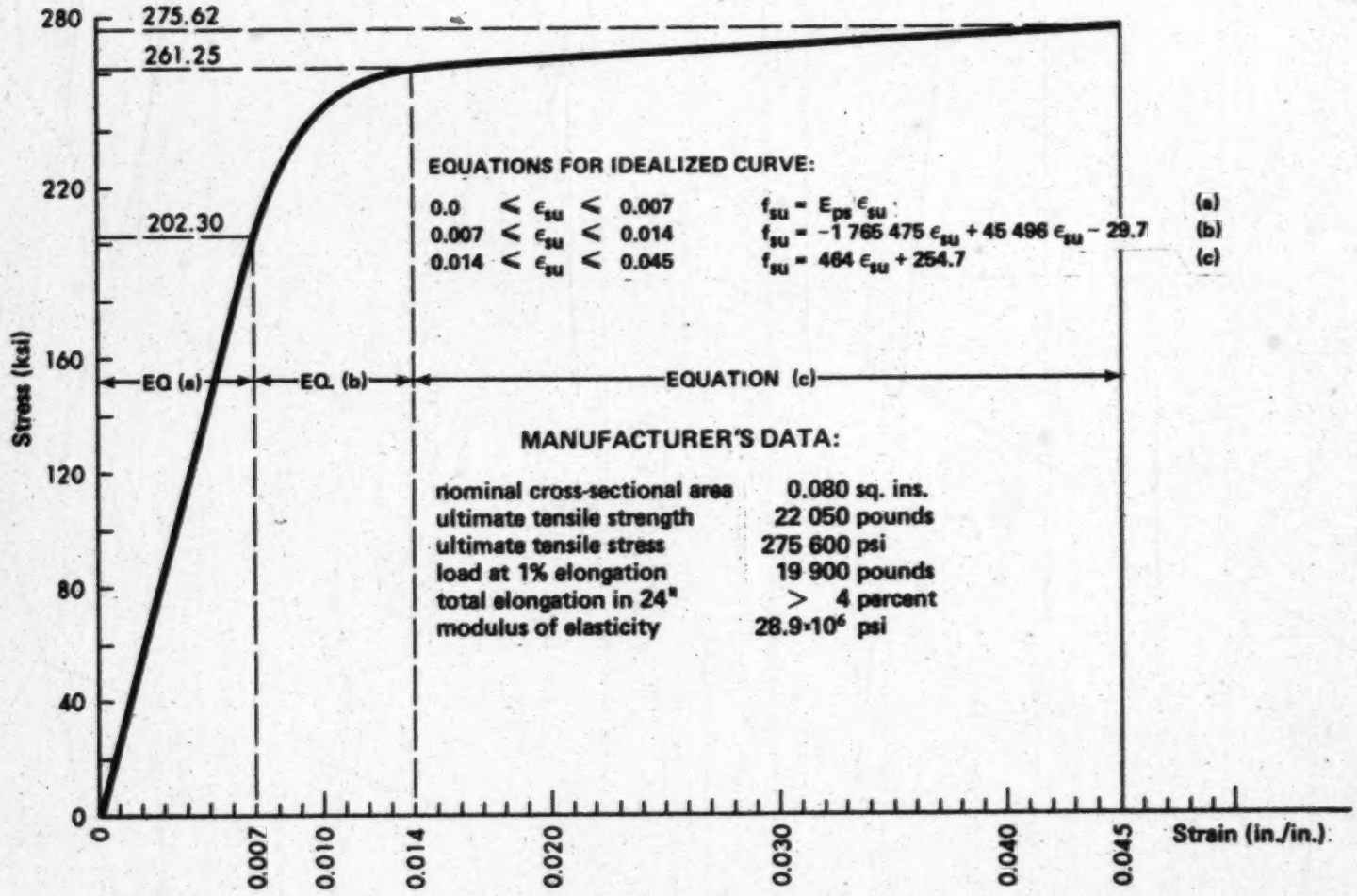

FIG. 3.5 IDEALIZED STRESS - STRAIN CURVE AND MANUFACTURER'S DATA FOR 3/8" DIA. STRAND

stirrups to the prestressing cables as shown in Figure 3.6. To ensure that failure occurred in the test zone, additional transverse and longitudinal reinforcement was provided outside the test zone. Prior to positioning and fastening of the steel forms they were cleaned and oiled. The 26 ft. long prestressing bed permitted fabrication of two beams at the same time.

Concrete mixing was performed in the laboratory using a nine cubic foot capacity mixer. Concrete was placed in the forms with the aid of a 1 inch diameter internal vibrator. Five six-by-twelve inch control cylinders were made with each specimen and cured under the same conditions as the beams. The steel forms were removed the day after casting and the beams together with test cylinders were covered with moist burlap and plastic sheets. After six days the burlap and plastic sheets were removed and final load cell readings were taken in order to determine prestress relaxation and anchorage losses.

The opening in the hollow beams was made using a styrofoam block of the same cross-section as the opening and a length of one foot longer than the test zone to avoid possible effects of stress concentration in this region. Although the contribution of styrofoam, if left inside the beam, would be insignificant in bending, it was felt that its contribution may be much higher in resisting torsion and shear due to confinement. To nullify its possible contribution to the beam torsional and shear strength, after curing of a beam was completed, the styrofoam was completely dissolved using an organic

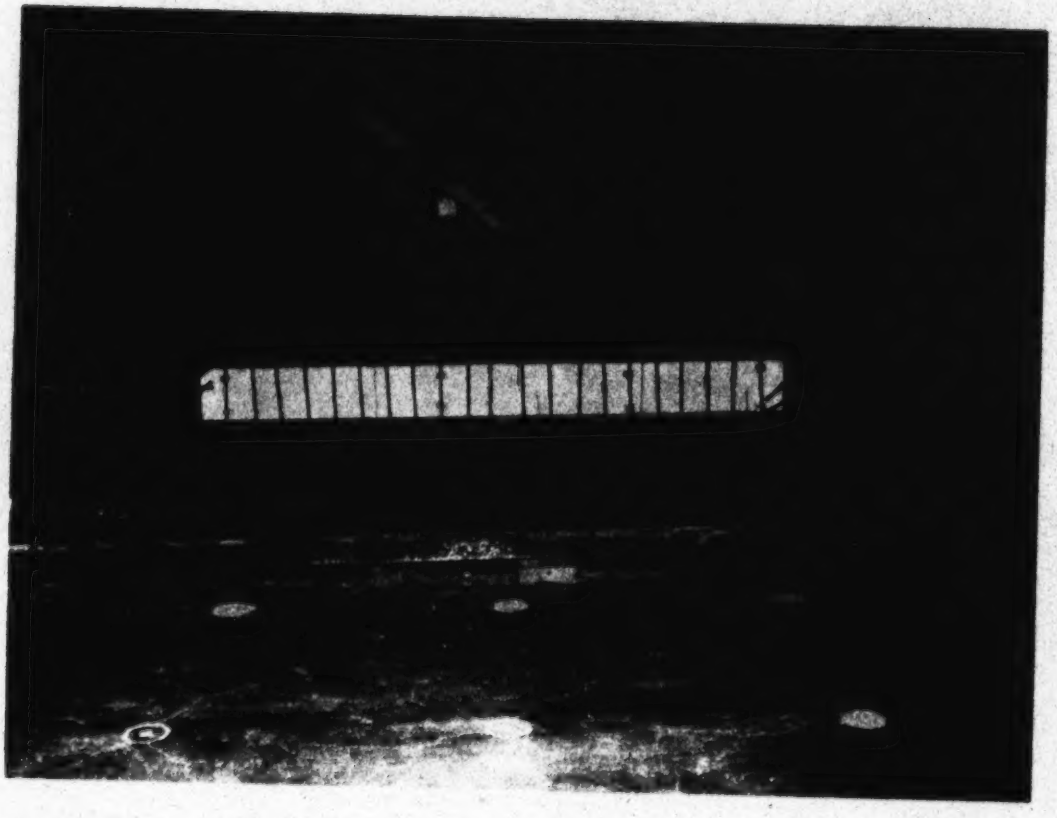

REINFORCEMENT CAGE FOR A HOLLOW BEAM

solvent, acetone. To insure accessibility to the styrofoam, two plastic tubes of 3/4 in. in diameter were cast in the solid portions of the beam as shown in Figure 3.6.

For both solid and hollow beams, five pairs of mechanical gauge points were positioned on both vertical sides of the beam and initial readings were taken using an 8 inch Demec deformation gauge. Readings were taken immediately after release of prestress providing data required for the calculation of prestress losses due to elastic shortening of the beam. The same procedure was repeated prior to test to determine losses due to creep, shrinkage and relaxation.

Three cylinders were tested in compression and the remaining two in tension the same day as the beam test. Compressive and tensile strengths of the concrete are reported in the following chapter.

3.3 Instrumentation of Specimens

3.3.1 Reinforcement Strains

In contrast to the beams of Series A where only four strain gauges were mounted on the vertical legs of stirrups, Series B and C were more extensively instrumented. Generally, seventeen strain gauges were used for each beam; five on the prestressing strands and twelve on the stirrups. Location and designation of these strain gauges is shown in Figures 3.7 through 3.11 and strain gauge readings for each load increment are given in Appendix B.

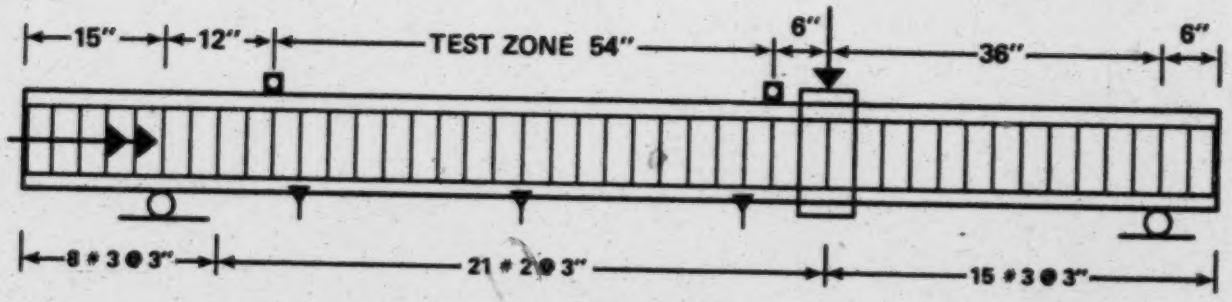

a) ELEVATION VIEW

LEGEND:

- TWISTMETER
- DEFLECTIONMETER (ONE EACH SIDE)
- STRAIN GAUGES ON STIRRUPS (FOUR ON EACH STIRRUP - S,B,N,T i.e. SOUTH, BOTTOM, NORTH AND TOP)
- STRAIN GAUGES ON PRESTRESSING STRANDS (ARROWS SHOW THEIR LOCATION IN CROSS-SECTION)

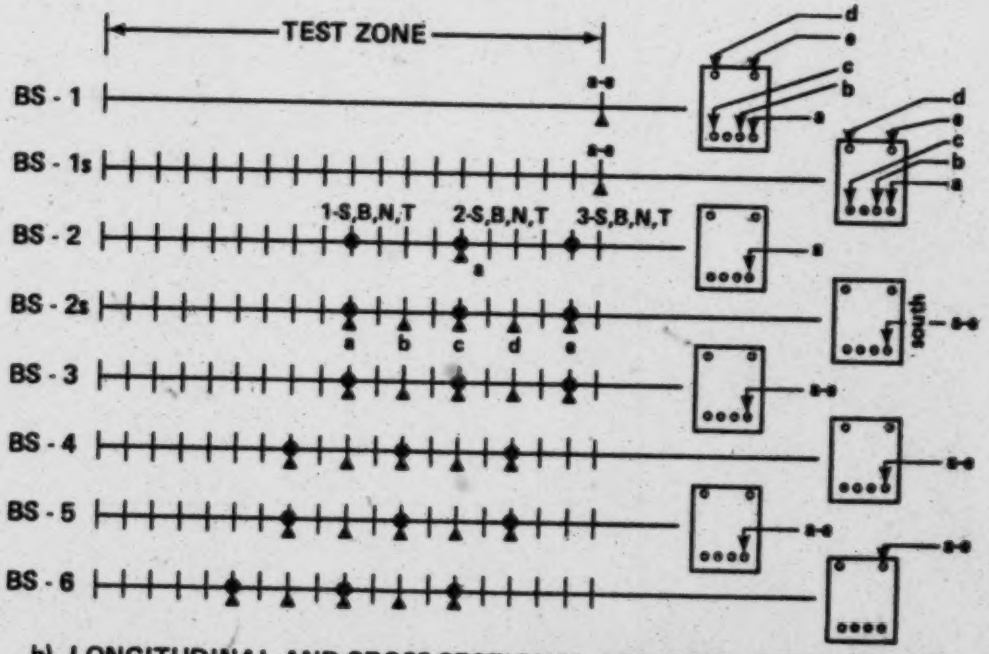

b) LONGITUDINAL AND CROSS-SECTIONAL ARRANGEMENT OF STRAIN GAUGES ON STIRRUPS AND PRESTRESSING STRANDS

FIG. 3.7 ELEVATION VIEW AND INSTRUMENTATION OF ∝S GROUP BEAMS

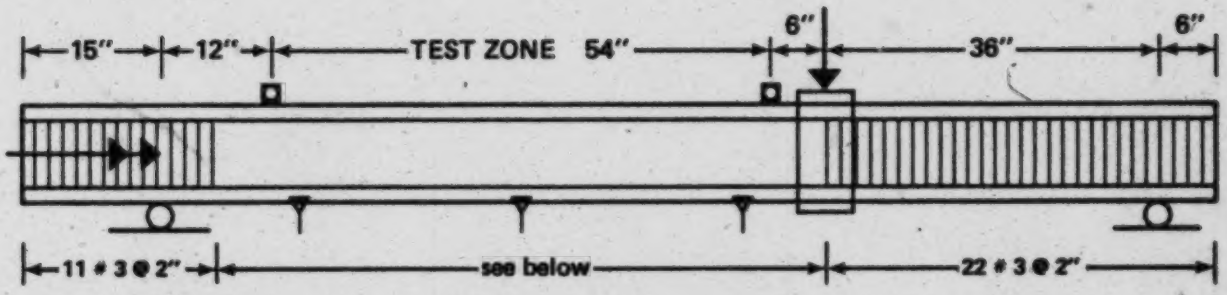

a) ELEVATION VIEW

LEGEND:

- TWISTMETER
- DEFLECTIONMETER (ONE EACH SIDE)
- STRAIN GAUGES ON STIRRUPS (FOUR ON EACH STIRRUP - S,B,N,T i.e. SOUTH, BOTTOM, NORTH AND TOP)
- STRAIN GAUGES ON PRESTRESSING STRANDS (ARROWS SHOW THEIR LOCATION IN CROSS-SECTION)

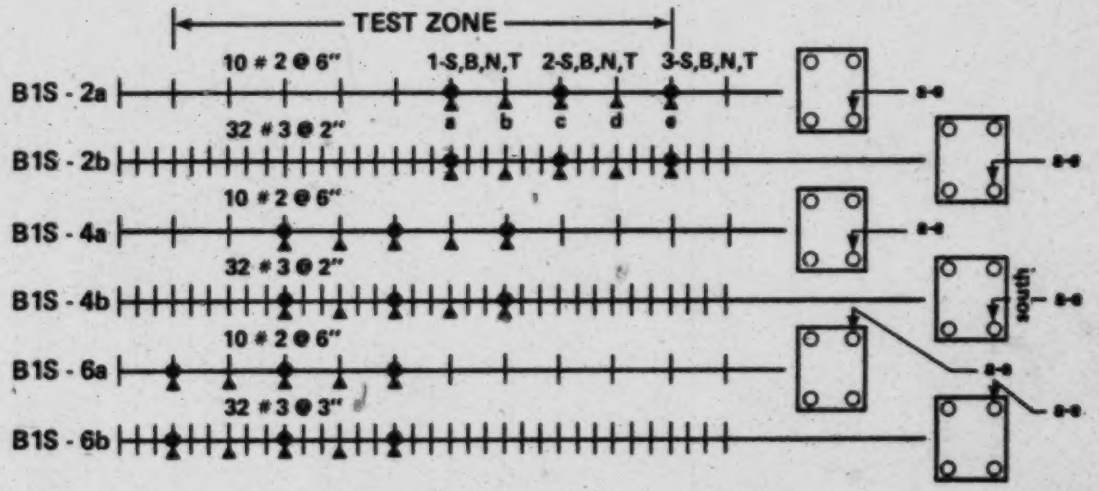

b) LONGITUDINAL AND CROSS-SECTIONAL ARRANGEMENT OF STRAIN GAUGES ON STIRRUPS AND PRESTRESSING STRANDS

FIG. 3.8 ELEVATION VIEW AND INSTRUMENTATION OF B1S GROUP BEAMS

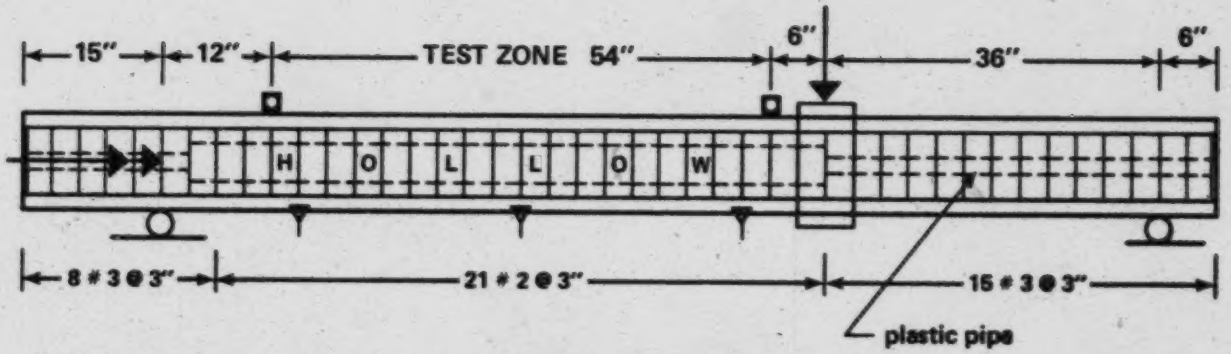

a) ELEVATION VIEW

LEGEND:

- TWISTMETER
- DEFLECTIONMETER (ONE EACH SIDE)
- STRAIN GAUGES ON STIRRUPS (FOUR ON EACH STIRRUP - S,B,N,T i.e. SOUTH' BOTTOM' NORTH AND TOP)
- STRAIN GAUGES ON PRESTRESSING STRANDS (ARROWS SHOW THEIR LOCATION IN CROSS-SECTION)

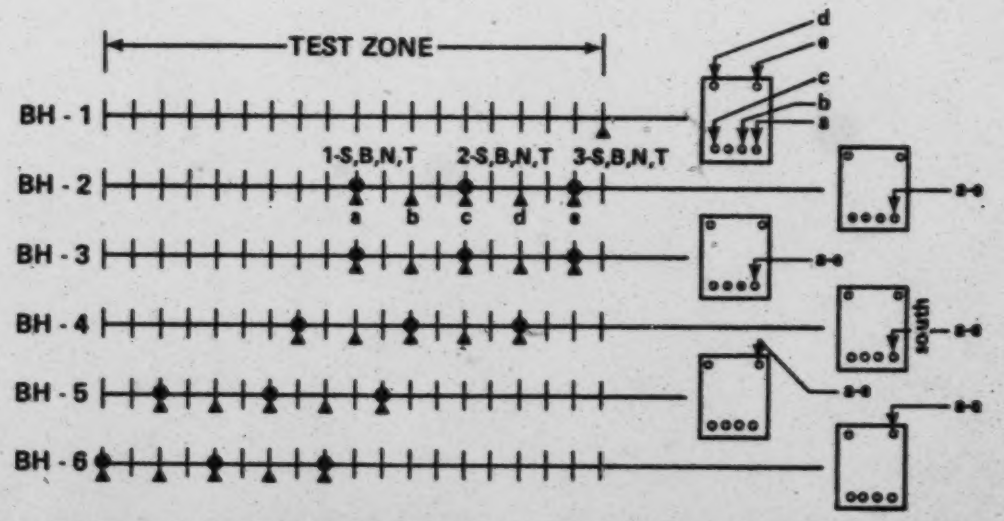

b) LONGITUDINAL AND CROSS-SECTIONAL ARRANGEMENT OF STRAIN GAUGES ON STIRRUPS AND PRESTRESSING STRANDS

FIG. 3.9 ELEVATION VIEW AND INSTRUMENTATION OF BH GROUP BEAMS

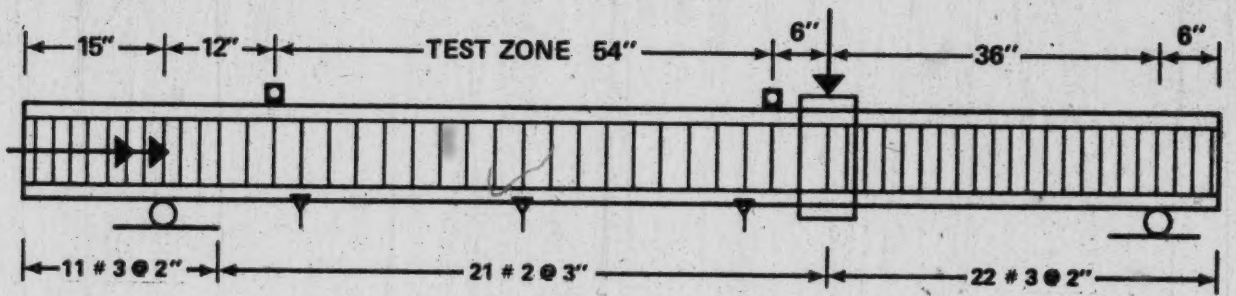

a) ELEVATION VIEW

LEGEND:

- TWISTMETER
- DEFLECTIONMETER (ONE EACH SIDE)
- STRAIN GAUGES ON STIRRUPS (FOUR ON EACH STIRRUP - S,B,N,T i.e. SOUTH, BOTTOM, NORTH AND TOP)
- STRAIN GAUGES ON PRESTRESSING STRANDS (ARROWS SHOW THEIR LOCATION IN CROSS-SECTION)

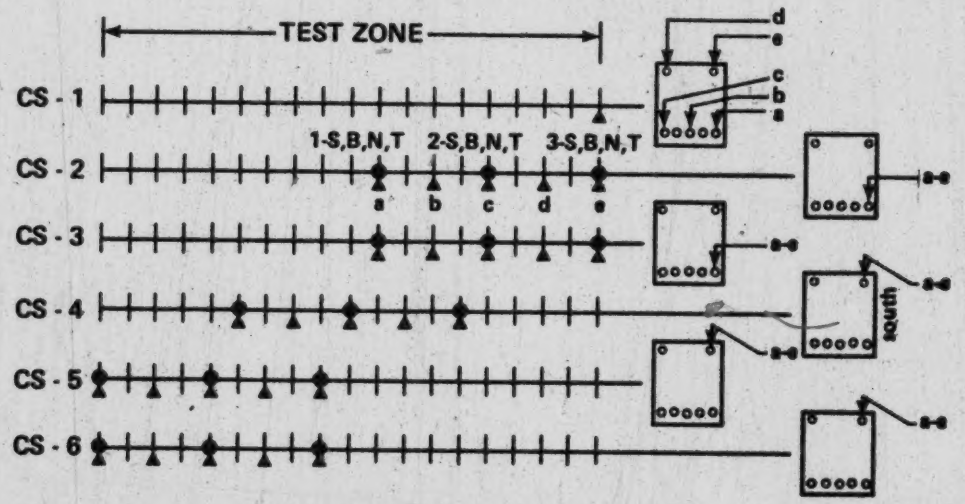

b) LONGITUDINAL AND CROSS-SECTIONAL ARRANGEMENT OF STRAIN GAUGES ON STIRRUPS PRESTRESSING STRANDS

FIG. 3.10 ELEVATION VIEW AND INSTRUMENTATION OF CS GROUP BEAMS

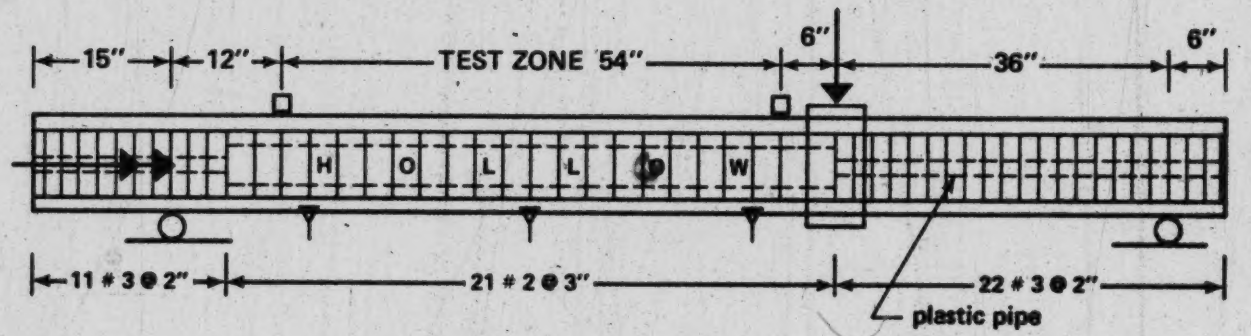

a) ELEVATION VIEW

LEGEND:

- TWISTMETER
- DEFLECTIONMETER (ONE EACH SIDE)
- STRAIN GAUGES ON STIRRUPS (FOUR ON EACH STIRRUP - S,B,N,T i.e. SOUTH, BOTTOM, NORTH AND TOP)
- STRAIN GAUGES ON PRESTRESSING STRANDS (ARROWS SHOW THEIR LOCATION IN CROSS-SECTION)

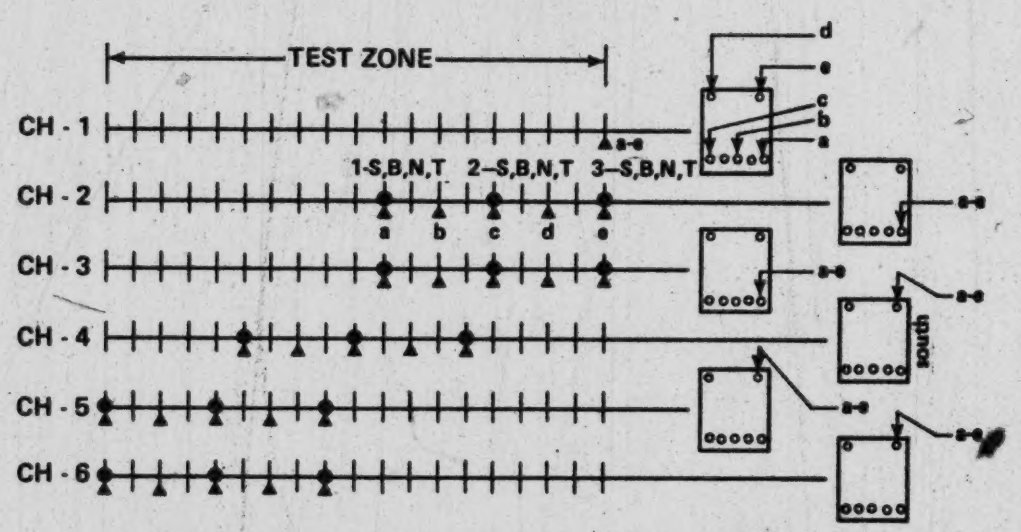

b) LONGITUDINAL AND CROSS-SECTIONAL ARRANGEMENT OF STRAIN GAUGES ON STIRRUPS AND PRETSTRESSING STRANDS

FIG. 3.11 ELEVATION VIEW AND INSTRUMENTATION OF CH GROUP BEAMS

Kyowa type KFC-5-C1-11 electrical resistance strain gauges were used for both prestressing steel and stirrups. While the installation of strain gauges on stirrups can be performed by standardized procedure, caution must be exercised in installing strain gauges on prestressing strands. Since each strand is composed of one straight and six twisted wires, "channels" between these wires make waterproofing virtually impossible. To eliminate this problem many researchers[24, 40, 65] used styrofoam plugs during casting of concrete which insured access to prestressing strands after concrete had hardened. These plugs were then removed and strain gauges placed on strands in the cavities. Although the problem of waterproofing is eliminated one of the main disadvantages of this procedure is that the gauge cannot be properly aligned in a 1 or 2 inch deep cavity. Since they are located on the outside boundaries of a cross-section these hollows, even though they are relatively small, reduce the moment of inertia of a cross-section by 10 to 15 percent thereby directly reducing the cracking strength by about the same amount. For these two reasons such a procedure was not used in this investigation. Instead, a new procedure described below, was developed.

After prestressing was completed at designated locations the outer portion of one single wire of prestressing strand was thoroughly cleaned after which a gauge was cemented with M-line Accessories' M-bond 200 and waterproofed with a coat of a Budd GW-2 compound. Lead wires were connected to the strain gauge and a small area where strain gauge was located was covered with an epoxy

compound. This step is very important since it ensured that moisture or water leaking during casting would be prevented. After curing the entire strand at strain gauge location was wrapped with tape. For additional protection against possible damage of a strain gauge during casting, the entire strand at this location was covered with the epoxy compound.

The main advantages of the above procedure are that, (i) gauge can be properly aligned and, (ii) no reduction of effective cross-sectional area occurs. Total loss of strain gauges is significantly reduced as compared to the first described procedure; it is interesting to note that in more than 500 strain gauges installed using this procedure only 3 strain gauges were lost.

3.3.2 Angle of Twist

Rotation of a member subjected to a torque was measured by two twistmeters. The location of these twistmeters is shown in Figures 3.7 through 3.11. Each twistmeter consisted of an elbow-type aluminum bracket with a spirit level, pin joined at one end and supported at the other by a micrometer screw with the smallest division of 0.001 inches. This assembly was attached to the top face of a beam by means of a rubber belt. The rotation of each twistmeter was computed from the difference in micrometer readings between two successive load increments, the total angle of twist over the test zone was the difference between twistmeter rotations. These angles are tabulated for each load increment in Appendix A.

3.3.3 Deflections

Figures 3.7 through 3.11 show locations of three pairs of deflection gauges for each group of beams. Essentially the deflection gauge consisted of a metal ruler with division of 0.01 inches hung on a small hook which was cemented on the beam face. Readings were taken using two precise levels located on either side of a specimen. The average value of a corresponding pair of readings, which was obtained in this manner, resulted in the determination of the deflection of the longitudinal beam axis. Deflection data for each load increment for beams of B and C series are tabulated in Appendix A.

3.4 Test Equipment

The loading apparatus which permits independent application of torsion and flexure or torsion and shear-flexure was first designed and used by McMullen and Warwaruk[55]. Only minor alterations, such as the enlargement of the torsionally fixed head were made in the course of this experimental investigation. Detailed description and illustration of loading apparatus is available elsewhere[55, 58]; only a brief description is presented here.

The loading arrangement used for testing of the beams under combined loading is illustrated in Figure 3.12. Transverse load was applied by means of an Amsler jack having a capacity of 100 kips. Load was transfered to the beam by a heavy plate laterally supported and resting on a pipe collar which was fastened to the specimen at the

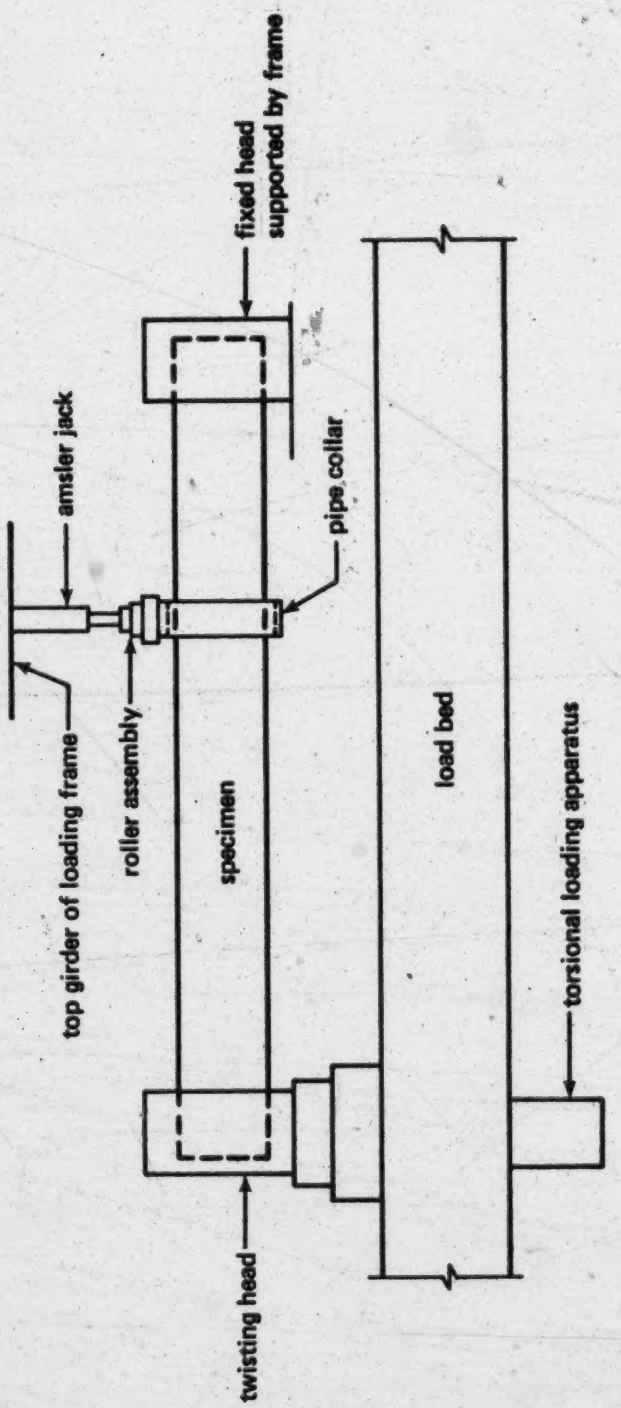

FIG. 3.12 EQUIPMENT ARRANGEMENT VIEWED FROM NORTH SIDE

point of loading. This system permitted transfer of a twisting moment along beam length and ensured that the transverse load remained in a vertical direction. The west end of the specimen was supported by a fixed head shown in Figure 3.13, while the east end was supported by a twisting head (Figure 3.14) where torque was applied. The east head allowed a beam to rotate about its longitudinal axis and also in the vertical plane. On the other hand, the west head restricted torsional rotation of a beam, while it permitted bending rotations and small movements in the longitudinal direction. Detailed view of complete test set-up for combined loading is shown in Figure 3.15.

The torque applied to a beam resulted from two loads applied by cables in opposite direction to the twisting head as shown in Figure 3.16. The cables, in turn, were attached to an assembly, located below the test floor, which was operated by a hand pump. Forces in the cables were measured using load cell and strain indicator.

3.5 Testing Procedure

Before a specimen was placed into the loading frame readings were taken on the mechanical demec points and electrical resistance strain gauges on the prestressing strand. These readings provided data required for prestress loss calculations. The dead weight of the pipe collar and plate assembly used for application of transverse load was calculated beforehand and allowance was made due to this weight in applying transverse load. Both transverse load and twisting moment

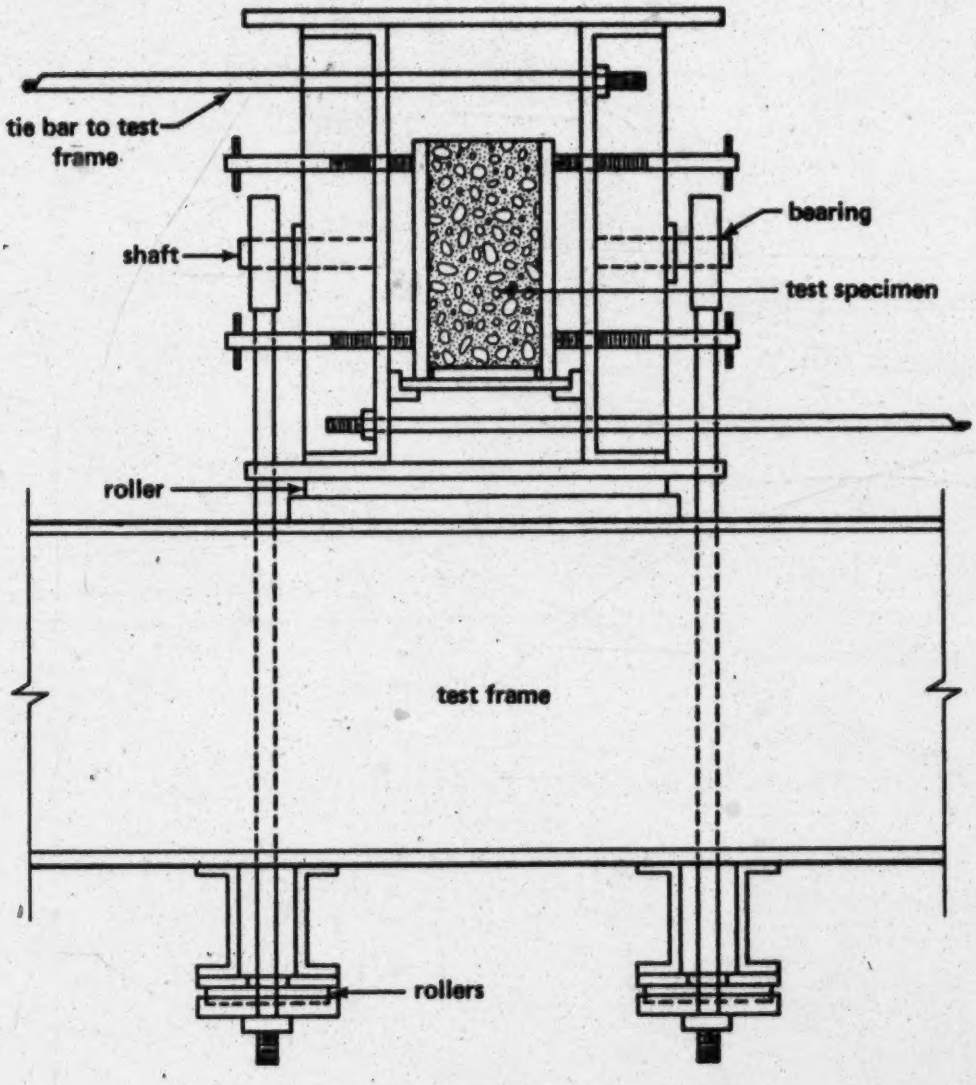

FIG. 3.13 FIXED HEAD

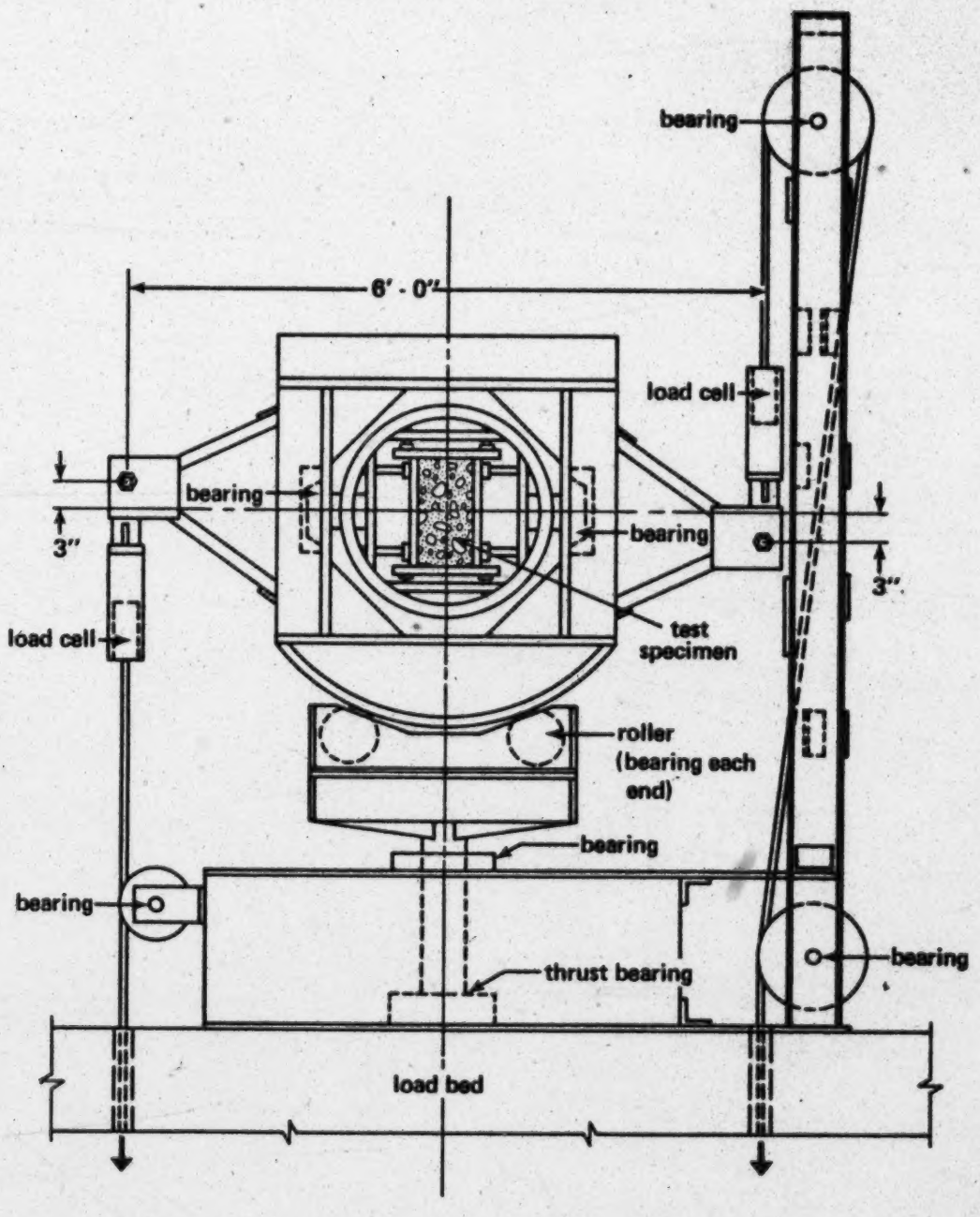

FIG. 3.14 TWISTING HEAD

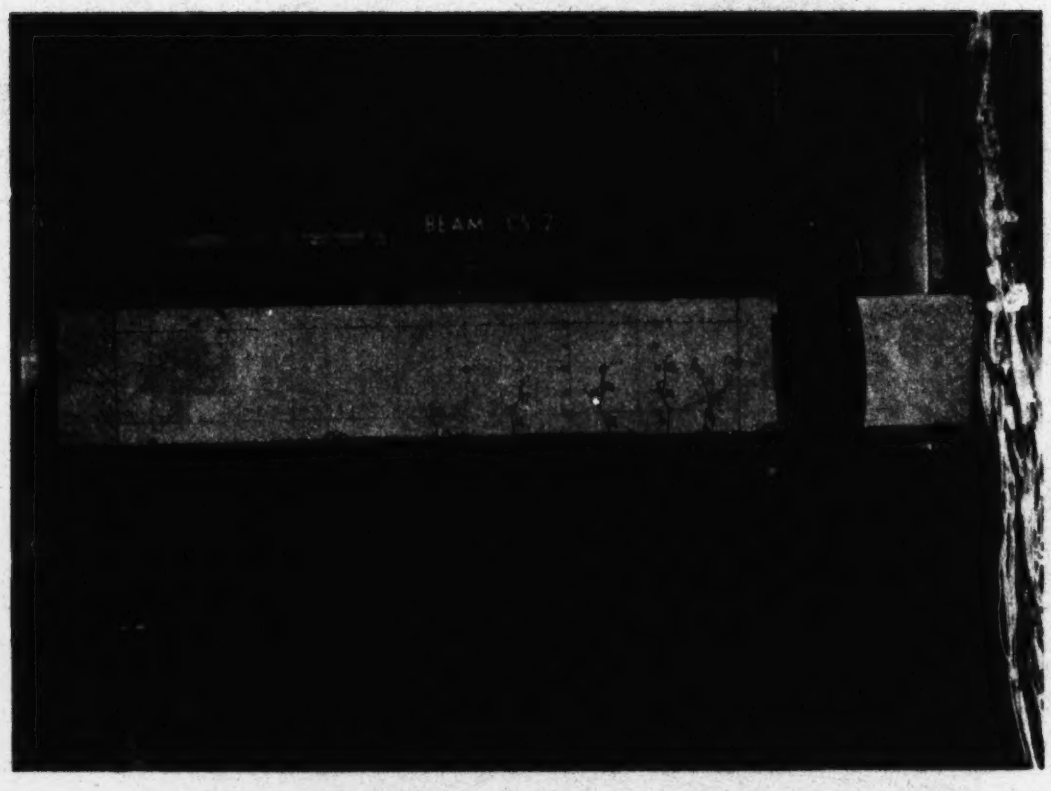

DETAILED VIEW OF TEST SETUP FOR COMBINED LOADING

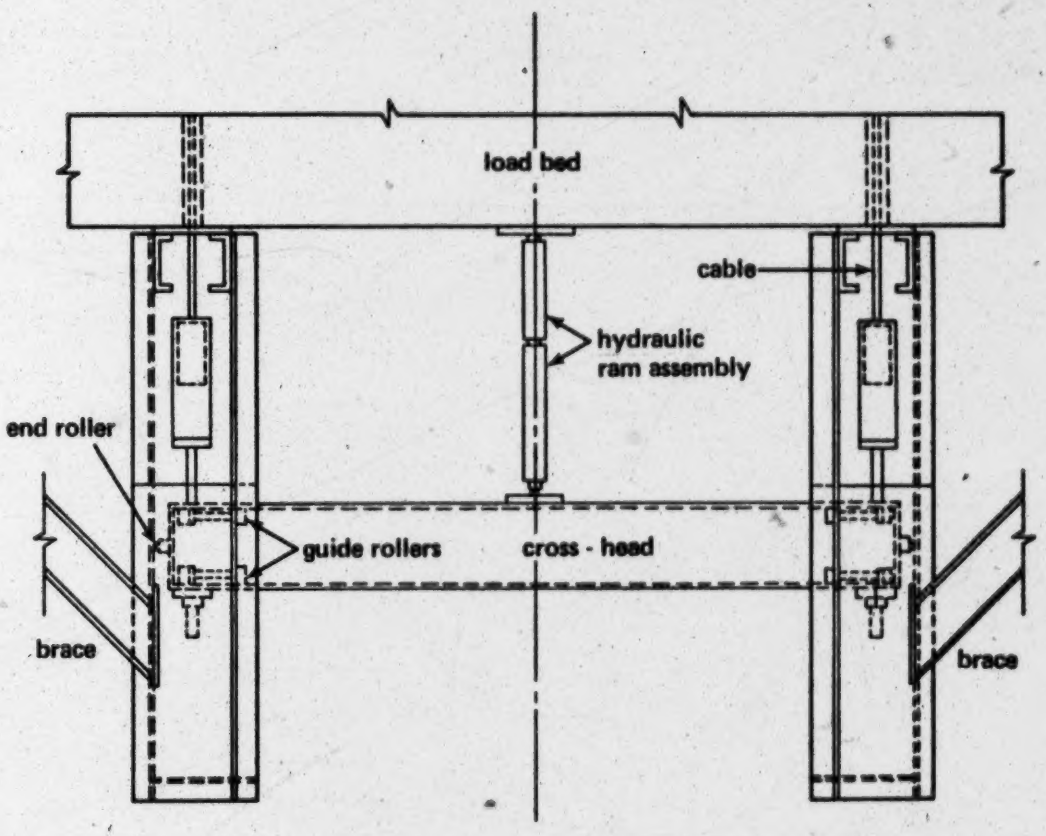

FIG. 3.16 TORSIONAL LOADING EQUIPMENT

were applied in a series of simultaneous increments of predetermined magnitude depending upon the ratio of torsional to bending moment. As cracking or ultimate load was approached loading increments were reduced in order to improve accuracy in determining these capacities. For each load increment all instrumentation was read and the crack patterns were marked. The number of increments for each test varied between 15 and 30. Test data for beams of series B and C is tabulated in Appendicies A and B, and crack patterns are shown in Appendix C.

CHAPTER IV

PRESENTATION AND DISCUSSION OF TEST RESULTS

4.1 General

In this chapter principal test results are presented and behavior of beams under combined loading is discussed. Additional information for each beam of Series B and C including loading, deformation and strain data for each load increment and crack pattern is presented in Appendices A, B and C. Data for beams of Series A is available elsewhere[39, 74]. The parameters studied in this investigation are listed in Table 4.1. Numerical values of these variables for each beam are presented in the following section. Variables included in Series A and the group identification of this series is shown in Table 4.2. The primary objective of Series B and C was to study the effect of a longitudinal opening. Each of these two series has been divided into two groups BS, BH and CS, CH; the second letter in each group refers to solid and hollow cross-section, respectively. Additionally, Series B contained group B1S in which the amount of transverse steel and the initial prestress were varied.

Each of the thirteen groups of beams reported in this investigation consisted of 6 to 8 beams. The first beam in each group was tested in pure bending and with the exception of groups AB, AD, AF and AH, the last beam of each group was subjected to pure torsion. The remaining beams were tested under various loading ratios in combined

TABLE 4.1 PARAMETERS CONSIDERED IN THIS STUDY

Series	Torsion and Bending only	Torsion, Bending and Shear	Torsion to Bending Ratio, ψ	Torsion to Shear Ratio, δ	Effective Prestress σ_o	Eccentricity of Prestressing Force, e	Amount of Transverse Steel	Solid beam	Hollow beam
A 6" x 12"	X	X	X	X		X	X	X	
B 8" x 12"		X	X	X	X	X	X	X	X
C 12" x 12"		X	X	X				X	X

TABLE 4.2 SERIES A, GROUP IDENTIFICATION

	Beams with transverse reinforcement		Beams without transverse reinforcement	
	torsion,bending	torsion,bending, shear	torsion,bending	torsion,bending, shear
Concentric Prestress	Group AA	AB	AC	AD
Eccentric Prestress	AE	AF	AG	AH

bending and torsion or bending, torsion and shear.

4.2 Principal Test Results

The principal test results for all three series of beams are presented in Table 4.3. They include compressive and splitting strengths of concrete, effective prestress, eccentricity of prestressing force, cracking and ultimate capacities, loading ratios, failure mode, angle of twist and centerline deflection. Geometric properties of beams are not included here, since they have been presented in Chapter 3. It should be noted that the effect of dead load for Series A was neglected, while because of larger dimensions it has been included for Series B and C. The effective prestressing force in each cable is not reported here since it can be easily generated from the effective prestress and eccentricity of prestressing force shown in Table 4.3.

The cracking and ultimate strengths, and loading ratios ψ and δ, are calculated with respect to the centroid of compression zone of the failure surface. For combined torsion, bending and shear ratios ψ and δ differ somewhat from the initial predetermined ratios used in the load application because the location of the actual failure cross-section usually did not coincide with the assumed failure cross-section. The maximum twist and deflection at the centerline of the test zone correspond to values recorded at the end of the load increment immediately preceding failure. It should be noted that failure is defined herein as a state when the beam could no longer sustain increases in loads to which it was subjected.

TABLE 4.3 TEST RESULTS

Beam		Concrete Strength (psi)		Effective Prestress $\sigma_o = \frac{P_{eff}}{A_n}$ (psi)	Eccentricity (positive downward) e (in)	Applied Load						Loading Ratios		Failure Mode	Angle of Twist (rad/in x 10^6)	Centerline deflection Δ_u (in)
						At Cracking			At Ultimate							
Group	no.	f'_c	f_{sp}			T_c (in.kips)	M_c (in.kips)	V_c (kips)	T_u (in.kips)	M_u (in.kips)	V_u (kips)	$\psi = \frac{T}{M}$	$\delta = \frac{2T}{bV}$			
AA	1	5148	569	1408	0.006	0.0	445.5	0.0	0	797	0	0.000	*	**	0	0.99
	2	4950	495	1418	0.012	55.9	389.5	0.0	95	662	0	0.144	∞	1	349	0.85
	3	4310	380	1410	-0.035	99.0	297.3	0.0	159	478	0	0.333	∞	2	746	0.73
	4	3896	394	1423	0.002	111.4	148.1	0.0	155	206	0	0.752	∞	2	970	0.17
	5	4255	433	1410	-0.030	126.0	94.7	0.0	157	118	0	1.331	∞	2	1167	0.04
	6	4496	380	1418	0.000	129.6	43.5	0.0	164	55	0	2.982	∞	2	817	0.01
	7	4883	464	1415	0.008	133.0	0.0	0.0	178	0	0	∞	∞	2	632	0.00
AB	1	5115	517	1413	0.016	0.0	312	5.00	0	747	11.67	0.000	0.000	**	0	0.53
	2	5056	531	1402	0.021	33.4	290.4	4.76	82	712	11.67	0.115	2.342	1	135	0.51
	3	4821	486	1301	0.022	65.0	294.1	4.98	120	543	9.20	0.221	4.346	2	536	0.41
	4	5092	486	1417	0.026	117.0	100.2	4.01	146	125	5.00	1.168	9.733	2	633	0.15
	5	5009	433	1417	-0.018	104.0	32.0	2.00	156	48	3.00	3.250	17.333	2	640	0.08
	6	4620	429	1422	-0.020	85.8	16.2	0.73	148	28	1.27	5.286	38.845	2	469	0.03

* Indeterminate

** Pure bending or shear-bending

TABLE 4.3 (Cont'd) TEST RESULTS

Beam		Concrete Strength (psi)		Effective Prestress $\sigma_o = \frac{P_{eff}}{A_n}$	Eccentricity (positive downward)	Applied Load						Loading Ratios		Failure Mode	Angle of Twist	Centerline deflection
						At Cracking			At Ultimate							
Group	no.	f'_c	f_{sp}	(psi)	e (in)	T_c (in.kips)	M_c (in.kips)	V_c (kips)	T_u (in.kips)	M_u (in.kips)	V_u (kips)	$\psi = \frac{T}{M}$	$\delta = \frac{2T}{bV}$		(rad/in x 10^6)	Δ_u (in)
AC	1	6083	495	1410	-0.014	0.0	364.7	0.0	0	770	0	0.000	*	**	0	1.07
	2	5818	540	1425	-0.005	38.6	241.2	0.0	106	662	0	0.160	-	1	166	0.81
	3	5606	528	1419	-0.005	108.0	290.3	0.0	141	379	0	0.372	-	2	142	0.21
	4	5491	442	1426	0.009	129.6	172.8	0.0	150	200	0	0.750	-	2	176	0.13
	5	5410	464	1407	-0.009	142.2	107.3	0.0	167	126	0	1.325	-	2	108	0.05
	6	5349	502	1411	0.013	129.6	43.2	0.0	168	56	0	3.000	-	2	166	0.01
	7	5120	530	1416	-0.004	106.3	0.0	0.0	171	0	0	-	-	2	58	0.00
AD	1	6408	568	1416	-0.017	0.0	426.6	6.64	0	787	12.30	0.000	0.000	**	0	0.47
	2	5906	526	1421	-0.019	22.3	265.5	4.02	63	748	11.33	0.084	1.854	1	97	0.41
	3	4750	482	1417	0.010	108.0	320.5	6.97	124	368	8.00	0.337	5.167	2	208	0.25
	4	6024	469	1422	0.022	117.9	112.5	4.02	130	124	4.43	1.048	9.782	2	134	0.19
	5	5223	435	1429	0.014	117.8	49.7	2.27	135	57	2.60	2.368	17.308	2	143	0.04
	6	5517	488	1430	0.014	113.0	15.7	0.96	137	19	1.17	7.211	46.837	2	125	0.00

* Indeterminate

** Pure bending or shear-bending

TABLE 4.3 (Cont'd) TEST RESULTS

Beam		Concrete Strength (psi)		Effective Prestress $\sigma_o = \frac{P_{eff}}{A_n}$ (psi)	Eccentricity (positive downward) e (in)	Applied Load						Loading Ratios		Failure Mode	Angle of Twist (rad/in x 10^6)	Centerline deflection Δ_u (in)
						At Cracking			At Ultimate							
Group	no.	f'_c	f_{sp}			T_c (in.kips)	M_c (in.kips)	V_c (kips)	T_u (in.kips)	M_u (in.kips)	V_u (kips)	$\psi = \frac{T}{M}$	$\delta = \frac{2T}{bV}$			
AE	1	4791	486	1428	1.664	0.0	486.0	0.0	0	904	0	0.000	*	**	0	0.98
	2	4703	451	1423	1.650	67.5	468.8	0.0	124	864	0	0.144	∞	1	123	1.26
	3	4573	394	1427	1.680	99.0	372.2	0.0	124	466	0	0.266	∞	2	1330	0.46
	4	5168	471	1415	1.700	121.5	162.4	0.0	172	230	0	0.748	∞	2	1160	0.10
	5	4056	394	1429	1.709	95.5	71.9	0.0	162	122	0	1.328	∞	2	624	0.03
	6	4432	438	1425	1.669	125.6	41.6	0.0	172	57	0	3.018	∞	2	1395	-0.12
	7	4667	462	1409	1.668	143.7	0.0	0.0	154	0	0	∞	∞	2	932	0
AF	1	4866	429	1396	1.630	0.0	600.0	10.00	0	880	14.67	0.000	0.000	**	0	0.57
	2	4657	520	1427	1.662	42.7	422.8	7.55	83	821	14.67	0.101	1.886	1	200	0.96
	3	4030	482	1353	1.627	95.4	249.7	7.35	134	351	10.33	0.382	4.324	2	635	0.44
	4	5075	420	1462	1.684	117.0	72.1	4.01	146	90	5.00	1.622	9.733	2	493	0.14
	5	4692	438	1427	1.689	78.0	31.4	1.50	149	60	2.87	2.483	17.306	2	693	0.03
	6	5110	442	1461	1.658	109.2	17.0	0.93	160	25	1.37	6.400	38.929	2	701	-0.02

* Indeterminate

** Pure bending or shear-bending

TABLE 4.3 (Cont'd) TEST RESULTS

Beam		Concrete Strength (psi)		Effective Prestress $\sigma_o = \frac{P_{eff}}{A_n}$ (psi)	Eccentricity (positive downward) e (in)	Applied Load						Loading Ratios		Failure Mode	Angle of Twist (rad/in x 10^6)	Centerline deflection Δ_u (in)
						At Cracking			At Ultimate							
Group	no.	f'_c	f_{sp}			T_c (in.kips)	M_c (in.kips)	V_c (kips)	T_u (in.kips)	M_u (in.kips)	V_u (kips)	$\psi = \frac{T}{M}$	$\delta = \frac{2T}{bV}$			
AG	1	5995	453	1411	1.664	0.0	610.7	0.0	0	1026	0	0.000	*	**	0	1.09
	2	5028	471	1411	1.663	58.8	376.9	0.0	118	756	0	0.156	∞	1	247	0.68
	3	5370	562	1409	1.673	112.5	123.2	0.0	136	409	0	0.913	∞	2	107	0.17
	4	5205	455	1413	1.685	126.5	186.7	0.0	150	200	0	0.750	∞	2	232	0.09
	5	5496	435	1409	1.647	95.5	71.3	0.0	146	109	0	1.339	∞	2	128	0.03
	6	5565	533	1402	1.673	129.5	43.2	0.0	150	50	0	3.000	∞	2	127	0.01
	7	5924	508	1412	1.671	122.8	0.0	0.0	144	0	0	∞	∞	2	105	0.00
AH	1	5240	391	1414	1.676	0.0	574.8	7.58	0	910	12.00	0.000	0.000	**	0	0.46
	2	5441	455	1422	1.688	44.6	299.3	4.99	107	720	12.00	0.149	2.972	1	129	0.35
	3	4644	498	1418	1.676	82.4	355.2	6.34	117	504	9.00	0.232	4.333	2	261	0.26
	4	3949	367	1414	1.671	97.5	60.0	3.33	117	72	4.00	1.625	9.750	2	133	0.17
	5	4969	438	1425	1.675	88.4	33.1	1.57	131	49	2.33	2.674	18.741	2	108	0.07
	6	4792	480	1408	1.671	105.2	15.4	0.71	143	21	0.97	6.810	49.141	2	123	0.01

* Indeterminate

** Pure bending or shear-bending

TABLE 4.3 (Cont'd) TEST RESULTS

Beam		Concrete Strength (psi)		Effective Prestress $\sigma_o = \frac{P_{eff}}{A_n}$ (psi)	Eccentricity (positive downward) e (in)	Applied Load						Loading Ratios		Failure Mode	Angle of Twist (rad/in x 10^6)	Centerline deflection Δ_u (in)
						At Cracking			At Ultimate							
Group	no.	f'_c	f_{sp}			T_c (in.kips)	M_c (in.kips)	V_c (kips)	T_u (in.kips)	M_u (in.kips)	V_u (kips)	$\psi = \frac{T}{M}$	$\delta = \frac{2T}{bV}$			
BH	1	5747	493	1402	1.167	0	537	7.95	0	933	13.95	0.000	0.000	**	0	0.44
	2	6325	533	1396	1.268	58	529	7.96	104	941	14.29	0.111	1.820	1	198	0.45
	3	5447	340	1448	1.207	102	369	5.99	164	589	9.66	0.278	4.244	1	260	0.26
	4	6071	458	1404	1.193	105	69	2.52	185	117	4.29	1.581	10.781	3	460	0.05
	5	5895	515	1358	1.349	114	55	1.40	189	86	2.23	2.198	21.188	3	405	-0.02
	6	6325	482	1352	1.395	104	6	0.19	182	6	0.19	30.333	239.474	3	604	0.00
BS	1	5588	389	1399	1.181	0	671	9.91	0	1067	15.91	0.000	0.000	**	0	0.46
	1S	6160	400	1412	1.225	0	693	10.23	0	1052	15.67	0.000	0.000	**	0	0.55
	2	6036	500	1388	1.202	54	731	10.56	87	1170	17.06	0.074	1.275	1	79	0.52
	2S	5995	427	1386	1.240	58	539	7.90	109	1001	14.90	0.109	1.829	2	90	0.45
	3	5624	495	1411	1.210	147	480	8.67	210	678	12.34	0.310	4.255	2	225	0.47
	4	6013	482	1336	1.131	165	95	3.93	232	132	5.43	1.758	10.681	2	570	0.04
	5	5906	453	1364	1.178	184	21	1.73	236	25	2.12	9.440	27.830	2	221	-0.06
	6	5818	435	1365	1.117	158	9	0.27	203	9	0.27	22.556	187.963	3	509	0.00

** Pure bending or shear-bending

TABLE 4.3 (Cont'd) TEST RESULTS

Beam		Concrete Strength (psi)		Effective Prestress $\sigma_o = \frac{P_{eff}}{A_n}$ (psi)	Eccentricity (positive downward) e (in)	Applied Load						Loading Ratios		Failure Mode	Angle of Twist (rad/in x 10^6)	Centerline deflection Δ_u (in)
						At Cracking			At Ultimate							
Group	no.	f'_c	f_{sp}			T_c (in.kips)	M_c (in.kips)	V_c (kips)	T_u (in.kips)	M_u (in.kips)	V_u (kips)	$\psi = \frac{T}{M}$	$\delta = \frac{2T}{bV}$			
B1S	2a	5836	475	448	0.758	23	212	2.90	50	446	6.40	0.112	1.953	1	78	0.47
	2b	5464	444	458	0.765	23	212	2.90	50	446	6.40	0.112	1.953	1	59	0.43
	4a	5783	453	461	0.825	96	172	2.63	132	232	3.63	0.569	9.091	1	154	0.10
	4b	5806	458	461	0.896	102	173	2.81	174	287	4.81	0.606	9.044	1	315	0.24
	6a	5435	453	470	0.778	117	8	0.25	144	8	0.25	18.000	144.000	2	764	0.00
	6b	5411	495	480	0.790	128	5	0.25	208	5	0.25	41.600	208.000	3	664	0.00
CH	1	5058	416	1102	1.334	0	608	891	0	1180	17.58	0.000	0.000	**	0	0.56
	2	4610	432	1030	1.279	50	563	8.24	131	1135	16.91	0.115	1.291	1	133	0.46
	3	4474	376	1051	1.302	138	474	7.64	282	954	15.64	0.296	3.005	1	323	0.47
	4	4893	400	1058	1.319	143	277	4.41	318	601	9.07	0.529	5.843	3	302	0.14
	5	4521	325	1048	1.228	192	36	3.09	336	60	5.09	5.600	11.002	3	310	0.02
	6	5476	287	1086	1.353	150	9	0.31	286	9	0.31	31.444	152.151	3	565	-0.10

** Pure bending or shear-bending

TABLE 4.3 (Cont'd) TEST RESULTS

Beam		Concrete Strength (psi)		Effective Prestress $\sigma_o = \frac{P_{eff}}{A_n}$ (psi)	Eccentricity (positive downward) e (in)	Applied Load						Loading Ratios		Failure Mode	Angle of Twist (rad/in x 10^6)	Centerline deflection Δ_u (in)
						At Cracking			At Ultimate							
Group	no.	f'_c	f_{sp}			T_c (in.kips)	M_c (in.kips)	V_c (kips)	T_u (in.kips)	M_u (in.kips)	V_u (kips)	$\phi = \frac{T}{M}$	$\delta = \frac{2T}{bV}$			
CS	1	5600	511	978	1.158	0	753	10.85	0	1222	17.85	0.000	0.000	**	0	0.38
	2	5629	559	963	1.182	80	698	10.19	139	1204	17.80	0.115	1.302	1	67	0.50
	3	5288	451	997	1.107	174	539	9.68	297	908	16.51	0.327	2.998	2	223	0.44
	4	5199	360	998	1.129	260	129	7.13	390	189	10.46	2.063	6.214	3	430	0.15
	5	5323	349	998	0.989	240	69	3.79	360	99	5.46	3.636	10.989	3	343	0.02
	6	5470	323	1007	1.089	192	6	0.53	352	6	0.53	58.667	110.692	3	267	-0.09

** Pure bending or shear-bending

4.3 Precracking Behavior and Cracking Strength

Torque-twist relationships for typical beams of Series B and C are shown in Figures 4.1 and 4.2, respectively. Beams BS-2 and BH-2 shown in Figure 4.1a were both subjected to predominant bending. With the exception that one beam was of solid (BS-2) and the other of hollow (BH-2) cross-section both beams were similar in every other respect, i.e., overall dimensions, level of prestress, amount of transverse steel, and concrete strength. Curves for two other beams of the same series which were subjected to predominant torsion are shown in Figure 4.1b. Similarly, torque-twist relationships for four beams of Series C are illustrated in Figure 4.2.

Examination of these curves reveals that the load-deformation relationship deviates from a linear function at about 50% of the cracking torque T_{cr} indicating that some stress redistribution takes place before cracking. However, it should be pointed out that no significant loss of torsional stiffness occurs at the precracking stages and, therefore, for all practical purposes a linear relationship can be used. Since stresses are distributed almost elastically throughout the cross-section it is not surprising that the hollow beams yielded a reduced stiffness as compared to solid beams, but this reduction is not very significant since the opening is located around the centroid of the cross-section where both stress resultants and lever arms are relatively small. While torsional stiffness differs from one series of beams to another owing to different cross-sectional properties, it is observed

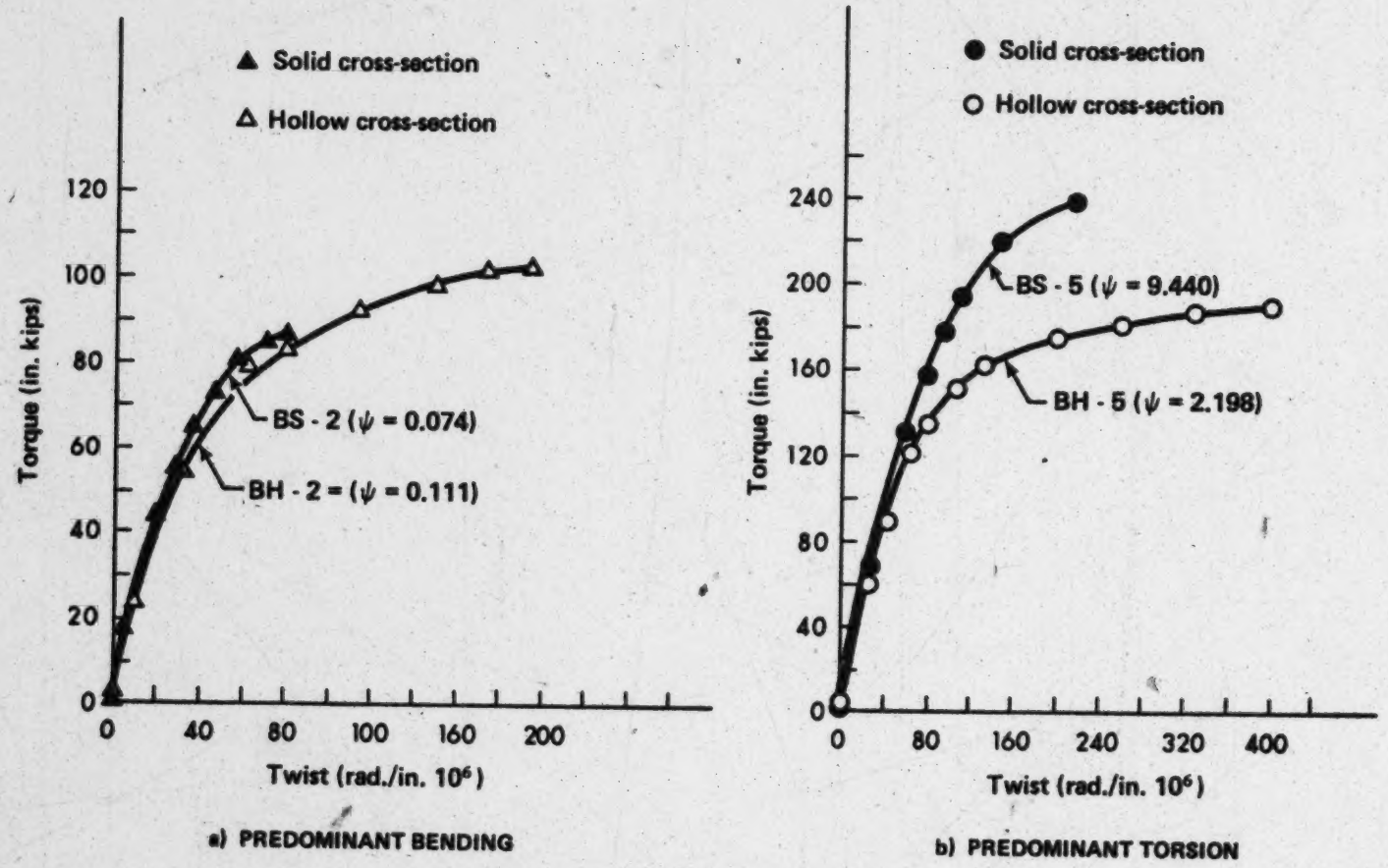

FIG. 4.1 TORQUE - TWIST CURVES, SERIES B

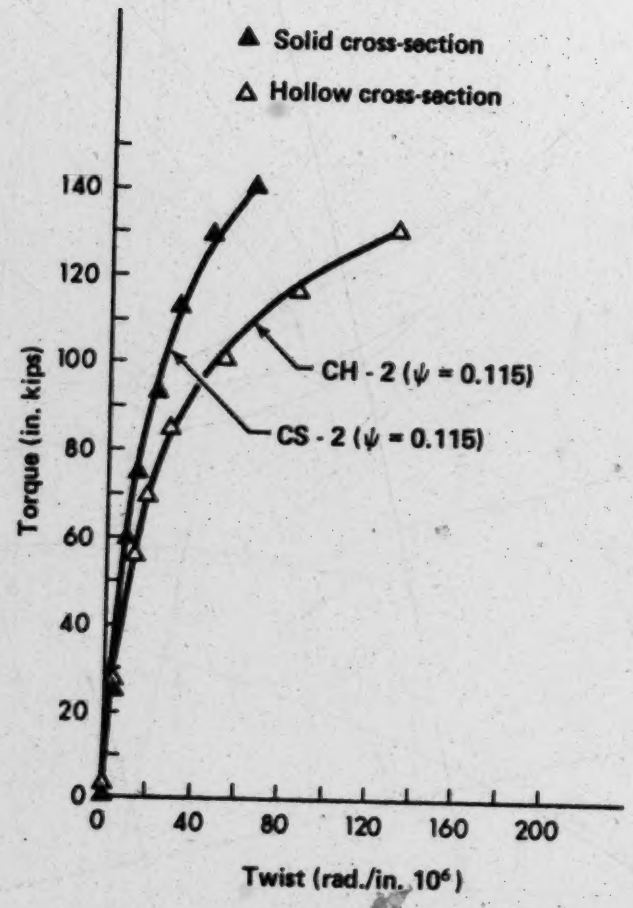

a) PREDOMINANT BENDING

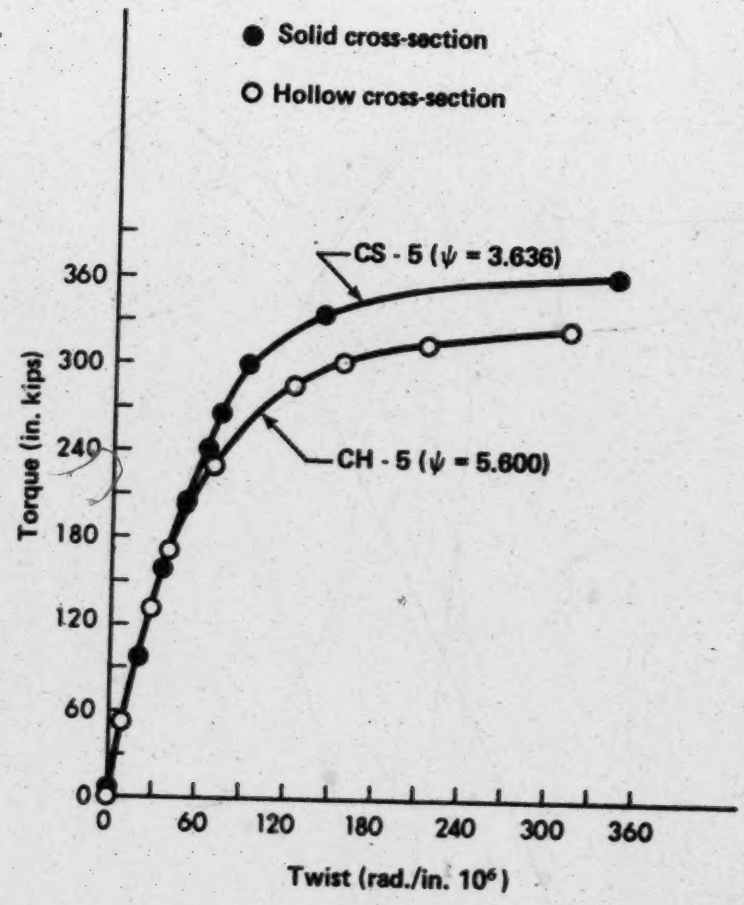

b) PREDOMINANT TORSION

FIG. 4.2 TORQUE - TWIST CURVES, SERIES C

that stiffness is independent of loading ratios ψ and δ. In comparing the curves in Figure 4.1 and 4.2, it should be noted that they are plotted using different scales. A detailed study of the influence of the other parameters on the torsional precracking stiffness is presented in Chapter 5.

The observations made regarding the torque-twist relationship before cracking apply also to the moment-deflection curves shown in Figures 4.3 and 4.4. Similar to torsional stiffness, flexural stiffness before cracking is directly influenced by the cross-sectional dimensions of the beams, therefore, comparisons can be made only within each series of beams. It is interesting to observe the upward deflection of beams BS-5 and BH-5 (Figure 4.3b). Such a behavior resulted from a positive (downward) eccentricity of the prestressing force and is associated with a high torsion to bending ratio, ψ. In this case the first crack appears on the top face and consequently the compression zone is adjacent to the bottom face. Data reported in Table 4.3 clearly shows that the major factors influencing cracking torque and cracking mode are the loading ratios ψ and δ. Other effects such as eccentricity of prestressing force and amount of transverse steel should be studied in conjunction with the above two loading ratios. For example, eccentric prestress increased cracking torques only for lower values of ψ where bending nullified the eccentricity of prestressing force. On the other hand, presence of stirrups increased torque only for beams subjected to high torsion to bending ratios,

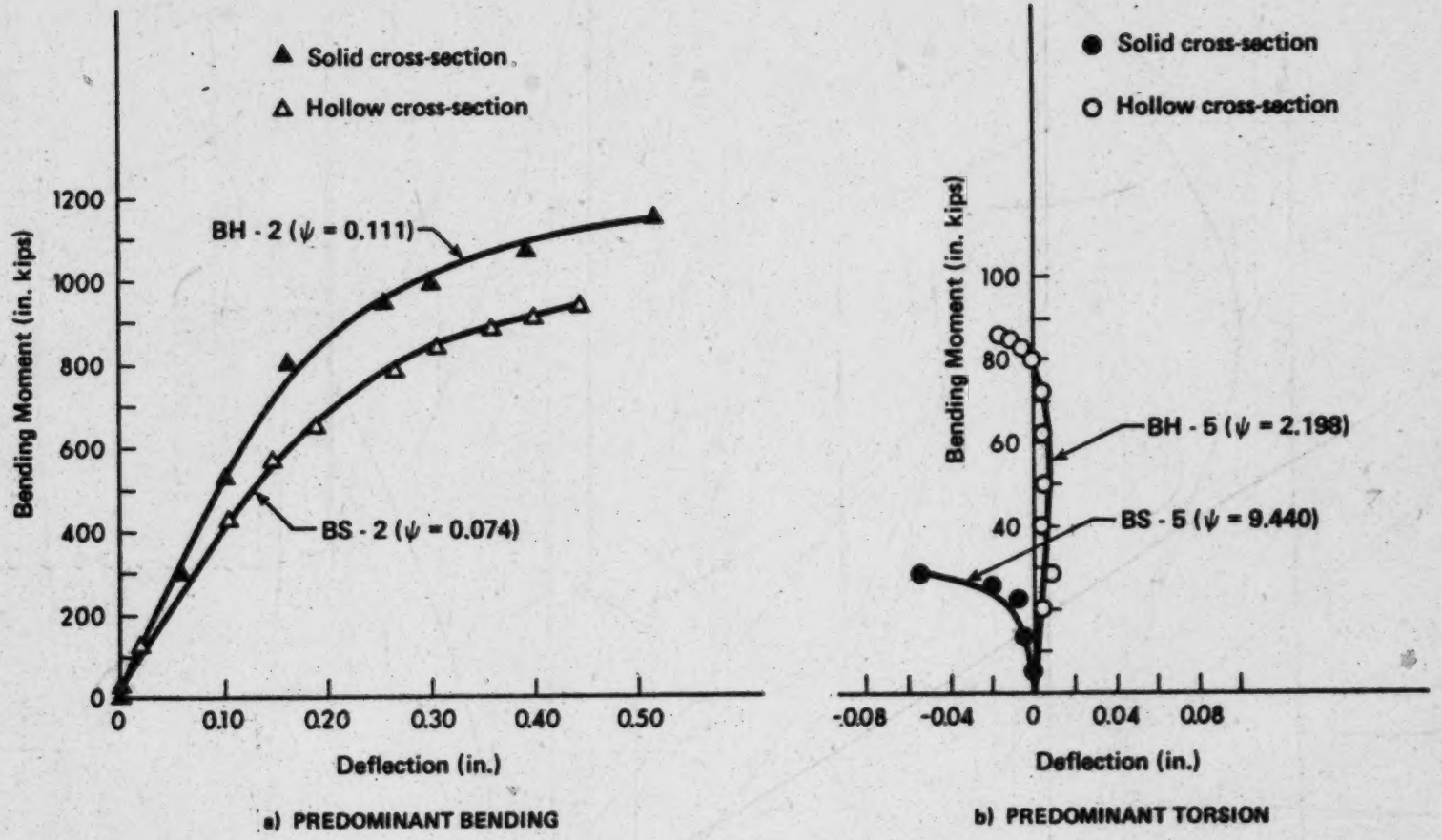

FIG. 4.3 MOMENT - DEFLECTION CURVES, SERIES B

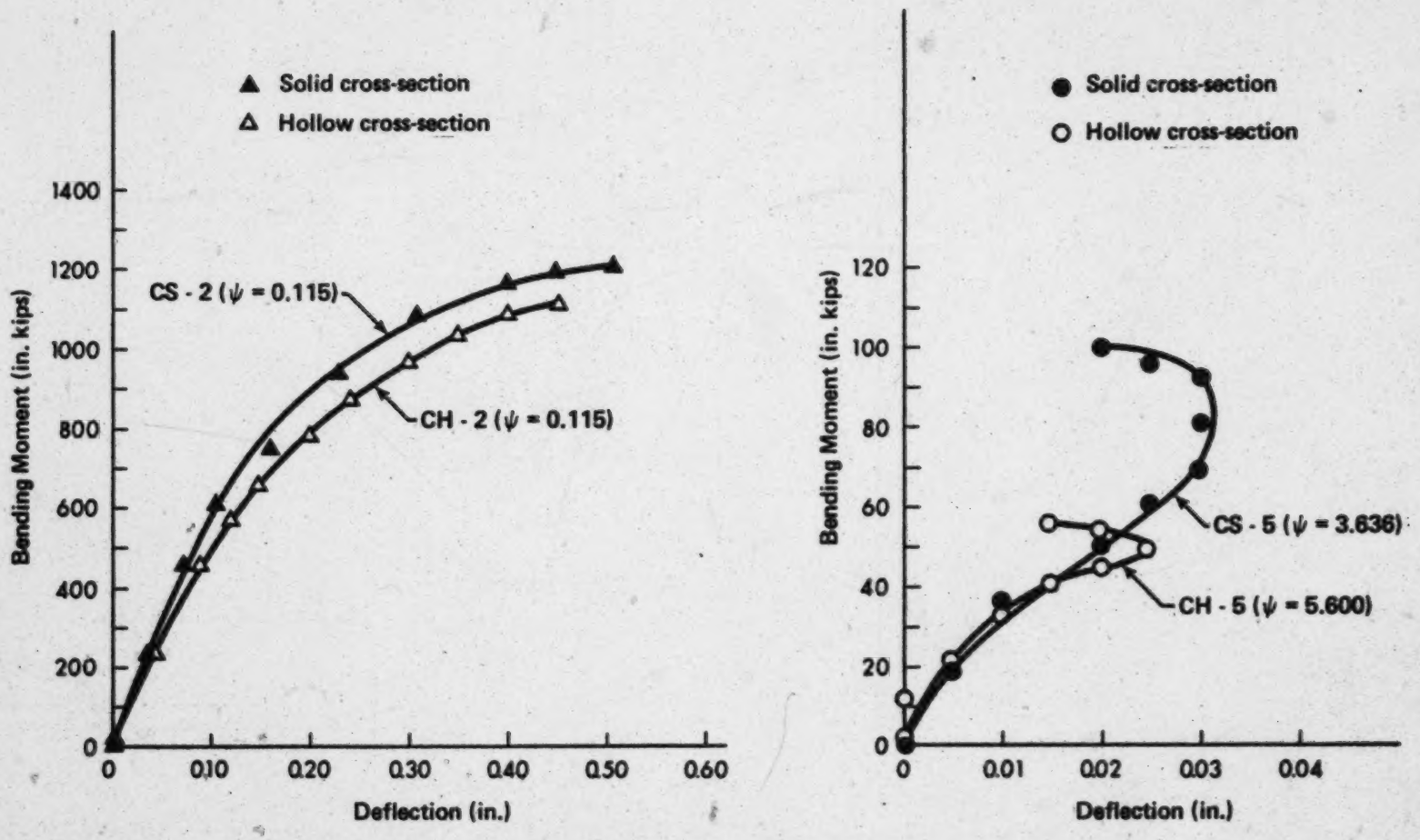

FIG. 4.4 MOMENT - DEFLECTION CURVES, SERIES C

since the number of stirrups "intersected" by a potential crack increased as ψ increased. Comparison of corresponding groups of beams in Series A subjected to combined torsion and bending only and torsion, bending and shear reveals that the presence of shear reduced cracking strength. When examining all the above effects on the cracking strength it is also important to note variations in tensile and compressive strengths of concrete.

Strain data shown in Appendix B indicate that increase in stirrup strains becomes significant after about 50% of T_{cr} and is associated only with predominant torsion. This observation is compatible with the stirrup contribution to the cracking strength noted above.

4.4 Development of Cracks, Postcracking Behavior, and Ultimate Strength

A typical crack pattern for a prestressed concrete beam under combined loading is shown in Figure 4.5. Appearance and crack formation is similar to that for reinforced concrete beams[55], except that the inclination of the cracks with respect to the longitudinal axis is generally smaller for prestressed than for reinforced concrete. Using a Mohr's circle approach[61], it can be shown that this angle in prestressed concrete can assume a value less than 30 degrees, while in reinforced concrete it always exceeds 45 degrees. For beams subjected to predominant bending the first crack started at the middle of the bottom face being almost perpendicular to the beam axis and as the load

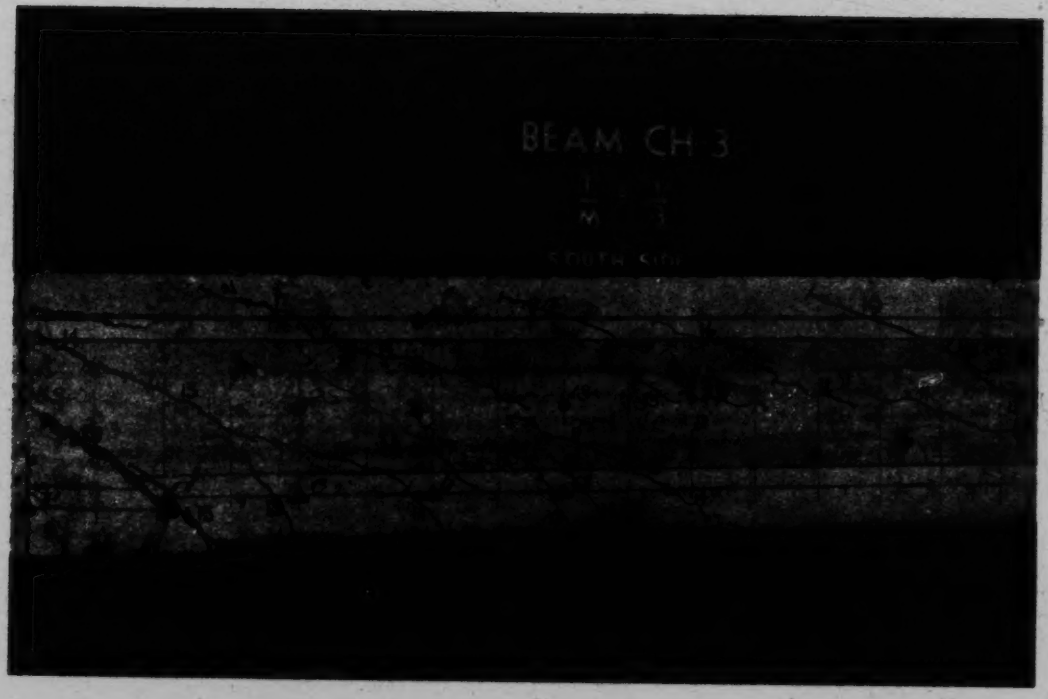

TYPICAL CRACK PATTERN OF A BEAM UNDER COMBINED LODING

was increased this crack extended to the vertical faces. Further increases in loading caused formation of new cracks on the bottom and the two vertical sides. For moderate torsion to bending ratios a crack began on the vertical face, always on the south face where the diagonal tension stresses due to flexural shear and torsional shear were additive. Finally, when torsion was predominant and eccentricity of prestressing force large, the first crack appeared on the top face. It should also be noted that the beam cross-sectional aspect ratio plays a significant role in the location of the first crack; contrary to the Series A (aspect ratio 2:1) where the first crack never appeared on the top face, for Series C (aspect ratio 1:1) cracking on the top face became common. This is not surprising since in an elongated cross-section torsional stresses are relatively much higher on the vertical than on the horizontal faces while for a square cross-section stresses due to torsion are of equal magnitude on all four faces. Similar to crack location, angle of cracks with respect to the longitudinal axis is primarily influenced by the loading ratios ψ and δ and the beam geometry.

Both torsional and flexural stiffness gradually decreased after the initial cracking had been reached. Generally, as shown in Figures 4.1 and 4.4, the loss in these stiffnesses was more pronounced for the hollow beams as compared to the solid beams. Comparisons of load-deformation curves show that the torsional stiffness increases as the torque to bending ratio decreases, while the torsional ductility

decreases as the torque to bending ratio decreases. On the other hand, both flexural stiffness and flexural ductility increase as ψ decreases. This implies that torsional and flexural stiffness and torsional and flexural ductility in the postcracking range are interdependent; this is in contrast to the precracking behavior. Data shown in Table 4.3 for beams of group B1S suggest that both the torsional and flexural stiffnesses increased as the amount of web reinforcement was increased; the increase being much higher for beams subjected to predominant torsion.

After extending across the tension face the crack propagated to the adjacent two faces at approximately the same angle as it began. As the ultimate load was approached the depth of the uncracked zone, which was located adjacent to the fourth face, decreases. In the case of predominant bending the uncracked zone was located adjacent to the top face and at ultimate, crushing of concrete in this zone was observed. However, if torsion was dominant this zone was located adjacent to the vertical north face or the bottom face. No crushing of concrete was observed but instead cracks appeared in this zone in the same direction as tension cracking described above resulting most likely from tension failure of the concrete subjected to a combined state of stress. This contradicts observations of many researchers, who reported crushing of concrete for all three modes on one hand, and on the other, supports the findings of those investigators who could not observe any significant compressive strain in the "compression" zone. In this investiga-

tion an attempt was also made to measure concrete strains using mechanical Demec points but no measurable compressive strain was observed even at the loading stage immediately preceding failure. It is reasonable to believe that crushing of the concrete in the case of moderate or predominant torsion, as reported by some researchers, is not a failure but is a postfailure phenomenon occurring only after significant loss of capacity and redistribution of internal forces carried by concrete and reinforcement. For this reason, some of the fundamental assumptions involved in the skew bending analysis for ultimate strength of beams under combined loading will be re-examined in detail in Chapter 6. Photographs of beams at failure presented in Appendix C also reinforce the above discussion.

4.5 Interaction of Torsion, Bending and Shear at Ultimate

The interaction between torsion, bending and shear at ultimate is a three-dimensional problem and as such can be represented only with a surface in a three-dimensional rectangular coordinate system. The major axes of such a coordinate system define three perpendicular planes; torsion-bending, torsion-shear and bending-shear, and for convenience, only intersections of the interaction surface with these planes is often studied. Thus the problem of a three-dimensional surface is reduced to a series of two-dimensional diagrams. Intersection of these diagrams with the coordinate axis represents the strength of a beam in pure torsion T_{uo}, pure bending M_{uo}, or

pure shear V_{uo}. While it is easy to subject a beam to pure torsion or pure bending, it is impossible to obtain shear in a beam over a finite length in the absence of a bending moment. This implies that the interaction between torsion and shear, and bending and shear, cannot be obtained experimentally. For this reason the flexural shear capacity has been usually defined as:

i. The theoretical shear strength calculated according to ACI equations, or

ii. The shear force acting when the ultimate flexural capacity is reached.

Although both definitions tend to distort interaction diagrams near the shear axis, the second definition is adopted here since it is based on tests.

Torsion-bending and torsion-shear diagrams in the nondimensionalized form for all groups of beams reported in this investigation are shown in Figures 4.6 through 4.9. With the exception of a few beams in Series A, it can be observed that the interaction between torsion and bending, and torsion and shear can be conservatively represented by the following expressions:

$$(T_u/T_{uo})^2 + (M_u/M_{uo})^2 = 1 \qquad (4.1)$$

$$(T_u/T_{uo})^2 + (V_u/V_{uo})^2 = 1 \qquad (4.2)$$

The above equations are identical to that proposed by Woodhead and McMullen[75]. Torque-bending interaction represented by Equation 4.1 has

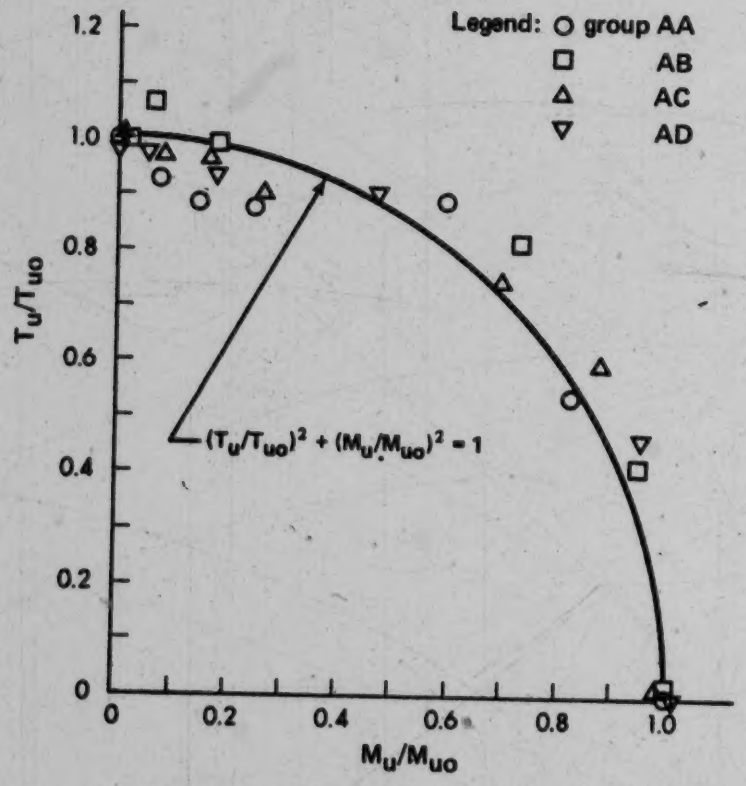

a) GROUPS: AA, AB, AC, AD

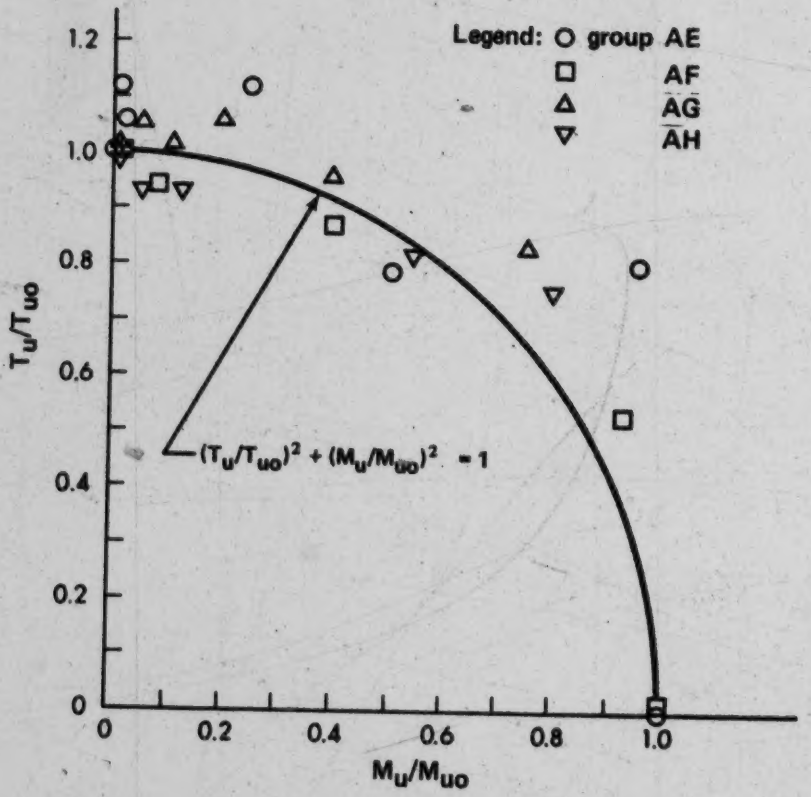

b) GROUPS: AE, AF, AG, AH

FIG. 4.6 INTERACTION BETWEEN TORSION AND BENDING AT ULTIMATE, SERIES A

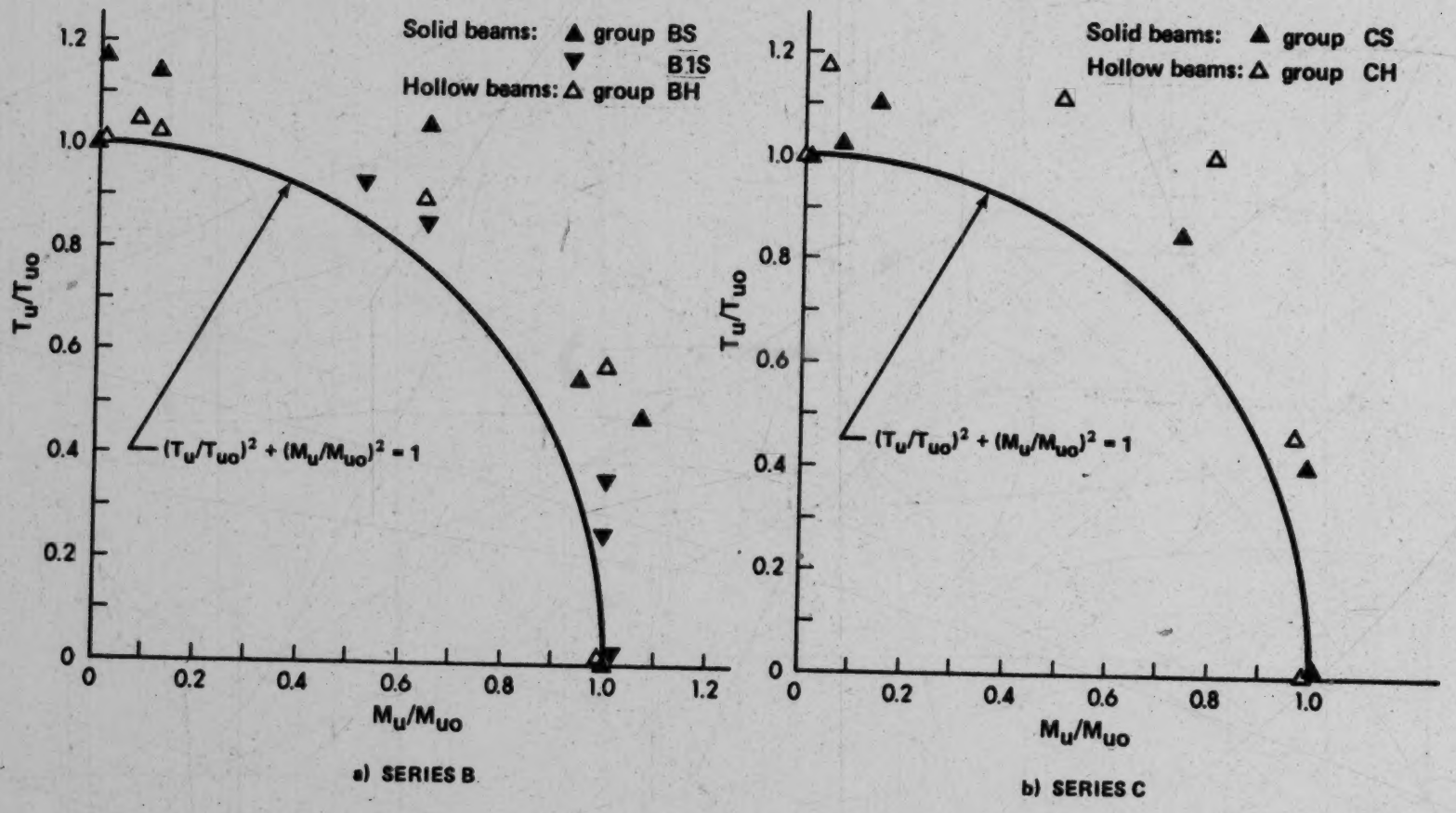

FIG. 4.7 INTERACTION BETWEEN TORSION AND BENDING AT ULTIMATE, SERIES B AND C

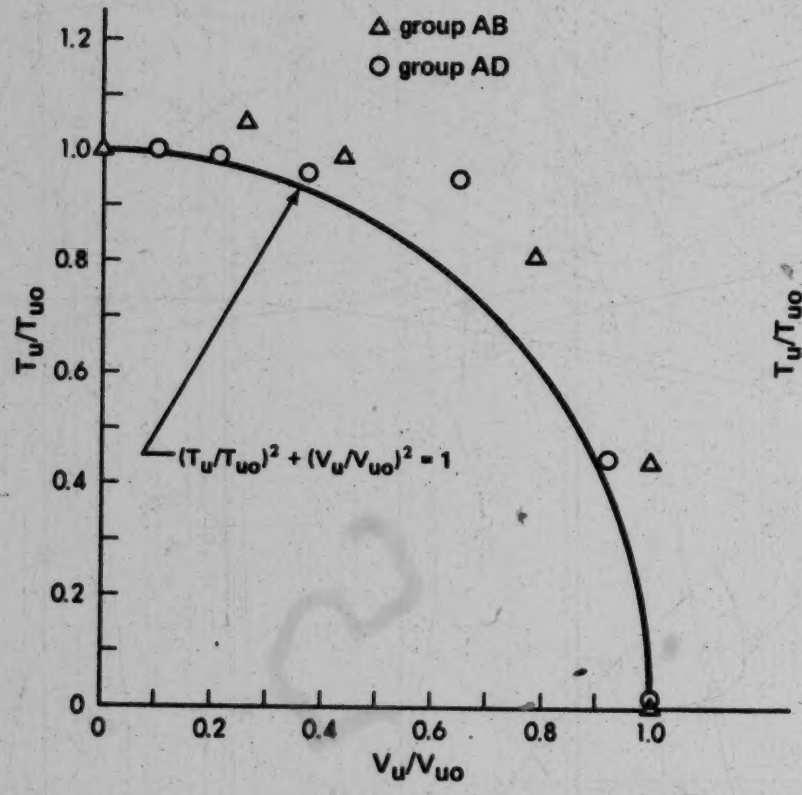

a) GROUPS AB AND AD

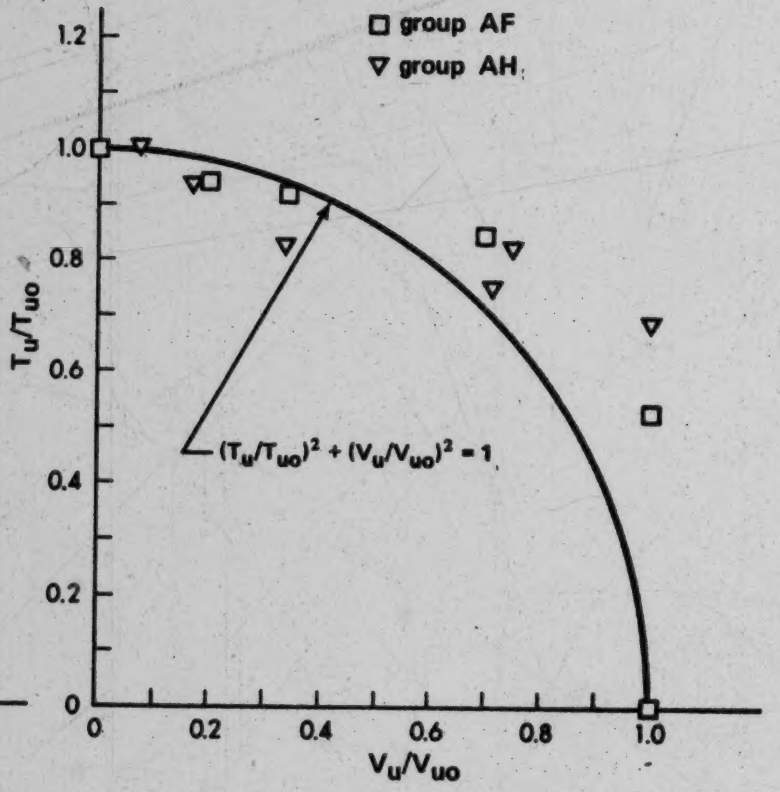

b) GROUPS AF AND AH

FIG. 4.8 INTERACTION BETWEEN TORSION AND SHEAR AT ULTIMATE, SERIES A

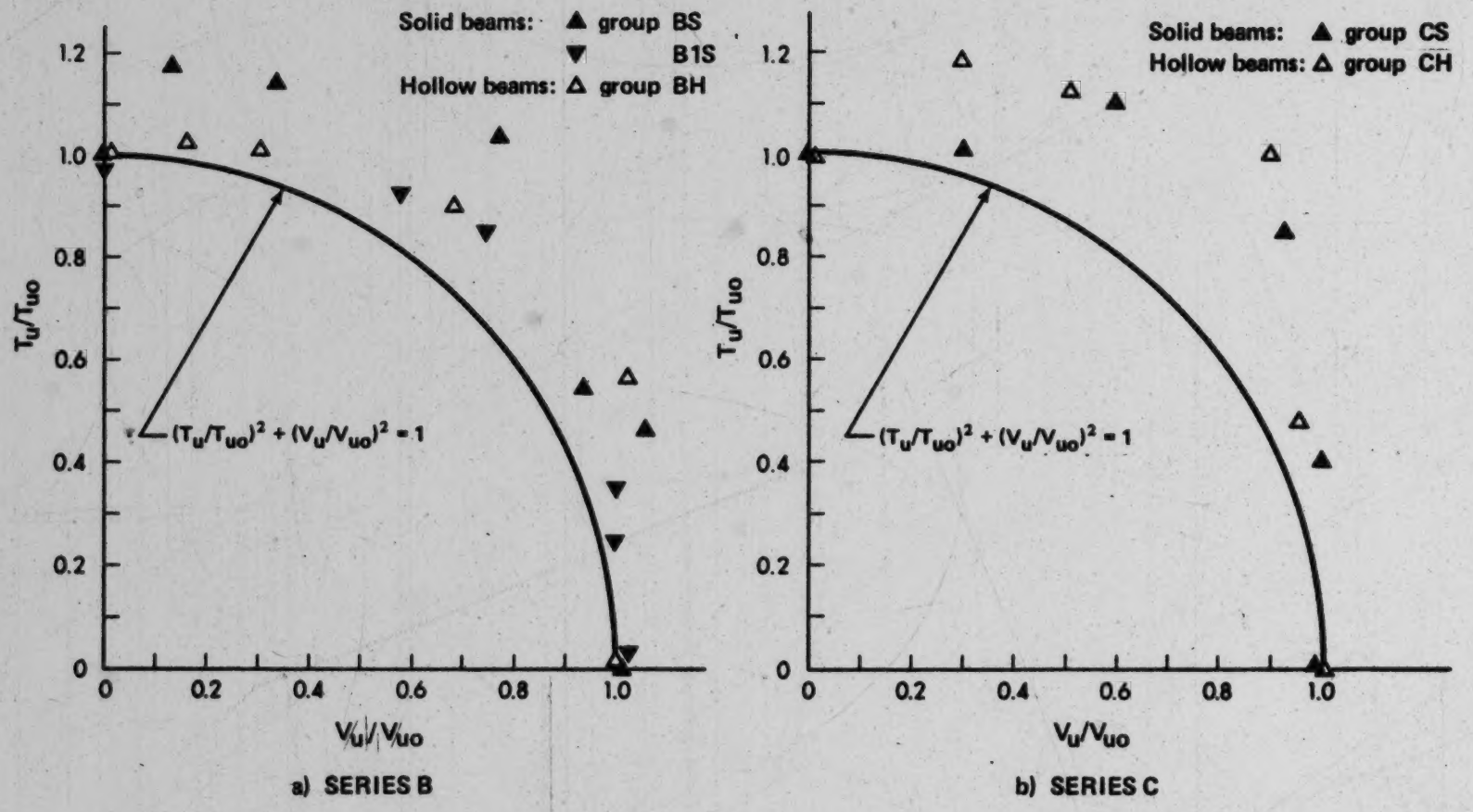

FIG. 4.9 INTERACTION BETWEEN TORSION AND SHEAR AT ULTIMATE, SERIES B AND C

been suggested by Henry and Zia[29], while they proposed the following relationship for the torque-shear interaction:

$$T_u/T_{uo} + V_u/V_{uo} = 1 \qquad (4.3)$$

It should, however, be noted that the value for pure shear V_{uo} in Equation 4.3 has been defined according to ACI[1].

Probably the most complete study dealing with interaction of torsion, bending and shear has been done by Mukherjee and Warwaruk[58]. Although somewhat complex, their equation for the curved interaction surface includes explicitly such effects as level of prestress, concrete strength and the eccentricity of prestressing force.

CHAPTER V

CRACKING STRENGTH, THEORIES AND COMPARISONS

5.1 Introduction

Although recent design approaches have been concerned mainly with the determination of ultimate loads that structures or structural members can sustain, in some cases the determination of the cracking load may be of equal importance. For example, structures exposed to atmospheric conditions that may cause corrosion must be designed to be crack free; serviceability rather than strength requirements will govern the design of water tanks or other similar containers. The necessity for a cracking analysis is even more pronounced in the area of prestressed concrete for two reasons: first, any corrosion is more dangerous here than in reinforced concrete, and second, the margin between the cracking load and the ultimate load could be very small. For example, in the case of beams that are lightly reinforced in a transverse direction, in which torsion dominates, the cracking and the ultimate load are almost identical.

While a cracking analysis is straightforward in the case of bending, the presence of torsion makes it quite complex, since the Navier hypothesis of a planar cross-section is not valid. It was not realized until the turn of this century that the shear stresses in a member subjected to torsion can not be solely interpreted by circular shear flow (Saint Venant torsion) but also may be caused by a change

in the axial stresses (warping torsion). If both of these effects are of the same order of magnitude, the interaction between Saint Venant torsion[43] and warping torsion[72] must be considered:

$$T = T_{sv} + T_w \tag{5.1}$$

where T_{sv} denotes Saint Venant torsion and T_w denotes warping torsion. A rigorous analysis of warping torsion is complex; fortunately, the effect of this component does not dominate the behavior of most reinforced or prestressed concrete members, particularly in the case of rectangular solid and hollow box sections (Figure 5.1). Therefore, its contribution will be neglected in this study.

In the following sections available theories are briefly reviewed and two procedures are proposed. One is based on the elasto-plastic behavior of concrete and includes the effects of principal stress interaction and recognizes stirrup contribution. In the other procedure rectangular cross-sections are treated as equivalent elliptical cross-sections and in the case of hollow box sections, as elliptical tubes. In all cases only combined loading (bending, torsion, shear, eccentric prestress) is considered; pure torsion, torsion and bending and concentric prestress alone constitute only special cases and can be easily deduced from the derived formulas. With the exception of Section 5.3.1 where principal stress interaction is taken into account, the tensile strength of concrete is taken as that obtained from the cylinder splitting test.

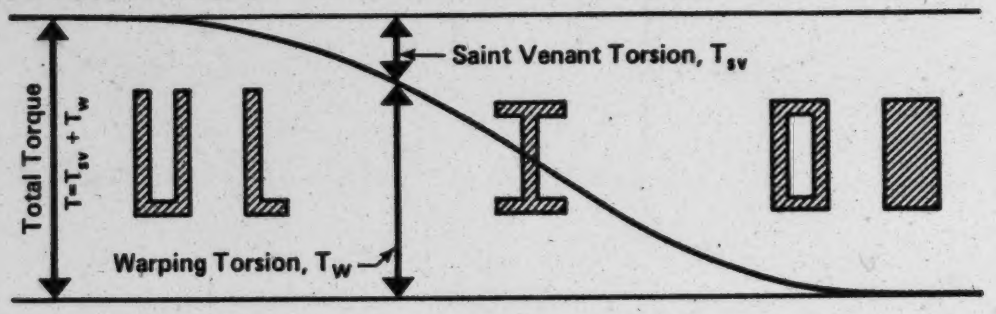

FIG. 5.1 INFLUENCE OF STRUCTURAL SHAPES ON THE RATIO OF WARPING TO SAINT VENANT TORSION (AFTER KOLLBRUNNER AND BASLER[43])

5.2 Available Theories

5.2.1 Elastic Analysis

According to this analysis concrete is assumed to be an ideally elastic material, therefore, the effects of combined loading can be superimposed. In the following discussion reference is made to the plane-stress transformation formulas[61] shown below:

$$\sigma_{max,\ min} = \sigma/2 \pm \sqrt{(\sigma/2)^2 + \tau^2} \qquad (5.2)$$

$$\tan(2\theta) = \tau/(\sigma/2) \qquad (5.3)$$

For a general case of loading a crack can start on either the vertical, bottom or top face; therefore all three locations must be examined, as discussed below, and the smallest value of torque represents cracking strength.

Bottom face: Assuming that the maximum principal stress at failure is equal to the cylinder splitting stress ($\sigma_{max} = f_{sp}$) and substituting the superimposed values of normal and shear stresses from Figure 5.2a into Equation 5.2, cracking torque can be obtained as follows:

$$f_{sp} = \frac{1}{2}\left[\frac{M}{S_x} - \sigma_o\left(1 + \frac{6e}{h}\right)\right] + \sqrt{\frac{1}{4}\left[\frac{M}{S_x} - \sigma_o\left(1 + \frac{6e}{h}\right)\right]^2 + \left[\frac{T}{\beta bh^2}\right]^2}$$

After transposing the first term from the right hand side to the left, squaring both sides and simplifying, this yields:

$$f_{sp}^2 - f_{sp}\left[\frac{M}{S_x} - \sigma_o\left(1 + \frac{6e}{h}\right)\right] = \left(\frac{T}{\beta bh^2}\right)^2$$

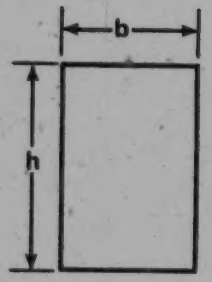

	NORMAL STRESS			SHEARING STRESS		
	side	bottom	top	side	bottom	top
TORSION				$T/(\alpha b^2 h)$	$T/(\beta bh^2)$	$T/(\beta bh^2)$
BENDING	0	M/S	$-M/S$			
SHEAR				$3V/(2bh)$	0	0
PRESTRESS	$\sigma_o = -P_{eff}/A$	$\sigma_o(1+6e/h)$	$\sigma_o(1-6e/h)$			

a) RECTANGULAR CROSS-SECTION

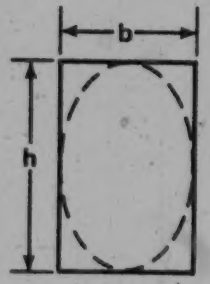

	NORMAL STRESS			SHEARING STRESS		
	side	bottom	top	side	bottom	top
TORSION				$16T/(\pi b^2 h)$	$16T/(\pi bh^2)$	$16T/(\pi bh^2)$
BENDING	0	M/S	$-M/S$			
SHEAR				$3V/(2bh)$	0	0
PRESTRESS	$\sigma_o = -P_{eff}/A$	$\sigma_o(1+6e/h)$	$\sigma_o(1-6e/h)$			

b) EQUIVALENT ELLIPTICAL CROSS-SECTION FOR TORSION

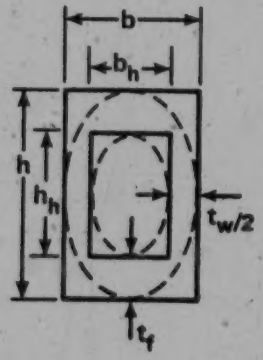

	NORMAL STRESS			SHEARING STRESS		
	side	bottom	top	side	bottom	top
TORSION				$16T/(\pi b^2 hc_h)$	$16T/(\pi bh^2 c_h)$	$16T/(\pi bh^2 c_h)$
BENDING	0	M/S_h	$-M/S_h$			
SHEAR				$VQ_h/(I_h t_w)$	0	0
PRESTRESS	$\sigma_h = -P_{eff}/A_h$	$\sigma_h(1+eA_h/S_h)$	$\sigma_h(1-eA_h/S_h)$			

c) EQUIVALENT ELLIPTICAL TUBE FOR TORSION

FIG. 5.2 STRESS COMPONENTS UNDER COMBINED LOADING

Substituting $M = T/\psi$ and solving the quadratic equation for positive root gives:

$$T^B_{cr} = bh^2 \beta f_{sp} \left[-\frac{3}{\psi}\beta + \sqrt{\left(\frac{3}{\psi}\beta\right)^2 + \frac{\sigma_o}{f_{sp}}\left(1 + \frac{6e}{h}\right) + 1} \right] \qquad (5.4)$$

where superscript B refers to bottom face. Having obtained T^B_{cr}, shear and bending at cracking can be found:

$$M_{cr} = T^B_{cr}/\psi \qquad \text{and} \qquad V^B_{cr} = 2\,T^B_{cr}/(b\delta)$$

When the resulting normal and shear stresses are substituted in Equation 5.3 the inclination of the initial crack with respect to longitudinal axis is:

$$\theta^B_{cr} = \frac{1}{2}\tan^{-1}\frac{2\,T^B_{cr}\,\psi}{\beta\left[6\,T^B_{cr} - \sigma_o bh^2\psi\left(1 + \frac{6e}{h}\right)\right]} \qquad (5.5)$$

Side face: No normal stresses due to bending exist in this case, however shear stresses due to flexural shear will be present, as indicated in Figure 5.2a. Substituting resulting stresses into Equation 5.2 gives:

$$f_{sp} = -\frac{\sigma_o}{2} + \sqrt{\left(\frac{\sigma_o}{2}\right)^2 + \left(\frac{T}{\alpha hb^2} + \frac{3V}{2bh}\right)^2}$$

or:

$$\left(f_{sp} + \frac{\sigma_o}{2}\right)^2 = \left(\frac{\sigma_o}{2}\right)^2 + \left(\frac{T}{\alpha hb^2} + \frac{3V}{2bh}\right)^2$$

Using $V = \frac{2T}{\delta b}$ and solving above equation for T, the following equation is obtained:

$$T_{cr}^{S} = \frac{hb^2 f_{sp} \sqrt{1 + \sigma_o/f_{sp}}}{(1/\alpha + 3/\delta)} \qquad (5.6)$$

where the superscript S refers to the side face. The inclination of the initial crack is obtained in a similar way to that described above:

$$\theta_{cr}^{S} = \frac{1}{2} \tan^{-1} \frac{2\sqrt{1 + \sigma_o/f_{sp}}}{\sigma_o/f_{sp}} \qquad (5.7)$$

Top face: A similar procedure, to that described for the bottom face applies here, except that the bending stresses are of opposite sign, as noted in Figure 5.2a. The following equations can be directly deduced from Equations 5.4 and 5.5:

$$T_{cr}^{T} = bh^2 \beta f_{sp} \left[\frac{3}{\psi} \beta + \sqrt{\left(\frac{3}{\psi} \beta\right)^2 + \frac{\sigma_o}{f_{sp}} \left(1 - \frac{6e}{h}\right) + 1} \right] \qquad (5.8)$$

$$\theta_{cr} = \frac{1}{2} \tan^{-1} \frac{2 T_{cr}^{T} \psi}{\beta [6 T_{cr}^{T} + \sigma_o bh^2 \psi (1 - \frac{6e}{h})]} \qquad (5.9)$$

Essentially the same formulas in implicit form for cracking analysis of prestressed concrete rectangular beams under combined loading, were first derived by Woodhead and McMullen[75], who used the Mohr's circle approach rather than stress transformation formulas. Torsional constants α and β for a rectangular cross-section are shown in Table 5.1. Theoretical predictions, using the above derived equations, for beams reported in this investigation are listed in Table 5.2 and a detailed discussion is given in Section 5.4.

A similar procedure can be used for any cross-section. Gen-

TABLE 5.1 TORSIONAL CONSTANTS FOR RECTANGULAR CROSS-SECTION

h/b	α	β	γ
1.0	0.208	0.208	0.141
1.2	0.219	0.196	0.166
1.4	0.227	0.184	0.187
1.6	0.234	0.174	0.208
1.8	0.240	0.169	0.217
2.0	0.246	0.155	0.229
2.5	0.258	0.135	0.249
3.0	0.267	0.120	0.264
5.0	0.292	0.079	0.291
10.0	0.312	0.042	0.312
∞	0.333	0	0.333

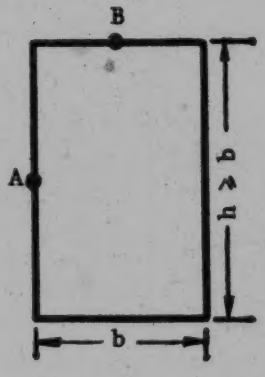

$$\tau_A = \frac{T}{\alpha b^2 h}$$

$$\tau_B = \frac{T}{\beta b h^2}$$

$$\phi = \frac{TL}{\gamma b^3 h G}$$

erally, for shear stress distribution due to torsion, the solution of the following differential equation is required:

$$\frac{\partial^2 F(x,y)}{\partial^2 x} + \frac{\partial^2 F(x,y)}{\partial^2 y} = -2 K_T \phi \qquad (5.10)$$

where $F(x,y)$ denotes the stress function in Cartesian coordinates, K_T the torsional rigidity, and ϕ the angle of twist per unit length. Unfortunately, this differential equation has been solved only for relatively few shapes; circle, rectangle (solid cross-section), ellipse, equilateral triangle and a segment of circle. For other shapes, numerical procedures in conjunction with a physical model, such as that from the membrane analogy, must be utilized. This analogy is credited to Prandtl[59] and is based on the similarity between the differential equations for torsion and a pressurized membrane over an opening having the same cross-sectional shape as the cross-section subjected to torsion. In this analogy torque is proportional to the volume under raised membrane and, at a given location shear stress is proportional to the slope of membrane.

5.2.2 Plastic Analysis

According to this theory concrete is assumed to be an ideally plastic material and, in the case of a rectangular cross-section shear stress is given by the following equation:

$$\tau_{max} = \frac{T}{k_p b^2 h} \qquad (5.11)$$

where:

$$k_p = \frac{1}{2}\left(1 - \frac{1}{3}\frac{b}{h}\right) \qquad (5.12)$$

Equation 5.11 has the same form as the one based on elastic theory, the only difference being in the magnitude of torsional coefficients. In Figure 5.3 these coefficients are plotted as a function of aspect ratios h/b. Comparison of values of τ_{max} would reveal that the plastic theory predicts approximately 50% higher values of τ_{max} (and therefore T_{cr}) over elastic theory. Nevertheless, a literature review shows that these two theories are equally used. To recapitulate, according to both theories torque can be expressed as:

$$T = f_t k b^2 h \tag{5.13}$$

where the torsional coefficient k is given by Equation 5.12 in the case of plastic theory or in Table 5.1 (denoted as α) in the case of elastic theory. Since concrete is neither an elastic or a plastic material it is not surprising that test results always fall between values predicted by the elastic and plastic theories. Tensile strength of concrete f_t used in Equation 5.13, is usually expressed as a function of compressive stress f'_c, as:

$$f_t = \text{coef } \sqrt{f'_c} \tag{5.14}$$

To fit experimental results, those researchers who used plastic theory have taken the coefficient in Equation 5.14 as low as 4 (Collins[11]) or 5 (Barton and Kirk[4]), whereas those who believed that the elastic behavior is more appropriate used, for the same coefficient, a value of 7.5 (Woodhead and McMullen[75]). The tensile strength of concrete is influenced by numerous factors including mix variables, size of speci-

men (strain gradient), type of loading (tension-compression interaction), etc., but is least dependent on the theory used. For the reasons mentioned above and because plastic theory represents an upper bound solution (which is not on the side of safety) it is not used herein for predicting cracking strength of beams subjected to combined loading.

5.2.3 Skew Bending Theory

Based on the hypothesis proposed by Lessig[51, 52], Hsu[31] derived the following equation for torsional strength of a rectangular longitudinally reinforced beam:

$$T = \frac{1}{3} bh^2 (0.85\ f_r) \tag{5.15}$$

Assuming that the factor $0.85\ f_r$ represents tensile strength under combined loading, Equation 5.15 can be directly compared with both the elastic and the plastic theories (Equation 5.13). Figure 5.3 shows that Hsu's solution is bounded by the two classical theories.

The same approach has been extended by Gangarao and Zia[24] to include torsion and bending. The general case of torsion, bending and shear in prestressed concrete rectangular beams has been presented by Henry and Zia[29]. For comparison, the final governing equations derived by Henry and Zia[29] are shown below:

Bending mode (crack starts at the bottom)

$$T_{cr} = \frac{bh^3}{3} \frac{f_{sp} + \frac{\sigma_o}{2}(1 + \frac{6e}{h})(1 - \cos 2\theta)}{\sin 2\theta + \frac{1}{\psi}(1 - \cos 2\theta)} \tag{5.16}$$

The value for θ corresponding to minimum cracking torque is

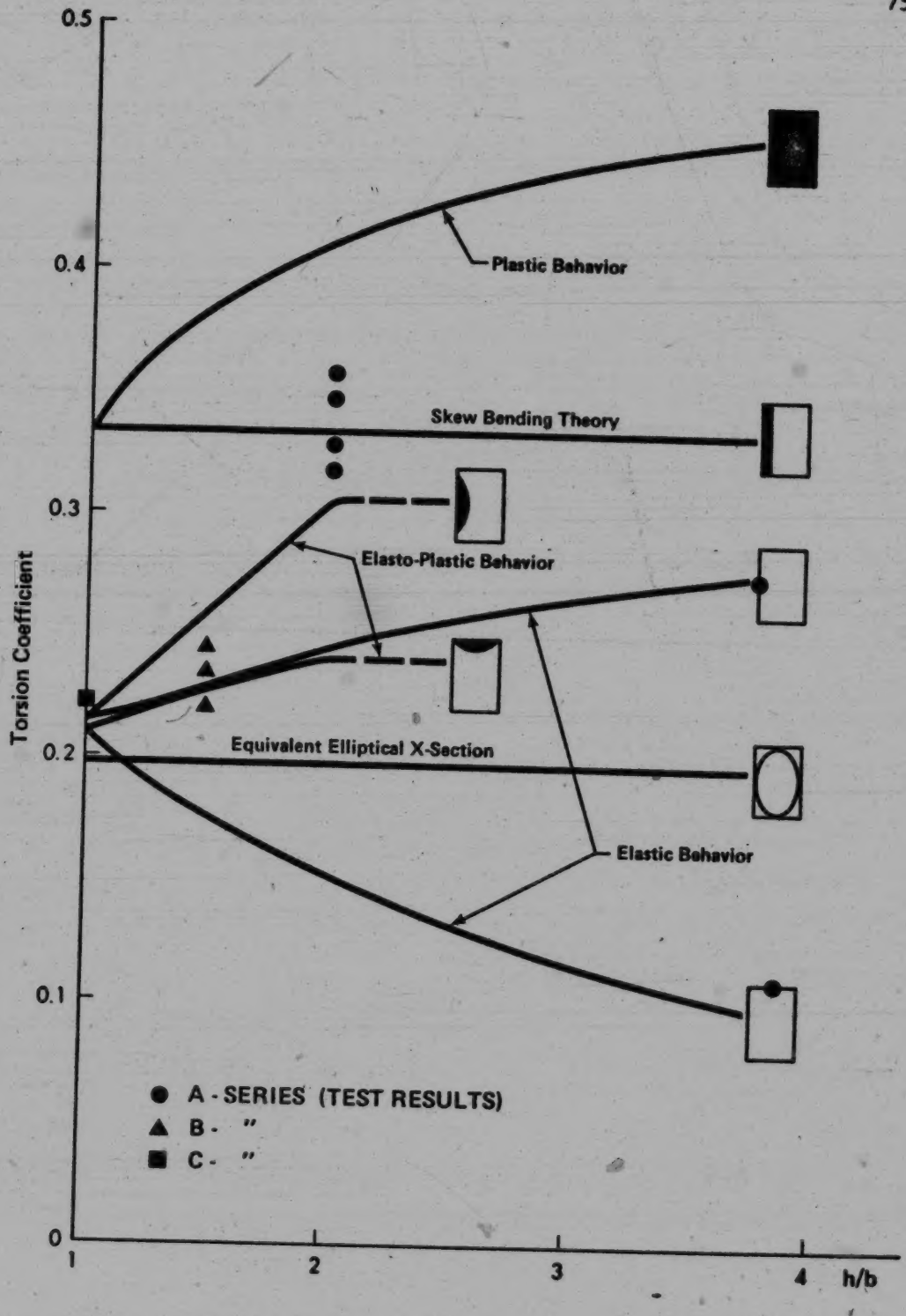

FIG. 5.3 COMPARISON OF TORSIONAL COEFFICIENT BY DIFFERENT THEORIES

found by differentiating Equation 5.16 with respect to θ and equating to zero, yielding:

$$\frac{\cos 2\theta + \frac{1}{\psi} \sin 2\theta}{1 - \cos 2\theta} = \frac{f_{sp} \left(1 + \frac{6e}{h}\right)}{2 f_{sp}} \qquad (5.17)$$

Crack inclination θ is then substituted back into Equation 5.16 and cracking torque is determined:

Torsion mode (crack starts at the side)

$$T_{cr} = \frac{f_t + \sigma_o \left[1 + \frac{6e}{h} (sgn)\right] \sin^2\theta}{\frac{3}{b^2 h} \sin 2\theta + \frac{3[1-(sgn)]}{2 b^2 h\delta} \sin 2\theta + \frac{12 z (sgn)}{b^2 h^2 \delta} \sin^2\theta} \qquad (5.18)$$

where sgn can take a value of +1 (crack starts at the bottom of front side) or 0 (crack starts at the center of front side), and z denotes the distance between the failure cross-section and the support in a simply supported beam. Inclination of the initial crack θ is given by the following transcendental equation:

$$\frac{\sigma_o \left[1 + \frac{6e}{h} (sgn)\right](1-\cos 2\theta) - 2 f_t \cos 2\theta}{\sin 2\theta} = \frac{f_t \frac{12 z (sgn)}{b^2 h^2 \delta}}{\frac{3}{b^2 h} + \frac{3[1-(sgn)]}{2 b^2 h\delta}} \qquad (5.19)$$

By solving Equations 5.18 and 5.19 for (sgn) = 1 and (sgn) = 0, and choosing the smaller of the two values the cracking torque is determined. For an aspect ratio of 1:2 good correlation between test results and skew bending theory has been reported in the literature, but for a cross-section that approaches a square, this theory over estimates cracking capacity significantly. Comparison of test results

in this investigation with skew bending theory also supports the above statement. This indicates that one of the fundamental assumptions on which this theory is based can be questioned: formation of a bending mechanism on an inclined plane, prior to cracking. Essentially, this implies that a crack will form across the whole tension face as soon as tensile strength is reached. On the contrary, experimental observations of beams subjected to combined loading clearly show (see photographs of crack patterns in the Appendix C) that cracks start at the center of either the bottom, top or side face and propagate towards the edges as loading is increased.

5.2.4 Statistical and Numerical Procedures

For the determination of factor k, shown in Equation 5.13, a statistical approach based on test data was first used at the University of West Virginia[10, 57]. Mukherjee and Kemp[57] proposed the equation for the torsional coefficient as:

$$k_s = 0.4124(1 - 0.2333\ b/h) \qquad (5.20)$$

and, subsequently, Chander, Kemp and Wilhelm[10] derived the following quadratic polynomial:

$$k_s = 0.4731(1 - 0.5924\ b/h + 0.2763\ b^2/h^2) \qquad (5.21)$$

It is interesting to note that both equations shown above result in values for torsional coefficient which are closer to the plastic solution for the entire range of practical aspect ratios. In both cases, a rather low value, $5\sqrt{f'_c}$, was used for the tensile

strength of concrete.

It has been mentioned in Section 5.2.1 that the governing differential equation for torsion cannot be solved for shapes having re-entrant corners such as T, L, I, H, or hollow box. Recourse is often made to numerical procedures such as finite difference or finite element methods in conjunction with physical models such as membrane analogy (elastic analysis) and sand heap analogy (plastic analysis). Wyss, Gerland and Mattock[76] employed a two dimensional finite element method in order to predict the cracking strength of I-girders. The finite difference technique has been used by Johnston and Zia[40] for hollow cross-sections. More recently Rao and Warwaruk[66] utilized three-dimensional hexadron finite elements in their analysis of pre-stressed I-girders under combined loading.

It should be mentioned that shear stresses due to torsion found by any of the above methods are superimposed with those caused by flexural shear, bending and prestress to yield the general state of stress to which a failure criteria is then applied.

In summary, it should be noted that the statistical analysis does not offer physical interpretation of the phenomenon. On the other hand, numerical approaches require solution of a large number of simultaneous equations and, therefore, cannot be conveniently used in everyday design practice.

5.3 Proposed Theories

5.3.1 Elasto-Plastic Analysis

5.3.1.1 General Remarks and Assumptions: In this section an attempt is made to include partial plastification of a cross-section subjected to torsion. Although this effect has been recognized in the case of bending, it also needs to be recognized in the presence of torsion and shear. However, if flexural shear does not govern cracking strength it is reasonable to assume that the shear stresses are distributed elastically. Similarly the effect of partial plastification in bending can be included indirectly using modulus of rupture rather than the direct tensile strength of concrete.

It was pointed out in previous sections that experimental results do not correspond to purely elastic or purely plastic behavior but always fall between these two solutions. This implies occurrence of some plastic regions. Figure 5.4 shows shearing stress distribution according to the elastic, the plastic and, the elasto-plastic solutions. According to both classical theories and the statistical analysis cracking torque for prestressed concrete beams can be expressed in the following form:

$$T_{cr} = k\, b^2 h\, f_t \sqrt{1 + \sigma_o / f_t} \qquad (5.22)$$

where the coefficient k depends on the analysis used and the cross-sectional aspect ratio, h/b. The term under the square root in Equation 5.22 denotes effect of prestress. In order to study the

degree of plastification, Equation 5.22 has been solved for k and test results of this parameter are plotted in Figure 5.3. It can be observed that the test results are close to the plastic solution if the aspect ratio, h/b, is equal to 2; those beams having aspect ratio of 1.5 and 1 are closer to the elastic solution. This may appear contrary to the expected behavior since in the case of a square cross-section the maximum stress is attained simultaneously at the centers of all beam faces, whereas in an elongated cross-section "yielding" will start first at the centers of longer sides. In order to explain this phenomenon, one can make use of the membrane analogy. Figure 5.5 shows a schematic view of membranes stretched over a square cross-section (Figure 5.5a) and over a slender rectangular cross-section (Figure 5.5b). At this point it should be recalled that shear stresses are proportional to the slope of a membrane at a given location. Proceeding from the middle to the corners along the edge, it can be visualized that the slope of the "dome" (Figure 5.5a) decreases at a faster rate than the slope of the "cylindrical shell" (Figure 5.5b) since the slope in the case of the cylindrical shell is nearly constant along this edge. This indicates that in the case of a rectangular cross-section yielding will be attained on a relatively longer length and consequently, this cross-section will be relatively more plastified at cracking than a square cross-section.

A theoretical analysis of a beam cross-section subjected to torsion in a transition between elastic to plastic state is extremely

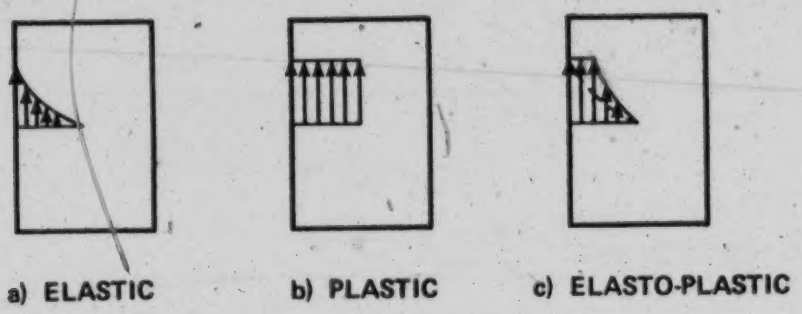

FIG. 5.4 SHEARING STRESS DISTRIBUTION IN A RECTANGULAR CROSS-SECTION SUBJECTED TO TORQUE

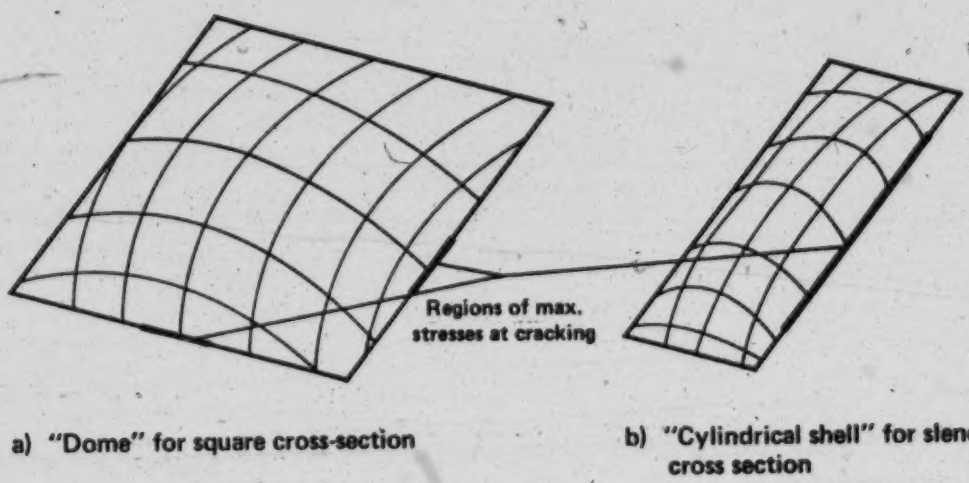

FIG. 5.5 MEMBRANE ANALOGY FOR SQUARE AND SLENDER CROSS SECTION

difficult for all cross-sections except the circular cross-section where the boundaries between the elastic and plastic regions remain always circular. On the basis of experimental data shown in Figure 5.3, the following equations for torsional coefficients α and β are proposed to account for the effects of partial plastification:

$$\alpha_{ep} = 0.215 + 0.09\ (h/b - 1) \tag{5.23}$$

$$\beta_{ep} = 0.215 + 0.03\ (h/b - 1) \tag{5.24}$$

where α_{ep} is used for the determination of shear stresses on the longer side and β_{ep} on the shorter side of the cross-section as noted on the sketch in Table 5.1. Plotted points corresponding to elasto-plastic behavior in Figure 5.3 are calculated using measured strengths for beams subjected to pure torsion. Since Equations 5.23 and 5.24 are based on limited test data they should be applied only within the following limits of aspect ratios:

$$1 \leq h/b \leq 2 \tag{5.25}$$

It should be noted that most of the practical aspect ratios for a rectangular cross-section do fall within above limits, being close to 1 in the case of predominant torsion and close to 2 only if bending and shear are present.

5.3.1.2 Biaxial Stress Failure Criteria: A considerable amount of discussion is available in the literature as to which tensile strength should govern the cracking of a beam subjected to combined loading. Hsu[31] suggested the use of a reduced modulus of rupture, while Johnston and Zia[40] used splitting strength on the basis of simi-

larity between states of stress in a cylinder under splitting test and a beam subjected to combined loading. However, most of the investigators (Woodhead and McMullen[75], Mukherjee and Kemp[57], Barton and Kirk[4], Rao and Warwaruk[65]) have expressed tensile strength as a function of cylinder compressive strength as shown in Equation 5.14. None of these approaches include the effect of loading ratios since in the case of predominant bending the use of the modulus of rupture would be more appropriate, whereas in the case of combined loading or torsion alone, interaction between principal stresses must be taken into account as no unique tensile stress can be used for the entire range of loading ratios.

Kupfer, Hilsdorf and Rusch[44] observed, in their experimental investigation, that the presence of compression in an orthogonal direction would reduce tensile strength and vice versa. Figure 5.6 shows their experimental results in the form of nondimensionalized (with f'_c) interaction diagrams, where σ_{max} and σ_{min} denote, respectively, tensile and compressive stresses. Since the proposed analysis uses a continuous biaxial interaction curve, the following interaction equation based on the experimental data by Kupfer, Hilsdorf and Rusch[44], is suggested:

$$(\sigma_{max}/f'_c)^2 = m(1 - \sigma_{min}/f'_c) \qquad (5.26)$$

Equation 5.26 represents a family of second-degree parabolas since parameter m is not yet defined. As mentioned earlier, one of the characteristics of the splitting test is that concrete is under a

biaxial state of stress with compression being approximately 0.25 f'_c at failure, or:

$$\text{when, } \sigma_{max} = f_{sp} \qquad \text{then, } \sigma_{min} = 0.25\ f'_c$$

Substituting these boundary conditions into Equation 5.26, parameter m can now be determined:

$$m = \frac{(f_{sp}/f'_c)^2}{1 - 0.25\ f'_c/f'_c}$$

or:

$$m = \frac{4}{3}\left(\frac{f_{sp}}{f'_c}\right)^2 \tag{5.27}$$

Substituting Equation 5.27 into Equation 5.26 yields (Figure 5.6):

$$\left(\frac{\sigma_{max}}{f'_c}\right)^2 = \frac{4}{3}\left(\frac{f_{sp}}{f'_c}\right)^2 \left(1 - \frac{\sigma_{min}}{f'_c}\right) \tag{5.28}$$

If f_{sp} is replaced with σ_{max} in Equations 5.4, 5.6 and 5.8, and torsional constants α_{ep} and β_{ep}, determined in the preceding section, substituted for elastic constants α and β, the following equations for cracking torques for prestressed concrete beams under combined loading are obtained:

$$T^B_{cr} = bh^2\beta_{ep}\sigma_{max}\left[-\frac{3}{\psi}\beta_{ep} + \sqrt{\left(\frac{3}{\psi}\beta_{ep}\right)^2 + \frac{\sigma_o}{\sigma_{max}}\left(1 + \frac{6e}{h}\right) + 1}\right] \tag{5.29}$$

$$T^S_{cr} = \frac{hb^2\sigma_{max}\sqrt{1 + \frac{\sigma_o}{\sigma_{max}}}}{\left(\frac{1}{\alpha_{ep}} + \frac{3}{\delta}\right)} \tag{5.30}$$

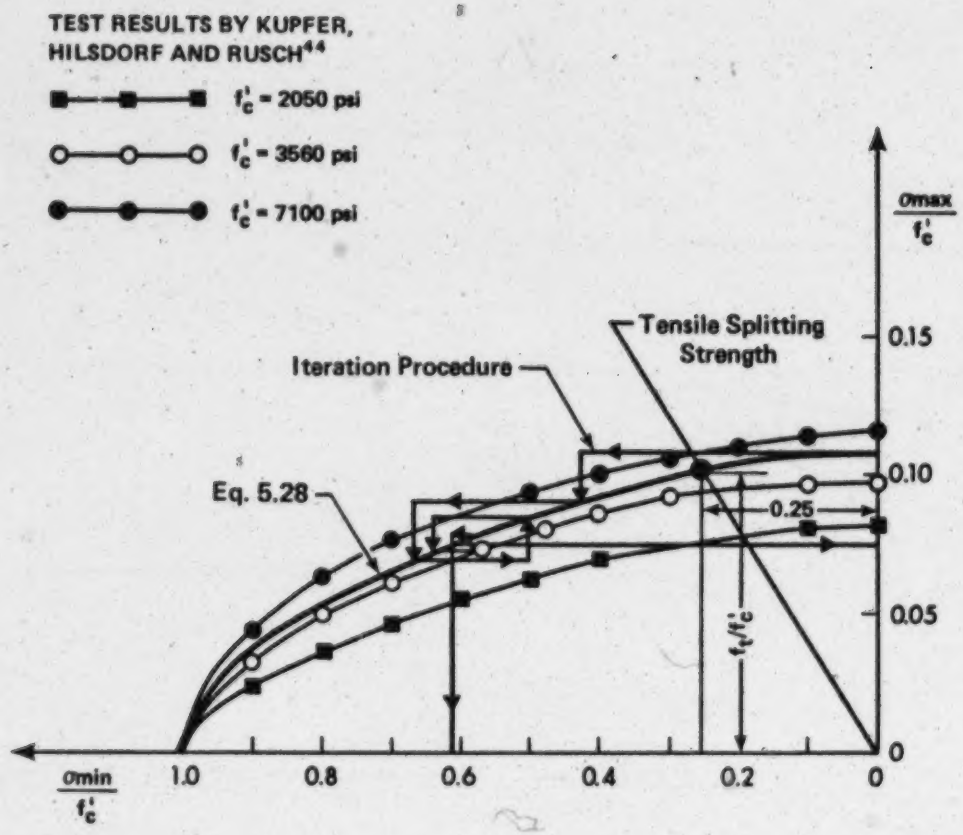

FIG. 5.6 STRENGTH OF CONCRETE UNDER COMBINED TENSION AND COMPRESSION

$$T_{cr}^{T} = bh^2 \beta_{ep} \sigma_{max} \left[\frac{3}{\psi} \beta_{ep} + \sqrt{\left(\frac{3}{\psi} \beta_{ep}\right)^2 + \frac{\sigma_o}{\sigma_{max}} \left(1 - \frac{6e}{h}\right) + 1} \right] \qquad (5.31)$$

Essentially, Equations 5.29, 5.30 and 5.31 are deduced from those derived in Section 5.2.1 dealing with elastic analysis. However, they include the effect of partial plastification of cross-section since torsional constants are determined according to Equations 5.23 and 5.24. More important they include the effects of principal stress interaction at cracking. Since tensile stress σ_{max}, is unknown in these equations, an iterative procedure as outline below, is used to determine σ_{max}:

1. Assume no compression stress exists ($\sigma_{min} = 0$) and calculate σ_{max} from Equation 5.28.
2. Calculate cracking capacities according to Equations 5.29, 5.30 and 5.31.
3. With the known cracking torque and loading ratios (ψ and δ) determine bending moment and flexural shear at cracking.
4. Find stress components due to torsion, bending, shear and prestress and calculate principal stresses according to Equation 5.2.
5. Substitute principal stresses from 4 into Equation 5.28. Generally, this equation will not be satisfied after the first iteration because two principal stresses exist (from step 4), whereas in the beginning (step 1) σ_{min} was assumed as zero.
6. Reduce σ_{max} by an increment, go to step 2 and repeat the procedure until Equation 5.28 is satisfied to the desired level of accuracy.

The iterative procedure, outlined in the above steps, is graphically illustrated in Figure 5.6. It is noted that the process of determination of the state of stress which satisfies Equation 5.26, converges rapidly.

Results of this analysis are presented in Table 5.2 in columns 8 through 14. It is interesting to compare the actual tensile stresses (column 13) at cracking with the tensile stresses obtained from the splitting test, presented in Chapter 4. This procedure was computerized and only 10 to 15 iterations were necessary to obtain the desired level of accuracy.

5.3.1.3 Contribution of Stirrups: Although some investigators[40] have noted that the contribution of stirrups to the cracking strength may be significant, no attempt has been made so far to include this effect. If an element is considered on the side of the beam at the level of neutral axis, according to rigorous theory, no strains in the vertical direction should be recorded under bending torsion and shear. However, experimental data (see strain data in Appendix B) does not support the above statement, implying that stress redistribution occurs prior to cracking. Figure 5.7 shows that stirrup strains are negligible only if the torque is less than about 50% of T_{cr}. On the basis of experimental data shown in Figure 5.7, it is assumed that the following relationship exists between concrete tensile strain in the inclined plane and strains in the vertical stirrups:

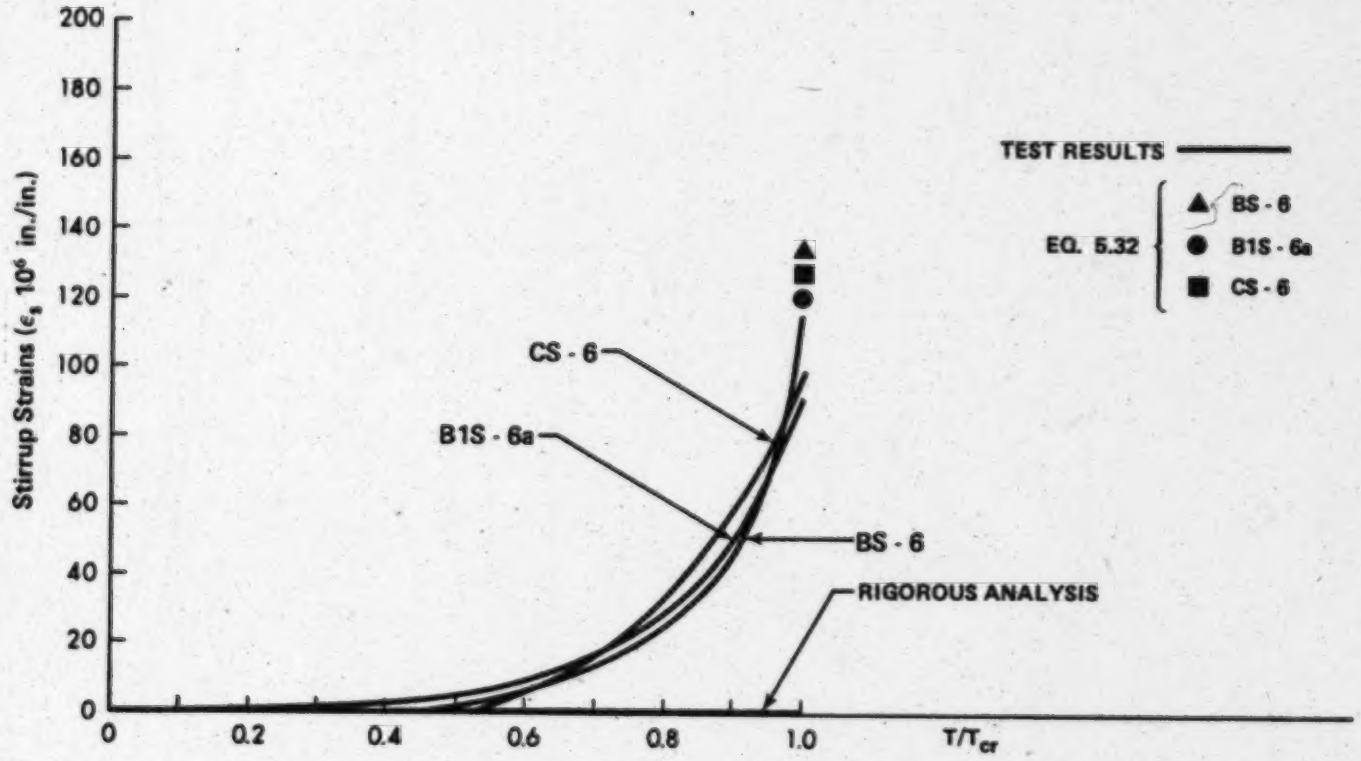

FIG. 5.7 STIRRUP STRAINS BEFORE CRACKING

$$\varepsilon_v = \varepsilon_t \cos\theta \tag{5.32}$$

where ε_v denotes strain in vertical leg of stirrup and ε_t tensile strain of concrete. Using an average value of 0.00015 (Johnston[41]) for ε_t, values of strains in vertical legs ε_v are found from Equation 5.32 and then plotted in Figure 5.7. Measured strains in the stirrups for three beams subjected to torsion are also shown in Figure 5.7 and a comparison can be made between these strains and those given by Equation 5.32. In order to determine contribution of stirrups to the cracking strength, the number of stirrups intersected by a potential crack has to be found. From the beam geometry following relationship is established:

$$n_v = \frac{h'}{s \tan\theta} \tag{5.32a}$$

$$n_h = \frac{b'}{s \tan\theta} \tag{5.32b}$$

where n_v and n_h denote, respectively, number of stirrups intersected by a potential crack on vertical and horizontal side of a beam. Taking moments with respect to the longitudinal axis of a beam, the torque due to presence of stirrups is:

$$T_{cr,st} = \sum_{i=1}^{n_v} E_{st}\, \varepsilon_{v,i} A_{st} b' + \sum_{i=1}^{n_h} E_{st}\, \varepsilon_{h,i} A_{st} h' \tag{5.33}$$

where $\varepsilon_{v,i}$ and $\varepsilon_{h,i}$ are, respectively, strain in vertical and horizontal i-th stirrup leg intersected by a potential crack. Assuming that the strain distribution is parabolic along the potential crack

(Figure 5.8), which is in conformance with the elastic theory, Equation 5.33 can be written as:

$$T_{cr,st} = \frac{2}{3} E_{st} A_{st} (n_v \varepsilon_v b' + n_h \varepsilon_h h') \qquad (5.34)$$

where ε_v and ε_h now denote the maximum stirrup strains found at the mid height and mid width of a stirrup, respectively. With the exception of a square cross-section subjected to pure torsion, ε_v and ε_h in Equation 5.34 will not be equal. In close accordance with the elastic theory the following relationship is assumed between ε_h and ε_v:

$$\varepsilon_h/\varepsilon_v = b'/h' \qquad (5.35)$$

If Equations 5.32a, 5.32b and 5.35 are substituted in Equation 5.34, the contribution of stirrups to the cracking torque is obtained as:

$$T_{cr,st} = \frac{2}{3} \frac{E_{st} A_{st}}{s \tan \theta} \varepsilon_v (h' + b') \qquad (5.36)$$

Using stirrup strain ε_v given by Equation 5.32 together with the following simplifications:

$$b' = 0.8\, b$$

$$h' = 0.8\, h$$

the resulting equation is:

$$T_{cr,st} = 0.43\, E_{st} A_{st} \varepsilon_t b(b + h) \cos \theta / \tan \theta \qquad (5.37)$$

If a crack starts on the shorter side, an identical equation can be

derived providing that stirrup strain on the uncracked, longer side is taken as the stirrup strain on the shorter side multiplied by b'/h'. The total cracking torque can now be taken as the sum of the torques carried by the concrete and the stirrups:

$$T_{cr,tot} = T_{cr,concr} + T_{cr,st} \qquad (5.38)$$

where the first term on the right hand side of Equation 5.38 is given by Equations 5.29, 5.30 or 5.31 and the second by Equation 5.37.

Columns 8 and 9 in Table 5.2, respectively list the values for cracking torque as predicted by this theory and test to theory ratios. Columns 10 through 14 show some additional data obtained in this analysis; contribution of stirrups to the cracking strength, angle of inclination of tensile crack, crack location and the values of the principal stresses at cracking. A detailed discussion is given in Section 5.4.

5.3.2 Analysis Based on an Equivalent Elliptical Cross-Section

5.3.2.1 General: From the proceeding sections it is observed that the formulas based on elastic theory are simpler in form than those based on skew bending theory. However, in order to use the elastic theory torsional constants α and β must be known. Evaluation of these coefficients even for a rectangular cross-section represents voluminous work since the solution involves infinite series of hyperbolic functions. In the usual strength of materials approach

these values are tabulated for particular aspect ratios and interpolation is used for non-tabulated ratios. For a hollow box section no exact solution exists. A few researchers have suggested a "shear flow" approach which makes use of a uniform shear stress distribution across the wall section, which in turn implies complete plastification of a cross-section with uniform wall thicknesses, or plastification of the thinnest wall in the case of cross-section with non-equal wall thicknesses. Since reinforced and prestressed concrete members usually have geometric proportions in excess of those to which thin-wall theory applies, assumption of a shear flow state for them may not be justified.

The proposed elasto-plastic solution for cracking strength under combined loading includes nonelastic behavior of concrete and interaction of principal stresses at cracking, but because it is an iterative procedure it may be more of academic than practical importance.

For reasons mentioned above it is proposed that the solid rectangular beam cross-section be replaced by an equivalent elliptical section as shown in Figure 5.9a, and the hollow box section by an elliptical tube shown in Figure 5.9b. Shear stress distribution due to torsion can now be evaluated using the elastic theory and does not require the use of torsional constants α and β. Referring to Figure 5.9a and according to theory of elasticity, shear stresses for a solid elliptical cross-section are given as:

$$\tau_A = \frac{16T}{\pi b^2 h} \tag{5.39}$$

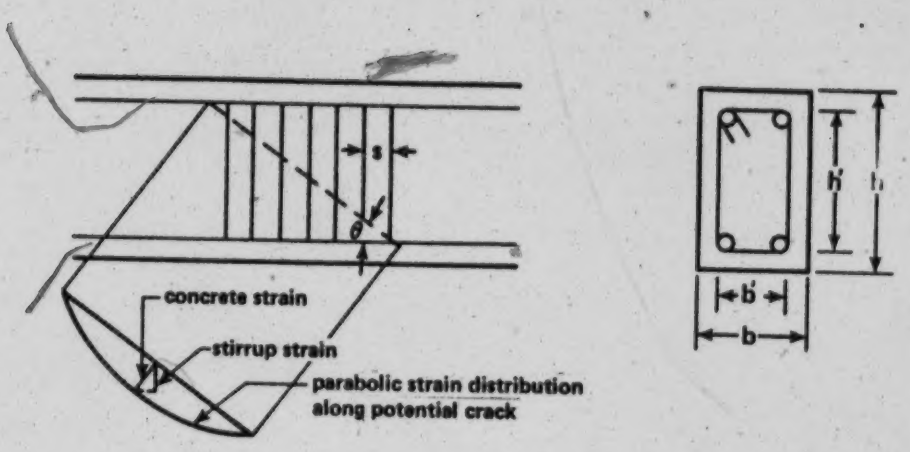

FIG. 5.8 CRACKING STRENGTH – CONTRIBUTION OF STIRRUPS

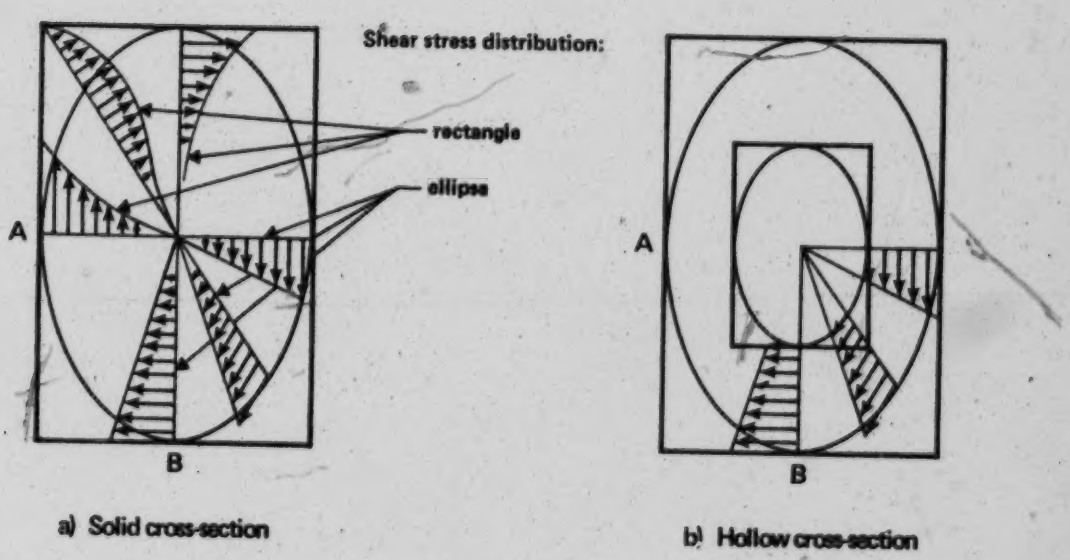

a) Solid cross-section

b) Hollow cross-section

FIG. 5.9 EQUIVALENT ELLIPTICAL CROSS SECTIONS FOR SOLID AND HOLLOW RECTANGLE

$$\tau_B = \frac{16T}{\pi bh^2} \qquad (5.39a)$$

or for elliptical tube:

$$\tau_A = \frac{16T}{\pi b^2 h c_h} \qquad (5.40)$$

$$\tau_B = \frac{16T}{\pi b h^2 c_h} \qquad (5.40a)$$

where:

$$c_h = 1-\left[\frac{b_h}{b}\right]^4 \quad \text{or} \quad c_h = 1-\left[\frac{h_h}{h}\right]^4 \qquad (5.41)$$

whichever is greater. From Figure 5.9 it can be observed that the contribution of the corners in the case of the rectangular cross-section is not significant and an approximation of it with an ellipse is on the conservative side.

In the following sections equations are derived for a hollow cross-section and then equations are deduced for a solid cross-section. It should be noted that the shear stress distribution due to flexural shear, and normal stresses due to bending moment, for both the solid and hollow cross-sections, are based on the original cross-section and not on the elliptical cross-sections.

5.3.2.2 Hollow Cross-Section: First, the shear and normal stresses are found at the centers of the bottom, top and vertical sides.

Shear stresses due to torsion:

side face $\tau = \frac{16T}{\pi b^2 h c_h}$

bottom or top face $\tau = \frac{16T}{\pi b h^2 c_h}$

Shear stresses due to flexural shear:

side face $\tau = \frac{VQ_h}{I_h t_w}$

bottom or top face $\tau = 0$

Normal stresses due to bending:

side face $\sigma = 0$

bottom face $\sigma = \frac{M}{S_h}$

top face $\sigma = -\frac{M}{S_h}$

Normal stresses due to prestress:

side face $\sigma = \frac{P_{eff}}{A_h}$

top face $\sigma = -\frac{P_{eff}}{A_h}(1 - \frac{A_h e}{S_h})$

bottom face $\sigma = -\frac{P_{eff}}{A_h}(1 + \frac{A_h e}{S_h})$

Next, these stresses are superimposed and the resulting normal and shear stresses are substituted in Equation 5.2. If the bending moment and shear force are expressed in terms of torques, the following equations for cracking torques are obtained:

Bottom face

$$T_{cr} = \frac{3}{8}\pi \frac{c_h}{r_h} S_h f_{sp}\left[-\frac{3\pi}{16\psi}\frac{c_h}{r_h} + \sqrt{(\frac{3\pi}{16\psi}\frac{c_h}{r_h})^2 + \frac{\sigma_h}{f_{sp}}(1 + \frac{eA_h}{S_h}) + 1}\right] \quad (5.42)$$

Side face

$$T_{cr} = \frac{f_{sp}\sqrt{1 + \frac{\sigma_h}{f_{sp}}}}{\frac{16}{\pi h b^2 c_h} + \frac{2Q_h}{bI_h t_w \delta}} \qquad (5.43)$$

Top face

$$T_{cr} = \frac{3}{8}\pi \frac{c_h}{r_h} S_h f_{sp}\left[\frac{3\pi}{16\psi}\frac{c_h}{r_h} + \sqrt{\left(\frac{3\pi}{16\psi}\frac{c_h}{r_h}\right)^2 + \frac{\sigma_h}{f_{sp}}\left(1 - \frac{eA_h}{S_h}\right) + 1}\right] \qquad (5.44)$$

where:

$$r_h = 1 - \left[\frac{b_h}{b}\right]\left[\frac{h_h}{h}\right]^3 \qquad (5.45)$$

and:

$$\sigma_h = \frac{P_{eff}}{A_h}$$

The smallest of three torques found by Equations 5.42, 5.43 and 5.44 governs the cracking strength of an eccentrically prestressed beam subjected to combined loading. Theoretical predictions according to this analysis and comparisons between test and theoretical values are given in Table 5.4. In Section 5.4 a detailed discussion is presented.

5.3.2.3 Solid Cross-Section: Equations derived in the preceding section can be easily transformed for solid cross-section if appropriate geometric constants (A, S, I, etc.) are taken for a solid, instead of a hollow cross-section. According to Equations 5.41 and 5.45 values for c_h and r_h for solid cross-section become equal to 1 and three equations for cracking torque , corresponding to first crack

at the bottom, side and top face of a beam, can be directly deduced from Equations 5.42, 5.43 and 5.44 as shown below:

Bottom face

$$T_{cr} = \frac{3}{8}\pi S f_{sp}\left[-\frac{3\pi}{16\psi} + \sqrt{\left(\frac{3\pi}{16\psi}\right)^2 + \frac{\sigma_o}{f_{sp}}\left(1 + \frac{6e}{h}\right) + 1}\right] \qquad (5.46)$$

Side face

$$T_{cr} = \frac{b^2 h f_{sp}}{16/\pi + 3/\delta}\sqrt{1 + \sigma_o/f_{sp}} \qquad (5.47)$$

Top face

$$T_{cr} = \frac{3}{8}\pi S f_{sp}\left[\frac{3\pi}{16\psi} + \sqrt{\left(\frac{3\pi}{16\psi}\right)^2 + \frac{\sigma_o}{f_{sp}}\left(1 - \frac{6e}{h}\right) + 1}\right] \qquad (5.48)$$

The smallest torque governs cracking strength of a beam. Predicted values according to this analysis are listed in Table 5.2. A discussion of these predictions is presented in the next section.

5.4 Comparative Study

Cracking torques for solid cross-sections as predicted by four different theories, namely skew bending theory, elastic analysis, elasto-plastic analysis and the procedure based on equivalent elliptical cross-sections are presented in Table 5.2. Average values of the test/theory ratios for each of three series of beams, according to each of the above theories are shown in Table 5.3. For rectangular hollow cross-sections the equivalent elliptical tube has been utilized

TABLE 5.2 CRACKING TORQUES FOR SOLID CROSS-SECTIONS BY DIFFERENT THEORIES

Beam		T_{test}	Skew bending theory		Elastic behavior, rectangular cross-section		Elasto-Plastic Behavior							Equivalent elliptical cross-section	
									Supplemental Information						
Group 6	No.	(in.kips)	T_{sb} (in.kips)	$\frac{T_{test}}{T_{sb}}$	T_e (in.kips)	$\frac{T_{test}}{T_e}$	T_{ep}† (in.kips)	$\frac{T_{test}}{T_{ep}}$	$T_{stirrup}$ (in.kips)	θ_{cr} (deg)	Crack Location	Principal stresses at cracking (psi)		T_{ee} (in.kips)	$\frac{T_{test}}{T_{ee}}$
												tension	compression		
1	2	3	4	5	6	7	8	9	10	11	12	13	14	15	16
AA (6" x 12")	2	55.9	38.8	1.441	36.5	1.532	40.1	1.394	0.3	71.7	B*	568	62	37.5	1.491
	3	99.0	75.9	1.304	59.6	1.661	74.8	1.323	1.5	50.8	B	424	282	65.7	1.507
	4	111.4	112.8	0.988	85.3	1.306	107.5	1.036	6.1	23.6	S	337	1760	71.8	1.552
	5	126.0	117.9	1.069	94.9	1.328	114.6	1.099	5.9	24.7	S	380	1790	75.8	1.662
	6	129.6	110.2	1.176	87.8	1.476	108.3	1.197	6.1	23.8	S	342	1760	70.1	1.648
	7	133.0	124.0	1.073	99.2	1.341	122.1	1.089	5.5	25.7	S	425	1841	79.2	1.679
AB (6" x 12")	2	33.4	25.3	1.320	24.7	1.352	26.3	1.270	0.1	78.5	B	611	25	25.0	1.336
	3	65.0	57.7	1.130	50.9	1.277	58.7	1.107	0.6	63.6	B	553	136	53.7	1.210
	4	117.0	118.8	0.985	95.0	1.232	115.3	1.015	5.4	26.1	S	447	1864	76.9	1.521
	5	104.0	119.7	0.869	91.2	1.140	112.2	0.927	5.7	25.1	S	399	1816	73.4	1.417
	6	85.8	123.0	0.698	92.9	0.924	113.4	0.757	5.7	24.8	S	386	1808	74.5	1.152

* B - bottom, S - side, T - top.

† T_{ep} includes stirrup contribution (column 10)

TABLE 5.2 (Cont'd) CRACKING TORQUES FOR SOLID CROSS-SECTIONS BY DIFFERENT THEORIES

Beam		T_{test}	Skew bending theory		Elastic behavior, rectangular cross-section		Elasto-Plastic Behavior							Equivalent elliptical cross-section	
									Supplemental Information						
Group	No.	(in.kips)	T_{sb} (in.kips)	$\frac{T_{test}}{T_{sb}}$	T_e (in.kips)	$\frac{T_{test}}{T_e}$	T_{ep} (in.kips)	$\frac{T_{test}}{T_{ep}}$	$T_{stirrup}$ (in.kips)	θ_{cr} (deg)	Crack Location	Principal stresses at cracking (psi)		T_{ee} (in.kips)	$\frac{T_{test}}{T_{ee}}$
												tension	compression		
1	2	3	4	5	6	7	8	9	10	11	12	13	14	15	16
AC (6" x 12")	2	38.6	39.7	0.972	37.4	1.032	40.8	0.946	0.0**	72.7	B*	620	60	38.5	1.003
	3	108.0	85.3	1.266	69.1	1.563	83.8	1.289		56.4	B	595	263	75.3	1.434
	4	129.6	120.9	1.072	90.6	1.430	115.4	1.123		25.4	S	416	1842	77.1	1.681
	5	142.2	127.8	1.113	99.0	1.436	118.0	1.205		25.9	S	435	1843	79.0	1.800
	6	129.6	129.9	0.998	104.1	1.245	123.4	1.050		26.5	S	467	1878	83.1	1.560
	7	106.3	139.5	0.782	107.9	0.985	126.6	0.840		26.8	S	485	1902	86.2	1.233
AD (6" x 12")	2	22.3	23.2	0.961	22.7	0.982	24.1	0.925		79.4	B	606	21	23.0	0.970
	3	108.0	72.4	1.492	60.5	1.785	71.7	1.506		58.1	B	544	211	65.2	1.656
	4	117.9	115.0	1.025	93.0	1.268	110.5	1.067		26.1	S	450	1872	75.3	1.566
	5	117.8	119.1	0.989	91.8	1.283	107.8	1.093		25.2	S	405	1834	73.9	1.594
	6	113.0	135.0	0.837	100.9	1.120	119.6	0.945		26.2	S	457	1887	80.8	1.399

* B - bottom, S - side, T - top.

** Beams of AC and AD groups are without stirrups

TABLE 5.2 (Cont'd) CRACKING TORQUES FOR SOLID CROSS-SECTIONS BY DIFFERENT THEORIES

Beam		T_{test}	Skew bending theory		Elastic behavior, rectangular cross-section		Elastic-Plastic Behavior							Equivalent elliptical cross-section	
									Supplemental Information						
Group	No.	(in.kips)	T_{sb} (in.kips)	$\frac{T_{test}}{T_{sb}}$	T_e (in.kips)	$\frac{T_{test}}{T_e}$	T_{ep}† (in.kips)	$\frac{T_{test}}{T_{ep}}$	$T_{stirrup}$ (in.kips)	θ_{cr} (deg)	Crack Location	Principal stresses at cracking (psi) tension	Principal stresses at cracking (psi) compression	T_{ee} (in.kips)	$\frac{T_{test}}{T_{ee}}$
1	2	3	4	5	6	7	8	9	10	11	12	13	14	15	16
AE (6" x 12")	2	67.5	60.7	1.112	55.0	1.227	61.5	1.098	0.8	60.7	B*	512	161	57.5	1.174
	3	99.0	122.2	0.810	89.7	1.104	110.9	0.893	6.0	24.1	S	355	1783	71.9	1.377
	4	121.5	152.8	0.795	100.1	1.214	123.7	0.982	5.4	25.9	S	436	1850	79.9	1.521
	5	95.5	140.0	0.682	86.2	1.108	108.5	0.880	6.1	23.7	S	342	1771	71.9	1.328
	6	125.6	147.2	0.853	82.4	1.524	116.4	1.079	5.7	24.8	S	389	1814	76.6	1.640
	7	143.7	150.6	0.954	75.9	1.893	120.4	1.194	5.6	25.5	S	416	1825	78.9	1.821
AF (6" x 12")	2	42.7	44.9	0.951	42.7	1.000	45.9	0.930	0.3	70.1	B	595	77	43.7	0.977
	3	95.4	107.8	0.885	85.5	1.116	98.9	0.965	5.4	25.9	S	417	1772	70.2	1.359
	4	117.0	133.1	0.879	87.8	1.333	107.7	1.086	5.9	24.6	S	387	1848	71.1	1.646
	5	78.0	141.5	0.551	83.8	0.931	111.9	0.697	5.7	25.0	S	395	1822	74.1	1.053
	6	109.2	151.9	0.719	79.2	1.379	118.6	0.921	5.7	25.1	S	411	1872	77.2	1.415

* B - bottom, S - side, T - top

† T_{ep} includes stirrup contribution (column 10)

TABLE 5.2 (Cont'd) CRACKING TORQUES FOR SOLID CROSS-SECTIONS BY DIFFERENT THEORIES

Beam		T_{test}	Skew bending theory		Elastic behavior, rectangular cross-section		Elastic-Plastic Behavior							Equivalent elliptical cross-section	
									Supplemental Information						
Group	No.	(in.kips)	T_{sb} (in.kips)	$\frac{T_{test}}{T_{sb}}$	T_e (in.kips)	$\frac{T_{test}}{T_e}$	T_{ep} (in.kips)	$\frac{T_{test}}{T_{ep}}$	$T_{stirrup}$ (in.kips)	θ_{cr} (deg)	Crack Location	Principal stresses at cracking (psi)		T_{ee} (in.kips)	$\frac{T_{test}}{T_{ee}}$
												tension	compression		
1	2	3	4	5	6	7	8	9	10	11	12	13	14	15	16
AG (6" x 12")	2	58.8	60.9	0.961	55.4	1.061	61.0	0.964	0.0**	61.7	B*	535	155	57.8	1.017
	3	112.5	132.9	0.847	101.8	1.105	125.9	0.894		45.9	B	613	577	89.3	1.260
	4	126.5	149.8	0.844	98.0	1.291	116.1	1.090		25.6	S	423	1836	78.2	1.618
	5	95.5	145.6	0.656	95.2	1.003	113.9	0.838		25.4	S	411	1820	76.0	1.257
	6	129.5	162.3	0.798	97.2	1.332	128.4	1.009		27.1	S	499	1902	86.1	1.504
	7	122.8	158.6	0.774	82.1	1.496	126.2	0.973		26.8	S	484	1896	83.8	1.465
AH (6" x 12")	2	44.6	40.6	1.099	38.8	1.149	41.1	1.085		69.6	B	522	72	39.6	1.126
	3	82.4	96.2	0.857	79.9	1.031	93.7	0.879		51.3	B	553	355	72.9	1.130
	4	97.5	122.0	0.799	78.5	1.242	89.3	1.092		23.2	S	318	1732	64.7	1.507
	5	88.4	141.3	0.626	84.4	1.047	107.3	0.824		25.1	S	402	1827	74.1	1.193
	6	105.2	154.5	0.681	84.1	1.251	115.2	0.913		25.9	S	435	1843	79.5	1.323

* B - bottom, S - side, T - top

** Beams of AG and AH groups are without stirrups

TABLE 5.2 (Cont'd) CRACKING TORQUES FOR SOLID CROSS-SECTIONS BY DIFFERENT THEORIES

Beam		T_{test}	Skew bending theory		Elastic behavior, rectangular cross-section		Elastic-Plastic Behavior							Equivalent elliptical cross-section	
									Supplemental Information						
Group	No.	(in.kips)	T_{sb} (in.kips)	$\frac{T_{test}}{T_{sb}}$	T_e (in.kips)	$\frac{T_{test}}{T_e}$	T_{ep}† (in.kips)	$\frac{T_{test}}{T_{ep}}$	$T_{stirrup}$ (in.kips)	θ_{cr} (deg)	Crack Location	Principal stresses at cracking (psi)		T_{ee} (in.kips)	$\frac{T_{test}}{T_{ee}}$
												tension	compression		
1	2	3	4	5	6	7	8	9	10	11	12	13	14	15	16
BIS (8" x 12")	2a	23.0	23.3	1.000	23.0	1.000	24.8	0.927	0.0	80.3	B*	548	16	23.0	1.000
	2b	23.0	23.0	1.000	22.6	1.018	24.8	0.927	0.6	79.9	B	512	16	22.7	1.013
	4a	96.0	103.2	0.930	82.3	1.166	98.9	0.971	1.0	54.1	B	511	266	85.9	1.118
	4b	102.0	110.1	0.926	86.4	1.181	110.9	0.920	7.6	52.9	B	515	295	90.4	1.128
	6a	117.0	169.5	0.690	114.2	1.025	136.2	0.859	3.0	35.3	S	475	946	97.1	1.205
	6b	128.0	182.3	0.702	122.7	1.043	161.4	0.793	18.9	35.8	S	516	996	104.4	1.226
BS (8" x 12")	2	54.0	38.4	1.406	37.7	1.432	39.5	1.367	0.3	75.6	B	576	38	37.9	1.425
	2S	58.0	54.9	1.056	52.7	1.101	56.2	1.032	0.9	66.9	B	489	89	53.2	1.090
	3	147.0	146.7	1.002	122.1	1.204	141.1	1.042	3.3	46.4	B	546	496	126.6	1.161
	4	165.0	230.5	0.715	156.0	1.058	179.4	0.920	8.9	26.9	S	466	1802	133.8	1.233
	5	184.0	251.5	0.732	145.2	1.267	181.4	1.014	9.3	26.2	S	436	1801	134.0	1.373
	6	158.0	252.5	0.626	140.7	1.123	181.2	0.872	9.4	25.8	S	419	1784	133.0	1.188

* B - bottom, S - side, T - top

† T_{ep} includes stirrup contribution (column 10)

TABLE 5.2 (Cont'd) CRACKING TORQUES FOR SOLID CROSS-SECTIONS BY DIFFERENT THEORIES

Beam		T_{test}	Skew bending theory		Elastic behavior, rectangular cross-section		Elastic-Plastic Behavior							Equivalent elliptical cross-section	
									Supplemental Information						
Group	No.	(in.kips)	T_{sb} (in.kips)	$\frac{T_{test}}{T_{sb}}$	T_e (in.kips)	$\frac{T_{test}}{T_e}$	T_{ep}† (in.kips)	$\frac{T_{test}}{T_{ep}}$	$T_{stirrup}$ (in.kips)	θ_{cr} (deg)	Crack Location	Principal stresses at cracking (psi)		T_{ee} (in.kips)	$\frac{T_{test}}{T_{ee}}$
												tension	compression		
1	2	3	4	5	6	7	8	9	10	11	12	13	14	15	16
G3	2	80.0	68.4	1.170	67.2	1.190	70.9	1.128	0.9	73.6	B*	642	56	66.9	1.196
	3	174.0	170.2	1.022	151.4	1.149	163.2	1.066	4.8	49.6	B	503	364	148.4	1.173
	4	260.0	372.7	0.698	227.5	1.143	249.3	1.043	15.0	27.2	S	357	1356	212.7	1.222
	5	240.0	385.9	0.622	218.9	1.096	245.0	0.980	12.9	29.9	T	360	1086	205.4	1.168
	6	192.0	418.7	0.459	181.8	1.056	207.8	0.924	11.3	33.0	T	344	814	171.6	1.119

* B - bottom, S - side, T - top

† T_{ep} includes stirrup contribution (column 10)

in developing cracking strength equations. Theoretical predictions according to this analysis together with test values are shown in Table 5.4. A brief critical examination of these theories and a comparative study is given in this section. No values for flexural shear and bending moments at cracking are listed since they can be easily generated knowing the torsion to bending ratio (ψ) and the torsion to shear ratio (δ).

The skew bending theory is in good agreement with test results only for beams of series A (6" x 12"), while the difference between test and theory is greater for beams of series B (8" x 12") and for some cases of beams of series C (12" x 12"). For beams of series C skew bending theory predicts as much as 100% higher capacities. For this reason the skew bending theory can be regarded as unsafe and its use, particularly for cross-sections that approach a square, can not be recommended. It would appear that the assumption of an instantaneously extended crack, discussed previously, compensates properly for plastic action only for beams having an aspect ratio approximately 2:1. Excluding the case of pure torsion (Equation 5.15) formulas based on this theory are rather complex and require the simultaneous solution of two equations, one for cracking torque and another for crack inclination.

Contrary to the skew bending theory, elastic analysis always underestimates cracking strength. This can be expected since concrete is not an elastic material and some portions of a cross-section become

TABLE 5.3 SUMMARY OF T_{test}/Theory VALUES FOR SOLID X-SECTIONS

Series	Skew Bending Theory	Elastic Behavior	Elasto-Plastic Behavior	Equivalent elliptical cross-section
A 44 beams 6" x 12"	0.948	1.262	1.034	1.409
B 12 beams 8" x 12"	0.899	1.135	0.970	1.180
C 5 beams 12" x 12"	0.794	1.127	1.028	1.176

TABLE 5.4 CRACKING TORQUES OF HOLLOW BEAMS

Beam		Test Results T_t (in.kips)	Theory Equivalent elliptical cross-section T_{eq} (in.kips)	T_t/T_{eq}
Group	number			
BH	2	58.0	47.1	1.231
	3	102.0	92.1	1.107
	4	105.0	111.9	0.938
	5	114.0	112.2	1.016
	6	104.0	112.2	0.924
			Ave.	1.043
CH	2	50.0	56.3	0.888
	3	138.0	122.9	1.123
	4	143.0	175.9	0.813
	5	192.0	194.0	0.990
	6	150.0	166.5	0.901
			Ave.	0.943

plastified (Figure 5.4c) and thereby additionally contribute to the cracking strength of a member. Higher discrepancies between this theory and test results are observed for beams of series A than for B and C series, as noted in Table 5.3. The formulas for cracking torques are simpler, but they involve torsional constants α and β.

The effects of nonelastic action and interaction between principal stresses are taken into account in the analysis described in Section 5.3.1. It can be observed from Table 5.3 that this analysis is in very good agreement with the test values for all ranges of aspect ratios.

If solid or hollow rectangular cross-sections are replaced by elliptical cross-sections defined by inscribed ellipses the need for torsional constants α and β is eliminated. This procedure is based on elastic behavior; however, it yields more conservative results than elastic analysis for rectangular cross-sections since the effect of corners is neglected. Test to theory ratio is highest for a 2:1 aspect ratio and lowest for a square cross-section. In the case of hollow cross-sections (Table 5.4) agreement between tests and theory is much better than for solid cross-sections. In this case the effect of neglecting the contribution of outside corners is compensated by rounding of inside corners as shown in Figure 5.9b.

5.5 Precracking Stiffness

The precracking torsional stiffness of a member can be ex-

pressed in several ways similar to that for bending where an initial, tangent or secant modulus is used. Of these the secant modulus is most commonly used and accordingly, in this study, the experimental value of torsional stiffness is taken as:

$$K_{test} = \frac{T_{cr}}{\phi_{cr}} \tag{5.49}$$

where T_{cr} and ϕ_{cr} are those values of torque-twist curves which correspond to the appearance of first crack.

The theoretical stiffness for a solid rectangular cross-section in accordance with St. Venant theory[69] is given by:

$$K_{rectangle} = \gamma G_c h b^3 \tag{5.50}$$

where γ is given in Table 5.1 and:

$$G_c = \frac{E_c}{2(1 + \mu)}$$

the modulus of elasticity for concrete E_c, as defined in ACI 318-71[1] is:

$$E_c = 57000 \sqrt{f'_c}$$

and Poisson's ratio μ is taken as 0.16.

Consistent with the analysis given in Section 5.3.2, use of elliptical cross-sections for stiffness evaluation is suggested. Based on theory of elasticity[69] the stiffness for an elliptical tube is:

$$K_{el,tube} = \frac{\pi}{16} c_h \frac{b^3 h^3}{b^2 + h^2} G_c \tag{5.51}$$

where c_h has been defined previously (Equation 5.41). Equation 5.51 can be easily modified for a solid cross-section since c_h becomes 1:

$$K_{el,solid} = \frac{\pi}{16} \frac{b^3 h^3}{b^2 + h^2} G_c \qquad (5.52)$$

Theoretical (Equations 5.50 and 5.51) and test (Equation 5.49) values for the torsional stiffnesses of solid cross-sections are listed in Table 5.5. Generally, the analysis based on use of a rectangle overestimates test values while that based on an ellipse yields smaller values as compared to test results. Experimental torque-twist curves in the range up to cracking and theoretical values of stiffnesses of solid beams of three groups are shown in Figure 5.10. Theoretical values are taken as average values for each group shown in Table 5.5. This essentially implies that the concrete compressive strength is averaged since it was the only variable in each group of beams.

A similar comparison can be made for hollow beams. Table 5.6 shows that Equation 5.51 underestimates the experimental stiffnesses by about 2% for the CH group. Graphical illustration of these comparisons is given in Figure 5.11.

TABLE 5.5 TORSIONAL STIFFNESS OF SOLID CROSS-SECTIONS

Beam no.	T_{cr} in-k	ϕ_{cr} $\frac{k\text{-in}}{rad} \times 10^{-6}$	K_{test} $\frac{k\text{-in}}{rad} \times 10^{-6}$	$K_{rectangle}$ (Eq. 4.50) $\frac{k\text{-in}}{rad} \times 10^{-6}$	$\frac{K_{test}}{K_{rectangle}}$	$K_{ellipse}$ (Eq. 4.52) $\frac{k\text{-in}}{rad} \times 10^{-6}$	$\frac{K_{test}}{K_{ellipse}}$
AF-2	42.7	42	1.017	0.995	1.022	0.683	1.489
AF-3	95.4	114	0.873	0.926	0.904	0.635	1.318
AF-4	117.0	142	0.824	1.073	0.793	0.713	1.156
AF-5	78.0	78	1.000	0.999	1.001	0.685	1.459
AF-6	109.2	119	0.918	1.042	0.881	0.715	1.284
Average			0.919	1.000	0.920	0.686	1.341
B1S-2a	23.0	10	2.300	2.260	1.018	1.568	1.467
B1S-2b	23.0	10	2.300	2.187	1.052	1.517	1.517
B1S-4a	96.0	48	2.000	2.250	0.889	1.560	1.282
B1S-4b	102.0	62	1.645	2.254	0.730	1.564	1.052
B1S-6a	117.0	70	1.671	2.181	0.766	1.513	1.104
B1S-6b	128.0	64	2.000	2.176	0.919	1.509	1.325
Average			1.986	2.218	0.896	1.539	1.293
CS-2	80.0	17	4.706	5.389	0.873	3.753	1.254
CS-3	174.0	51	3.412	5.224	0.653	3.637	0.938
CS-4	260.0	70	3.714	5.180	0.717	3.606	1.030
CS-5	240.0	65	3.692	5.241	0.704	3.649	1.012
CS-6	192.0	44	4.364	5.313	0.821	3.699	1.180
Average			3.978	5.269	0.754	3.669	1.082

TABLE 5.6 TORSIONAL STIFFNESS OF HOLLOW CROSS-SECTIONS

Beam no.	Test values (from T-ϕ curves)			Theory (Eq. 4.51)	
	T_{cr} in-k	ϕ_{cr} $\frac{rad}{in} \times 10^{6}$	K_{test} $\frac{k\text{-}in}{rad} \times 10^{-6}$	K_{theory} $\frac{k\text{-}in}{rad} \times 10^{-6}$	$\frac{K_{test}}{K_{theory}}$
BH-2	58	31	1.871	1.530	1.223
BH-3	102	70	1.457	1.420	1.026
BH-4	105	60	1.750	1.499	1.167
BH-5	114	62	1.839	1.477	1.245
BH-6	104	65	1.600	1.530	1.046
Average			1.703	1.491	1.141
CH-2	50	20	2.500	3.184	0.785
CH-3	138	32	4.313	3.136	1.375
CH-4	143	41	3.488	3.280	1.063
CH-5	192	78	2.462	3.153	0.781
CH-6	150	49	3.061	3.470	0.882
Average			3.164	3.225	0.977

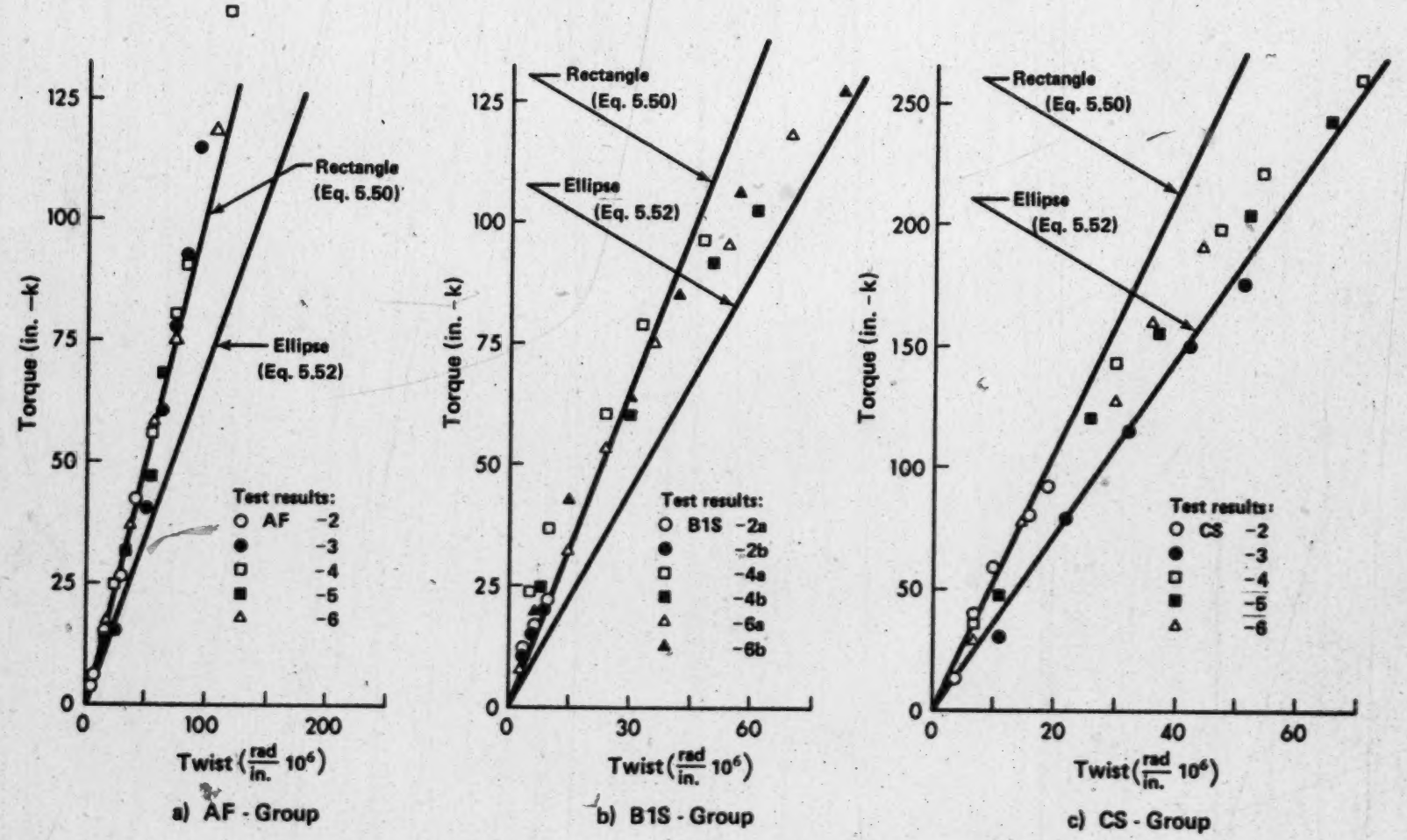

FIG. 5.10 PRECRACKING TORSIONAL STIFFNESS, SOLID CROSS - SECTIONS

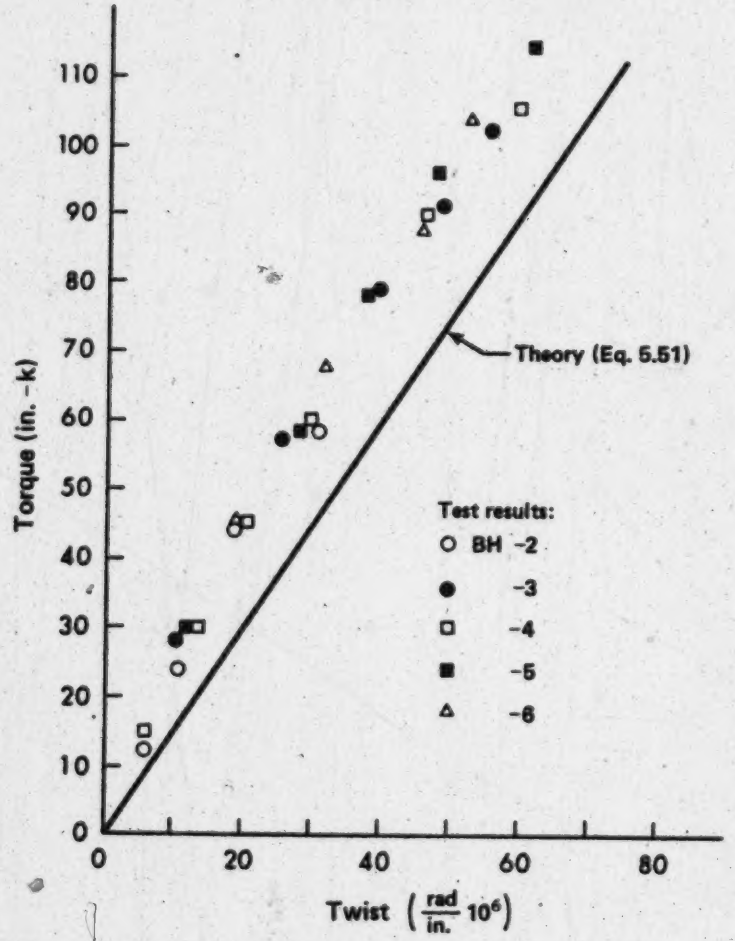

a) BH - Group

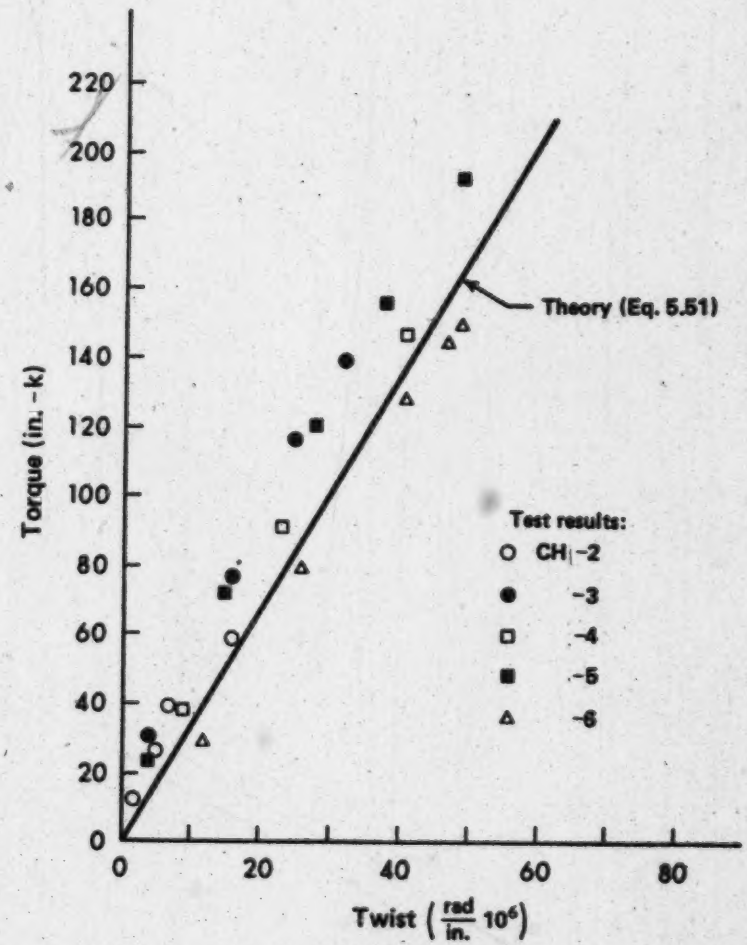

b) CH - Group

FIG. 5.11 PRECRACKING TORSIONAL STIFFNESS, HOLLOW CROSS - SECTION

CHAPTER VI

ULTIMATE STRENGTH - THEORY, EXPERIMENTS AND COMPARISON

6.1 Introduction

From the discussion in Chapter 2, available theories for the ultimate strength of beams subjected to combined loading include the Truss analogy, the Skew bending theory and the Equivalent thin tube theory. These three approaches are schematically shown in Figure 6.1. It should be noted that the thin tube approach has been used for the case of pure torsion only and attempts at predicting postcracking torsional stiffness have been based on this model[11, 36]. Elfgren[18] showed that Truss theory and skew bending analysis yield the same results, providing the same assumptions and simplifications are made in both cases. He used the method of virtual work in deducing this important conclusion.

In this chapter the skew bending theory is reviewed with the emphasis on failure mechanism and failure criteria. Some shortcomings and limitations of this theory are pointed out and a new approach which considers the torsional component on the inclined uncracked zone in addition to bending component is presented. A failure criteria for concrete based on a biaxial state of strain is suggested and equations for the ultimate torsional strength of prestressed rectangular concrete solid and hollow beams subjected to combined torsion, bending and shear, are developed. Finally, comparison between experimental results and

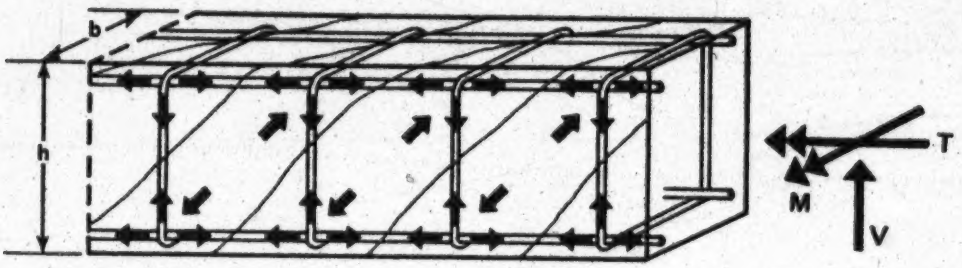

a) TRUSS ANALOGY

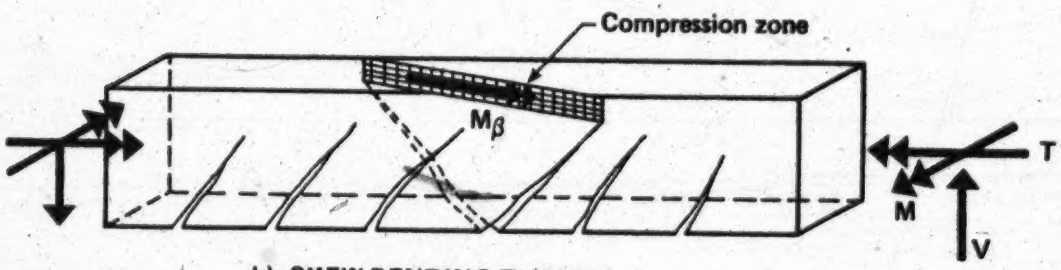

b) SKEW BENDING THEORY

c) EQUIVALENT THIN TUBE THEORY

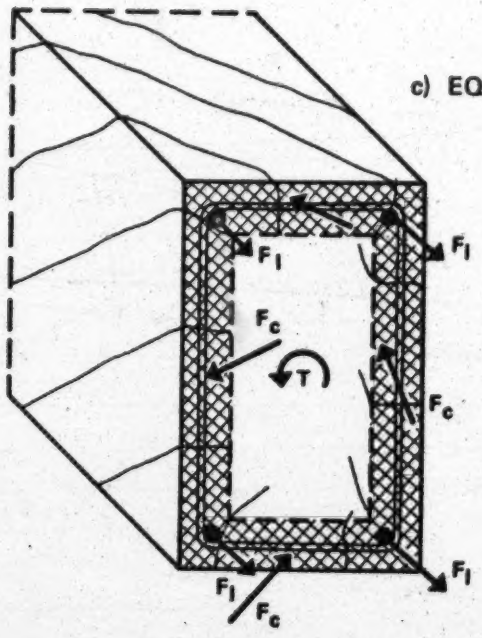

FIG. 6.1 THREE APPROACHES TO THE PROBLEM OF COMBINED LOADING

theoretical predictions is given.

6.2 Remarks on the Skew Bending Theory

A skew bending mechanism is defined as one in which a spiral crack develops on three faces of a beam, the ends of which are joined by an inclined compression zone on the fourth face as shown in Figure 6.1b. Failure is reached when the strain in the compression zone ε_β, due to bending M_β, reaches a limiting value. Depending on beam geometry, amounts of transverse and longitudinal reinforcements, ψ and δ ratios, the compression zone can be located adjacent to the top, side or bottom of a beam. These three cases shown in Figure 6.2 are commonly referred to in the literature as mode 1, mode 2 and mode 3. That mode which results in the least torque governs the strength of a beam. Torsional capacities, corresponding to each mode can be obtained if the total moment of the external forces about the compression hinge is equated to M_β:

$$\text{mode 1:} \qquad T = \frac{\psi M_\beta}{\psi \cos\beta + \sin\beta} \tag{6.1}$$

$$\text{mode 2:} \qquad T = \frac{M_\beta}{\cos\beta(1 + 1/\delta - 2a/b\delta)} \tag{6.2}$$

$$\text{mode 3:} \qquad T = \frac{\psi M_\beta}{\psi \cos\beta - \sin\beta} \tag{6.3}$$

where T = theoretical ultimate torque

β = angle of inclination of compression zone with respect to the longitudinal axis

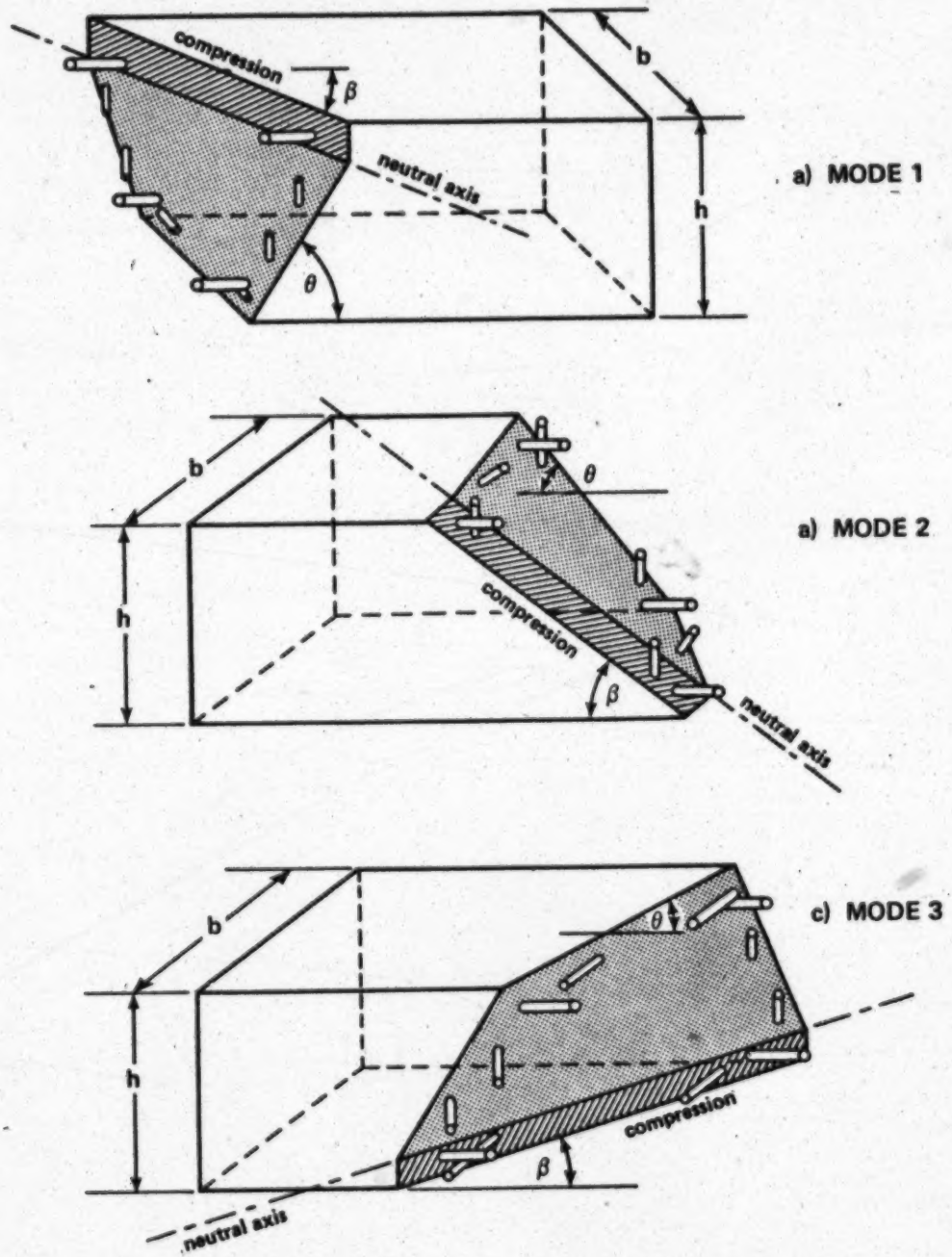

FIG. 6.2 FAILURE MODES ACCORDING TO SKEW BENDING THEORY

M_β = bending capacity in the inclined direction

ψ = torque to bending ratio, T/M

δ = torque to shear ratio, 2T/bV

Once the torque is determined, bending and shear can be calculated as follows:

$$M = \frac{T}{\psi} \tag{6.4}$$

$$V = \frac{2T}{b\delta} \tag{6.5}$$

The above analysis, usually referred to as Lessig's theory, is applicable only for under-reinforced beams in which both longitudinal and transverse steel yield prior to failure. In addition, for a skew bending analysis, the following assumptions are normally introduced:

(i) tension of concrete is neglected

(ii) no local loads are present within length of compression zone

(iii) stirrups are uniformly spaced along the length of the beam

(iv) dowel action of the longitudinal and transverse reinforcement is neglected

One of the crucial assumptions in Lessig's theory is that concrete in the inclined compression zone reaches full flexural strength. This assumption, however, can be true only for the pure bending case. When a beam is subjected to a combined loading, the uncracked zone is

subjected to a complex state of stress. The term "uncracked zone" is used here purposely since the term "compression zone" can be somewhat misleading, because concrete in this zone is subjected to tension as well as compression. This biaxial state of stress, which is actually a simplification of a more general triaxial state of stress, results from forces acting on the skewed surface which consist of not only the bending component M_β, but also the torque T_β and shear V_β shown in Figure 6.3. Large numbers of reinforced concrete beams tested and reported in the literature suggest that torque T_β can be neglected. However, it has been noted by some researchers that this assumption overestimates beam capacities. Hsu[34] modified this analysis by assuming a planar, not a warped failure surface, or in other words, he assumed that the tension crack on the two sides of a beam is perpendicular to the beam corners. This implies that no stirrups are intercepted by the tension crack on two sides of a beam, resulting in no contribution from these stirrups to the beam strength. Hsu noticed that beams having square or nearly square cross-sections did not obey this assumption. The experimental findings reported here do not support Hsu's assumption, both for rectangular (series A and B) and square (series C) cross-sections. Crack patterns shown in the photographs in Appendix C clearly confirm this. It is justified to examine other reasons for the reduction of beam capacities.

In the late sixties, when research shifted from reinforced to prestressed concrete, assumptions applicable to reinforced concrete when extended to prestressed concrete resulted in unrealistic predic-

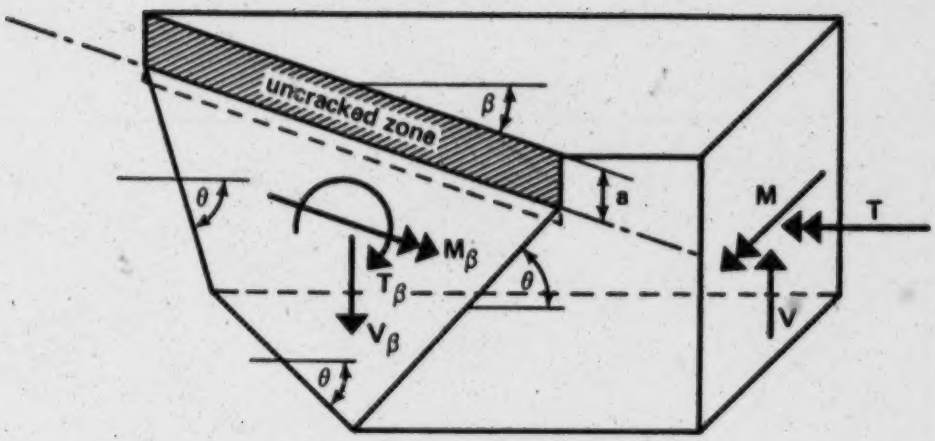

FIG. 6.3 MODE 1 – FREE BODY DIAGRAM

tions. For example, in an attempt to analyse beams reported herein, according to the original skew bending theory, in some cases the strength was overestimated by more than 250 percent. Faced with the above problem, researchers in North Carolina[24, 29, 40] in their analysis assumed that failure of a beam corresponded to yielding of the stirrups or longitudinal steel, whichever came first. Therefore, for each mode, two cases were examined; the smallest torque governed the strength for each mode. While this analysis represents a step ahead in the solution to this problem, it is difficult to justify one of its main assumptions, i.e., steel strains at failure correspond to first yielding strains; recorded strains in longitudinal or transverse steel have been measured much higher.

Evans and Khalil[22] pursued the problem in a somewhat different direction. They proposed a reduction of concrete compressive strain at ultimate as follows:

$$\varepsilon_c = \varepsilon_{cu} (M_u/M_{ub})^2 \qquad (6.6)$$

where ε_c = compressive strain in concrete in combined state of stress

ε_{cu} = compressive strain in concrete in pure bending

M_u = ultimate bending in combined loading

M_{ub} = pure bending capacity

Woodhead and McMullen[75] further reduced strain given by Equation 6.6 by assuming:

$$\varepsilon_\beta = \varepsilon_c \sin^2\beta \qquad (6.7)$$

where ε_β = concrete strain in the inclined compression zone

ε_c = reduced strain, given by Equation 6.6

β = angle of inclination of compression zone with respect to longitudinal beam axis

Rao and Warwaruk[65] in the proposed analysis of I-beams used the following expression for concrete strain:

$$\varepsilon_c = \varepsilon_{cu} \sin^2\beta \qquad (6.8)$$

It should be noted that Equation 6.6, 6.7 and 6.8 are of an empirical nature. More important, these expressions have been proposed for mode 1 only. For modes 2 and 3, the stress block for pure flexure was suggested. In the discussion that follows it will be shown that the torsion component on the inclined zone is more pronounced for mode 2 and mode 3 than for mode 1. Consequently, the necessity for concrete strain reduction in the case of these two modes is more justified than for mode 1.

To recapitulate the preceding discussion, consider the behavior of a beam under test. Prior to test a grid of horizontal and vertical lines is plotted on the tension face of the beam. The tension face is defined here as that face which lies opposite to the side where the compression zone is located, or, one where first cracking commences. Figure 6.4a illustrates such a grid on the side of a beam, corresponding to mode 2. For simplicity, consider that the angle of the tension crack with respect to the longitudinal axis is 45 degrees.

Of primary interest is the direction of the crack opening in the post-cracking stage. If the bending component above is present in the inclined zone, and steel stiffnesses in both longitudinal and transverse directions are the same, the opening will take place perpendicular to the crack as shown in Figure 6.4b. Because the crack angle is 45 degrees, "shifts" between lines on the two uncracked sides will be the same in longitudinal and transverse directions. It is important to note that this phenomenon corresponds to the original skew bending concept. Because of the presence of torsion in the inclined zone and possible differences in the stiffnesses of transverse steel and longitudinal steel, the opening of the crack may take place in a manner shown in Figure 6.4c. No discontinuity of the lines in the transverse direction is observed here. On the other hand, a large amount of stirrups as compared to longitudinal steel would result in a shift in the longitudinal direction shown in Figure 6.4d. To verify these hypothetical assumptions a square grid of 1 centimeter was made on beam B1S-6a, on the south face of the beam, since mode 2 was expected. Three postcracking stages of loading are shown in Figure 6.5. This figure clearly indicates that a sideway shift took place, rather than one corresponding to skew bending. It should be remembered that this beam had light stirrups and moderate longitudinal reinforcement. From the above discussion a very important qualitative conclusion can be drawn: the bending component on the inclined zone does not necessarily dominate the behavior of the beam subjected to combined loadings.

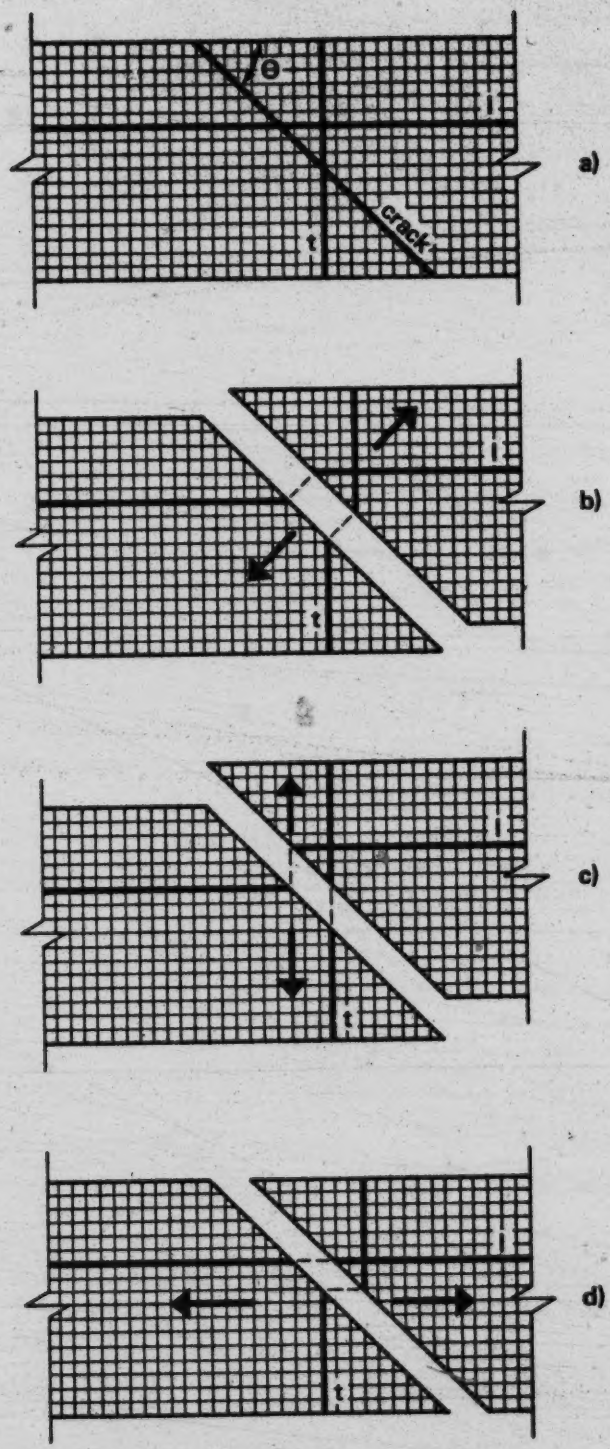

FIG. 6.4 CRACK OPENING UNDER COMBINED LOADING

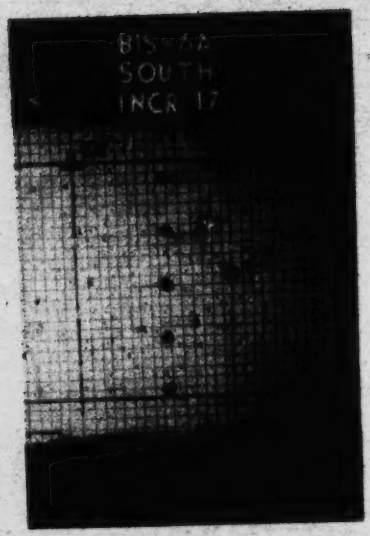

a

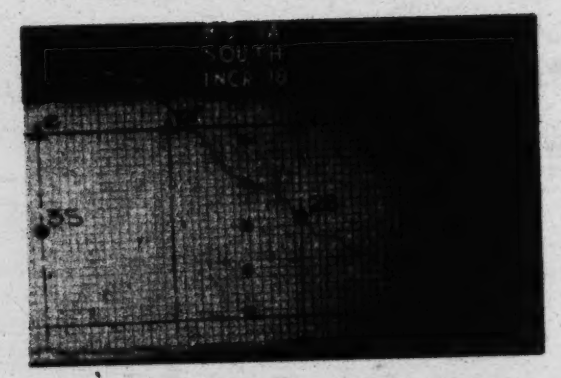

b

c

FIG. 6.5 CRACK OPENING UNDER COMBINED LODING (BEAM B1S-6a)

6.3 Proposed Analysis

6.3.1 General Remarks

In the preceding sections of this chapter the principles of skew bending theory were examined and some inconsistencies were pointed out. Examination of equilibrium equations on the plane containing the uncracked zone (β-plane) would give not only the bending component M_β, but also the torsional component T_β, and the shear V_β. Traditionally, the latter two components have been neglected, implying that the concrete in the compression zone reaches its full flexural strength. In the proposed analysis, it is suggested that the torsional component T_β be taken into account. It should be emphasized that this component is not only of academic, but also of practical importance, since it can dominate both strength and behavior of a beam under combined loading. In the following section its magnitude is examined.

6.3.2 Torsion to Bending Ratio, ψ_β

The resolution of the external force and couples into the β-plane result in the following expressions:

mode 1 (Figure 6.6a)

$$M_\beta = T \cos \beta + M \sin \beta \qquad (6.9)$$

$$T_\beta = T \sin \beta - M \cos \beta \qquad (6.10)$$

$$V_\beta = V \qquad (6.11)$$

Using the torsion to bending ratio ψ, Equations 6.9 and 6.10 can be

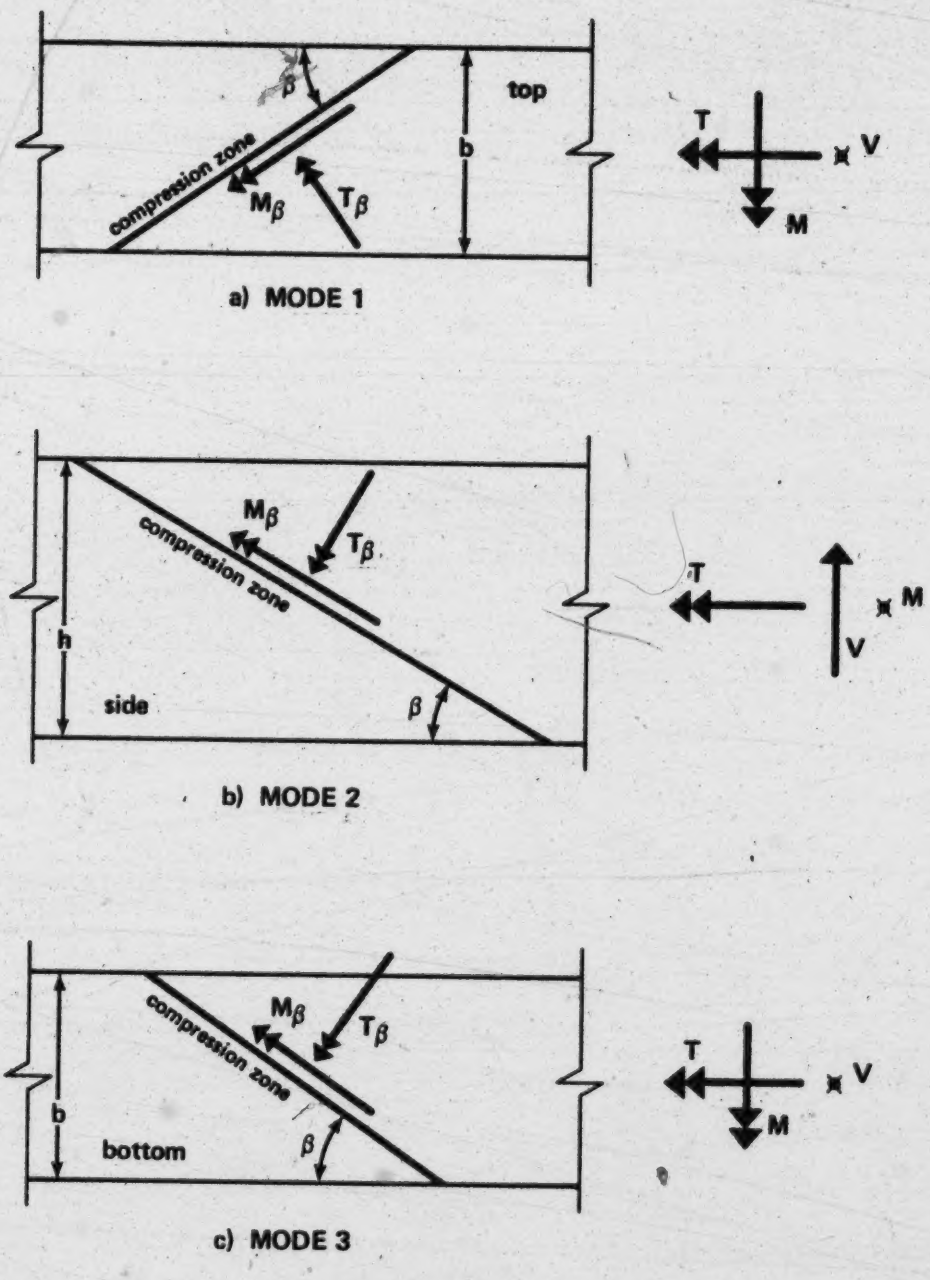

FIG. 6.6 TORSION TO BENDING RATIO ON β – PLANE

rewritten:

$$M_\beta = M\psi \cos\beta + M \sin\beta \tag{6.12}$$

$$T_\beta = M\psi \sin\beta - M \cos\beta \tag{6.13}$$

Dividing Equation 6.13 by Equation 6.12 gives:

$$\frac{T_\beta}{M_\beta} = \frac{\psi \tan\beta - 1}{\psi + \tan\beta} \tag{6.14}$$

Let:

$$\frac{T_\beta}{M_\beta} = \psi_\beta \tag{6.15}$$

then:

$$\psi_\beta = \frac{\psi \tan\beta - 1}{\psi + \tan\beta} \tag{6.16}$$

In a similar manner this ratio can be found for mode 2 (Figure 6.6b):

$$\psi_\beta = \tan\beta \tag{6.17}$$

and for mode 3 (Figure 6.6c):

$$\psi_\beta = \frac{\psi \tan\beta + 1}{\psi - \tan\beta} \tag{6.18}$$

It is interesting to note that ψ_β for mode 2 is never zero, while for mode 1 it can have a zero value. From Equation 6.16 it follows:

$$\psi_\beta = \frac{\psi \tan\beta - 1}{\psi + \tan\beta} = 0$$

or:

$$\psi \tan\beta = 1$$

and: $$\psi = \cot \beta \qquad (6.19)$$

This supports the idea that the reduction of strain is more important for mode 2 than for mode 1. To illustrate the relationship between ψ, ψ_β and β, Equations 6.16, 6.17 and 6.18 are plotted in Figure 6.7. It is shown in Figure 6.7b that ψ_β can reach values higher than 1, meaning that the torsion will be higher than bending on the β-plane. Negative values of ψ_β signify that one of the couples (bending moment or torque) has an opposite sign of that assumed in Figure 6.6. This corresponds to mode 3 failure or, for example, failure that occurs in the regions of applied negative bending moments.

6.3.3 Failure Criteria and Stress-Strain Characteristics for Concrete

Presence of bending, torsion and shear in the β-plane implies the existence of a multiaxial state of stress in the uncracked concrete zone. Similar to the cracking analysis, where a biaxial state of stress was used, it is proposed here that a biaxial state of strain exists at failure. Figure 6.8 illustrates the assumed principal strain interaction relationship. Limiting values for compressive and tensile strains are taken as 0.0038 and 0.00015, respectively. The first represents the maximum strain in Hognestad's stress-strain curve[30], while the second (tensile strain) is based on the study done by Johnston[41]. If these values are joined by a second degree parabola, the resulting equation is:

$$\varepsilon_t^2 = 5.921 \times 10^{-6}(0.0038 - \varepsilon_c) \qquad (6.20)$$

where ε_t = principal tensile strain

ε_c = principal compressive strain

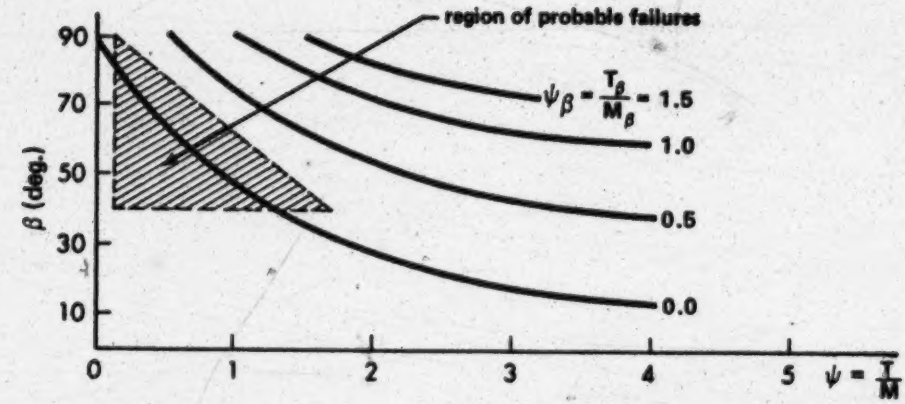

a) MODE 1

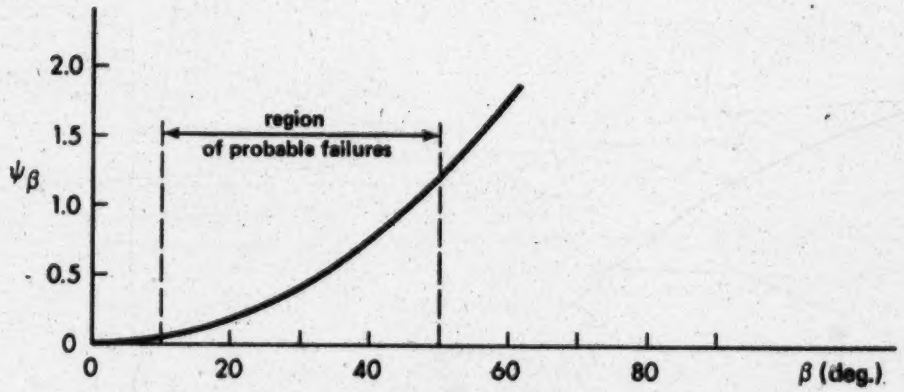

b) MODE 2

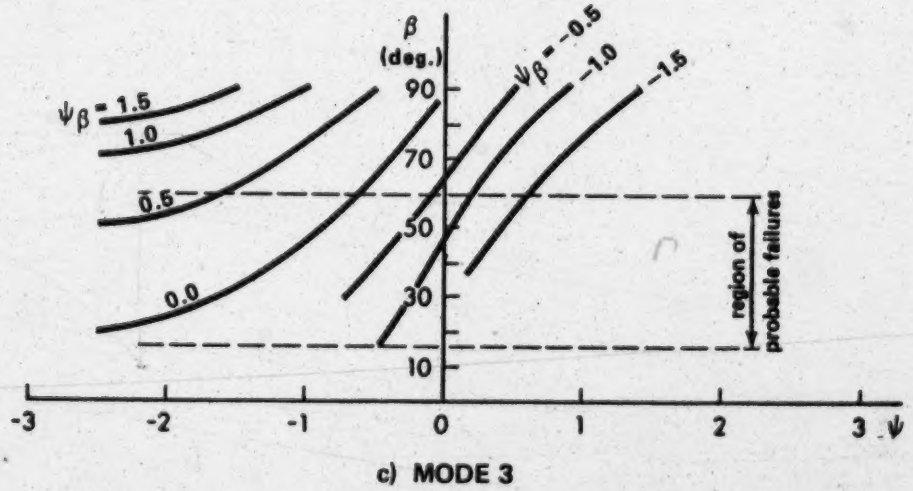

c) MODE 3

FIG. 6.7 RELATIONSHIP BETWEEN ψ, ψ_β, AND β

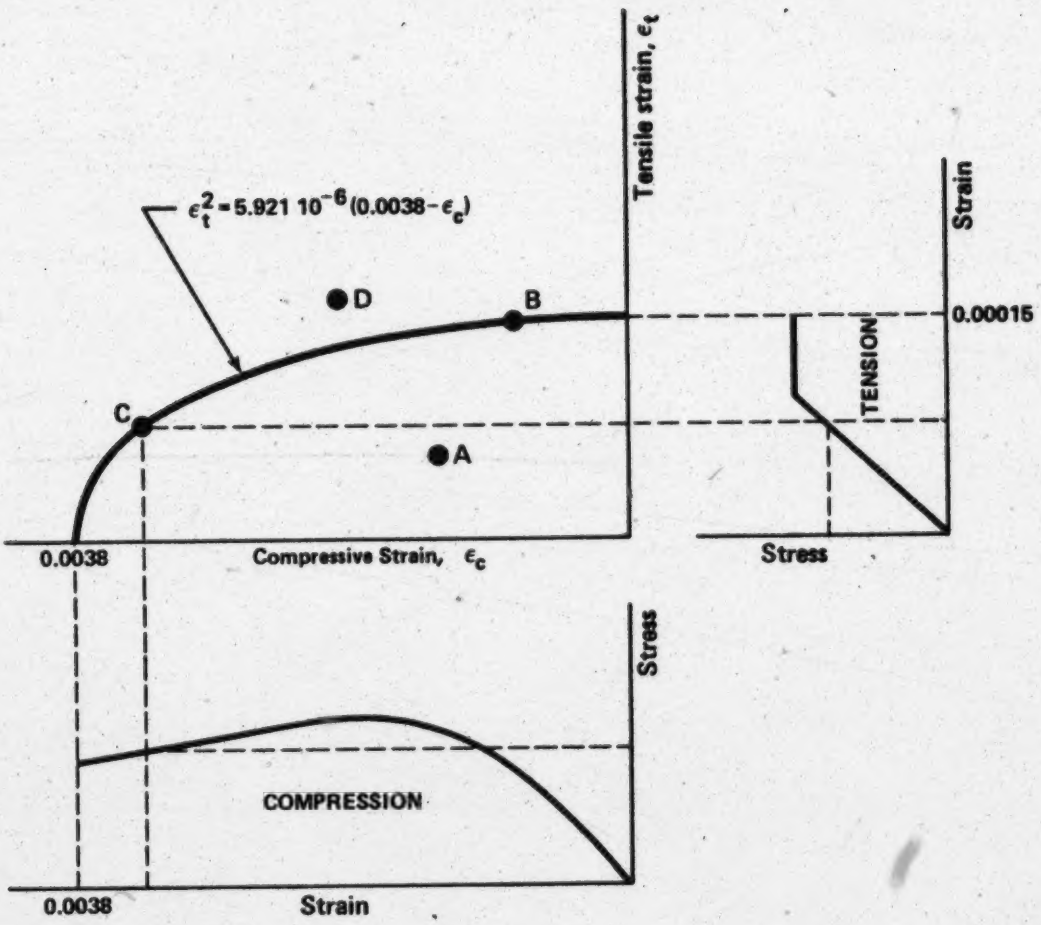

FIG. 6.8 BIAXIAL STRAIN OF CONCRETE

Failure occurs when any combination of principal strains satisfies Equation 6.20.

In Figure 6.8 stress-strain curves for compression and tension are also shown. They are given only to supplement the biaxial strain diagram. Figure 6.9 defines in detail the stress-strain characteristics of concrete, adopted in this study. While a number of stress-strain curves for concrete in compression have been suggested in the literature, probably Hognestad's curve[30] is most realistic. On the other hand little has been reported in the literature regarding the stress-strain relationship of concrete in tension. It has been recognized, however, that the maximum tensile strain, in most cases, is between 0.0001 and 0.0002. Researchers also agree that the concrete in tension is more brittle than in compression. Although a nonlinear stress-strain relationship probably exists for concrete in tension, a simplified relationship, shown in Figure 6.9b, is suggested. It should be recalled from Chapter 5 that the maximum uniaxial stress does not correspond to tensile strength from the splitting test, but has a somewhat higher value:

$$f_t = 2 f_{sp}/\sqrt{3} \qquad (6.21)$$

where f_t = tensile stress in a uniaxial state of stress

f_{sp} = tensile stress obtained from splitting test

Equation 6.21 can be derived from Equation 5.28 if f_t is substituted for σ_{max} and σ_{min} taken as zero.

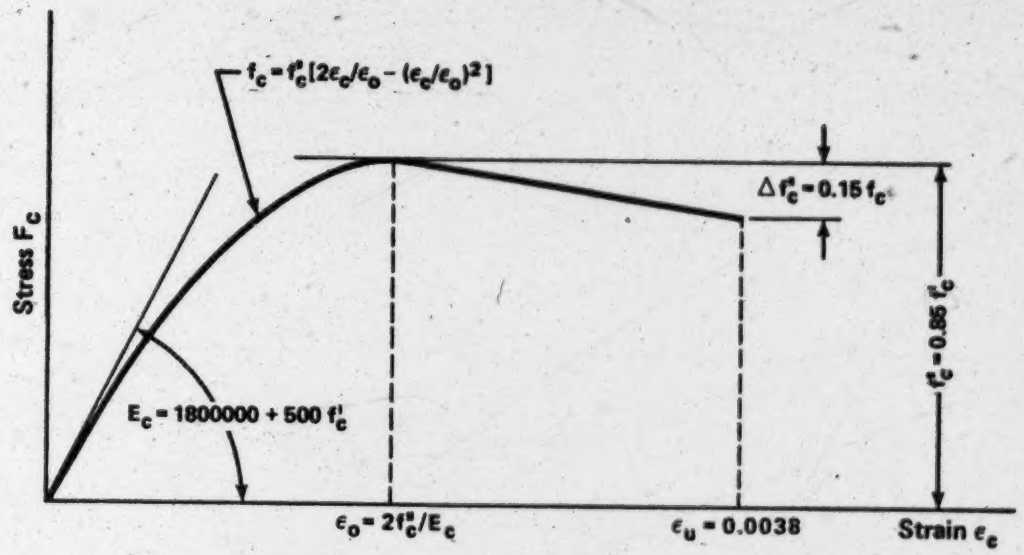

a) COMPRESSION

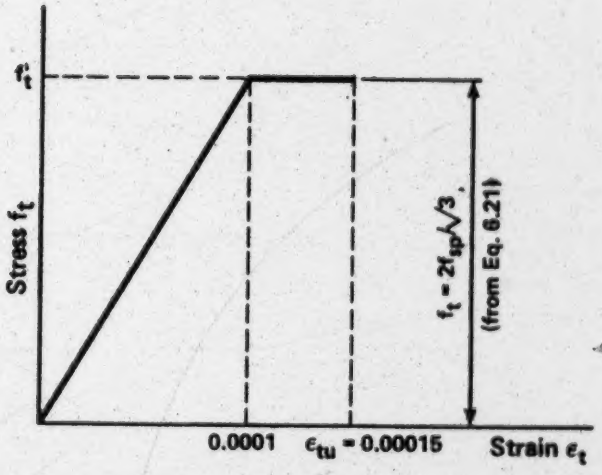

b) TENSION

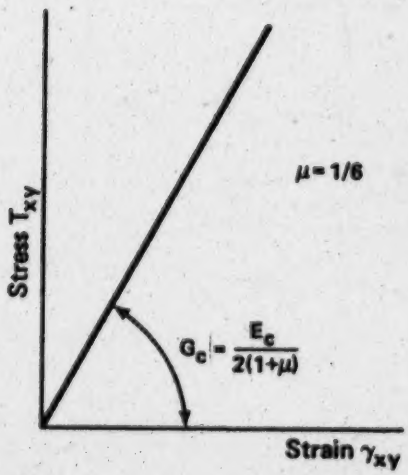

c) SHEAR

FIG. 6.9 STRESS - STRAIN CHARACTERISTICS OF CONCRETE

Since shear stresses are present in the uncracked zone, a shear stress-strain relationship needs to be defined. No research is available in this area. It is known that pure shear strength approaches compressive strength. However, in all practical cases actual shear stress reaches only a fraction of maximum pure shear stress since failure of concrete in tension would precede a pure shear failure. Consequently, a linear stress-strain relationship, shown in Figure 6.9c is suggested.

6.3.4 Assumptions of the Analysis

The following assumptions are made in the development of equations for the ultimate torque of rectangular prestressed concrete solid and hollow beams subjected to combined torsion bending and shear:

1. Failure occurs on a warped surface, whose boundaries are defined on three sides of the beam by a spiral crack, and on the fourth side by an uncracked zone which joins the ends of the spiral crack.
2. The crack defining the failure surface on three sides is composed of three straight lines spiralling around the beam at a constant angle with respect to the longitudinal beam axis.
3. The crack inclination θ can be found using one of the procedures described in Chapter 5.
4. The uncracked zone is rectangular, perpendicular to the uncracked face of a beam, and is inclined at an angle β with respect to the longitudinal beam axis.

5. Failure occurs when the combination of principal strains in the uncracked concrete zone satisfies Equation 6.20.

6. The contribution of concrete subjected to tension is neglected.

7. The contribution of transverse reinforcement in the compression zone is neglected.

8. The contribution of shearing stresses in the compression zone is considered.

9. Dowel action of longitudinal and transverse reinforcement in the tension zone is taken into account.

10. The stress-strain characteristics of longitudinal and transverse reinforcements are known. The nonlinear portion of the stress-strain curve for prestressing steel is utilized. Transverse reinforcement has a well defined yield plateau.

11. The stress-strain characteristics of the concrete in compression, tension, and shear are known.

12. The strain perpendicular to the β-plane is proportional to its distance from the neutral axis. Components of this strain (at various steel levels) in both longitudinal and transverse directions represent, respectively, strains in the longitudinal and transverse reinforcement:

$$\varepsilon_{\ell} = \varepsilon_{\beta} \sin \beta \qquad (6.22)$$

$$\varepsilon_{tr} = \varepsilon_{\beta} \cos \beta \qquad (6.23)$$

Assumptions 1 through 4 define the failure surface. They are similar to the assumptions made in skew bending theory and are strongly supported by experimental observations.

Assumption 5 defines the failure criteria adopted in this analysis. Although additional research may be required in this area it is felt that the parabolic strain interaction relationship is most appropriate for the case of combined loading. This assumption parallels the assumed stress interaction used in the cracking analysis. Essentially it represents an extension of the maximum compressive strain concept used in pure flexure or combined flexure and axial load.

Assumptions 6 and 7 are introduced to simplify the analysis.

Assumptions 8 and 9 relate to the resisting torque T_β and will be discussed in detail later in this chapter.

Equations for reinforcement stress-strain curves (assumption 10) are given in Chapter 3.

Stress-strain characteristics of concrete (assumption 11) are based on the work of Hognestad[30], and Johnston[41].

Finally, assumption 12 is supported by work done by Johnston and Zia[40], and Woodhead and McMullen[75]. It should be, however, observed that no simple relationship exists between strains in longitudinal and transverse reinforcement (see discussion in Section 6.2); linear relationship is assumed in order to simplify analysis.

6.3.5 Bending and Torsion Transfer on β-Plane

It was mentioned previously that the tensile crack propagates in a spiral manner as loading is increased. The ends of the crack define the uncracked zone, which may be located adjacent to the top,

side or bottom face of the beam depending on whether mode 1, 2 or 3 dominates beam behavior. For every assumed depth of the neutral axis the inclination of the compression zone β can be found directly from geometry. From Figure 6.10 the following relationships can be deduced:

$$\text{mode 1:} \quad \cot \beta = \frac{b + 2(h - a)}{b} \cot \theta \tag{6.24}$$

$$\text{mode 2:} \quad \cot \beta = \frac{h + 2(b - a)}{h} \cot \beta \tag{6.25}$$

$$\text{mode 3:} \quad \cot \beta = \frac{b + 2(h - a)}{h} \cot \beta \tag{6.26}$$

where a = depth of neutral axis

b = beam width

h = beam height

The analysis in Section 6.3.2 shows that a definite relationship exists between ψ_β, ψ and β. This means, if ψ and β are known, ψ_β can be calculated for each mode, which in turn, defines torsion to bending ratio on the β-plane (T_β/M_β).

The problem of bending transfer (Figure 6.11) does not require special attention since the rules of flexural theory apply: for any position of the neutral axis, forces perpendicular to the β-plane can be equilibrated and the corresponding bending moment M_β can be found. These steps are analogous to those for the determination of moment-curvature for pure flexure. However, there is a difference

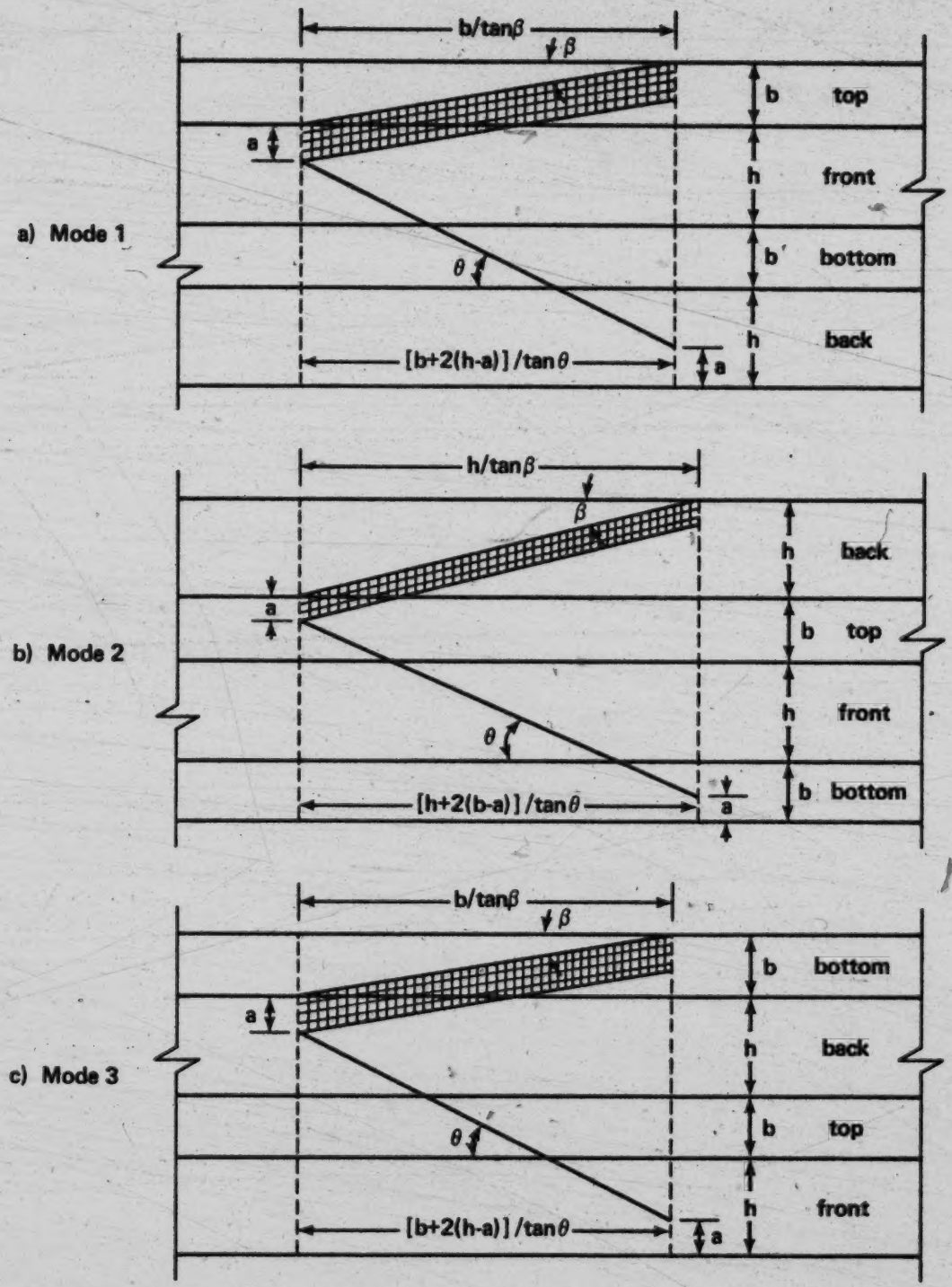

FIG. 6.10 RELATIONSHIP BETWEEN INCLINATION OF SPIRAL CRACK θ, AND ANGLE OF UNCRACKED ZONE β

since for every position of the neutral axis the angle β changes, implying a different width of compression zone. It should be noted that strains in both longitudinal and transverse steel are taken as rectangular components of the corresponding strain in the β-plane (assumption 12).

Figure 6.12 shows the torque T_β on the β-plane with the unknowns being the shear force taken by concrete V_c and component of dowel force F_d, which is parallel to β-plane. It is assumed that the dowel force F_d is located at the intersection of longitudinal and transverse steel on the tension face of the beam. Other dowel forces due to stirrups on the sides are neglected since their magnitudes and lever arms are smaller. To find V_c and F_d, two equations can be established; one is the summation of forces in β-plane, in the direction parallel to neutral axis, the other is the summation of moments about the axis perpendicular to β-plane. Of course, the right hand side of the first equation will be equal to zero, since no external loads exist in the direction in which the summation is taken; however, in the moment equation the right hand side will be equal to T_β which itself is related to external loads as given by the equations in Section 6.3.2:

$$V_c - F_d - \sum_{i=1}^{n} F_{\ell,i} \cos\beta - F_t \sin\beta = 0 \qquad (6.27)$$

$$V_c \frac{a}{2} - F_d d_d + \sum_{i=1}^{n} F_{\ell,i} \cos\beta \, d_{\ell,i} + F_t d_v \sin\beta + F_v d_v \sin\beta = T_\beta \qquad (6.28)$$

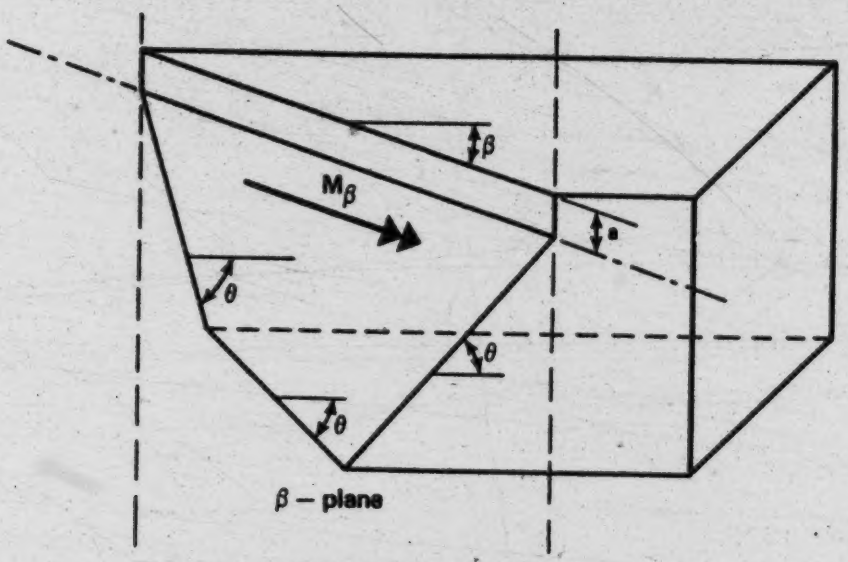

FIG. 6.11 BENDING ON THE INCLINED β – PLANE

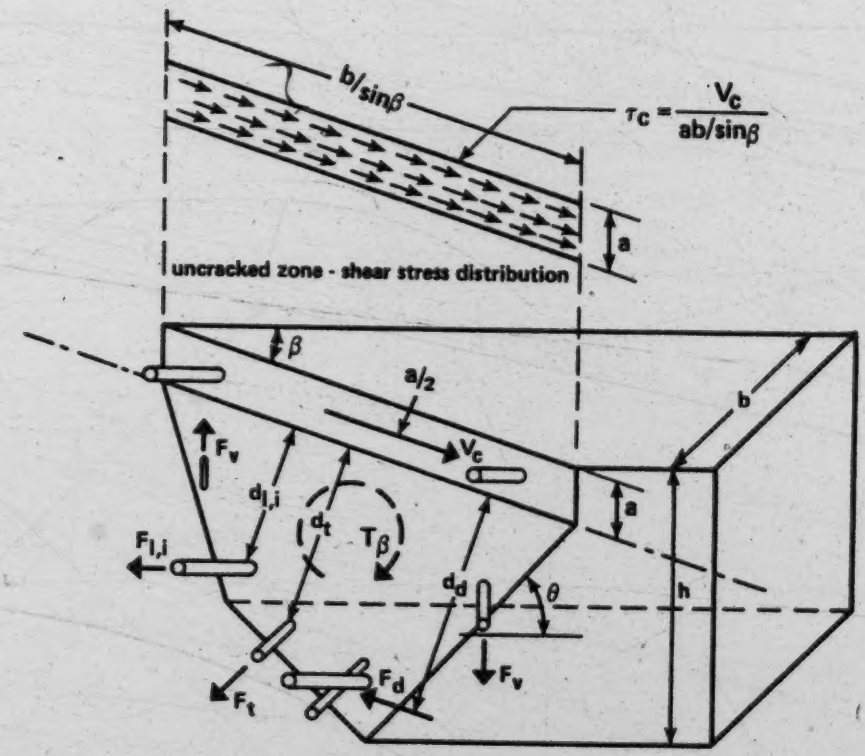

FIG. 6.12 MECHANISM OF TORSION TRANSFER ON β – PLANE

where V_c = shear force carried by concrete compression zone

F_d = component of dowel force in the direction of neutral axis

F_ℓ = force in longitudinal steel

n = number of longitudinal bars or prestressing cables

d_ℓ = distance from longitudinal steel to neutral axis

F_t = total tensile force in stirrups adjacent to tension face of the beam

d_t = lever arm of F_t

d_d = dowel force lever arm

F_v = total force in stirrups on one side of the spiral crack

d_v = distance between stirrups on two sides of the spiral crack, equal to h' for mode 1 and mode 3, and h' for mode 2

b',h' = centerline width and height of a closed stirrup, respectively

Multiplying Equation 6.27 by d_d and adding to Equation 6.28 gives:

$$V_c(a/2 + d_d) - \cos\beta \sum_{i=1}^{n} F_{\ell,i}(d_d - d_{\ell,i}) - F_t \sin\beta\,(d_t - d_d) + F_v d_v \sin\beta = T_\beta \qquad (6.29)$$

In the second term of Equation 6.29 a summation has to be carried out since forces and lever arms are not the same for every longitudinal bar or prestressing strand. If this summation is started from the bar located in the tension corner, then $d_{\ell,1}$ denotes distance between

this bar and the neutral axis. Consequently, the following simplification can be made without any significant loss of accuracy:

$$d_{\ell,1} = d_t = d_d \tag{6.30}$$

and the third term of the left hand side of the Equation 6.29 will cancel out. For i=1 the second term will be equal to zero. Equation 6.29 can then be written as:

$$V_c(a/2 + d_{\ell,1}) - \cos\beta \sum_{i=2}^{n} F_{\ell,i}(d_{\ell,1} - d_{\ell,i}) + F_v d_v \sin\beta = T_\beta \tag{6.31}$$

and:

$$V_c = (T_\beta + \cos\beta \sum_{i=2}^{n} F_{\ell,i}(d_{\ell,1} - d_{\ell,i}) - F_v d_v \sin\beta)/(a/2 + d_{\ell,1}) \tag{6.32}$$

Equation 6.32 is completely general and, therefore, is valid for any of the three modes. It should be mentioned that forces, lever arms, depth of neutral axis and angle β in Equation 6.32 are those determined during the solution of M_β.

The final assumption in this analysis is related to distribution of shear force V_c in the concrete compression zone. For simplicity, a uniform distribution is assumed as shown in Figure 6.12:

$$\tau_c = V_c/(ab/\sin\beta) \tag{6.33}$$

for modes 1 and 3. For mode 2, b has to be replaced with h, i.e.:

$$\tau_c = V_c/(ah/\sin\beta) \tag{6.34}$$

where a = depth of uncracked zone

b = width of a rectangular cross-section

h = depth of a rectangular cross-section

β = angle of inclination of compression zone with respect to longitudinal beam axis

The corresponding shearing strain γ_β can be found as:

$$\gamma_\beta = \tau_c/G_c \tag{6.35}$$

where G_c denotes shear modulus of concrete. The normal strain ε_β in the concrete is available from the steps involved in the evaluation of M_β. Principal strains can now be calculated:

$$\varepsilon_{max,min} = \varepsilon_\beta/2 \pm \sqrt{(\varepsilon_\beta/2)^2 + (\gamma_\beta/2)^2} \tag{6.36}$$

Finally, these strains can be compared with the proposed strain interaction equation (Equation 6.20) and checked as to whether or not the element is in the failure state. Details of the interaction steps are included in the following sections.

6.3.6 Summary of the Proposed Analysis

The proposed analysis is summarized in the following steps:

1. Obtain inclination of first crack θ , using one of the methods described under cracking analysis.
2. Assume depth of neutral axis, a.
3. Calculate inclination of compression zone β (formulas 6.24, 6.25 and 6.26).
4. By varying "curvature" equilibrate forces perpendicular to β-plane and find bending moment, M_β.
5. Using formulas 6.16, 6.17 and 6.18 find torsion to bending ratio on the inclined plane, ψ_β.
6. Find torsion on β-plane using Equation 6.15, $T_\beta = \psi_\beta M_\beta$.
7. Find shear force carried by concrete, V_c (Equation 6.32), then shearing stress (Equation 6.33 and Equation 6.34) and shearing strain (Equation 6.35).
8. Calculate principal strains (Equation 6.36) and compare state of strain with the parabolic strain diagram (Figure 6.8, Equation 6.20). Any combination of strains which fall inside the interaction diagram (e.g., point A in Figure 6.8) indicates that the ultimate state has not been reached; depth of compression zone should be decreased and all steps from 3 onwards repeated. Any state of stress falling outside of the interaction diagram (point D, Figure 6.8) indicates that the solution is approached from the upper bound; depth of compression zone should be increased and all steps repeated. These iteration steps are to be continued until the desired accuracy is reached.
9. Calculate torsional capacity using formulas 6.1, 6.2 and 6.3,

then bending and shear capacity using Equations 6.4 and 6.5, respectively.

The major steps of the proposed procedure are illustrated in Figure 6.13, where the solution has been approached from the lower bound. Figure 6.14 shows typical iteration paths for different modes. If the iteration is started using a deep compression zone, small principal strains in the concrete will result. As the depth of compression zone is decreased principal strains will become larger until Equation 6.20 is satisfied. It is interesting to note that mode 1 would always result in larger compressive strains than mode 2 or 3. On the other hand, modes 2 and 3 yield higher tensile strains than mode 1, as shown in Figure 6.14. This is not surprising since mode 1 is usually associated with higher bending as compared to torque and shear.

A slightly different approach is given in Figure 6.15 where the maximum compressive strain (0.0038) is assumed first and depth of neutral axis is varied until the forces perpendicular to β-plane are in equilibrium. It should be remembered again that, for every position of neutral axis angle β changes. In this approach, only steps 2, 3 and 4 described in the preceding paragraph need to be altered. With the assumed maximum principal compressive strain, completion of all steps in the first iteration will result in a state of strain which does not satisfy Equation 6.20 (Figure 6.12, iteration 1) since shearing strains are also present in the compression zone. Consequently, the depth of compression zone has to be decremented and the process

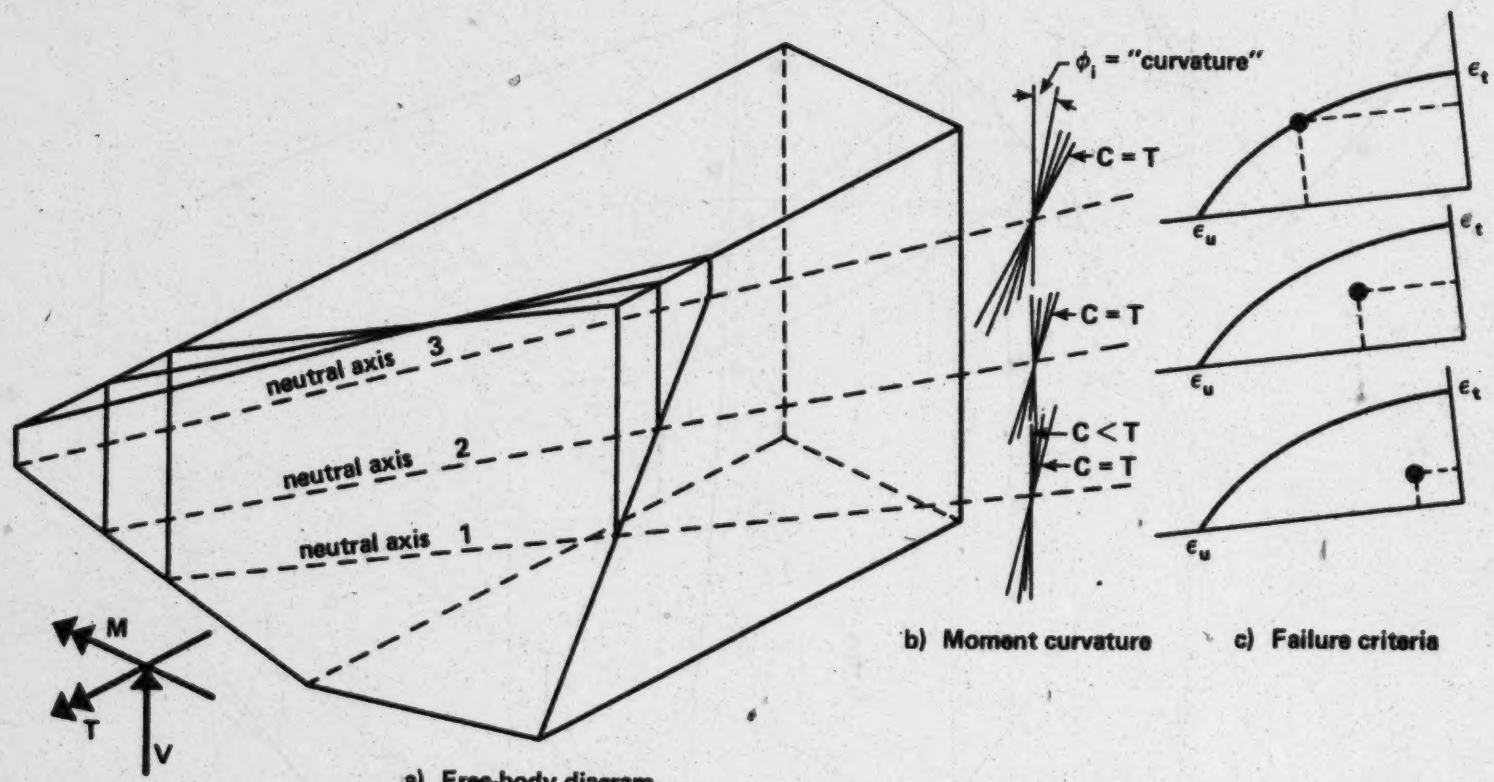

a) Free-body diagram

b) Moment curvature

c) Failure criteria

FIG. 6.13 SCHEMATICAL CONCEPT OF PROPOSED PROCEDURE

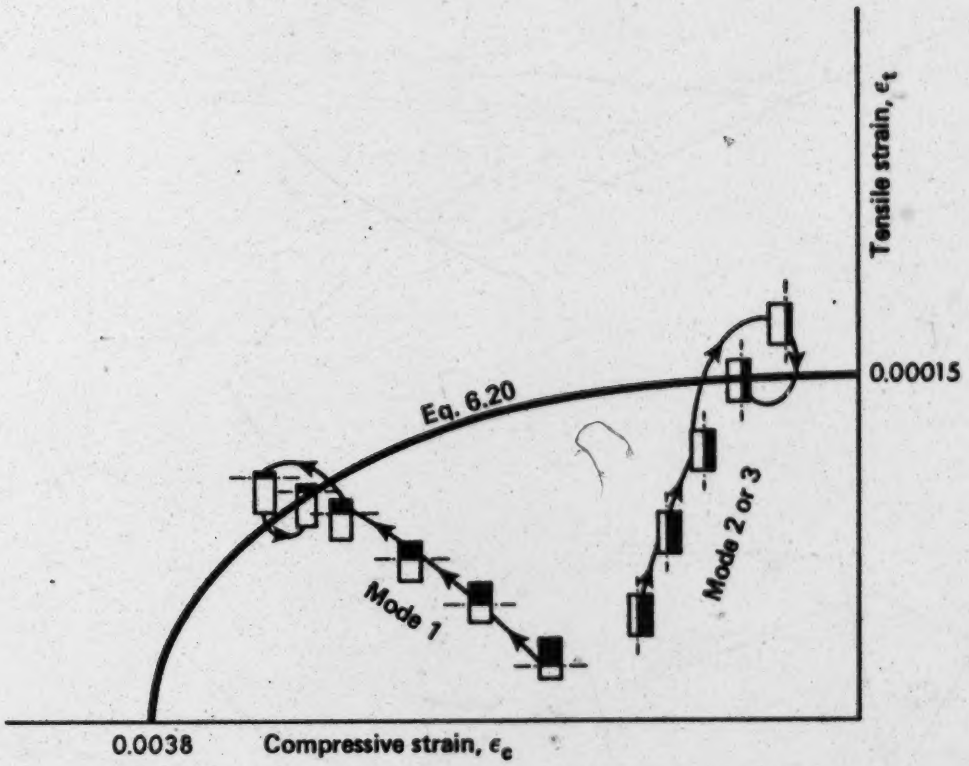

FIG. 6.14 TYPICAL ITERATION PATHS FOR DIFFERENT MODES

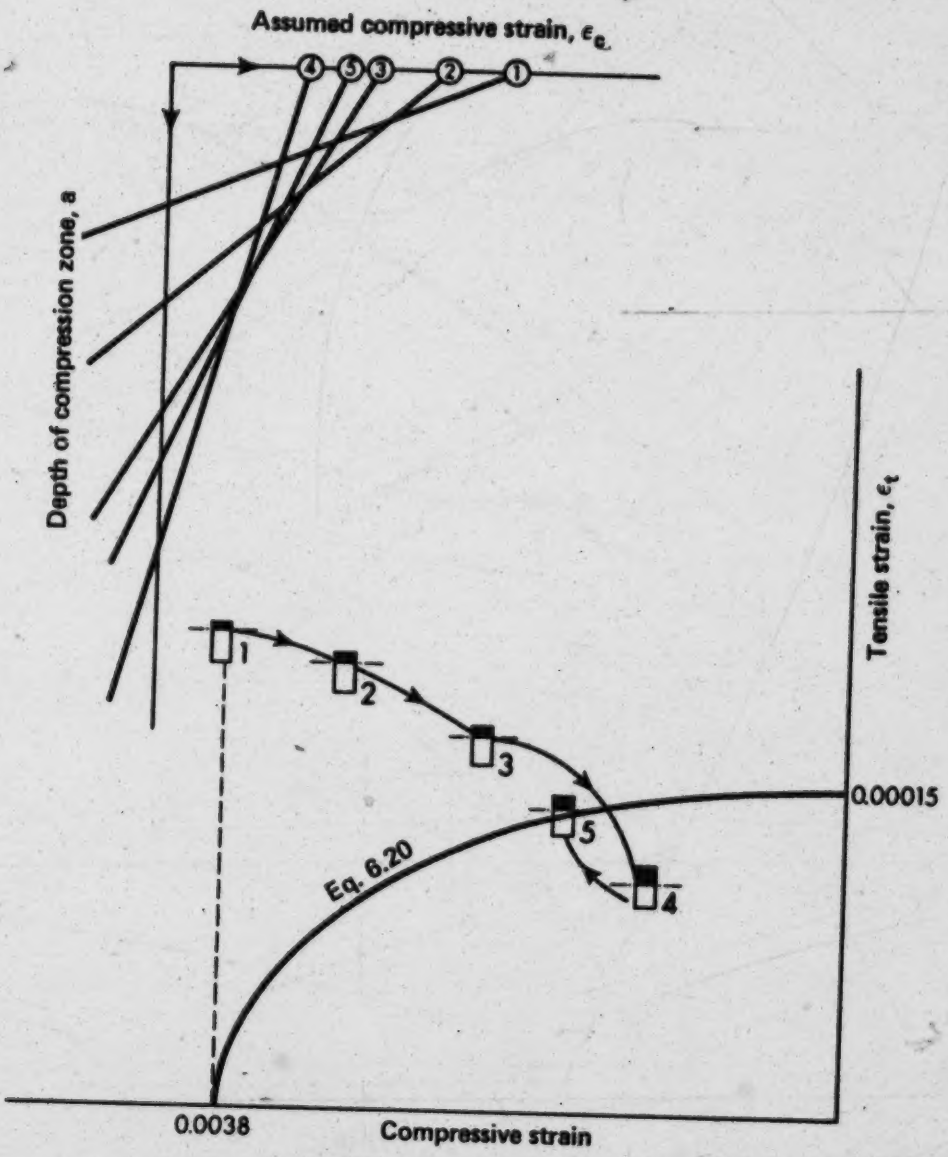

FIG. 6.15 ALTERNATE PROCEDURE

repeated.

Both approaches yield the same result. Generally, the second is somewhat more efficient since convergence is faster. Modes 1 and 3 in the computer program, presented in Appendix D utilize the second approach, while mode 2 is based on the first approach.

6.3.7 Concluding Remarks on the Proposed Analysis

The proposed biaxial strain failure criteria for the beams under combined loading is a logical extension of uniaxial strain criteria used in pure flexure or compression. To account for the biaxial state of strain two equations are utilized: first, summation of torsional moments about the axis perpendicular to the β-plane and second, summation of forces in the β-plane in the direction of the neutral axis. It should be noted that consideration of these two equations is supplemented by another two equilibrium conditions; bending moments about neutral axis and forces perpendicular to the β-plane. Therefore, four equilibrium conditions are satisfied. For hollow beams reported here, no separate procedure is necessary since the compression zone was always located in a wall. However, for thin-walled beams where the neutral axis may be located outside compression flange (wall) it is suggested that the contribution of shearing stresses, in the outstanding flanges of a channel-shaped uncracked zone, be neglected.

The assumed uniform shearing stress distribution in the uncracked zone is not correct for the loading stages immediately after

cracking, since circulatory (torsional) shear may be predominant. However, as failure is approached a state of shear flow will be reached.

The proposed theory would considerably overestimate capacities of beams B1S-4b and B1S-6b. Theoretical values for these beams are given in brackets in Table 6.2. Beams B1S-2b, B1S-4b, and B1s-6b contain excessive amounts of transverse steel (Chapter 3). Studies by Hsu[34] and McGee and Zia[54] suggest that strength cannot be increased with an excessive increase of transverse or longitudinal steel. They suggested the following limitation:

$$0.7 < m < 1.5$$

where:

$$m = \frac{A_{\ell} \cdot s}{A_t (b' + h')}$$

A_{ℓ} = total area of longitudinal steel

A_t = area of one leg of a closed stirrup

s = stirrup spacing

b' = centerline width of a closed stirrup

h' = centerline height of a closed stirrup

The actual value of m for above three beams is 0.42. For this reason an equivalent stirrup spacing has been obtained based on $m = 0.7$ and theory then applied.

6.4 Comparison of Experimental and Theoretical Results

In order to verify accuracy of the theory presented in this

chapter, this analysis was applied to eighty-four beams reported in the experimental phase of this investigation. Tables 6.1, 6.2 and 6.3 summarize experimental and theoretical results for series A, B and C, respectively. Since torsion to bending ratio (ψ), and torsion to shear ratio (δ) are known, theoretical values for bending and shear are not reported here for the case of combined loading, as they can be easily calculated from torques and loading ratios. Theoretical values for pure bending are, however, reported in column 7. Test/theory values for bending and torsion are tabulated in columns 8 and 10, respectively. In columns 12 through 14 principal strains and stresses of concrete in the compression zone at failure are reported. It is interesting to observe higher tensile strains and stresses for modes 2 and 3 than for mode 1.

Test/theory values are in a range of 1 ± 0.20 for all beams, indicating good correlation between experimental and theoretical results. Table 6.4 gives a summary of average test/theory values for all three series. It is important to note a very good correlation, not only between experimental and theoretical results, but also from two other aspects. Table 6.4 shows that an average test/theory value for beams subjected to bending is 0.996 while in the case of combined loading is 1.008. This table also shows that a uniform accuracy is obtained for all three modes in the case of combined loading. It is strongly felt that the excellent correlation in all aspects resulted from the use of a uniform failure criteria over the entire range of loading ratios.

TABLE 6.1 ULTIMATE STRENGTH, COMPARISON OF EXPERIMENTAL AND THEORETICAL RESULTS, SERIES A

Beam no.	Experimental Results					Theoretical Results								
	M_{test} in.k.	T_{test} in.k.	V_{test} k.	ψ	δ	M in.k.	$\frac{M_{test}}{M}$	T in.k.	$\frac{T_{test}}{T}$	Failure mode	Princ. strains & stresses			
											ε_{comp} x 100	ε_{tens} x 100	σ_{comp} psi	σ_{tens} psi
1	2	3	4	5	6	7	8	9	10	11	12	13	14	15
AA-1	797	0	0	0.000		661	1.206	0			0.3800	0.0000	3719	0
-2	662	95	0	0.144	∞			114	0.833	1	0.3791	0.0011	3654	65
-3	478	159	0	0.333	∞			133	1.195	2	0.0432	0.0140	1402	439
-4	206	155	0	0.752	∞			132	1.174	2	0.0440	0.0140	1347	455
-5	118	157	0	1.331	∞			136	1.154	2	0.0454	0.0139	1453	500
-6	55	164	0	2.982	∞			141	1.163	2	0.0447	0.0142	1478	439
-7	0	178	0	∞	∞			149	1.195	2	0.0479	0.0141	1667	536
AB-1	747	0	11.67	0.000	0.000	659	1.134	0			0.3800	0.0000	3696	0
-2	712	82	11.67	0.115	2.342			68	1.206	1	0.3786	0.0007	3650	44
-3	543	120	9.20	0.221	4.348			123	0.976	2	0.0474	0.0138	1622	561
-4	125	146	5.00	1.168	9.733			137	1.066	2	0.0475	0.0140	1677	561
-5	48	156	3.00	3.250	17.333			139	1.122	2	0.0458	0.0139	1609	500
-6	28	148	1.27	5.286	38.845			139	1.065	2	0.0456	0.0140	1528	495

TABLE 6.1 (Cont'd) ULTIMATE STRENGTH, COMPARISON OF EXPERIMENTAL AND THEORETICAL RESULTS, SERIES A

Beam no.	Experimental Results					Theoretical Results								
	M_{test} in.k.	T_{test} in.k.	V_{test} k.	ψ	δ	M in.k.	$\frac{M_{test}}{M}$	T in.k.	$\frac{T_{test}}{T}$	Failure mode	Princ. strains & stresses			
											ε_{comp} x 100	ε_{tens} x 100	σ_{comp} psi	σ_{tens} psi
1	2	3	4	5	6	7	8	9	10	11	12	13	14	15
AC-1	770	0	0	0.000		723	1.065				0.3800	0.0000	4395	0
-2	662	106	0	0.160	∞			117	0.906	1	0.3791	0.0011	3650	70
-3	379	141	0	0.372	∞			153	0.922	2	0.0487	0.0140	1819	610
-4	200	150	0	0.750	∞			148	1.014	2	0.0455	0.0139	1691	511
-5	126	167	0	1.325	∞			148	1.128	2	0.0469	0.0139	1705	536
-6	56	168	0	3.000	∞			151	1.113	2	0.0485	0.0141	1760	580
-7	0	171	0	∞	∞			149	1.148	2	0.0487	0.0138	1720	612
AD-1	787	0	12.30	0.000	0.000	742	1.061				0.3800	0.0000	4630	0
-2	748	63	11.33	0.084	1.854			66	0.955	1	0.3798	0.0008	4263	49
-3	368	124	8.00	0.337	5.167			127	1.016	2	0.0472	0.0139	1601	557
-4	124	130	4.43	1.048	9.782			143	0.909	2	0.0458	0.0140	1836	542
-5	57	135	2.60	2.368	17.308			140	0.964	2	0.0456	0.0140	1645	502
-6	19	137	1.17	7.211	46.837			146	0.938	2	0.0469	0.0141	1743	563

TABLE 6.1 (Cont'd) ULTIMATE STRENGTH, COMPARISON OF EXPERIMENTAL AND THEORETICAL RESULTS, SERIES A

Beam no.	Experimental Results					Theoretical Results								
											Princ. strains & stresses			
	M_{test} in.k.	T_{test} in.k.	V_{test} k.	ψ	δ	M in.k.	$\frac{M_{test}}{M}$	T in.k.	$\frac{T_{test}}{T}$	Failure mode	ε_{comp} x 100	ε_{tens} x 100	σ_{comp} psi	σ_{tens} psi
1	2	3	4	5	6	7	8	9	10	11	12	13	14	15
AE-1	904	0	0	0.000		788	1.147				0.3800	0.0000	3462	0
-2	864	124	0	0.144	∞			125	0.992	1	0.1400	0.0120	3550	521
-3	466	124	0	0.266	∞			144	0.861	2	0.0454	0.0142	1513	455
-4	230	172	0	0.748	∞			150	1.147	2	0.0475	0.0140	1694	544
-5	122	162	0	1.328	∞			134	1.209	2	0.0439	0.0142	1374	455
-6	57	172	0	3.018	∞			137	1.256	2	0.0452	0.0139	1480	506
-7	0	154	0	∞	∞			141	1.092	2	0.0454	0.0137	1480	504
AF-1	880	0	14.67	0.000	0.000	790	1.114				0.3800	0.0000	3516	0
-2	821	83	14.67	0.101	1.886			101	0.822	1	0.2371	0.0092	3263	550
-3	351	134	10.33	0.382	4.324			117	1.145	2	0.0480	0.0139	1478	557
-4	90	146	5.00	1.622	9.733			134	1.090	2	0.0452	0.0142	1603	485
-5	60	149	2.87	2.483	17.306			134	1.112	2	0.0455	0.0140	1540	506
-6	25	160	1.37	6.400	38.929			139	1.151	2	0.0450	0.0140	1603	515

TABLE 6.1 (Cont'd) ULTIMATE STRENGTH, COMPARISON OF EXPERIMENTAL AND THEORETICAL RESULTS, SERIES A

Beam no.	Experimental Results					Theoretical Results								
	M_{test} in.k.	T_{test} in.k.	V_{test} k.	ψ	δ	M in.k.	$\frac{M_{test}}{M}$	T in.k.	$\frac{T_{test}}{T}$	Failure mode	Princ. strains & stresses			
											ε_{comp} x 100	ε_{tens} x 100	σ_{comp} psi	σ_{tens} psi
1	2	3	4	5	6	7	8	9	10	11	12	13	14	15
AG-1	1026	0	0	0.000		899	1.141				0.3800	0.0000	4331	0
-2	756	118	0	0.156	∞			124	0.952	1	0.1359	0.0119	3676	544
-3	409	136	0	0.913	∞			150	0.907	2	0.0493	0.0140	1792	649
-4	200	150	0	0.750	∞			147	1.020	2	0.0464	0.0140	1667	525
-5	109	146	0	1.339	∞			152	0.961	2	0.0463	0.0139	1719	502
-6	50	150	0	3.000	∞			153	0.980	2	0.0493	0.0142	1830	615
-7	0	144	0	∞	∞			153	0.941	2	0.0475	0.0141	1842	587
AH-1	910	0	12.00	0.000	0.000	833	1.092				0.3800	0.0000	3786	0
-2	720	107	12.00	0.149	2.972			91	1.176	1	0.1847	0.0107	4477	525
-3	504	117	9.00	0.232	4.333			120	0.975	2	0.0472	0.0139	1581	575
-4	72	117	4.00	1.625	9.750			122	0.959	2	0.0429	0.0140	1327	424
-5	49	131	2.33	2.674	18.741			136	0.963	2	0.0453	0.0142	1587	506
-6	21	143	0.97	6.810	49.141			140	1.021	2	0.0470	0.0140	1603	554

TABLE 6.2 ULTIMATE STRENGTH, COMPARISON OF EXPERIMENTAL AND THEORETICAL RESULTS, SERIES B

Beam no.	Experimental Results					Theoretical Results								
											Princ. strains & stresses			
	M_{test} in.k.	T_{test} in.k.	V_{test} k.	ψ	δ	M in.k.	$\frac{M_{test}}{M}$	T in.k.	$\frac{T_{test}}{T}$	Failure mode	ε_{comp} x 100	ε_{tens} x 100	σ_{comp} psi	σ_{tens} psi
1	2	3	4	5	6	7	8	9	10	11	12	13	14	15
BS-1	1067	0	15.91	0.000	0.000	1072	0.995				0.3800	0.0000	4037	0
-1S	1052	0	15.67	0.000	0.000	1134	0.928				0.3800	0.0000	4451	0
-2	1170	87	17.06	0.074	1.275			93	0.936	1	0.3448	0.0048	4152	275
-2S	1001	109	14.90	0.109	1.829			129	0.845	2	0.1880	0.0106	4896	493
-3	678	210	12.34	0.310	4.255			202	1.040	2	0.0458	0.0139	1728	572
-4	132	232	5.43	1.758	10.681			232	1.000	2	0.0467	0.0140	1831	557
-5	25	236	2.12	9.440	27.830			236	1.000	2	0.0450	0.0139	1752	523
-6	9	203	0.27	22.556	187.963			195	1.041	3	0.0437	0.0141	1690	502
BH-1	933	0	13.95	0.000	0.000	1023	0.912				0.3800	0.0000	4159	0
-2	941	104	14.29	0.111	1.820			101	1.030	1	0.1041	0.0129	3658	443
-3	589	164	9.66	0.278	4.244			179	0.916	3	0.0578	0.0138	2080	418
-4	117	185	4.29	1.581	10.781			193	0.959	3	0.0344	0.0143	1399	477
-5	86	189	2.23	2.198	21.188			175	1.080	3	0.0404	0.0142	1589	457
-6	6	182	0.19	30.333	239.474			170	1.071	3	0.0449	0.0141	1828	428

TABLE 6.2 (Cont'd) ULTIMATE STRENGTH, COMPARISON OF EXPERIMENTAL AND THEORETICAL RESULTS, SERIES B

Beam no.	Experimental Results					Theoretical Results								
	M_{test} in.k.	T_{test} in.k.	V_{test} k.	ψ	δ	M in.k.	$\frac{M_{test}}{M}$	T in.k.	$\frac{T_{test}}{T}$	Failure mode	Princ. strains & stresses			
											ε_{comp} x 100	ε_{tens} x 100	σ_{comp} psi	σ_{tens} psi
1	2	3	4	5	6	7	8	9	10	11	12	13	14	15
B1S-2a	446	50	6.40	0.112	1.953			47	1.064	1	0.3789	0.0009	4222	47
-2b	446	50	6.40	0.112	1.953			(50) 48*	1.042	1	0.3771	0.0011	3961	56
-4a	232	132	3.63	0.569	9.091			124	1.065	1	0.0718	0.0135	2850	523
-4b	287	174	4.81	0.606	9.044			(253) 196*	0.888	1	0.3772	0.0012	4209	64
-6a	8	144	0.25	18.000	144.000			153	0.941	2	0.0503	0.0139	1835	523
-6b	5	208	0.25	41.600	208.000			(351) 224*	0.929	3	0.0575	0.0139	2057	572

* Based on stirrup spacing s = 3.37"

(values in brackets correspond to actual s = 2")

TABLE 6.3 ULTIMATE STRENGTH, COMPARISON OF EXPERIMENTAL AND THEORETICAL RESULTS, SERIES C

Beam no.	Experimental Results					Theoretical Results								
	M_{test} in.k.	T_{test} in.k.	V_{test} k.	ψ	δ	M in.k.	$\frac{M_{test}}{M}$	T in.k.	$\frac{T_{test}}{T}$	Failure mode	Princ. strains & stresses			
											ϵ_{comp} x 100	ϵ_{tens} x 100	σ_{comp} psi	σ_{tens} psi
1	2	3	4	5	6	7	8	9	10	11	12	13	14	15
CS-1	1222	0	17.85	0.000	0.000	1369	0.893				0.3800	0.0000	4046	0
-2	1204	139	17.80	0.115	1.302			172	0.808	1	0.3635	0.0035	3654	226
-3	908	297	16.51	0.327	2.998			234	1.010	2	0.0340	0.0141	1103	521
-4	189	390	10.46	2.063	6.214			332	1.175	3	0.0479	0.0141	1710	415
-5	99	360	5.46	3.636	10.989			329	1.094	3	0.0493	0.0140	1782	403
-6	6	352	0.53	58.667	110.692			327	1.077	3	0.0596	0.0138	2132	373
CH-1	1180	0	17.58	0.000	0.000	1242	0.950				0.0380	0.0000	3654	0
-2	1136	131	16.91	0.115	1.291			137	0.956	1	0.1635	0.0115	3763	402
-3	954	282	15.64	0.296	3.005			273	1.033	3	0.0988	0.0128	2591	413
-4	601	318	9.07	0.529	5.843			312	1.019	3	0.0355	0.0143	1263	350
-5	60	336	5.09	5.600	11.002			306	1.098	3	0.0573	0.0139	1836	419
-6	9	286	0.31	31.444	152.151			312	0.917	3	0.0621	0.0137	2211	375

TABLES 6.4 AVERAGE TEST/THEORY VALUES

	M_{test}/M_{theory} Bending		T_{test}/T_{theory} Combined Loading		
Series A	1.120	MODES	1	0.980	1.018
			2	1.057	
			3		
Series B	0.945	MODES	1	0.977	1.004
			2	0.995	
			3	1.041	
Series C	0.922	MODES	1	0.932	1.001
			2	1.010	
			3	1.061	
0.996					1.008

CHAPTER VII

SUMMARY AND CONCLUSIONS

7.1 Summary

The behavior, cracking and ultimate capacities of solid and hollow prestressed concrete beams subjected to combined torsion, bending and shear have been studied in this investigation. In the experimental phase of this study, tests on eighty-four prestressed beams were performed in order to examine the effects of level of prestress, torsion-bending and torsion-shear loading ratios, amount of longitudinal and transverse reinforcement, longitudinal opening, and the size of cross-section. The analytical phase of this investigation includes an examination of available theories for cracking and ultimate strengths. Two methods for cracking analysis are proposed; the first method is based on the biaxial stress criteria for concrete, and the second which is more straight forward, utilizes equivalent elliptical cross-sections for the determination of torsional shear stresses. Some shortcomings of the commonly used theories for ultimate analysis are pointed out and a new iterative procedure, based on the biaxial strain criteria is presented.

7.2 Conclusions

The following conclusions and recommendations are based on the results of this investigation:

1. Prestressed concrete beams without web reinforcement fail immediately after occurrence of the initial crack, while beams with web reinforcement have considerable strength and ductility beyond cracking.

2. Depending upon the cross-sectional aspect ratio, magnitude and eccentricity of prestress, and the loading ratios, the initial crack can develop on either bottom, side or top face of the beam. Cracking at the bottom generally resulted from predominant bending, at the side, from moderate values of torsion to bending ratios, and at the top, from predominant torsion and high eccentricity of prestressing force.

3. The precracking torsional and flexural stiffnesses were not significantly influenced by loading ratios, ψ and δ nor by the amount of web reinforcement.

4. No stirrup strain was observed up to approximately 50% of the cracking strength, however, beyond this level the increase in stirrup strain occurred at an increasing rate. The contribution of stirrups to the cracking strength can be assessed if a parabolic strain distribution along the potential crack is assumed and the tensile strain of concrete is related to the strain in stirrups. Since an elastic stress-strain relationship exists in the reinforcement at the cracking stage, the stirrup contribution to the cracking strength is directly proportional to the amount of web reinforcement.

5. A very good correlation between experimental and theoretical results for cracking strength can be obtained if the failure criteria for concrete is based on a biaxial stress interaction. This criteria was used in conjunction with the modified elastic theory to include partial "yielding" of the cross-section at cracking. The extent of the yielded regions is larger for

elongated cross-sections than for square or nearly square cross-sections. More data is needed in order to determine α_{ep} and β_{ep} for a greater range of cross-section aspect ratios.

6. Torsional shear stress distribution in a rectangular or hollow box cross-section can be determined using elliptical cross-sections; thus the use of torsion constants α, β, and γ is avoided. This approach is particularly useful for hollow box sections where the only available shear flow theory can not be applied since geometry of reinforced or prestressed beams does not conform to the assumptions of thin-wall theory.

7. The cracking strength and pre-cracking stiffness of a hollow beam is reduced as compared to a similarly reinforced solid beam implying a contribution of the core to the cracking strength and pre-cracking stiffness. However, this reduction is not very significant, indicating an excellent efficiency of hollow beams in torsion and flexure. On the other hand, the use of hollow cross-sections cannot be recommended in the presence of high flexural shear.

8. Experimental torque-moment and torque-shear interaction relationships for hollow and solid cross-sections have been presented. A conservative relationship can be represented by a circular arc providing that the ultimate shear is defined as shear force acting when ultimate flexural capacity is reached. It should be stressed, however, that this is only true for slender beams where shear does not dominate behavior and strength of a beam.

9. The eccentricity of prestressing force, in the case of predominant bending, is beneficial for the ultimate capacity and ductility of a beam, in comparison to a concentrically prestressed beam.

10. The effect of flexural shear in a member is to reduce ultimate strength and ductility of a member subjected to combined loading.

11. Similar to reinforced concrete, prestressed concrete solid and hollow beams exhibited the skew bending mechanism at failure. The failure surface was formed by a tensile crack extending across three faces at approximately the same angle, and the uncracked zone was located adjacent to the fourth face. Depending on loading ratios, beam geometry and relative amounts of transverse and longitudinal reinforcement, the uncracked zone can be located adjacent to top, side or bottom face of the beam.

12. Proposed biaxial strain failure criteria in the ultimate analysis is a logical extension of the uniaxial strain criteria used for flexure and compression. An assumed uniform shear stress distribution in the uncracked zone, though not correct at the pre-cracking or at the stages immediately after cracking can be justified at failure since the depth of the uncracked zone at failure is reduced and hence circulatory stresses are also reduced. This parallels usual assumptions of shear stress distribution in a steel wide flange cross-section subjected to torsion; concrete in the uncracked zone acts as the top flange while the components of tensile forces in reinforcement and dowels act as the bottom flange.

13. No significant difference between ultimate strengths of solid and similarly reinforced hollow cross-sections was observed implying that the neutral axis at ultimate was located in a wall of a hollow cross-section. However, the proposed method can handle also those cases where the neutral axis falls outside the wall thickness; for the determination of shear stresses it is suggested that the outstanding flanges of

channel-shaped uncracked zone be neglected.

14. The developed equations apply to underreinforced and moderately overreinforced beams, however, an excessive amount of reinforcement limits their use. More research is needed to establish the limits of longitudinal and web reinforcement for beams subjected to combined loading.

15. If flexural shear sominates beam behavior, vertical shear stresses in the uncracked zone must be taken into account in the analysis. Depending on the ratio of these vertical shear stresses to the shear-flow stresses (parallel to neutral axis, those considered in the analysis) and normal stresses, use of a three dimensional failure criteria may be appropriate. This would, however, require detailed study of the complex mechanism of shear transfer in a cracked concrete.

REFERENCES

1. American Concrete Institute, "*Building Code Requirements for Reinforced Concrete (ACI 318-71)*", Detroit, Michigan, 1971.

2. American Concrete Institute, "*Commentary on Building Code Requirements for Reinforced Concrete (ACI 318-71)*", Detroit, Michigan, 1971.

3. ASCE-ACI, Joint Task Committee 426, "*The Shear Strength of Reinforced Concrete Members*", Journal of the Structural Division, ASCE 99 (ST6), 1973.

4. Barton, T.G., and Kirk, D.W., "*Concrete T-Beams Subjected to Combined Loading*", Journal of the Structural Division, ASCE 99 (ST4), 1973.

5. Behera, U., Rajagopalan, K.S., and Ferguson, P.M., "*Reinforcement for Torque in Spandrel L-Beams*", Journal of the Structural Division, ASCE 96 (ST2), 1970.

6. Behera, U., and Ferguson, P.M., "*Torsion, Shear and Bending on Stirruped L-Beams*", Journal of the Structural Division, ASCE 96 (ST7), 1970.

7. Birkeland, C.J., Hamilton, M.E., and Mattock, A.H., "*Strength of Reinforced Concrete Beams Without Web Reinforcement in Combined Torsion, Shear and Bending*", The Trend in Engineering 19(4), University of Washington, Seattle, 1967.

8. Bishara, A., "*Prestressed Concrete Beams Under Combined Torsion, Bending, and Shear*", Journal of the American Concrete Institute, 66 (7), 1969.

9. Bresler, B., and Pister, K., "*Strength of Concrete Under Combined Stresses*", Journal of the American Concrete Institute, 30 (3), 1958.

10. Chander, H., Kemp, E.L., and Wilhelm, W.J., "*Prestressed Concrete Rectangular Members Subjected to Pure Torsion*", Civil Engineering Studies Report No. 2007, West Virginia University, Morgantown, West Virginia, 1970.

11. Collins, M.P., "*Torque-Twist Characteristics of Reinforced Concrete Beams*", University of Waterloo Press, SM Study No. 8, 1972.

12. Collins, M.P., and Lampert, P., "*Redistribution of Moments at Cracking - The Key to Simpler Torsion Design*", American Concrete Institute, SP-35, Detroit, Michigan, 1973.

13. Collins, M.P., and Lampert, P., "*Designing for Torsion*", Structural Concrete Symposium, Department of Engineering, University of Toronto, 1971.

14. Collins, M.P., Walsh, P.F., Archer, F.E., and Hall, A.S., "*Ultimate Strength of Reinforced Concrete Beams Subjected to Combined Torsion and Bending*", American Concrete Institute, SP-18, Detroit, Michigan, 1968.

15. Cowan, H.J., "*Reinforced and Prestressed Concrete in Torsion*", Edward Arnold (Publishers) Limited, London, 1950.

16. Cowan, H.J., "*An Elastic Theory for the Torsional Strength of Rectangular Reinforced Concrete Beams*", Magazine of Concrete Research, 2 (4), 1950.

17. Cowan, H.J., and Armstrong, S., "*Experiments on the Strength of Reinforced and Prestressed Concrete Beams and of Concrete-Encased Steel Joists in Combined Bending and Torsion*", Magazine of Concrete Research 7 (19), 1955.

18. Elfgren, L., "*Reinforced Concrete Beams Loaded in Combined Torsion, Bending and Shear*", Publication 71:3, Division of Concrete Structures, Chalmers University of Technology, Göteborg, 1972.

19. Elfgren, L., Karlsson, I., and Losberg, A., "*Torsion-Bending-Shear Interaction for Reinforced Concrete Beams*", Private Communication, 1973.

20. Elfgren, L., Karlsson, I., and Losberg, A., "*Nodal Forces in the Analysis of the Ultimate Torsion Moment for Rectangular Reinforced Concrete Beams*", Private Communication, 1973.

21. Ersoy, U., and Ferguson, P.M., "*Concrete Beams Subjected to Combined Torsion and Shear - Experimental Trends*", American Concrete Institute, SP No. 18, Detroit, Michigan, 1968.

22. Evans, R.H., and Khalil, M.G.A., "*The Behavior and Strength of Prestressed Concrete and Rectangular Beams Subjected to Combined Bending and Torsion*", The Structural Engineer, 48 (2), 1970.

23. Evans, P.R., Kemp, E.L., and Wilhelm, W.J., "*The Behavior of T- and L-Shaped Plain and Reinforced Concrete Beams Loaded in Torsion*", Civil Engineering Studies Report No. 2006, West Virginia University, Morgantown, West Virginia, 1970.

24. Gangarao, H.V.S., and Zia, P., "*Rectangular Prestressed Concrete Beams Under Combined Bending and Torsion*", Department of Civil Engineering, N. Carolina State University at Raleigh, 1970.

25. Gesund, H., and Boston, L.A., "*Ultimate Strength in Combined Bending and Torsion of Concrete Beams Containing Only Longitudinal Reinforcement*", Journal of the American Concrete Institute, 61 (11), 1964.

26. Gesund, H., Schuette, F.J., Buchanan, G.R., and Gray, G.A., "*Ultimate Strength in Combined Bending and Torsion of Concrete Beams Containing Both Longitudinal and Transverse Reinforcement*", Journal of the American Concrete Institute, 61, 1964.

27. Goode, C.D., and Helmy, M.A., "*Ultimate Strength of Reinforced Concrete Beams in Combined Bending and Torsion*", American Concrete Institute, SP-18, 1968.

28. Gvozdev, A.A., Lessig, N.N., and Rulle, L.K., "*Research on Reinforced Concrete Beams Under Combined Bending and Torsion in the Soviet Union*", American Concrete Institute, SP-18, 1968.

29. Henry, R.L., and Zia, P., "*Behavior of Rectangular Prestressed Concrete Beams Under Combined Torsion, Bending and Shear*", Department of Civil Engineering, North Carolina State University at Raleigh, 1971.

30. Hognestad, E., "*A Study of Combined Bending and Axial Load in Reinforced Concrete Members*", University of Illinois Engineering Experiment Station, Bulletin Series No. 399, Urbana, Illinois, 1951.

31. Hsu, T.T.C., "*Torsion of Structural Concrete - Plain Concrete Rectangular Section*", American Concrete Institute, SP-18, 1968.

32. Hsu, T.T.C., "*Torsion of Structural Concrete - A Summary on Pure Torsion*", American Concrete Institute, SP-18, 1968.

33. Hsu, T.T.C., "*Torsion of Structural Concrete - Uniformly Prestressed Rectangular Members Without Web Reinforcement*", Journal of Prestressed Concrete Institute, 13 (2), 1968.

34. Hsu, T.T.C., "*Ultimate Torque of Reinforced Rectangular Beams*", Journal of Structural Division, ASCE, 94 (ST2), 1968.

35. Hsu, T.T.C., "*Torsion of Structural Concrete - Behavior of Reinforced Concrete Rectangular Members*", American Concrete Institute, SP-18, 1968.

36. Hsu, T.T.C., "*Post-Cracking Torsional Rigidity of Reinforced Concrete Sections*", Journal of the American Concrete Institute, 70 (5), 1973.

37. Hsu, T.T.C., and Kemp, E.L., "*Background and Practical Application of Tentative Design Criteria for Torsion*", Journal of the American Concrete Institute, 66 (1), 1969.

38. Humphreys, R., "*Torsional Properties of Prestressed Concrete*", The Structural Engineer, 35 (6), 1957.

39. Jacobsen, E.B., "*Torsion, Bending and Shear in Prestressed Concrete Beams*", M.Sc. Thesis, University of Alberta, Edmonton, 1970.

40. Johnston, D.W., and Zia, P., "*Hollow Prestressed Concrete Beams Under Combined Torsion, Bending, and Shear*", Department of Civil Engineering, North Carolina State University at Raleigh, 1971.

41. Johnston, C.D., "*Strength and Deformation of Concrete in Uniaxial Tension and Compression*", Magazine of Concrete Research, Volume 22, No. 70, March 1970.

42. Kemp, E.L., Sozen, M.A., and Siess, C.P., "*Torsion in Reinforced Concrete*", Structural Research Series No. 226, Department of Civil Engineering, University of Illinois, Urbana, Illinois, 1961.

43. Kollbrunner, C.F., and Basler, K., "*Torsion in Structures - An Engineering Approach*", (Translated from the German Edition by E.C. Glauser), Springler-Verlag, Berlin, 1969.

44. Kupfer, H., Hilsdorf, H.K., and Rusch, H., "*Behavior of Concrete Under Biaxial Stresses*", Journal of the American Concrete Institute, 66 (8), 1969.

45. Kuyt, B., "*A Theoretical Investigation of Ultimate Torque as Calculated by the Truss Theory and by the Russian Equilibrium Method*", Magazine of Concrete Research, 23 (77), 1971.

46. Kuyt, B., "*A Method for Ultimate Strength Design of Rectangular Reinforced Concrete Beams in Combined Torsion, Bending and Shear*", Magazine of Concrete Research, 23 (78), 1972.

47. Lampert, P., "*Torsion and Bending in Reinforced and Prestressed Concrete Members*", Proceedings of the Institution of Civil Engineers, Volume 50, 1971.

48. Lampert, P., and Collins, M.P., "*Torsion, Bending and Confusion - An Attempt to Establish the Facts*", Journal of the American Concrete Institute, 69 (8), 1972.

49. Lampert, P., *"Postcracking Stiffness of Reinforced Concrete Beams in Torsion and Bending"*, American Concrete Institute, SP-35, 1973.

50. Leonhardt, F., *"Shear and Torsion in Prestressed Concrete"*, Lecture, Session IV, VI FIP Congress, Prague, Czechoslovakia, 1970.

51. Lessig, N.N., *"Theoretical and Experimental Investigation of Reinforced Concrete Members Subjected to Combined Bending and Torsion"*, (in Russian), Theory of Design and Construction of Reinforced Concrete Structures, Moscow, Russia, 1958.

52. Lessig, N.N., *"Determination of the Load-Bearing Capacity of Reinforced Concrete Elements with Rectangular Cross Section Subjected to Flexure and Torsion"*, (in Russian), Trudy No. 5, Concrete and Reinforced Concrete Institute, Moscow, Russia, 1959.

53. Liao, H., and Ferguson, P.M., *"Combined Torsion in Reinforced Concrete L-Beams with Stirrups"*, Journal of the American Concrete Institute, 66 (12), 1969.

54. McGee, W.D., and Zia, P., *"Prestressed Concrete Members Under Torsion, Shear and Bending"*, Department of Civil Engineering, North Carolina State University at Raleigh, 1973.

55. McMullen, A.E., and Warwaruk, J., *"The Torsional Strength of Rectangular Reinforced Concrete Beams Subjected to Combined Loading"*, Report No. 2, Department of Civil Engineering, University of Alberta, Edmonton, 1967.

56. Mitchell, D., Lampert, P., and Collins, M.P., *"The Effects of Stirrup Spacing and Longitudinal Restraint on the Behavior of Reinforced Concrete Beams Subjected to Torsion"*, Publication 71-22, Department of Civil Engineering, University of Toronto, Toronto, 1971.

57. Mukherjee, P.R., and Kemp, E.L., *"Ultimate Torsional Strength of Plain, Prestressed, and Reinforced Concrete Members of Rectangular Cross Section"*, Civil Engineerin Studies No. 2003, Department of Civil Engineering, University of West Virginia, Morgantown, 1970.

58. Mukherjee, P., and Warwaruk, J., *"Prestressed Concrete Beams with Web Reinforcement Under Combined Loading"*, Structural Engineering Report No. 24, University of Alberta, Edmonton, 1970.

59. Nadai, A., *"Theory of Flow and Fracture of Solids"*, McGraw Hill Book Company, Inc., New York, 1950.

60. Pandit, G.S., and Warwaruk, J., "*Reinforced Concrete Beams in Combined Bending and Torsion*", American Concrete Institute, SP-18, Detroit, Michigan, 1968.

61. Popov, E.P., "*Introduction to Mechanics of Solids*", Prentice-Hall, Inc., New Jersey, 1968.

62. Rajagopalan, K.S., Behera, U., and Ferguson, P.M., "*Partially Over-Reinforced Beams Under Pure Torsion*", Journal of the American Concrete Institute, 68 (10), 1971.

63. Rajagopalan, K.S., Behera, U., and Ferguson, P.M., "*Total Interaction Method for Torsion Design*", Journal of the Structural Division, ASCE 98 (ST9), 1972.

64. Rangan, B.V., and Hall, A.S., "*Strength of Rectangular Prestressed Concrete Beams in Combined Torsion, Bending and Shear*", Journal of the American Concrete Institute, 70 (4), 1973.

65. Rao, D.L.N. and Warwaruk, J., "*Prestressed Concrete I-Beams Subjected to Combined Loadings*", Structural Engineering Report No. 46, University of Alberta, Edmonton, 1973.

66. Rao, D.L.N., and Warwaruk, J., "*Finite Element Analysis for Combined Loadings with Improved Hexahedrons*", Structural Engineering Report No. 47, University of Alberta, Edmonton, 1973.

67. Shaw, F.S., "*Torsion of Solid and Hollow Prisms in the Elastic and Plastic Range by Relaxation Methods*", Report ACA-11, Australian Council for Aeronautics, Melbourne, Australia, 1944.

68. Swamy, N., "*The Behavior and Ultimate Strength of Prestressed Concrete Hollow Beams Under Combined Bending and Torsion*", Magazine of Concrete Research, 14 (40), 1962.

69. Timoshenko, S.P., and Goodier, J.N., "*Theory of Elasticity*", McGraw Hill Book Company, Inc., New York, 1970.

70. Turner, L. and Davies, V.C., "*Plain and Reinforced Concrete in Torsion, with Particular Reference to Reinforced Concrete Beams*", Selected Engineering Papers No. 165, The Institute of Civil Engineers, London, England, 1934.

71. Victor, D.J., and Ferguson, P.M., "*Reinforced Concrete T-Beams Without Stirrups Under Combined Moment and Torsion*", Journal of the American Concrete Institute, 65 (1), 1968.

72. Vlasov, V.Z., "*Thin-Walled Elastic Beams*", (Translated from Russian), 2nd Edition, Israel Program for Scientific Translations, Jerusalem, 1961.

73. Victor, D.J, and Ferguson, P.M., "*Beams Under Distributed Load Creating Moment, Shear, and Torsion*", Journal of the American Concrete Institute, 65 (4), 1968

74. Warwaruk, J., and Misic, J., "*Prestressed Concrete Beams Subjected to Combined Bending, Torsion and Shear - An Experimental Study (In Serbo-Croatian)*", Civil Engineer VI, Zagreb, Yugoslavia, 1971.

75. Woodhead, H.R., and McMullen, A.E., "*A Study of Prestressed Concrete Under Combined Loading*", Research Report No. CE 72-43, University of Calgary, Calgary, 1972.

76. Wyss, A.N., Garland, J.B., and Mattock, A.H., "*A Study of the Behavior of I-Section Prestressed Concrete Girders Subject to Torsion*", Structures and Mechanics Report SM 9-1, University of Washington, Seattle, 1969.

77. Wyss, A.N., and Mattock, A.H., "*A Study of I-Section Prestressed Concrete Girders Subject to Torsion, Shear and Bending*", Structures and Mechanics Report SM 71-1, University of Washington, Seattle, 1971.

78. Yudin, V.K., "*Determination of Load-Bearing Capacity of Reinforced Concrete Members of Rectangular Cross Section Under Combined Torsion and Bending*", (in Russian), Beton and Zhelezobeton 6, Moscow, Russia, 1962.

79. Zia, P., "*Torsional Strength of Prestressed Concrete Members*", Ph.D. Thesis, Department of Civil Engineering, University of Florida, Gainsville, 1960.

80. Zia, P., "*Torsional Strength of Prestressed Concrete Members*", Journal of the American Concrete Institute, 57 (10), 1961.

81. Zia, P., "*Torsion Theories for Concrete Members*", American Concrete Institute, SP-18, 1968.

82. Zia, P., "*What do We Know About Torsion in Concrete Members*", Journal of the Structural Division, ASCE 96 (ST6), 1970.

APPENDIX A

TEST RESULTS FOR SERIES B AND C

Complete test results for each beam of series B and C are presented in this appendix. Tables A-1 to A-32 contain torques, bending moments, shears, twists and deflections for each increment obtained in the experimental phase of this investigation. In essence, this chapter represents detailed information for series B and C as compared to that in Chapter 4 where only final results are given. Series A is not included here for two reasons: first as mentioned previously, beams of this series were not instrumented well, and second, some data for this series is available elsewhere[39, 74].

The locations of twisting meters and deflection guages are presented in Chapter 3.

In some cases, collapse of a beam occurred as final readings were being taken; therefore some information is missing for the last increment for several beams. Increments corresponding to first cracking and ultimate are designated in these tables for each beam using a single and double asterisk, respectively. With the exception of beam CH-6, no deflections were taken for beams tested in pure torsion; this was done for beam CH-6 primarily to observe upward deflection, since a mode 3 was expected. Similarly, for beams tested in pure bending no stirrup strains were taken.

TABLE A-1

TEST RESULTS - OBSERVED DATA FOR BEAM BS-1

Load Stage	Torque (in.kips)	Bend.M. (in.kips)	Shear (kips)	Twist (rad/in x 10^4)	Deflections (inches x 10^3)		
					East	Center	West
0		19	0.02		0	0	0
1		121	1.57		10	15	20
2		231	3.23		25	35	50
3		342	4.91		45	65	90
4		451	6.57		60	95	125
5		517	7.57		70	120	150
6		583	8.57		80	140	173
7		627	9.24		95	150	185
8*		671	9.91		95	160	203
9		715	10.57		110	180	225
10		759	11.24		120	195	250
11		803	11.91		135	225	280
12		847	12.57		145	245	315
13		891	13.24		165	280	360
14		935	13.91		180	315	405
15		979	14.57		200	350	435
16		1023	15.24		210	380	520
17**		1067	15.91		240	455	610

* First Crack
** Ultimate

TABLE A-2

TEST RESULTS - OBSERVED DATA FOR BEAM BS-1S

Load Stage	Torque (in.kips)	Bend.M. (in.kips)	Shear (kips)	Twist (rad/in x 10^4)	Deflections (inches x 10^3)		
					East	Center	West
0		19	0.02		0	0	0
1		121	1.59		15	25	25
2		231	3.23		35	55	60
3		341	4.90		50	80	90
4		407	5.90		55	100	110
5		473	6.90		70	120	130
6		517	7.57		75	130	150
7		561	8.25		85	140	160
8		605	8.90		90	155	180
9		627	9.23		95	160	190
10		649	9.57		95	170	200
11		671	9.90		100	175	205
12*		693	10.23		100	180	215
13		715	10.57		110	200	220
14		759	11.23		125	220	245
15		803	11.90		135	235	270
16		847	12.57		145	260	305
17		891	13.23		155	290	350
18		935	13.90		175	325	395
19		979	14.57		195	365	445
20		1023	15.23		285	550	540
21**		1052	15.67		-	-	-

* First Crack
** Ultimate

TABLE A-3

TEST RESULTS - OBSERVED DATA FOR BEAM BS-2

Load Stage	Torque (in.kips)	Bend.M. (in.kips)	Shear (kips)	Twist (rad/in x 10^6)	Deflections (inches x 10^3)		
					East	Center	West
0	0	19	0.01	0	0	0	0
1	8	124	1.56	5	15	15	25
2	17	235	3.21	6	25	40	50
3	25	348	4.88	9	40	60	85
4	34	461	6.56	14	50	83	115
5	39	528	7.56	15	65	105	135
6	44	596	8.56	20	70	125	160
7	48	641	9.23	22	80	140	125
8	51	686	9.92	22	85	145	190
9*	54	731	10.56	25	90	165	205
10	59	798	11.56	28	70	165	220
11	65	866	12.56	36	85	190	260
12	70	933	13.56	38	110	235	333
13	73	998	14.23	48	145	305	395
14	76	1024	14.90	56	165	340	460
15	80	1068	15.56	59	195	390	525
16	82	1102	16.06	72	205	430	600
17	84	1125	16.36	73	220	470	640
18	86	1147	16.73	79	235	520	710
19**	87	1170	17.06	-	-	-	-

* First Crack
** Ultimate

TABLE A-4

TEST RESULTS - OBSERVED DATA FOR BEAM BS-2S

Load Stage	Torque (in.kips)	Bend.M. (in.kips)	Shear (kips)	Twist (rad/in x 10^6)	Deflections (inches x 10^3)		
					East	Center	West
0	0	19	0.02	0	0	0	0
1	12	134	1.77	1	10	20	25
2	24	231	3.23	9	25	40	50
3	34	319	4.57	14	35	65	75
4	44	407	5.90	21	45	85	100
5	49	451	6.57	23	55	95	120
6	53	495	7.23	23	55	110	130
7*	58	539	7.90	27	60	120	140
8	63	583	8.57	33	65	130	160
9	64	605	8.90	35	80	140	170
10	68	627	9.23	35	80	150	180
11	70	649	9.57	36	80	155	185
12	73	671	9.90	37	85	165	200
13	78	715	10.57	42	90	175	210
14	83	759	11.23	48	100	190	240
15	87	803	11.90	53	110	225	265
16	92	847	12.57	57	125	240	295
17	97	891	13.23	65	135	275	330
18	100	913	13.57	68	145	305	380
19	102	935	13.90	78	155	330	420
20	104	957	14.23	84	175	365	455
21	107	979	14.57	90	180	390	500
22**	109	1001	14.90	-	-	445	570

* First Crack
** Ultimate

TABLE A-5

TEST RESULTS - OBSERVED DATA FOR BEAM BS-3

Load Stage	Torque (in.kips)	Bend.M. (in.kips)	Shear (kips)	Twist (rad/in x 10^6)	Deflections (inches x 10^3)		
					East	Center	West
0	0	18	0.12	0	0	0	0
1	28	102	1.67	10	-10	5	25
2	57	192	3.34	22	30	45	55
3	79	264	4.67	33	40	65	75
4	91	300	5.34	42	45	75	95
5	102	336	6.01	46	45	85	110
6	113	372	6.67	54	50	100	120
7	125	408	7.34	58	55	105	130
8	136	444	8.01	73	60	115	140
9*	147	480	8.67	76	60	125	145
10	159	516	9.34	88	65	135	170
11	170	552	10.01	99	75	160	195
12	176	570	10.34	109	95	180	225
13	181	588	10.67	119	100	205	255
14	187	606	11.01	140	105	215	280
15	193	624	11.34	151	105	235	310
16	198	642	11.67	168	125	265	340
17	201	651	11.84	185	140	295	405
18	204	660	12.01	202	145	320	435
19	207	669	12.17	225	155	345	485
20**	210	678	12.34	-	-	465	-

* First Crack
** Ultimate

TABLE A-6

TEST RESULTS - OBSERVED DATA FOR BEAM BS-4

Load Stage	Torque (in.kips)	Bend.M. (in.kips)	Shear (kips)	Twist (rad/in x 10^6)	Deflections (inches x 10^3)		
					East	Center	West
0	0	10	0.38	0	0	0	0
1	30	23	0.93	7	-35	-35	-30
2	45	32	1.27	15	-40	-35	-30
3	60	40	1.60	20	-40	-35	-45
4	75	47	1.93	27	-40	-40	-40
5	90	56	2.27	37	-40	-45	-40
6	105	64	2.60	44	-40	-40	-30
7	120	71	2.93	53	-40	-35	-25
8	135	80	3.27	62	-45	-30	-20
9	150	88	3.60	70	-40	-25	-15
10*	165	95	3.93	80	-35	-20	-10
11	180	104	4.27	92	-35	-15	- 5
12	195	112	4.60	105	-45	-10	5
13	210	119	4.93	122	-50	- 5	15
14	215	122	5.03	133	-50	0	20
15	219	124	5.13	143	-50	5	25
16	225	128	5.27	153	-45	5	25
17	229	130	5.37	194	-45	0	25
18	231	131	5.40	480	-15	20	35
19**	232	132	5.43	570	+15	40	55

* First Crack
**Ultimate

TABLE A-7

TEST RESULTS - OBSERVED DATA FOR BEAM BS-5

Load Stage	Torque (in.kips)	Bend.M. (in.kips)	Shear (kips)	Twist (rad/in x 10^4)	Deflections (inches x 10^3)		
					East	Center	West
0	0	6	0.48	0	0	0	0
1	45	8	0.70	16	0	0	5
2	68	10	0.87	30	0	5	0
3	90	12	1.03	37	-10	5	5
4	104	14	1.13	44	-10	- 5	10
5	117	15	1.23	52	-20	- 5	5
6	130	16	1.33	60	-20	-10	5
7	140	17	1.40	67	-25	-10	5
8	149	18	1.47	74	-20	-10	5
9	158	18	1.53	79	-25	-10	5
10	167	19	1.60	84	-20	-10	5
11	176	20	1.67	90	-25	-10	5
12*	184	21	1.73	101	-25	-10	0
13	194	22	1.80	110	-25	-15	5
14	203	22	1.87	119	-30	-15	5
15	212	23	1.93	128	-35	-15	5
16	221	24	2.00	147	-35	-20	0
17	225	24	2.03	165	-35	-15	0
18	230	25	2.07	186	-40	-20	5
19	234	25	2.10	221	-40	-20	0
20**	236	25	2.12	-	-40	-35	-25

* First Crack
** Ultimate

TABLE A-8

TEST RESULTS - OBSERVED DATA FOR BEAM BS-6

Load Stage	Torque (in.kips)	Bend.M. (in.kips)	Shear (kips)	Twist (rad/in x 10^4)	Deflections (inches x 10^3)		
					East	Center	West
0	0	9	0.27	0			
1	45	9	0.27	22			
2	68	9	0.27	46			
3	90	9	0.27	64			
4	104	9	0.27	72			
5	117	9	0.27	88			
6	130	9	0.27	105			
7	140	9	0.27	125			
8	149	9	0.27	135			
9*	158	9	0.27	151			
10	167	9	0.27	153			
11	168	9	0.27	164			
12	170	9	0.27	160			
13	176	9	0.27	179			
14	176	9	0.27	184			
15	184	9	0.27	191			
16	194	9	0.27	217			
17	197	9	0.27	264			
18	202	9	0.27	253			
19**	203	9	0.27	326			
20	185	9	0.27	509			

* First Crack
** Ul

TABLE A-9

TEST RESULTS - OBSERVED DATA FOR BEAM BH-1

Load Stage	Torque (in.kips)	Bend.M. (in.kips)	Shear (kips)	Twist (rad/in x 10^4)	Deflections (inches x 10^3)		
					East	Center	West
0		17	0.07		0	0	0
1		119	1.62		10	25	20
2		229	3.28		30	55	55
3		339	4.95		50	90	85
4		403	5.95		60	100	110
5		449	6.62		60	120	120
6		493	7.28		70	130	140
7*		537	7.95		75	145	160
8		581	8.62		85	155	180
9		625	9.28		90	180	205
10		669	9.95		100	200	240
11		713	10.62		115	230	280
12		757	11.28		130	260	320
13		801	11.95		150	295	365
14		845	12.62		165	335	430
15		867	12.95		180	380	470
16		889	13.28		190	395	500
17		911	13.62		210	440	570
18**		933	13.95		-	-	615

* First Crack
** Ultimate

TABLE A-10

TEST RESULTS - OBSERVED DATA FOR BEAM BH-2

Load Stage	Torque (in.kips)	Bend.M. (in.kips)	Shear (kips)	Twist (rad/in x 10^4)	Deflections (inches x 10^3)		
					East	Center	West
0	0	17	0.08	0	0	0	0
1	12	118	1.63	6	10	25	25
2	24	226	3.29	11	25	50	55
3	34	313	4.63	17	40	70	85
4	44	399	5.96	19	45	90	110
5	49	443	6.63	23	50	110	130
6	53	486	7.29	27	60	120	140
7*	58	529	7.96	31	70	135	160
8	63	573	8.63	36	75	145	175
9	68	616	9.29	40	80	170	200
10	73	659	9.96	47	90	190	230
11	78	703	10.63	57	100	210	260
12	83	746	11.29	81	115	240	300
13	87	789	11.96	93	120	270	345
14	92	833	12.63	117	145	310	385
15	95	854	12.96	133	150	325	415
16	97	876	13.29	157	165	360	455
17	99	887	13.46	167	175	380	485
18	100	898	13.63	175	180	395	505
19	101	908	13.79	182	190	410	525
20	102	919	13.96	191	195	425	545
21	103	930	14.13	198	200	445	570
22**	104	941	14.29	-	-	-	590

* First Crack
** Ultimate

TABLE A-11

TEST RESULTS - OBSERVED DATA FOR BEAM BH-3

Load Stage	Torque (in.kips)	Bend.M. (in.kips)	Shear (kips)	Twist (rad/in x 10^4)	Deflections (inches x 10^3)		
					East	Center	West
0	0	16	0.11	0	0	0	0
1	28	109	1.66	11	10	20	25
2	57	209	3.32	26	30	50	55
3	79	389	4.66	40	40	75	85
4	91	329	5.32	49	40	90	90
5*	102	369	5.99	56	45	95	110
6	113	409	6.66	70	55	110	125
7	125	449	7.32	104'	65	135	150
8	130	469	7.66	125	70	145	165
9	136	489	7.99	142	80	155	190
10	142	509	8.32	167	85	170	205
11	147	529	8.66	198	90	195	235
12	153	549	8.99	235	105	225	270
13	159	569	9.32	301	115	260	270
14**	164	589	9.66	-	-	-	-

* First Crack
** Ultimate

TABLE A-12

TEST RESULTS - OBSERVED DATA FOR BEAM BH-4

Load Stage	Torque (in.kips)	Bend.M. (in.kips)	Shear (kips)	Twist (rad/in x 10^4)	Deflections (inches x 10^3)		
					East	Center	West
0	0	10	0.31	0	0	0	0
1	15	15	0.52	6	5	15	5
2	30	25	0.86	14	10	15	5
3	45	33	1.19	21	10	10	15
4	60	42	1.52	30	15	15	25
5	75	52	1.86	37	20	20	30
6	90	60	2.19	47	20	20	35
7	97	65	2.36	56	20	25	35
8*	105	69	2.52	60	15	25	40
9	112	74	2.69	69	20	30	40
10	120	79	2.86	81	15	35	50
11	128	83	3.02	95	20	35	50
12	135	87	3.19	105	15	40	55
13	142	92	3.36	117	20	40	60
14	150	96	3.52	127	15	40	60
15	157	101	3.69	146	15	45	65
16	165	106	3.86	157	20	45	70
17	173	110	4.02	180	20	45	75
18	177	113	4.12	262	15	50	75
19	180	114	4.19	299	20	45	75
20	183	116	4.26	354	30	45	75
21**	185	117	4.29	460	25	50	75
22	179	118	4.31	-	-	-	-

* First Crack
** Ultimate

TABLE A-13

TEST RESULTS - OBSERVED DATA FOR BEAM BR-5

Load Stage	Torque (in.kips)	Bend.M. (in.kips)	Shear (kips)	Twist (rad/in x 10^4)	Deflections (inches x 10^3)		
					East	Center	West
0	0	12	0.25	0	0	0	0
1	30	20	0.44	13	- 5	5	5
2	48	28	0.64	22	0	10	5
3	60	33	0.80	30	- 5	5	10
4	72	38	0.93	37	- 5	5	10
5	78	40	1.00	30	0	5	15
6	84	42	1.04	42	- 5	0	10
7	90	43	1.13	44	- 5	5	5
8	96	48	1.20	48	-10	5	10
9	102	50	1.26	53	-10	5	10
10	108	52	1.33	56	-10	5	10
11*	114	55	1.40	62	- 5	5	15
12	120	57	1.46	65	- 5	5	15
13	126	59	1.53	69	- 5	5	10
14	132	62	1.60	80	- 5	5	10
15	138	65	1.66	96	- 5	5	10
16	144	67	1.73	107	-10	5	15
17	150	70	1.80	116	-15	5	15
18	156	72	1.86	125	-10	5	10
19	162	75	1.93	138	-15	5	15
20	168	77	2.00	141	-20	5	15
21	174	77	2.06	201	-25	0	10
22	177	81	2.10	231	-25	- 5	15
23	179	83	2.13	262	-25	- 5	10
24	182	83	2.16	286	-25	-10	10
25	186	85	2.20	331	-25	-10	10
26**	189	86	2.23	405	-25	-15	5

* First Crack
** Ultimate

TABLE A-14

TEST RESULTS - OBSERVED DATA FOR BEAM BR-6

Load Stage	Torque (in.kips)	Bend.M. (in.kips)	Shear (kips)	Twist (rad/in x 10^4)	Deflections (inches x 10^3)		
					East	Center	West
0	0	6	0.19	0			
1	45	6	0.19	19			
2	68	6	0.19	32			
3	90	6	0.19	47			
4*	104	6	0.19	53			
5	117	6	0.19	85			
6	130	6	0.19	85			
7	140	6	0.19	102			
8	149	6	0.19	137			
9	152	6	0.19	154			
10	155	6	0.19	163			
11	157	6	0.19	174			
12	160	6	0.19	186			
13	165	6	0.19	193			
14	168	6	0.19	207			
15	172	6	0.19	236			
16	174	6	0.19	291			
17	176	6	0.19	302			
18	179	6	0.19	367			
19	181	6	0.19	438			
20**	182	6	0.19	484			

* First Crack ** Ultimate

TABLE A-15

TEST RESULTS - OBSERVED DATA FOR BEAM B15-2a

Load Stage	Torque (in.kips)	Bend.M. (in.kips)	Shear (kips)	Twist (rad/in x 10^4)	Deflections (inches x 10^3)		
					East	Center	West
0	0	19	0.02	0	0	0	0
1	5	56	0.57	-	0	15	15
2	8	78	0.90	-	0	15	25
3	10	100	1.23	4	5	15	30
4	14	123	1.57	5	10	25	35
5	15	145	1.90	6	10	30	40
6	18	167	2.23	9	10	35	50
7	21	190	2.57	7	15	40	50
8*	23	212	2.90	10	20	45	60
9	26	234	3.23	11	25	50	75
10	31	279	3.90	15	35	85	105
11	33	301	4.23	19	45	100	135
12	36	324	4.57	22	50	125	155
13	39	346	4.90	27	65	145	195
14	41	368	5.23	33	85	190	255
15	42	379	5.40	38	90	210	290
16	44	391	5.57	46	100	235	335
17	45	401	5.73	54	115	270	380
18	46	413	5.90	58	125	295	415
19	48	424	6.07	69	140	340	475
20	49	435	6.23	78	155	385	540
21**	50	446	6.40	-	195	470	675

* First Crack
** Ultimate

TABLE A-16

TEST RESULTS - OBSERVED DATA FOR BEAM B15-2b

Load Stage	Torque (in.kips)	Bend.M. (in.kips)	Shear (kips)	Twist (rad/in x 10^4)	Deflections (inches x 10^3)		
					East	Center	West
0	0	19	0.02	0	0	0	0
1	5	56	0.57	-	5	10	10
2	8	78	0.90	-	5	10	15
3	10	100	1.23	-	10	20	25
4	14	123	1.57	4	10	20	35
5	15	145	1.90	5	10	30	35
6	18	167	2.23	7	15	35	45
7	21	190	2.57	7	15	40	55
8*	23	212	2.90	10	25	45	60
9	26	234	3.23	10	25	55	70
10	31	279	3.90	14	35	85	100
11	36	324	4.57	14	60	130	175
12	39	346	4.90	23	85	165	215
13	41	368	5.23	31	90	200	270
14	44	391	5.57	35	110	250	335
15	45	401	5.73	42	125	290	350
16	46	413	5.90	51	140	325	435
17	48	424	6.07	53	160	365	485
18	49	435	6.23	59	185	425	590
19**	50	446	6.40	-	-	-.	-

* First Crack
** Ultimate

TABLE A-17

TEST RESULTS - OBSERVED DATA FOR BEAM B15-4a

Load Stage	Torque (in.kips)	Bend.M. (in.kips)	Shear (kips)	Twist (rad/in x 10^4)	Deflections (inches x 10^3)		
					East	Center	West
0	0	19	0.08	0	0	0	0
1	12	31	0.29	0	0	5	0
2	24	52	0.63	4	0	5	5
3	36	71	0.96	10	5	15	10
4	48	91	1.29	16	5	25	20
5	54	101	1.46	17	5	25	20
6	60	112	1.63	23	5	25	30
7	66	121	1.79	28	10	25	30
8	72	131	1.96	30	10	30	30
9	78	145	2.13	33	15	35	35
10	84	151	2.29	40	15	40	45
11	90	161	2.46	46	15	45	50
12*	96	172	2.63	48	15	45	50
13	102	181	2.79	54	15	50	55
14	108	191	2.96	64	20	60	65
15	114	202	3.13	75	20	65	75
16	120	211	3.29	98	25	75	95
17	126	221	3.46	134	35	100	125
18**	132	232	3.63	-	-	-	-

* First Crack
** Ultimate

TABLE A-18

TEST RESULTS - OBSERVED DATA FOR BEAM B15-4b

Load Stage	Torque (in.kips)	Bend.M. (in.kips)	Shear (kips)	Twist (rad/in x 10^4)	Deflections (inches x 10^3)		
					East	Center	West
0	0	18	0.10	0	0	0	0
1	24	50	0.65	19	5	5	10
2	36	68	0.98	16	5	10	15
3	48	87	1.31	22	5	15	25
4	60	107	1.65	30	10	25	35
5	72	125	1.98	37	10	25	40
6	84	144	2.31	46	15	30	45
7	90	154	2.48	51	10	35	50
8	96	164	2.65	57	15	40	55
9*	102	173	2.81	62	15	40	60
10	108	182	2.98	68	20	45	65
11	114	192	3.15	73	20	50	75
12	120	201	3.31	80	25	60	85
13	126	211	3.48	93	30	65	100
14	132	221	3.65	106	30	80	105
15	138	230	3.81	125	40	90	130
16	144	239	3.98	148	45	115	160
17	150	249	4.15	172	55	135	190
18	156	258	4.31	211	60	160	225
19	162	268	4.48	256	75	185	270
20	168	278	4.65	315	85	235	325
21**	174	287	4.81	-	-	-	-

* First Crack
** Ultimate

TABLE A-19

TEST RESULTS - OBSERVED DATA FOR BEAM B15-6b

Load Stage	Torque (in.kips)	Bend.M. (in.kips)	Shear (kips)	Twist (rad/in x 10^4)	Deflections (inches x 10^3)		
					East	Center	West
0	0	5	0.25	0			
1	11	0	0.25	4			
2	22	0	0.25	8			
3	32	0	0.25	13			
4	43	0	0.25	19			
5	53	0	0.25	25			
6	64	0	0.25	31			
7	75	0	0.25	36			
8	85	0	0.25	46			
9	96	0	0.25	53			
10	101	0	0.25	58			
11	107	0	0.25	62			
12	112	0	0.25	64			
13*	117	0	0.25	70			
14	122	0	0.25	78			
15	128	0	0.25	83			
16	133	0	0.25	91			
17	138	0	0.25	99			
18**	144	0	0.25	230			
19	115	0	0.25	511			
20	101	0	0.25	764			

* First Crack ** Ultimate

TABLE A-20

TEST RESULTS - OBSERVED DATA FOR BEAM B15-6b

Load Stage	Torque (in.kips)	Bend.M. (in.kips)	Shear (kips)	Twist (rad/in x 10^4)	Deflections (inches x 10^3)		
					East	Center	West
0	0	5	0.25	0			
1	22	5	0.25	7			
2	32	5	0.25	11			
3	43	5	0.25	15			
4	53	5	0.25	21			
5	64	5	0.25	30			
6	75	5	0.25	33			
7	85	5	0.25	42			
8	96	5	0.25	47			
9	107	5	0.25	57			
10	117	5	0.25	64			
11*	128	5	0.25	74			
12	133	5	0.25	80			
13	138	5	0.25	84			
14	144	5	0.25	90			
15	149	5	0.25	95			
16	155	5	0.25	102			
17	160	5	0.25	109			
18	166	5	0.25	114			
19	171	5	0.25	128			
20	176	5	0.25	144			
21	182	5	0.25	175			
22	187	5	0.25	228			
23	190	5	0.25	280			
24	192	5	0.25	323			
25	195	5	0.25	363			
26	197	5	0.25	410			
27	200	5	0.25	448			
28	203	5	0.25	529			
29	206	5	0.25	600			
30**	208	5	0.25	644			
31	197	5	0.25	-			

* First Crack ** Ultimate

TABLE A-21

TEST RESULTS - OBSERVED DATA FOR BEAM CS-1

Load Stage	Torque (in.kips)	Bend.M. (in.kips)	Shear (kips)	Twist (rad/in x 10^4)	Deflections (inches x 10^3)		
					East	Center	West
0		24	0.02		0	0	0
1		128	1.52		5	10	15
2		239	3.18		20	35	40
3		351	4.85		30	60	70
4		463	6.52		45	85	95
5		552	7.85		55	105	115
6		641	9.18		65	125	150
7		708	10.18		75	145	180
8*		733	10.85		80	155	190
9		798	11.52		90	175	210
10		842	12.18		100	185	225
11		887	12.85		105	200	250
12		932	13.52		110	220	270
13		976	14.18		120	235	300
14		1021	14.85		130	260	325
15		1066	15.52		140	290	365
16		1110	16.18		160	320	410
17		1155	16.85		175	360	465
18		1200	17.52		205	380	560
19**		1222	17.85		-	-	-

* First Crack
** Ultimate

TABLE A-22

TEST RESULTS - OBSERVED DATA FOR BEAM CS-2

Load Stage	Torque (in.kips)	Bend.M. (in.kips)	Shear (kips)	Twist (rad/in x 10^4)	Deflections (inches x 10^3)		
					East	Center	West
0	0	28	0.03	0	0	0	0
1	12	127	1.53	4	10	15	20
2	26	236	3.19	4	25	33	40
3	39	346	4.86	7	35	55	70
4	51	457	6.53	9	45	75	90
5	59	523	7.53	10	55	90	110
6	64	568	8.19	11	60	100	125
7	69	610	8.86	12	65	110	140
8	75	655	9.53	14	70	120	150
9*	80	698	10.19	16	75	130	165
10	85	742	10.86	17	80	160	190
11	93	808	11.86	22	90	180	215
12	100	874	12.86	23	100	200	240
13	108	940	13.86	26	115	230	280
14	113	985	14.53	32	125	255	315
15	118	1028	15.19	37	135	280	350
16	123	1072	15.86	37	145	310	385
17	129	1116	16.53	48	165	350	445
18	134	1160	17.19	53	185	400	515
19	136	1183	17.53	58	205	455	590
20**	139	1204	17.80	67	230	500	1165

* First Crack
** Ultimate

TABLE A-23

TEST RESULTS - OBSERVED DATA FOR BEAM CS-3

Load Stage	Torque (in.kips)	Bend.M. (in.kips)	Shear (kips)	Twist (rad/in x 10^{-6})	Deflections (inches x 10^{-3})		
					East	Center	West
0	0	24	6.18	0	0	0	0
1	30	107	1.68	11	10	20	10
2	60	197	3.34	19	15	35	25
3	78	251	4.34	22	25	50	35
4	96	305	5.34	27	30	60	45
5	114	359	6.34	32	40	75	55
6	126	395	7.01	35	45	85	65
7	138	431	7.68	40	50	95	75
8	150	467	8.34	42	55	105	80
9	162	503	9.01	47	45	110	75
10*	174	539	9.68	51	50	115	80
11	186	575	10.34	54	55	125	90
12	198	611	11.01	59	65	135	105
13	210	647	11.68	68	70	150	120
14	222	683	12.34	74	80	165	130
15	234	719	13.01	72	90	190	145
16	246	755	13.68	99	100	215	170
17	258	791	14.34	111	110	245	190
18	264	809	14.68	126	120	265	210
19	270	827	15.01	138	130	285	225
20	276	845	15.34	153	135	310	240
21	[illegible]	863	15.68	169	145	335	265
22	288	881	16.01	184	160	370	295
23	291	890	16.18	202	180	405	330
24	294	899	16.34	223	185	435	355
25**	297	908	16.51	-	-	-	400

* First Crack ** Ultimate

TABLE A-24

TEST RESULTS - OBSERVED DATA FOR BEAM CS-4

Load Stage	Torque (in.kips)	Bend.M. (in.kips)	Shear (kips)	Twist (rad/in x 10^{-6})	Deflections (inches x 10^{-3})		
					East	Center	West
0	0	12	0.63	0	0	0	0
1	39	27	1.46	7	25	35	45
2	65	39	2.13	15	30	45	40
3	91	51	2.79	19	35	50	45
4	117	63	3.46	26	40	50	50
5	143	75	4.13	30	45	55	60
6	169	87	4.79	41	45	70	60
7	195	99	5.46	47	50	75	70
8	209	105	5.79	51	50	80	75
9	221	111	6.13	54	55	80	75
10	234	117	6.46	59	50	85	75
11	247	123	6.79	65	55	90	75
12*	260	129	7.13	70	60	95	80
13	273	135	7.46	74	60	100	85
14	286	141	7.79	80	60	105	85
15	299	147	8.13	86	65	115	90
16	312	153	8.46	91	65	115	95
17	325	159	8.79	99	65	120	95
18	338	165	9.13	109	65	125	100
19	351	171	9.46	123	70	135	110
20	364	177	9.79	147	70	145	115
21	377	183	10.13	221	80	145	120
22	383	186	10.29	430	90	145	105
23**	390	189	10.46	-	-	-	-

* First Crack ** Ultimate

TABLE A-25

TEST RESULTS - OBSERVED DATA FOR BEAM CS-5

Load Stage	Torque (in.kips)	Bend.M. (in.kips)	Shear (kips)	Twist (rad/in x 10^6)	Deflections (inches x 10^3)		
					East	Center	West
0	0	13	0.43	0	0	0	0
1	44	21	1.13	21	5	5	5
2	96	33	1.79	23	5	10	10
3	139	39	2.13	26	5	10	15
4	144	43	2.46	35	5	15	20
5	154	48	2.63	37	5	15	20
6	168	51	2.79	40	10	20	20
7	180	54	2.96	47	10	25	25
8	192	57	3.13	49	10	25	25
9	204	60	3.29	52	10	25	25
10	216	63	3.46	58	5	30	30
11	228	66	3.63	59	10	25	30
12*	240	69	3.79	65	10	30	35
13	252	72	3.96	68	5	25	40
14	264	75	4.13	74	5	30	40
15	276	78	4.29	78	10	30	45
16	288	81	4.46	85	5	30	40
17	300	84	4.63	91	10	25	45
18	312	87	4.79	96	5	30	30
19	324	90	4.96	110	5	30	45
20	336	93	5.13	140	0	30	50
21	348	96	5.29	189	5	25	45
22**	360	99	5.46	343	15	30	45

* First Crack ** Ultimate

TABLE A-26

TEST RESULTS - OBSERVED DATA FOR BEAM CS-6

Load Stage	Torque (in.kips)	Bend.M. (in.kips)	Shear (kips)	Twist (rad/in x 10^6)	Deflections (inches x 10^3)		
					East	Center	West
0	0	6	0.53	0	0	0	0
1	27	6	0.53	7	0	5	0
2	53	6	0.53	10	- 5	0	0
3	80	6	0.53	15	- 5	0	0
4	107	6	0.53	22	-10	- 5	- 5
5	117	6	0.53	25	- 5	0	- 5
6	128	6	0.53	30	-10	- 5	-10
7	138	6	0.53	31	-15	- 5	-10
8	149	6	0.53	33	-15	- 5	- 5
9	160	6	0.53	36	-10	- 5	- 5
10	171	6	0.53	38	-10	- 5	- 5
11	182	6	0.53	41	-15	-10	-10
12*	192	6	0.53	44	-15	- 5	-10
13	208	6	0.53	52	-15	-10	-15
14	225	6	0.53	56	-20	-15	-15
15	241	6	0.53	61	-20	-15	-20
16	256	6	0.53	67	-20	-15	-15
17	272	6	0.53	73	-25	-20	-20
18	288	6	0.53	78	-25	-25	-25
19	304	6	0.53	91	-30	-30	-25
20	315	6	0.53	107	-35	-40	-40
21	326	6	0.53	139	-40	-50	-45
22	331	6	0.53	154	-50	-60	-50
23	342	6	0.53	184	-45	-45	-40
24**	352	6	0.53	267	-50	-85	-45
25	329	6	0.52	-	-	-	-

* First Crack ** Ultimate

TABLE A-27

TEST RESULTS - OBSERVED DATA FOR BEAM CB-1

Load Stage	Torque (in.kips)	Bend.M. (in.kips)	Shear (kips)	Twist (rad/in x 10^6)	Deflections (inches x 10^3)		
					East	Center	West
0		25	0.08		0	0	0
1		124	1.58		0	10	20
2		233	3.24		20	40	55
3		344	4.91		40	65	80
4		410	5.91		50	80	100
5		476	6.91		60	100	120
6		520	7.85		65	105	130
7		563	8.24		70	115	145
8*		608	8.91		75	130	165
9		652	9.58		85	145	175
10		695	10.24		85	155	190
11		740	10.91		90	175	205
12		784	11.58		100	190	230
13		827	12.24		110	210	260
14		872	12.91		120	225	285
15		916	13.58		130	250	310
16		959	14.24		140	270	345
17		1004	14.91		155	295	385
18		1048	15.58		170	335	435
19		1091	16.24		185	375	490
20		1114	16.58		200	405	525
21		1136	16.91		215	435	580
22		1157	17.24		240	490	655
23**		1180	17.58		260	535	730

* First Crack
** Ultimate

TABLE A-28

TEST RESULTS - OBSERVED DATA FOR BEAM CB-2

Load Stage	Torque (in.kips)	Bend.M. (in.kips)	Shear (kips)	Twist (rad/in x 10^6)	Deflections (inches x 10^3)		
					East	Center	West
0	0	25	0.08	0	0	0	0
1	12	124	1.58	2	10	20	25
2	26	233	3.24	5	25	40	55
3	39	344	4.91	7	35	65	80
4	41	454	6.58*	15	50	90	110
5	49	520	7.58	16	55	105	130
6*	50	563	8.24	17	60	120	140
7	69	608	8.91	20	65	130	160
8	73	652	9.58	21	65	145	180
9	80	695	10.24	26	85	165	200
10	85	740	10.91	28	90	180	215
11	90	784	11.58	35	100	200	250
12	95	827	12.24	46	110	215	275
13	100	872	12.91	53	125	245	305
14	105	916	13.58	62	135	275	340
15	111	959	14.24	72	145	300	380
16	116	1004	14.91	88	160	330	425
17	121	1048	15.58	101	175	370	475
18	126	1091	16.24	115	190	400	515
19	129	1114	16.58	126	195	425	550
20**	131	1136	16.91	133	210	455	580

* First Crack
** Ultimate

TABLE A-29

TEST RESULTS - OBSERVED DATA FOR BEAM CH-3

Load Stage	Torque (in.kips)	Bend.M. (in.kips)	Shear (kips)	Twist (rad/in x 10^6)	Deflections (inches x 10^3)		
					East	Center	West
0	0	24	0.14	0	0	0	0
1	30	114	1.64	4	5	15	15
2	60	214	3.30	12	20	35	40
3	78	274	4.30	16	25	50	60
4	96	334	5.30	20	30	60	75
5	108	374	5.97	27	40	70	85
6	120	414	6.64	28	45	85	100
7	132	454	7.30	33	45	95	110
8*	138	474	7.64	32	50	100	115
9	150	514	8.30	38	55	110	130
10	162	554	8.97	44	65	125	145
11	174	594	9.64	52	70	140	160
12	186	634	10.30	62	75	160	185
13	198	674	10.97	79	85	175	215
14	210	714	11.64	101	100	205	245
15	222	754	12.30	120	110	235	290
16	234	794	12.97	137	125	270	330
17	246	834	13.64	186	135	305	375
18	252	854	13.97	211	150	335	415
19	258	874	14.30	236	155	355	445
20	264	894	14.64	258	170	390	485
21	270	913	14.97	290	180	420	525
22	276	934	15.30	323	195	470	590
23**	282	934	15.64	-	-	-	-

* First Crack
** Ultimate

TABLE A-30

TEST RESULTS - OBSERVED DATA FOR BEAM CH-4

Load Stage	Torque (in.kips)	Bend.M. (in.kips)	Shear (kips)	Twist (rad/in x 10^6)	Deflections (inches x 10^3)		
					East	Center	West
0	0	25	0.91	0	0	0	0
1	39	85	1.74	9	5	5	10
2	65	133	2.41	16	10	10	25
3	91	181	3.07	23	10	25	30
4	117	229	3.74	32	10	30	40
5*	143	277	4.41	41	5	35	45
6	169	325	5.07	48	5	35	55
7	195	373	5.74	60	10	50	70
8	221	421	6.41	74	15	55	80
9	247	469	7.07	93	20	70	95
10	260	493	7.41	110	20	80	110
11	267	517	7.74	128	25	90	125
12	286	541	8.07	147	30	100	135
13	299	565	8.41	177	35	110	150
14	312	589	8.74	232	40	130	175
15**	318	601	8.91	302	40	140	195
16	284	613	9.07	-	-	-	-

* First Crack
** Ultimate

TABLE A-31

TEST RESULTS - OBSERVED DATA FOR BEAM CB-5

Load Stage	Torque (in.kips)	Bend.M. (in.kips)	Shear (kips)	Twist (rad/in x 10^6)	Deflections (inches x 10^3)		
					East	Center	West
0	0	6	0.59	0	0	0	0
1	24	8	0.75	4	5	0	5
2	48	12	1.09	9	- 5	0	0
3	72	16	1.42	15	0	0	5
4	96	20	1.75	20	0	0	5
5	108	22	1.92	22	0	5	10
6	120	24	2.09	28	- 5	5	10
7	132	26	2.25	30	-10	5	10
8	144	28	2.42	32	- 5	5	10
9	156	30	2.59	38	-10	5	15
10	168	32	2.75	41	- 5	10	20
11	180	34	2.92	43	- 5	10	25
12*	192	36	3.09	49	0	15	25
13	216	40	3.42	78	0	15	30
14	240	44	3.75	83	0	20	35
15	264	48	4.09	104	0	25	35
16	288	52	4.42	131	0	20	40
17	300	54	4.59	162	- 5	15	40
18	312	56	4.75	223	0	15	40
19	324	58	4.92	310	10	20	40
20**	336	60	5.09	-	-	-	-

* First Crack
** Ultimate

TABLE A-32

TEST RESULTS - OBSERVED DATA FOR BEAM CB-6

Load Stage	Torque (in.kips)	Bend.M. (in.kips)	Shear (kips)	Twist (rad/in x 10^6)	Deflections (inches x 10^3)		
					East	Center	West
0	0	9	0.31	0	0	0	0
1	27	9	0.31	12	0	0	0
2	53	9	0.31	17	- 5	- 5	- 5
3	80	9	0.31	26	-20	- 5	- 5
4	107	9	0.31	31	-25	-10	- 5
5	116	9	0.31	37	-30	-15	- 5
6	128	9	0.31	41	-25	-15	-10
7	133	9	0.31	43	-25	-20	-10
8	139	9	0.31	46	-25	-20	-10
9	144	9	0.31	47	-20	-20	-10
10*	150	9	0.31	49	-20	-20	-10
11	155	9	0.31	52	-20	-20	-10
12	160	9	0.31	54	-20	-20	-10
13	171	9	0.31	60	-25	-20	-15
14	181	9	0.31	65	-25	-20	-10
15	190	9	0.31	73	-25	-25	-15
16	214	9	0.31	122	-30	-30	-15
17	230	9	0.31	148	-35	-40	-25
18	240	9	0.31	186	-40	-45	-35
19	251	9	0.31	217	-50	-55	-40
20	262	9	0.31	253	-55	-60	-45
21	272	9	0.31	317	-55	-65	-55
22**	283	9	0.31	365	-60	-80	-60
23	244	9	0.31	-	-45	-100	-65

* First Crack
** Ultimate

APPENDIX B

STRAIN GAUGE READINGS

Strain gauge readings, recorded during the test of each beam of series B and C, are presented in Tables B-1 through B-59 of this appendix. Generally, each beam was instrumented with seventeen strain gauges; five on the longitudinal prestressing steel, and twelve on stirrups. All gauges were placed at the probable failure region. If a beam was tested in pure bending, no strain gauges were mounted on the stirrups, however, for pure torsion all seventeen strain gauges were used. Detailed location of strain gauges is presented in Chapter 3.

With the exception of beams tested in pure bending, two tables are given for each beam on one page; the first presents strain data for prestressing steel, and the second strain data for transverse steel. It should be remembered that the strain in the prestressing steel, recorded in these tables represents only the increase in strain between zero and ultimate stage of loading. This has to be distinguished from the total strain which includes, in addition, the prestrain.

Increments corresponding to first cracking and ultimate are designated in these tables using a single and double asterisk, respectively.

TABLE B-1

PRESTRESSING STEEL STRAINS (MICRO INCHES PER INCH), BEAM BB-1

Load Stage	Strain Gauge Location				
	a	b	c	d	e
0	0	0	0	0	0
1	75	40	70	-80	-75
2	160	75	155	-180	-160
3	250	115	240	-280	-260
4	355	160	340	-390	-360
5	420	185	405	-470	-425
6	550	225	480	-555	-520
7	645	255	530	-625	-570
8*	720	290	675	-685	-635
9	800	330	820	-770	-770
10	885	380	990	-830	-790
11	995	435	1160	-1040	-870
12	1135	520	1380	-1090	-1020
13	1310	610	1610	-1270	-1120
14	1480	700	1820	-1440	-1320
15	1530	835	1935	-1580	-1465
16	1780	990	2045	-1845	-1580
17**	1970	1220	2070	-2140	-1500

* First Crack
** Ultimate

TABLE B-2

PRESTRESSING STEEL STRAINS (MICRO INCHES PER INCH), BEAM BB-15

Load Stage	Strain Gauge Location				
	a	b	c	d	e
0	0	0	0	0	0
1	70	65	70	-85	-90
2	155	135	150	-185	-190
3	240	210	240	-295	-300
4	300	260	295	-360	-370
5	360	310	360	-440	-450
6	405	345	405	-495	-505
7	450	380	455	-550	-560
8	505	430	510	-615	-620
9	540	455	550	-650	-655
10	570	485	610	-690	-690
11	670	545	680	-730	-730
12*	720	575	735	-765	-765
13	795	620	795	-815	-810
14	890	720	905	-890	-890
15	1040	790	1030	-990	-975
16	1140	860	1130	-1090	-1080
17	1210	895	1225	-1210	-1190
18	1320	850	1320	-1350	-1335
19	1300	830	1415	-1530	-1515
20	1330	825	1575	-1750	-1770
21**	1130	860	6300	-5000	-6400

* First Crack ** Ultimate

TABLE B-3

PRESTRESSING STEEL STRAINS (MICRO INCHES PER INCH), BEAM BS-2

Load Stage	Strain Gauge Location				
	a	b	c	d	e
0	0				
1	50				
2	115				
3	175				
4	245				
5	290				
6	340				
7	375				
8	415				
9*	460				
10	545				
11	615				
12	860				
13	1055				
14	1285				
15	1550				
16	1780				
17	1985				
18	2100				
19**	2900				

* First Crack ** Ultimate

TABLE B-4

STIRRUP STRAINS (MICRO INCHES PER INCH), BEAM BS-2

Load Stage	Strain Gauge Location											
	1-T	1-S	1-B	1-W	2-T	2-S	2-B	2-W	3-T	3-S	3-B	3-W
0	0	0	0	0	0	0	0	0	0	0	0	0
1	10	5	- 5	0	10	0	0	0	10	5	- 5	0
2	20	10	-15	5	25	- 5	- 5	0	20	5	-20	- 5
3	35	15	-25	0	35	- 5	-10	- 5	35	5	-35	- 5
4	45	15	-35	0	50	-10	-15	- 5	45	0	-50	-10
5	55	15	-40	0	60	-15	-15	- 5	50	- 5	-55	-15
6	60	15	-45	0	70	-15	-15	- 5	60	-15	-65	-20
7	65	20	-50	0	75	-20	-15	- 5	65	-20	-65	-25
8	75	20	-55	0	85	-35	-15	- 5	75	-35	-60	-30
9*	75	25	-55	0	90	-25	+ 5	- 5	80	-45	-45	-35
10	85	25	-60	- 5	105	-40	+20	- 5	90	-35	-15	-40
11	95	25	-65	- 5	120	-55	+15	- 5	100	95	115	-25
12	105	15	-70	- 5	140	-30	0	-10	115	210	240	30
13	115	15	-75	-10	155	-15	- 5	-20	125	285	330	120
14	125	10	-75	-15	170	+40	- 5	-30	140	335	405	140
15	135	5	-75	-15	185	+160	-15	-55	155	475	425	175
16	140	0	-75	-15	200	+250	-15	-70	160	555	525	190
17	145	- 5	-70	-20	210	+320	-20	-80	170	560	615	195
18	155	-10	-70	-20	225	+405	-25	-90	190	625	565	205
19**	-	-	-	-	-	-	-	-	-	-	-	-

* First Crack ** Ultimate

TABLE B-5

PRESTRESSING STEEL STRAINS (MICRO INCHES PER INCH), BEAM BS-2S

Load Stage	Strain Gauge Location				
	a	b	c	d	e
0	0	0	0	0	0
1	50	55	60	60	45
2	100	110	115	95	85
3	140	155	165	105	115
4	180	200	210	165	155
5	200	225	235	150	175
6	225	250	265	240	195
7*	245	275	295	305	230
8	270	305	325	430	265
9	280	320	340	530	280
10	295	335	360	520	295
11	305	350	375	560	315
12	320	365	395	585	335
13	345	400	440	600	370
14	370	440	500	620	435
15	400	480	570	680	525
16	425	535	660	965	640
17	460	595	780	1135	745
18	480	640	855	1045	800
19	500	700	915	950	860
20	520	780	1005	860	935
21	540	850	1105	730	1000
22**	555	-	1250	-	-

* First Crack ** Ultimate

TABLE B-6

STIRRUP STRAINS (MICRO INCHES PER INCH), BEAM BS-2S

Load Stage	Strain Gauge Location											
	1-T	1-S	1-B	1-N	2-T	2-S	2-B	2-N	3-T	3-S	3-B	3-N
0	0	0	0	0	0	0	0	0	0	0	0	0
1	10	0	0	10	10	10	0	5	10	5	0	5
2	15	0	0	10	25	10	-10	10	25	10	0	10
3	30	5	-10	10	45	15	-20	10	45	10	- 5	10
4	40	0	-20	15	55	15	-30	10	60	10	- 5	10
5	45	0	-20	15	60	20	-30	10	65	10	- 5	10
6	50	0	-25	15	70	20	-35	10	70	10	0	10
7*	50	0	-25	20	80	20	-40	10	80	5	10	5
8	55	0	-30	15	85	20	-40	10	90	0	40	5
9	60	0	-30	20	90	20	-40	10	95	0	60	5
10	65	0	-30	20	95	25	-40	10	105	- 5	75	5
11	65	0	-30	20	100	25	-40	10	110	-10	90	5
12	70	0	-30	20	105	25	-40	10	115	-15	95	5
13	75	0	-30	20	115	25	-40	10	130	-30	95	10
14	80	0	-30	20	125	25	-30	0	140	-45	95	10
15	90	0	-25	25	140	30	-20	0	155	-30	80	15
16	95	0	-20	25	150	35	-15	- 5	175	0	70	30
17	100	0	-20	25	165	45	-10	-10	195	60	70	35
18	105	0	-10	30	170	45	0	-15	210	110	70	30
19	110	- 5	-10	30	180	45	5	-20	225	145	70	15
20	115	-10	-10	30	190	50	15	-30	250	175	70	0
21	120	-10	-10	35	195	45	20	-40	270	200	75	-15
22**	125	-15	0	35	205	55	20	-40	390	310	90	-35

* First Crack ** Ultimate

TABLE B-7

PRESTRESSING STEEL STRAINS (MICRO INCHES PER INCH), BEAM BS-3

Load Stage	Strain Gauge Location				
	a	b	c	d	e
0	0	0	0	0	0
1	40	50	40	55	60
2	85	110	85	115	135
3	125	155	115	165	195
4	145	185	135	195	230
5	165	210	155	225	265
6	185	235	170	255	305
7	205	265	190	290	345
8	230	295	215	330	385
9*	255	325	235	360	430
10	275	365	265	415	575
11	300	435	295	515	690
12	330	485	315	720	815
13	445	515	320	840	905
14	595	575	340	980	1010
15	705	665	370	1090	1100
16	780	765	395	1195	1190
17	830	845	505	1250	1245
18	790	940	560	1325	1325
19	640	1050	600	1480	1580
20**	-	-	-	-	2400

* First Crack ** Ultimate

TABLE B-8

STIRRUP STRAINS (MICRO INCHES PER INCH), BEAM BS-3

Load Stage	Strain Gauge Location											
	1-T	1-S	1-B	1-N	2-T	2-S	2-B	2-N	3-T	3-S	3-B	3-N
0	0	0	0	0	0	0	0	0	0	0	0	0
1	10	0	0	0	10	0	-10	0	-35	0	0	0
2	20	- 5	0	10	25	- 5	-15	5	-105	0	- 5	0
3	35	-10	0	10	35	-10	-25	10	-85	0	- 5	5
4	40	-10	0	15	45	- 5	-25	10	-175	5	- 5	5
5	45	-10	0	15	50	-10	-30	10	-165	5	- 5	5
6	50	-10	0	15	55	-10	-35	15	-165	5	- 5	5
7	55	-10	0	20	65	- 5	-35	15	-135	5	0	5
8	55	- 5	0	20	70	5	-35	15	-150	- 5	20	0
9*	60	10	0	20	80	35	-25	15	-135	-25	55	- 5
10	65	15	10	20	90	50	-20	10	-125	-35	115	-20
11	70	25	20	20	100	115	-25	5	-105	15	125	-30
12	75	40	25	20	110	205	-25	0	-85	210	120	-80
13	80	45	40	20	115	405	-35	-15	-85	370	130	-95
14	85	45	145	25	120	635	-45	-30	-70	580	150	-85
15	90	45	345	40	130	940	-45	-15	-55	680	185	-110
16	90	75	395	45	140	1230	-25	20	-40	715	225	-140
17	95	140	440	55	145	1540	0	65	-15	770	250	-165
18	95	225	515	70	155	1825	20	125	70	800	295	-530
19	100	310	690	140	165	2050	35	245	320	905	460	-2730
20**	-	-	-	-	-	-	-	-	-	-	-	-

* First Crack ** Ultimate

TABLE B-9

PRESTRESSING STEEL STRAINS (MICRO INCHES PER INCH), BEAM BS-4

Load Stage	Strain Gauge Location				
	a	b	c	d	e
0	0	0	0	0	0
1	15	15	20	25	20
2	25	25	30	40	35
3	40	40	45	55	45
4	45	50	55	65	55
5	60	60	65	80	65
6	75	75	80	100	75
7	90	90	100	120	95
8	95	105	110	130	105
9	110	115	125	150	120
10*	125	130	140	170	135
11	140	150	160	190	155
12	160	170	175	210	190
13	170	190	195	235	740
14	180	200	205	240	875
15	190	205	210	250	900
16	195	215	220	260	900
17	165	190	215	255	895
18	150	135	180	245	885
19**	110	125	165	230	875

* First Crack ** Ultimate

TABLE B-10

STIRRUP STRAINS (MICRO INCHES PER INCH), BEAM BS-4

Load Stage	Strain Gauge Location											
	1-T	1-S	1-B	1-N	2-T	2-S	2-B	2-N	3-T	3-S	3-B	3-N
0	0	0	0	0	0	0	0	0	0	0	0	0
1	5	5	0	5	5	- 5	5	0	5	0	5	0
2	10	5	0	5	5	- 5	10	0	10	- 5	5	- 5
3	15	5	0	5	10	- 5	15	0	15	- 5	10	- 5
4	13	5	- 5	5	10	- 5	15	0	15	- 5	10	- 5
5	15	10	- 5	5	15	- 5	20	0	20	- 5	15	- 5
6	20	20	0	10	15	5	25	5	30	0	20	0
7	25	40	0	20	20	10	40	10	40	0	25	0
8	30	50	5	35	30	25	40	20	40	5	30	- 5
9	30	75	5	25	25	40	50	20	45	15	35	- 5
10*	30	110	10	30	30	90	55	25	50	30	40	0
11	30	175	10	30	30	135	60	30	50	50	50	0
12	35	245	10	35	30	200	65	35	60	65	60	0
13	40	340	15	40	40	310	75	35	65	75	75	-10
14	40	390	15	40	35	360	80	35	65	90	85	-15
15	40	430	15	45	35	400	85	60	70	100	105	-15
16	45	475	15	50	40	445	90	60	70	115	120	-20
17	30	505	10	420	40	450	90	60	70	130	125	-20
18	830	1030	25	1475	50	525	95	70	70	140	135	-25
19**	1265	1085	70	1415	45	470	105	95	65	145	120	-20

* First Crack ** Ultimate

TABLE B-11

PRESTRESSING STEEL STRAINS (MICRO INCHES PER INCH), BEAM BS-5

Load Stage	Strain Gauge Location				
	a	b	c	d	e
0	0	0	0	0	0
1	10	10	10	10	10
2	25	20	20	15	15
3	25	25	20	15	20
4	30	30	25	20	25
5	35	35	25	20	25
6	35	35	25	25	30
7	40	40	30	25	35
8	45	45	30	25	35
9	45	45	35	30	35
10	50	50	35	35	40
11	55	55	35	35	45
12*	60	55	40	35	45
13	70	60	40	40	50
14	70	65	45	45	50
15	75	65	50	45	55
16	75	70	55	50	60
17	75	70	55	55	60
18	75	70	60	55	65
19	55	50	55	55	65
20**	150	-55	15	40	60

* First Crack ** Ultimate

TABLE B-12

STIRRUP STRAINS (MICRO INCHES PER INCH), BEAM BS-5

Load Stage	Strain Gauge Location											
	1-T	1-S	1-B	1-N	2-T	2-S	2-B	2-N	3-T	3-S	3-B	3-N
0	0	0	0	0	0	0	0	0	0	0	0	0
1	0	0	10	- 5	5	5	5	0	0	0	10	0
2	0	- 5	20	- 5	5	10	10	5	5	0	20	0
3	0	- 5	25	0	10	10	10	5	5	5	25	0
4	0	- 5	30	0	10	15	10	5	5	5	25	0
5	0	- 5	35	10	10	20	15	10	10	5	30	0
6	0	0	40	15	10	25	15	10	10	10	35	0
7	0	5	40	25	15	30	15	15	10	15	40	5
8	0	5	45	30	15	35	15	15	10	15	45	5
9	0	10	45	35	15	45	20	15	10	25	45	10
10	0	15	50	45	15	55	20	15	10	30	50	15
11	0	20	55	55	20	75	30	25	10	35	50	15
12*	0	20	55	60	20	90	30	40	10	45	55	20
13	0	15	60	70	20	105	30	50	15	50	55	25
14	30	10	65	80	20	135	30	65	15	70	60	30
15	45	10	65	90	20	175	30	70	15	80	60	40
16	50	0	70	105	20	230	30	75	20	95	60	50
17	55	- 5	70	105	20	270	30	85	25	100	65	55
18	60	0	70	115	20	300	30	90	35	110	65	60
19	60	5	90	115	20	310	25	90	45	115	65	60
20**	60	575	470	855	20	260	20	65	45	110	50	55

* First Crack ** Ultimate

TABLE B-13

PRESTRESSING STEEL STRAINS (MICRO INCHES PER INCH), BEAM BS-6

Load Stage	Strain Gauge Location				
	a	b	c	d	e
0	0	0	0	0	
1	- 5	- 5	- 5	0	
2	0	0	- 5	- 5	
3	0	0	-10	-10	
4	0	5	-10	- 5	
5	10	0	-10	- 5	
6	15	0	-15	- 5	
7	20	0	-15	- 5	
8	5	5	-15	- 5	
9*	10	5	-15	- 5	
10	5	10	-15	-10	
11	10	10	-15	- 5	
12	10	15	-15	- 5	
13	10	15	-15	- 5	
14	15	15	-10	0	
15	15	20	-10	0	
16	20	25	- 5	0	
17	20	35	15	-10	
18	25	45	15	-10	
19**	75	70	35	-10	
20	105	70	30	- 5	

* First Crack ** Ultimate

TABLE B-14

STIRRUP STRAINS (MICRO INCHES PER INCH), BEAM BS-6

Load Stage	Strain Gauge Location											
	1-T	1-S	1-B	1-N	2-T	2-S	2-B	2-N	3-T	3-S	3-B	3-N
0	0	0	0	0	0	0	0	0	0	0	0	0
1	5	0	5	0	- 5	5	15	- 5	10	0	0	0
2	10	- 5	15	0	-10	5	25	0	15	5	5	0
3	10	- 5	25	0	-10	5	40	- 5	15	5	5	5
4	15	-10	25	0	-10	5	55	0	20	15	10	5
5	20	-10	30	5	-10	10	50	-10	20	15	10	10
6	40	-10	35	10	-15	10	60	0	25	15	10	15
7	65	- 5	40	20	-10	5	65	0	30	20	10	25
8	90	- 5	40	35	- 5	20	75	10	35	25	10	25
9*	95	-20	45	130	0	20	85	15	40	30	10	30
10	100	-35	40	205	0	20	85	15	45	30	10	35
11	100	-45	40	255	0	25	95	25	55	30	15	35
12	105	-60	35	325	5	20	105	25	75	30	15	40
13	105	-70	35	390	10	25	115	25	85	30	15	45
14	105	-85	30	455	10	25	115	25	90	35	15	45
15	105	-100	25	560	10	20	120	25	100	35	15	50
16	110	-110	- 5	720	15	5	125	40	110	40	15	60
17	160	-10	-20	715	15	0	145	45	115	40	15	85
18	185	105	-20	690	15	- 5	165	45	115	40	15	110
19**	235	385	150	940	20	15	460	45	110	40	15	135
20	255	630	410	1060	20	150	760	45	110	40	20	135

*First Crack ** Ultimate

TABLE B-13

PRESTRESSING STEEL STRAINS (MICRO INCHES PER INCH), BEAM BH-1

Load Stage	Strain Gauge Location				
	a	b	c	d	e
0	0	0	0	0	0
1	70	65	-90	65	-70
2	150	150	-195	150	-170
3	235	240	-315	240	-265
4	290	300	-400	305	-335
5	335	340	-455	350	-380
6	390	385	-515	430	-425
7*	460	440	-585	520	-480
8	560	500	-660	610	-530
9	720	690	-735	730	-595
10	870	920	-830	815	-665
11	1010	1120	-930	890	-735
12	1215	1370	-1055	970	-825
13	1410	1600	-1185	1125	-920
14	1620	1830	-1360	1290	-1030
15	1770	1970	-1530	1400	-1130
16	1880	2065	-1610	1505	-1180
17	2025	2205	-2235	1585	-1700
18**	2205	2450			

* First Crack ** Ultimate

TABLE B-16

PRESTRESSING STEEL STRAINS (MICRO INCHES PER INCH), BEAM BH-2

Load Stage	Strain Gauge Location				
	a	b	c	d	e
0	0	0	0	0	0
1	40	50	60	60	65
2	85	105	130	120	125
3	125	155	170	175	225
4	160	200	230	235	315
5	185	225	260	270	365
6	205	255	295	305	430
7*	225	285	330	345	520
8	250	315	370	440	620
9	270	350	410	600	760
10	300	390	500	785	955
11	335	445	705	950	1060
12	370	610	875	1100	1510
13	435	845	1060	1325	-
14	720	1080	1190	1520	-
15	795	1185	1275	1620	-
16	895	1305	1370	1475	-
17	960	1395	1440	1210	-
18	995	1465	1500	1160	-
19	1030	1520	1550	1135	-
20	1060	1595	1620	1130	-
21	1100	1680	1705	1150	-
22**	-	-	1760	1245	-

* First Crack ** Ultimate

TABLE B-17

STIRRUP STRAINS (MICRO INCHES PER INCH), BEAM BH-2

Load Stage	Strain Gauge Location											
	1-T	1-S	1-B	1-N	2-T	2-S	2-B	2-N	3-T	3-S	3-B	3-N
0	0	0	0	0	0	0	0	0	0	0	0	0
1	10	5	0	10	15	- 5	0	5	15	0	- 5	5
2	15	10	0	10	25	- 5	-10	5	30	5	-15	5
3	15	15	- 5	10	40	- 5	-15	5	45	20	-20	5
4	20	20	- 5	10	50	5	-15	10	55	35	-25	5
5	25	25	- 5	15	60	15	-15	10	65	40	-30	10
6	25	30	- 5	15	65	25	-20	10	70	45	-35	15
7*	25	35	- 5	15	75	35	-20	10	80	50	-45	15
8	30	40	- 5	15	85	50	-20	5	90	40	-45	10
9	30	70	-10	10	90	50	- 5	0	100	15	-50	15
10	35	90	- 5	10	100	60	30	0	110	95	-35	40
11	35	105	- 5	15	110	55	220	- 5	125	290	- 5	90
12	40	125	- 5	10	125	35	355	-15	150	335	350	170
13	40	150	- 5	15	140	25	420	-30	185	340	615	190
14	45	205	20	30	155	185	460	-35	225	365	815	105
15	45	220	180	40	160	310	495	-40	260	400	905	70
16	45	230	270	55	175	695	505	-40	315	435	965	35
17	45	235	355	55	185	750	525	-35	350	460	1000	20
18	45	240	405	60	190	785	540	-35	390	475	1040	5
19	45	245	440	65	195	815	550	-35	420	490	1080	0
20	45	250	485	65	200	850	565	-35	460	500	1120	-10
21	45	255	540	70	205	900	585	-40	520	510	1165	-20
22**	50	260	580	-	-	-	-	-	-	-	-	-

* First Crack ** Ultimate

TABLE B-18

PRESTRESSING STEEL STRAINS (MICRO INCHES PER INCH), BEAM BH-3

Load Stage	Strain Gauge Location				
	a	b	c	d	e
0	0	0	0	0	0
1	45	60	60	65	65
2	100	120	125	135	135
3	150	170	185	210	195
4	175	200	200	250	230
5*	205	235	270	295	265
6	240	390	330	340	305
7	255	735	440	395	355
8	270	830	510	625	575
9	295	925	615	745	655
10	340	1005	710	760	640
11	425	1130	835	790	645
12	610	1235	1030	1010	730
13	880	1345	1280	1190	860
14**	-	-	1940	-	-

* First Crack ** Ultimate

TABLE B-19

STIRRUP STRAINS (MICRO INCHES PER INCH), BEAM BH-3

Load Stage	Strain Gauge Location											
	1-T	1-S	1-B	1-N	2-T	2-S	2-B	2-N	3-T	3-S	3-B	3-N
0	0	0	0	0	0	0	0	0	0	0	0	0
1	10	5	- 5	10	15	0	- 5	5	10	0	-10	0
2	25	0	-15	15	25	5	-10	10	30	5	-25	0
3	35	0	-20	20	35	10	-10	10	45	20	-35	0
4	40	15	-25	35	45	15	-10	10	50	60	-35	0
5*	45	220	-40	35	50	10	- 5	5	60	240	-35	0
6	60	590	-45	35	58	70	30	5	65	695	-20	0
7	55	835	-40	10	60	270	80	- 5	75	1090	110	-25
8	60	920	-30	20	70	360	110	- 5	90	1105	420	-35
9	65	1015	-25	45	75	440	135	15	100	1175	520	-40
10	65	1105	-15	15	80	480	165	100	120	1250	595	165
11	70	1210	-15	35	90	530	245	210	165	1540	655	325
12	75	1285	-10	5	115	560	365	530	220	2600	675	440
13	85	1320	270	10	170	775	695	720	380	5000	690	660
14**	-	-	-	-	-	-	-	-	-	-	-	-

* First Crack ** Ultimate

TABLE B-20

PRESTRESSING STEEL STRAINS (MICRO INCHES PER INCH), BEAM BB-4

Load Stage	Strain Gauge Location				
	a	b	c	d	e
0	0	0	0	0	0
1	0	10	10	10	10
2	15	20	20	20	20
3	25	30	30	30	30
4	35	35	40	40	40
5	40	45	55	50	50
6	60	60	65	55	60
7	65	65	70	60	65
8*	70	70	80	65	70
9	95	90	85	70	80
10	115	100	95	75	95
11	135	115	105	85	115
12	150	125	115	95	130
13	195	135	125	105	140
14	385	150	130	115	150
15	390	165	140	130	165
16	400	195	150	150	195
17	445	225	150	180	275
18	490	240	145	205	300
19	500	255	145	225	335
20	495	265	145	255	355
21**	490	285	135	275	355
22	-	-	-	-	-

* First Crack ** Ultimate

TABLE B-21

STIRRUP STRAINS (MICRO INCHES PER INCH), BEAM BB-4

Load Stage	Strain Gauge Location											
	1-T	1-S	1-B	1-H	2-T	2-S	2-B	2-H	3-T	3-S	3-B	3-H
0	0	0	0	0	0	0	0	0	0	0	0	0
1	0	0	0	0	0	0	0	0	0	10	0	0
2	0	0	10	5	10	0	0	5	5	10	0	0
3	5	0	10	10	15	0	0	10	10	15	0	0
4	10	0	15	10	20	0	0	15	15	25	- 5	0
5	10	5	20	10	20	10	0	15	15	35	-10	0
6	10	15	20	15	25	145	- 5	20	20	70	-10	- 5
7	10	55	25	15	25	195	- 5	25	20	85	-10	- 5
8*	10	105	25	15	25	340	-10	25	20	105	-10	- 5
9	15	155	30	20	30	525	-15	30	20	165	-10	- 5
10	5	205	25	20	30	725	-15	30	20	260	-15	- 5
11	5	215	35	25	35	825	-15	30	25	495	-15	- 5
12	5	225	40	25	40	925	-15	35	25	560	-15	- 5
13	5	230	55	25	45	955	-15	35	25	620	-15	- 5
14	10	235	85	25	50	1000	-10	40	25	675	-10	- 5
15	10	240	110	30	65	1050	- 5	40	30	735	0	- 5
16	15	250	130	30	75	1075	0	40	30	795	25	0
17	20	260	245	30	120	1090	10	50	30	875	30	0
18	20	270	345	180	140	1100	0	55	35	915	80	0
19	20	295	385	255	195	1125	- 5	70	40	950	95	5
20	35	360	400	340	165	1160	-10	80	40	980	105	10
21**	730	480	815	490	175	1130	-20	380	40	935	215	0
22	-	-	-	-	-	-	-	-	-	-	-	-

* First Crack ** Ultimate

TABLE B-22

LONGITUDINAL STEEL STRAINS (MICRO INCHES PER INCH), BEAM BM-1

Load Stage	Strain Gauge Location				
	a	b	c	d	e
0	0	0	0	0	0
1	0	0	0	0	0
2	0	0	0	- 5	- 5
3	0	0	0	- 5	-10
4	0	0	0	-10	-20
5	0	0	0	-10	-20
6	0	5	0	-10	-25
7	0	5	0	-10	-25
8	0	5	0	-10	-30
9	0	5	0	-10	-30
10	0	5	0	-15	-35
11*	0	10	0	-15	-35
12	0	15	- 5	-15	-45
13	0	25	- 5	-20	-45
14	15	30	5	-10	-45
15	25	35	10	- 5	-30
16	35	40	15	- 5	-30
17	40	40	25	- 5	-30
18	55	45	35	0	-25
19	45	70	50	0	-20
20	-160	70	60	5	- 5
21	-210	160	65	- 5	- 5
22	-330	160	70	- 5	-10
23	-260	125	75	- 5	10
24	-280	100	75	- 5	65
25	-290	90	85	- 5	125
26**	-260	75	213	- 5	140

* First Crack ** Ultimate

TABLE B-23

STIRRUP STRAINS (MICRO INCHES PER INCH), BEAM BM-1

Load Stage	Strain Gauge Location											
	1-T	1-S	1-B	1-U	2-T	2-S	2-B	2-U	3-T	3-S	3-B	3-U
0	0	0	0	0	0	0	0	0	0	0	0	0
1	10	0	10	0	5	0	5	5	0	0	10	10
2	15	0	15	0	10	0	10	5	0	0	15	10
3	15	5	15	0	10	0	10	10	0	0	20	10
4	15	5	20	0	10	0	10	10	0	0	20	10
5	20	10	20	0	10	0	15	10	0	0	20	10
6	20	10	25	0	15	5	20	10	0	0	25	15
7	20	10	25	0	15	5	20	10	0	0	25	15
8	20	15	30	0	15	5	20	15	0	0	30	15
9	25	15	30	0	20	10	20	15	0	0	30	15
10	25	15	30	0	20	10	20	15	0	0	30	20
11*	25	20	35	0	20	20	25	20	0	0	35	20
12	25	25	35	0	20	35	25	20	0	5	35	25
13	30	30	40	5	20	45	25	20	0	10	35	25
14	30	35	40	5	20	65	30	20	0	20	35	25
15	30	60	55	0	30	265	35	15	0	90	45	30
16	35	70	65	0	35	375	35	10	0	105	50	30
17	40	80	75	5	35	380	30	10	0	130	55	30
18	50	90	100	15	30	430	40	10	5	150	60	30
19	60	90	170	305	30	465	35	0	10	185	65	30
20	65	90	265	680	190	490	180	0	10	230	75	30
21	80	1220	530	865	1350	500	200	20	35	230	110	735
22	90	1420	645	1030	1470	535	235	60	55	250	130	895
23	125	1565	830	1190	1565	570	290	260	70	280	160	970
24	160	1540	1005	1305	1840	600	315	375	75	340	300	1020
25	220	1570	1340	1460	1765	645	330	650	85	420	395	1080
26**	1090	1595	2180	1650	1775	670	385	905	90	615	375	1070

* First Crack ** Ultimate

TABLE B-24

PRESTRESSING STEEL STRAINS (MICRO INCHES PER INCH), BEAM BB-6

Load Stage	Strain Gauge Location				
	a	b	c	d	e
0	0	0	0	0	0
1	10	10	- 5	0	10
2	10	15	- 5	10	10
3	15	20	- 5	10	15
4*	15	20	- 5	15	25
5	15	30	0	20	45
6	10	30	5	30	130
7	15	35	25	65	225
8	20	35	30	220	375
9	25	40	45	245	430
10	30	45	55	260	455
11	30	50	60	280	495
12	30	50	70	295	520
13	30	55	80	310	550
14	30	60	110	330	565
15	30	75	150	345	595
16	35	85	160	360	610
17	85	85	175	380	650
18	100	270	420	410	585
19	115	460	585	530	660
20**	130	420	580	795	655

* First Crack ** Ultimate

TABLE B-25

STIRRUP STRAINS (MICRO INCHES PER INCH), BEAM BB-6

Load Stage	Strain Gauge Location											
	1-T	1-S	1-B	1-N	2-T	2-S	2-B	2-N	3-T	3-S	3-B	3-N
0	0	0	0	0	0	0	0	0	0	0	0	0
1	0	0	20	10	5	0	15	5	10	-10	15	0
2	0	5	25	10	5	0	20	10	10	-10	20	0
3	-10	10	30	230	5	0	30	25	15	-20	30	0
4*	-10	20	35	275	10	0	35	30	20	20	35	10
5	-15	150	35	335	5	220	35	110	25	35	40	15
6	-15	280	40	395	5	605	45	120	60	50	45	15
7	-15	635	50	540	10	740	50	125	275	140	55	10
8	-15	820	60	620	15	955	60	120	730	185	65	0
9	-15	900	70	730	15	1090	65	120	805	225	70	0
10	-15	940	80	865	15	1150	70	120	840	265	80	0
11	-15	960	90	930	20	1200	75	125	880	375	80	0
12	-15	995	100	980	20	1255	80	130	905	440	85	0
13	10	1010	115	1015	20	1300	90	145	930	490	90	- 5
14	30	1055	140	1080	30	1355	105	225	965	540	105	- 5
15	510	1045	205	1045	95	1230	180	920	970	570	110	-10
16	720	1080	305	1175	105	1295	470	1190	995	625	115	5
17	790	1050	350	1220	125	1350	660	1285	1020	670	110	20
18	830	1105	390	1190	825	1370	1010	1310	1025	690	120	785
19	875	1180	570	1380	1010	1740	1295	1530	1180	780	135	1030
20**	1120	1090	970	1420	1140	1735	1300	1460	1375	825	400	1030

* First Crack ** Ultimate

TABLE B-26

PRESTRESSING STEEL STRAINS (MICRO INCHES PER INCH), BEAM B18-2a

Load Stage	Strain Gauge Location				
	a	b	c	d	e
0	0	0	0	0	0
1	40	30	30	30	35
2	45	40	45	30	50
3	60	50	60	40	70
4	75	70	75	50	95
5	85	80	95	55	125
6	100	95	120	65	180
7	120	115	140	75	250
8*	135	130	160	90	320
9	155	150	190	110	500
10	230	220	260	180	1210
11	270	240	350	215	1610
12	330	280	530	270	2010
13	395	320	715	390	2490
14	530	525	1280	610	3220
15	660	670	1590	660	3650
16	855	950	1915	780	4290
17	980	1275	2180	630	4990
18	1130	1530	-	-	5770
19	1300	1780	-	-	-
20	1450	2050	-	-	-
21**	1590	2230	-	-	-

* First Crack ** Ultimate

TABLE B-27

STIRRUP STRAINS (MICRO INCHES PER INCH), BEAM B18-2a

Load Stage	Strain Gauge Location											
	1-T	1-S	1-B	1-N	2-T	2-S	2-B	2-N	3-T	3-S	3-B	3-N
0	0	0	0	0	0	0	0	0	0	0	0	0
1	10	0	10	10	10	5	0	5	10	10	0	10
2	10	0	0	10	10	0	0	5	10	5	- 5	5
3	10	0	0	10	10	0	- 5	5	10	10	- 5	5
4	10	0	0	10	15	0	- 5	5	20	10	- 5	5
5	15	0	0	10	15	0	- 5	5	20	5	- 5	5
6	15	0	0	10	20	0	- 5	5	30	10	10	5
7	20	0	0	10	20	0	- 5	10	40	10	35	5
8*	20	0	0	10	20	0	- 5	5	50	10	65	5
9	20	0	0	10	25	0	- 5	5	90	10	75	15
10	25	- 5	20	10	30	0	- 5	0	-90	-10	80	210
11	30	- 5	40	15	35	30	0	-10	-415	15	85	340
12	30	-10	55	15	40	145	10	-30	-500	100	110	430
13	35	-10	80	15	40	220	10	-40	-535	170	150	550
14	40	-15	135	20	40	260	10	-80	-550	180	210	490
15	40	-20	190	25	40	260	10	-75	-550	170	240	470
16	40	-30	270	45	45	290	15	-75	-550	170	290	470
17	45	-40	330	60	50	300	15	-75	-540	170	320	480
18	45	-40	390	85	50	320	20	-75	-490	190	340	530
19	45	-40	420	160	50	330	20	-80	-135	190	370	590
20	50	-50	450	210	50	370	20	-85	-320	190	410	660
21**	50	-50	440	250	50	455	20	-10	-600	140	455	570

* First Crack ** Ultimate

TABLE B-28

PRESTRESSING STEEL STRAINS (MICRO INCHES PER INCH), BEAM B18-2b

Load Stage	Strain Gauge Location				
	a	b	c	d	e
0	0	0	0	0	0
1	25	25	25	25	30
2	40	40	40	45	45
3	50	50	55	60	60
4	65	65	70	80	80
5	80	80	90	100	100
6	95	95	110	125	130
7	110	110	135	140	175
8*	125	125	155	160	220
9	145	145	185	185	300
10	185	195	275	245	770
11	220	265	665	1095	1360
12	255	420	1000	1580	1855
13	425	745	1270	2040	2145
14	790	1170	1690	2740	2230
15	940	1380	1930	3150	-
16	1070	1560	2130	3600	-
17	1205	1795	2385	3770	-
18	1340	2020	2670	-	-
19**	-	-	3380	-	-

* First Crack ** Ultimate

TABLE B-29

STIRRUP STRAINS (MICRO INCHES PER INCH), BEAM B18-2b

Load Stage	Strain Gauge Location											
	1-T	1-S	1-B	1-N	2-T	2-S	2-B	2-N	3-T	3-S	3-B	3-N
0	0	0	0	0	0	0	0	0	0	0	0	0
1	5	0	0	0	5	10	0	0	5	5	0	0
2	5	0	- 5	5	10	0	- 5	5	10	0	- 5	0
3	10	0	- 5	5	15	0	- 5	5	10	0	- 5	0
4	10	0	- 5	5	15	0	-10	5	15	0	-10	0
5	10	0	- 5	5	20	0	-10	5	20	0	-10	0
6	15	0	-10	5	20	0	-10	5	20	0	- 5	0
7	15	0	-10	5	25	0	-15	5	25	5	10	10
8*	15	0	-10	5	25	0	-15	5	30	5	20	10
9	20	0	-10	5	30	0	-15	5	35	10	30	15
10	25	- 5	-10	5	35	-15	-15	5	55	65	40	65
11	25	0	0	10	50	-50	-25	35	70	205	55	215
12	30	5	10	10	50	-65	-30	65	90	215	105	245
13	35	10	15	10	55	-80	-30	75	115	200	200	265
14	35	5	15	0	65	-90	-35	75	170	180	380	295
15	40	20	15	0	70	-90	-35	75	220	170	470	320
16	40	40	25	0	70	-95	-35	75	260	170	530	345
17	45	75	45	0	75	-95	-30	70	345	170	565	365
18	45	130	50	0	80	-95	-30	65	445	135	450	380
19**	-	-	-	-	-	-	-	-	-	-	-	-

* First Crack ** Ultimate

TABLE B-30

PRESTRESSING STEEL STRAINS (MICRO INCHES PER INCH), BEAM B18-4a

Load Stage	Strain Gauge Location				
	a	b	c	d	e
0	0	0	0	0	0
1	10	5	10	0	0
2	20	15	20	10	15
3	25	25	35	20	25
4	35	35	45	30	40
5	40	40	55	35	45
6	45	45	60	45	55
7	50	55	70	50	65
8	55	60	75	55	70
9	60	65	85	65	80
10	70	75	95	75	95
11	75	80	105	80	105
12*	80	90	115	90	115
13	90	100	125	95	145
14	100	110	135	105	220
15	110	115	165	110	265
16	120	125	195	120	300
17	125	135	215	125	325
18**	-	-	-	-	-

* First Crack ** Ultimate

TABLE B-31

STIRRUP STRAINS (MICRO INCHES PER INCH), BEAM B18-4a

Load Stage	Strain Gauge Location											
	1-T	1-S	1-B	1-N	2-T	2-S	2-B	2-N	3-T	3-S	3-B	3-N
0	0	0	0	0	0	0	0	0	0	0	0	0
1	5	0	0	5	10	0	0	0	0	5	0	10
2	5	0	0	5	10	0	0	0	5	5	0	10
3	5	0	5	5	15	- 5	0	0	5	5	0	10
4	5	- 5	5	5	15	0	0	0	10	5	0	15
5	5	- 5	5	5	15	0	0	0	10	5	0	15
6	5	- 5	10	10	20	10	5	5	15	10	0	15
7	5	- 5	10	10	20	10	5	5	15	10	0	15
8	5	0	10	10	20	15	10	5	15	15	5	15
9	5	5	15	10	20	25	25	5	15	25	5	15
10	5	10	15	15	25	35	35	5	20	30	10	20
11	5	15	15	15	25	45	40	5	20	35	20	20
12*	5	25	20	25	25	55	45	5	20	45	30	20
13	5	35	20	30	25	60	50	5	20	45	55	20
14	5	40	25	40	25	70	60	5	25	35	110	30
15	5	45	25	45	25	80	80	5	25	20	135	35
16	5	80	25	45	30	95	90	0	25	0	150	100
17	5	100	20	45	25	105	95	- 5	25	-10	170	125
18**	-	-	-	-	-	-	-	-	-	-	-	-

* First Crack, ** Ultimate

TABLE B-32

PRESTRESSING STEEL STRAINS (MICRO INCHES PER INCH), BEAM B18-4b

Load Stage	Strain Gauge Location				
	a	b	c	d	e
0	0	0	0	0	0
1	5	30	25	15	20
2	10	40	35	25	35
3	10	50	50	35	50
4	15	60	65	45	65
5	20	75	80	60	85
6	20	90	95	75	105
7	25	95	105	85	115
8	25	105	115	100	125
9*	30	110	125	110	135
10	35	120	135	125	160
11	40	135	145	140	220
12	45	150	155	145	415
13	45	170	170	155	625
14	55	190	180	170	760
15	70	205	190	185	885
16	85	225	205	210	1120
17	100	245	240	255	1330
18	115	255	835	480	1510
19	135	280	1110	730	1740
20	180	350	1280	1175	1930
21**	-	-	-	-	-

* First Crack ** Ultimate

TABLE B-33

STIRRUP STRAINS (MICRO INCHES PER INCH), BEAM B18-4b

Load Stage	Strain Gauge Location											
	1-T	1-S	1-S	1-N	2-T	2-S	2-S	2-N	3-T	3-S	3-S	3-N
0	0	0	0	0	0	0	0	0	0	0	0	0
1	0	0	0	0	0	0	0	0	10	0	- 5	0
2	0	0	5	0	0	0	0	0	10	0	-10	5
3	0	5	5	0	5	0	0	0	15	0	-15	10
4	0	10	5	0	0	- 5	5	5	20	0	-20	15
5	0	20	10	0	0	- 5	5	5	25	5	-30	20
6	- 5	30	10	5	0	-10	5	10	30	20	-35	30
7	- 5	35	10	5	0	-10	10	15	30	20	-35	35
8	- 5	40	10	10	0	-10	10	20	35	30	-35	40
9*	- 5	45	15	10	0	-10	10	20	40	30	-25	45
10	- 5	55	15	10	0	-10	10	30	40	40	5	50
11	- 5	65	20	10	0	- 5	10	35	45	45	60	55
12	0	80	20	15	0	5	10	50	50	20	235	50
13	0	90	20	20	0	15	10	60	55	0	425	35
14	0	105	20	25	- 5	40	10	70	60	-15	545	30
15	0	125	20	35	- 5	55	5	80	60	-30	610	30
16	0	165	15	40	-10	75	10	95	70	-35	760	35
17	0	210	15	45	-15	90	10	110	75	-45	905	30
18	0	240	10	55	-15	55	100	195	85	-45	1060	65
19	0	295	10	65	-15	45	330	295	100	-15	1180	75
20	5	355	15	75	-10	100	470	400	110	35	1280	85
21**	-	-	-	-	-	-	-	-	-	-	-	-

* First Crack ** Ultimate

TABLE B-34

PRESTRESSING STEEL STRAINS (MICRO INCHES PER INCH), BEAM B18-6a

Load Stage	Strain Gauge Location				
	a	b	c	d	e
0	0	0	0	0	0
1	0	0	0	0	0
2	5	0	5	- 5	5
3	5	0	5	- 5	5
4	10	0	10	- 5	5
5	10	5	10	- 5	10
6	10	5	10	- 5	0
7	15	5	10	- 5	5
8	15	10	10	- 5	0
9	20	10	15	0	5
10	20	15	20	0	5
11	20	20	20	0	5
12	20	20	20	0	5
13*	20	20	25	5	10
14	25	25	25	15	10
15	25	25	20	20	10
16	30	25	25	50	10
17	30	25	20	160	10
18**	- 5	-10	180	255	150
19	-15	-30	-170	-2340	-340
20	+10	-20	-1265	-3330	-955

* First Crack ** Ultimate

TABLE B-35

STIRRUP STRAINS (MICRO INCHES PER INCH), BEAM B18-6a

Load Stage	Strain Gauge Location											
	1-T	1-S	1-B	1-N	2-T	2-S	2-B	2-N	3-T	3-S	3-B	2-N
0	0	0	0	0	0	0	0	0	0	0	0	0
1	0	0	0	0	0	0	0	0	0	0	0	0
2	5	0	0	0	5	0	5	0	5	0	5	- 5
3	5	0	5	- 5	5	0	5	- 5	10	- 5	5	- 5
4	5	0	5	- 5	5	0	10	- 5	10	- 5	5	0
5	5	0	10	- 5	5	5	10	- 5	15	- 5	10	0
6	5	0	10	- 5	5	5	15	- 5	20	- 5	5	0
7	5	0	15	- 5	5	5	15	0	20	- 5	10	5
8	5	0	15	10	5	10	20	5	25	- 5	10	5
9	5	0	20	15	5	15	20	10	30	0	5	10
10	5	5	20	25	5	35	20	10	35	10	10	10
11	0	5	20	35	5	45	25	15	35	10	10	15
12	0	10	20	50	0	70	25	20	40	15	10	15
13*	0	10	20	70	0	115	25	30	40	15	10	20
14	0	15	20	100	0	200	25	35	40	20	10	30
15	0	15	20	130	-10	270	20	40	45	25	10	25
16	- 5	15	15	180	-15	400	10	35	45	30	10	30
17	-10	15	15	230	-20	610	10	20	45	30	10	35
18**	-15	- 3	-	550	-10	4485	55	505	660	80	0	390
19	80	-10	-	900	100	4070	205	1890	-	10	-10	280
20	80	0	-	675	125		230	4510	-	0	-20	360

* First Crack ** Ultimate

TABLE D-36

REINFORCING STEEL STRAINS (MICRO INCHES PER INCH), BEAM B13-4b

Load Stage	Strain Gauge Location				
	a	b	c	d	e
0	0	0	0	0	0
1	0	-5	-5	0	10
2	10	0	0	-5	10
3	10	0	0	-5	10
4	10	5	5	-5	10
5	15	10	5	-5	15
6	15	10	10	-5	15
7	20	15	10	-5	20
8	20	15	10	-10	20
9	25	20	10	-10	20
10	30	25	15	-10	20
11*	35	30	20	-10	20
12	35	35	30	-5	25
13	35	40	30	-5	30
14	40	40	25	-5	35
15	40	30	20	0	40
16	45	35	30	0	45
17	50	60	30	5	50
18	50	70	40	10	60
19	60	90	50	20	70
20	70	105	65	30	90
21	75	240	90	110	130
22	75	270	125	200	230
23	90	305	150	280	300
24	105	400	170	430	340
25	130	450	200	500	405
26	170	480	225	610	445
27	315	495	270	690	510
28	335	530	310	770	590
29	940	890	355	840	670
30**	1500	1750	840	910	690

* First Crack ** Ultimate

TABLE D-37

STIRRUP STRAINS (MICRO INCHES PER INCH), BEAM B13-4b

Load Stage	Strain Gauge Location											
	1-T	1-M	1-B	1-B	2-T	2-M	2-B	2-B	3-T	3-M	3-B	3-B
0	0	0	0	0	0	0	0	0	0	0	0	0
1	0	0	0	0	0	5	0	0	0	0	5	0
2	0	0	5	-5	-5	5	5	0	5	0	5	10
3	0	5	5	0	0	5	10	5	5	0	0	5
4	0	5	10	0	-5	5	10	10	10	0	5	10
5	0	10	10	0	-5	0	10	10	10	0	0	10
6	0	10	10	0	-10	0	10	15	10	0	0	15
7	0	15	10	0	-10	5	10	15	10	0	0	20
8	0	20	10	0	-10	5	10	20	10	0	0	20
9	0	20	15	10	-15	10	15	30	15	10	0	20
10	-5	20	15	20	-20	10	15	45	15	20	0	30
11*	-10	25	20	40	-20	20	20	60	30	15	10	40
12	-10	30	20	40	-20	40	20	70	25	20	15	40
13	-10	35	20	45	-15	45	20	75	30	20	15	45
14	-10	40	20	50	-10	60	20	90	45	25	20	60
15	-15	45	25	60	15	85	20	100	55	30	20	70
16	-20	50	40	75	45	110	30	105	60	35	30	85
17	-20	45	50	130	70	130	20	110	75	45	35	100
18	-20	40	45	240	100	155	30	130	100	50	30	100
19	-30	45	50	300	130	205	85	170	125	65	40	110
20	-30	120	70	350	260	310	50	115	140	75	75	105
21	-35	210	90	430	470	440	130	200	260	220	170	85
22	-25	290	100	495	670	530	170	280	440	320	210	130
23	-30	300	125	540	760	560	240	530	730	390	410	220
24	0	630	360	700	860	590	280	590	790	360	480	305
25	70	750	470	800	905	630	315	635	850	380	550	370
26	190	860	570	860	960	670	355	675	900	480	610	440
27	365	930	675	925	990	690	395	750	930	410	640	490
28	880	980	800	1010	1070	730	430	806	970	425	670	565
29	1055	960	940	1070	1030	765	490	830	1010	430	700	640
30**	1155	1700	1370	1055	940	890	735	1005	910	430	680	640

* First Crack ** Ultimate

TABLE B-18

PRESTRESSING STEEL STRAINS (MICRO INCHES PER INCH), BEAM CS-1

Load Stage	Strain Gauge Location				
	a	b	c	d	e
0	0	0	0	0	0
1	45	50	50	-55	-50
2	95	100	100	-115	-125
3	155	150	160	-185	-195
4	215	220	225	-255	-270
5	270	280	280	-315	-335
6	340	360	355	-385	-410
7	460	465	480	-440	-470
8*	565	555	575	-485	-525
9	675	645	685	-530	-570
10	805	775	810	-570	-615
11	940	910	930	-610	-670
12	1085	1055	1075	-660	-720
13	1230	1210	1225	-705	-775
14	1370	1355	1360	-745	-825
15	1490	1560	1330	-795	-895
16	1560	1805	1250	-850	-960
17	1480	2050	1190	-905	-1035
18	1520	2280	1035	-990	-1165
19**	-	3100	-	-	-

* First Crack ** Ultimate

TABLE B-39

PRESTRESSING STEEL STRAINS (MICRO INCH'S PER INCH), BEAM CS-2

Load Stage	Strain Gauge Location				
	a	b	c	d	e
0	0	0	0	0	0
1	30	35	40	40	40
2	70	75	80	85	90
3	105	120	120	130	120
4	140	160	165	180	195
5	170	190	195	210	225
6	185	210	220	235	265
7	200	235	245	265	300
8	220	255	265	300	350
9*	240	280	290	340	400
10	265	315	335	395	505
11	295	355	415	470	680
12	340	420	500	610	935
13	400	500	635	835	1245
14	440	585	780	1025	3400
15	490	700	1000	1235	-
16	550	835	1200	1450	-
17	630	1020	1405	1675	-
18	740	1240	1635	1810	-
19	820	1360	1720	1895	-
20**	-	-	-	-	-

* First Crack ** Ultimate

TABLE B-40

STIRRUP STRAINS (MICRO INCHES PER INCH), BEAM CS-2

Load Stage	Strain Gauge Location											
	1-T	1-S	1-B	1-N	2-T	2-S	2-B	2-N	3-T	3-S	3-B	3-N
0	0	0	0	0	0	0	0	0	0	0	0	0
1	25	0	0	5	5	5	0	0	10	0	0	0
2	35	0	-10	5	15	10	-10	5	25	0	-10	0
3	45	0	-15	5	20	10	-15	5	40	5	-20	5
4	50	0	-20	5	30	15	-25	5	50	5	-30	0
5	55	0	-20	5	35	15	-30	5	60	5	-40	0
6	65	0	-25	10	40	15	-30	5	65	0	-40	0
7	60	0	-25	10	40	15	-30	5	70	0	-45	0
8	60	0	-25	10	45	15	-35	5	75	0	-45	- 5
9*	60	0	-25	10	50	15	-35	0	85	- 5	-50	-10
10	70	0	-30	10	55	15	-30	0	95	-15	-40	-10
11	70	- 5	-30	10	60	10	-20	10	100	-40	-20	-25
12	75	-10	-25	5	65	5	55	5	110	-45	15	-40
13	85	-15	-10	5	50	- 5	110	10	125	-90	75	-70
14	85	-20	20	0	75	-15	150	10	135	-100	115	-85
15	90	-25	55	- 5	75	-20	220	15	150	-100	170	-105
16	95	-35	90	-10	80	-20	290	30	155	-85	220	-120
17	100	-40	135	-15	85	-20	375	65	180	-80	275	-135
18	145	-50	205	-25	90	70	470	125	235	-95	390	-40
19	100	-50	255	-30	95	110	535	155	340	-90	550	+145
20**	-	-	-	-	-	-	-	-	-	-	-	-

* First Crack ** Ultimate

TABLE B-41

PRESTRESSING STEEL STRAINS (MICRO INCHES PER INCH), BEAM CB-3

Load Stage	Strain Gauge Location				
	a	b	c	d	e
0	0	0	0	0	0
1	30	35	35	40	60
2	70	80	80	90	125
3	95	110	110	120	165
4	120	135	135	150	205
5	140	165	165	185	240
6	160	185	190	210	270
7	175	205	210	235	305
8	195	230	235	260	355
9	213	253	260	290	415
10*	235	280	285	330	495
11	255	310	315	385	630
12	275	335	340	450	815
13	300	370	375	535	980
14	320	410	410	670	1150
15	340	455	515	895	1300
16	360	525	685	1085	1455
17	380	695	875	1265	1670
18	400	895	1025	1400	1840
19	415	1050	1145	1520	1980
20	465	1230	1320	1690	2170
21	545	1360	1435	1830	2325
22	740	1485	1600	1970	2510
23	1070	1555	1680	2070	2675
24	1150	1635	1760	2175	2830
25**	-	-		-	3050

* First Crack ** Ultimate

TABLE B-42

STIRRUP STRAINS (MICRO INCHES PER INCH), BEAM CB-3

Load Stage	Strain Gauge Location											
	1-T	1-S	1-B	1-N	2-T	2-S	2-B	2-N	3-T	3-S	3-B	3-N
0	0	0	0	0	0	0	0	0	0	0	0	0
1	5	5	0	5	10	5	0	5	15	0	- 5	5
2	15	5	0	10	20	5	-10	5	30	0	-15	5
3	20	0	0	10	25	10	-10	10	40	0	-25	0
4	25	0	0	10	30	10	-15	10	45	- 5	-30	0
5	30	0	0	10	35	10	-15	10	55	-10	-35	0
6	30	0	0	15	40	10	-20	10	65	-10	-35	0
7	30	0	0	15	45	15	-20	10	70	-10	-40	0
8	35	0	0	15	50	15	-20	10	80	-10	-40	0
9	35	0	10	15	55	25	-35	5	90	-10	-45	- 5
10*	35	0	30	15	60	30	-25	0	100	-15	-35	-10
11	40	0	60	15	65	30	-15	0	105	-25	-40	-25
12	40	10	80	15	70	35	0	- 5	110	-50	-70	-40
13	40	10	110	15	70	40	20	-15	120	-70	-60	-50
14	45	10	130	15	75	35	25	-20	125	-85	-30	-70
15	45	10	135	15	75	25	65	-10	135	-85	45	-70
16	45	10	185	15	70	25	100	- 5	150	-65	105	-45
17	45	0	225	20	65	95	165	0	185	-30	125	120
18	40	- 5	255	30	65	255	220	5	240	-35	140	250
19	40	-10	260	60	65	390	270	10	290	-20	155	565
20	35	-10	265	100	70	585	415	25	375	- 5	170	810
21	25	-10	275	145	90	725	565	45	450	10	185	990
22	25	-15	285	220	120	870	760	90	590	20	205	1180
23	15	-35	445	310	140	980	870	120	585	30	230	1325
24	15	-40	565	340	160	1060	985	145	585	45	260	1410
25**	-	-	-	-	-	-	-	-	-	-	-	-

* First Crack ** Ultimate

TABLE B-43

PRESTRESSING STEEL STRAIN: (MICRO INCHES PER INCH), BEAM CS-4

Load Stage	Strain Gauge Location				
	a	b	c	d	e
0	0	0	0	0	0
1	-10	-15	-15	-20	-20
2	-30	-30	-30	-40	-40
3	-30	-40	-50	-60	-60
4	-40	-55	-65	-80	-85
5	-50	-70	-80	-105	-115
6	-70	-85	-105	-125	-140
7	-90	-105	-120	-145	-165
8	-105	-115	-130	-160	-180
9	-110	-125	-135	-170	-190
10	-130	-140	-145	-180	-205
11	-130	-160	-155	-190	-215
12*	-140	-175	-165	-200	-230
13	-150	-200	-175	-215	-245
14	-165	-215	-185	-235	-255
15	-180	-230	-200	-240	-270
16	-190	-245	-210	-250	-280
17	-200	-250	-220	-260	-300
18	-210	-260	-230	-270	-310
19	-215	-265	-240	-285	-330
20	-230	-280	-255	-300	-350
21	-280	-340	-300	-330	-375
22	-315	-425	-345	-380	-410
23**					

* First Crack ** Ultimate

TABLE B-44

STIRRUP STRAINS (MICRO INCHES PER INCH), BEAM CS-4

Load Stage	Strain Gauge Location											
	1-T	1-S	1-B	1-N	2-T	2-S	2-B	2-N	3-T	3-S	3-B	3-N
0	0	0	0	0	0	0	0	0	0	0	0	0
1	0	0	0	0	0	0	0	0	0	0	0	0
2	0	0	0	0	0	0	0	0	10	0	0	0
3	0	0	0	0	0	0	0	0	15	0	0	0
4	0	0	0	5	5	0	0	0	20	5	-10	- 5
5	0	0	0	5	5	0	0	5	25	10	-10	- 5
6	10	5	0	10	10	5	0	5	30	10	-10	- 5
7	25	10	0	15	10	15	0	10	40	20	-10	- 5
8	25	20	0	20	10	20	0	10	45	35	- 5	- 5
9	30	30	0	20	10	25	0	15	50	45	5	-10
10	40	40	0	25	10	30	0	15	50	50	15	-10
11	50	55	0	30	10	30	0	15	55	60	30	-10
12*	80	70	- 5	35	10	35	0	20	60	85	45	-10
13	105	85	- 5	40	10	40	5	20	60	100	60	-10
14	130	100	- 5	50	10	45	5	20	85	115	70	-10
15	145	115	-10	55	15	50	5	20	65	125	75	-10
16	155	140	-10	65	15	60	5	25	70	140	80	-10
17	160	170	-15	75	15	65	10	25	70	145	75	- 5
18	170	200	-20	85	15	60	5	25	70	145	90	-25
19	195	220	-20	100	20	75	10	30	65	130	140	-30
20	260	220	-30	110	25	90	15	35	65	135	215	-25
21	340	235	25	480	15	95	15	35	65	145	255	-20
22	540	750	345	860	5	80	10	30	70	155	290	-10
23**	-	-	-	-	-	-	-	-	-	-	-	-

* First Crack ** Ultimate

TABLE D-45

PRESTRESSING STEEL STRAINS (MICRO INCHES PER INCH), BEAM CB-5

Load Stage	Strain Gauge Location				
	a	b	c	d	e
0	0	0	0	0	0
1	- 5	- 5	- 5	-10	-10
2	-15	-10	-15	-20	-25
3	60	30	30	30	40
4	130	75	35	35	50
5	180	110	60	40	55
6	230	150	90	50	60
7	270	190	135	65	65
8	305	220	165	85	70
9	330	255	200	100	80
10	355	280	225	115	90
11	380	300	250	130	100
12*	400	320	270	145	105
13	435	345	300	175	125
14	445	370	340	220	150
15	525	415	395	280	190
16	565	445	450	360	255
17	590	520	505	410	295
18	600	560	550	435	330
19	490	595	580	510	385
20	360	600	590	553	410
21	-245	-425	-435	-545	-430
22**	-160	- 20	-605	-585	-475

* First Crack ** Ultimate

TABLE D-46

STIRRUP STRAINS (MICRO INCHES PER INCH), BEAM CB-5

Load Stage	Strain Gauge Location											
	1-T	1-S	1-B	1-N	2-T	2-S	2-B	2-N	3-T	3-S	3-B	3-N
0	0	0	0	0	0	0	0	0	0	0	0	0
1	0	0	5	- 5	0	5	- 5	- 5	5	0	0	0
2	0	10	10	-10	0	10	-10	-10	10	0	- 5	5
3	0	15	10	-10	0	10	-10	-10	10	0	-10	5
4	0	20	15	-15	5	15	-15	-10	15	0	-10	5
5	0	25	15	-15	10	15	-15	- 5	15	0	-10	5
6	0	35	15	-15	10	15	-20	- 5	20	0	-10	5
7	0	40	15	-15	10	15	-20	- 5	20	5	-10	5
8	0	50	15	-20	10	20	-20	- 5	20	10	-10	10
9	0	55	20	-20	15	20	-20	0	25	10	-10	15
10	10	65	20	-20	15	25	-20	5	25	15	- 5	15
11	10	70	20	-20	15	25	-20	10	30	20	0	15
12*	10	75	30	-20	20	30	-20	20	35	30	0	20
13	10	80	20	-25	20	35	-20	30	40	35	0	25
14	15	80	10	-45	15	40	-20	45	40	45	0	25
15	35	75	0	-55	10	40	-20	65	45	60	5	25
16	65	80	-10	-60	10	50	-20	80	50	70	10	30
17	90	95	-25	-55	10	60	-20	90	55	85	10	30
18	125	200	-40	-50	10	70	-20	100	60	105	30	35
19	240	500	65	5	30	60	-45	130	70	120	25	35
20	340	950	355	1030	40	65	-10	180	80	345	35	35
21	620	1115	740	1505	130	85	160	250	90	365	45	40
22**	1410	1030	-	1490	950	445	565	480	85	140	25	40

* First Crack ** Ultimate

TABLE B-47

LONGITUDINAL STEEL STRAINS (MICRO INCHES PER INCH), BEAM CB-6

Load Stage	Strain Gauge Location				
	a	b	c	d	e
0		0	0	0	0
1		0	0	0	10
2		0	0	0	10
3		0	0	0	10
4		0	0	- 5	10
5		- 5	0	- 5	10
6		-30	- 5	- 5	5
7		-35	-15	- 5	5
8		-45	-35	-10	5
9		-80	-50	-25	5
10		-105	-70	-45	- 5
11		-125	-90	-65	-15
12*		-140	-105	-85	-35
13		-160	-120	-115	-55
14		-185	-135	-145	-85
15		-220	-170	-185	-145
16		-255	-210	-235	-235
17		-295	-245	-265	-290
18		-305	-265	-295	-375
19		-390	-300	-340	-440
20		-510	-330	-430	-515
21		-600	-320	-430	-545
22		-100	-305	-420	-850
23		10	-295	-415	-535
24**		125	-290	-490	-570
25		-	-	-	-

* First Crack ** Ultimate

TABLE B-48

STIRRUP STRAINS (MICRO INCHES PER INCH), BEAM CB-6

Load Stage	Strain Gauge Location											
	1-T	1-S	1-B	1-N	2-T	2-S	2-B	2-N	3-T	3-S	3-B	3-N
0	0	0	-	0	0	0	0	0	0	0	0	0
1	0	0	-	0	0	0	0	0	0	0	0	0
2	0	0	-	0	0	0	0	0	0	0	0	0
3	0	0	-	0	0	0	5	0	0	0	5	0
4	- 5	0	-	5	0	0	10	0	0	- 5	- 5	10
5	- 5	0	-	10	0	0	10	5	5	-10	- 5	10
6	- 5	0	-	15	0	0	10	5	5	-10	- 5	10
7	- 5	0	-	25	5	0	15	5	5	-15	- 5	15
8	- 5	- 5	-	35	30	-10	15	10	10	-15	- 5	15
9	0	- 5	-	50	45	-10	15	10	10	-15	- 5	15
10	0	- 5	-	60	55	-10	15	10	10	-20	- 5	20
11	5	- 5	-	75	65	-15	15	15	15	-20	- 5	20
12*	10	- 5	-	95	75	-15	15	15	15	-30	- 5	20
13	10	-10	-	150	100	-20	20	25	20	-25	-10	25
14	5	-15	-	200	125	-30	20	30	25	-30	-10	30
15	0	-25	-	305	155	-30	30	35	35	-35	-10	30
16	-10	-35	-	530	215	-25	30	35	30	-45	-10	35
17	-10	-50	-	590	275	-35	30	35	75	-50	-10	40
18	0	-60	-	640	390	-45	15	25	115	-65	-15	50
19	20	-70	-	690	645	-70	5	5	140	-85	-20	70
20	790	365	-	775	745	-85	-15	0	160	-95	-25	90
21	1050	700	-	905	905	-90	-30	90	175	-105	-35	115
22	1270	1045	-	1060	1055	-100	40	360	185	-115	-45	160
23	1430	1390	-	1220	1170	-45	230	655	200	-125	-55	220
24**	1450	1495	-	1445	1295	275	540	1160	205	-130	-70	260

* First Crack **Ultimate

TABLE B-49

PRESTRESSING STEEL STRAINS (MICRO INCHES PER INCH), BEAM CH-1

Load Stage	Strain Gauge Location				
	a	b	c	d	e
0	0	0	0	0	0
1	45	50	50	-60	-55
2	100	110	115	-140	-125
3	165	175	185	-225	-205
4	200	220	230	-275	-260
5	250	270	280	-330	-315
6	280	310	315	-370	-350
7	315	345	350	-415	-390
8*	355	390	390	-455	-430
9	400	450	450	-515	-480
10	475	535	545	-565	-530
11	570	625	640	-620	-580
12	715	765	805	-680	-635
13	875	935	980	-745	-690
14	1055	1085	1160	-800	-730
15	1240	1275	1385	-865	-785
16	1425	1465	1620	-920	-830
17	1625	1660	1795	-990	-890
18	1830	1900	1855	-1050	-950
19	2040	2240	1910	-1100	-1005
20	2145	2445	1910	-1150	-1055
21	2175	2520	1930	-1170	-1065
22	2200	2440	1935	-1205	-1080
23**	2280	2460	1970	-1240	-1130

* First Crack ** Ultimate

TABLE B-50

PRESTRESSING STEEL STRAINS (MICRO INCHES PER INCH), BEAM CH-2

Load Stage	Strain Gauge Location				
	a	b	c	d	e
0	0	0	0	0	0
1	30	30	40	45	45
2	65	70	90	100	115
3	105	115	145	160	190
4	150	160	205	225	280
5	175	190	245	265	340
6*	195	215	270	310	400
7	220	240	300	350	490
8	240	265	335	475	610
9	265	295	385	565	780
10	290	310	585	740	1010
11	315	335	830	950	1210
12	355	365	1145	1200	1425
13	460	405	1300	1430	1615
14	710	515	1460	1665	1890
15	850	740	1640	1915	2160
16	975	1185	1825	2160	2440
17	1150	1365	2055	2450	2735
18	1270	1520	2250	2735	3025
19	1355	1620	2355	2880	3180
20**	1430	1700	2450	3025	3320

* First Crack ** Ultimate

TABLE B-51

STIRRUP STRAINS (MICRO INCHES PER INCH), BEAM CH-2

Load Stage	Strain Gauge Location											
	1-T	1-S	1-B	1-N	2-T	2-S	2-B	2-N	3-T	3-S	3-B	3-N
0	0	0	0	0	0	0	0	0	0	0	0	0
1	0	0	0	0	10	10	0	0	10	0	0	0
2	5	0	-10	10	20	15	-10	10	35	0	-15	0
3	15	5	-20	10	30	20	-15	15	50	0	-30	0
4	25	15	-25	10	35	25	-25	15	60	0	-45	- 5
5	25	30	-30	15	40	35	-25	15	65	- 5	-60	-15
6*	30	35	-35	15	45	40	-25	15	70	- 5	-65	-15
7	35	45	-35	15	50	45	-30	15	75	- 5	-70	-20
8	40	50	-40	15	55	50	-25	15	85	25	- 5	-15
9	45	65	-40	15	60	60	0	15	95	125	5	0
10	50	70	-45	20	65	70	135	20	110	220	110	15
11	65	80	-50	20	70	70	275	25	125	310	185	20
12	55	95	-45	25	80	75	475	20	140	435	235	40
13	65	105	-10	25	90	60	605	20	155	515	270	80
14	70	105	170	15	105	90	700	20	175	600	315	95
15	75	110	285	15	115	115	805	30	200	680	335	95
16	85	105	380	30	135	275	870	45	240	760	395	85
17	95	105	475	40	150	370	955	60	280	895	435	85
18	105	100	570	50	165	435	1025	80	300	985	470	80
19	115	180	600	60	180	500	1065	90	325	1030	500	85
20**	120	215	625	70	190	550	1080	100	325	1050	500	85

* First Crack ** Ultimate

TABLE B-32

PRESTRESSING STEEL STRAINS (MICRO INCHES PER INCH), BEAM CB-1

Load Stage	Strain Gauge Location				
	a	b	c	d	e
0	0	0	0	0	0
1	35	35	45	35	85
2	70	75	95	75	150
3	90	100	130	105	190
4	110	130	160	135	225
5	125	150	185	155	260
6	145	170	210	180	300
7	155	190	225	205	335
8*	160	200	250	215	380
9	180	225	275	245	425
10	195	245	295	285	545
11	210	270	325	430	715
12	225	295	390	600	935
13	235	310	745	835	1045
14	260	650	1030	1180	1170
15	370	925	1180	1410	1330
16	410	1045	1325	1635	1505
17	455	1150	1485	1810	1645
18	475	1245	1610	1910	1630
19	510	1340	1730	2030	1640
20	550	1440	1850	2160	1760
21	590	1560	1985	2315	1925
22	620	1655	2115	2475	2160
23**	-	-	-	2700	-

* First Crack ** Ultimate

TABLE B-33

STIRRUP STRAINS (MICRO INCHES PER INCH), BEAM CB-1

Load Stage	Strain Gauge Location											
	1-T	1-I	1-B	1-O	2-T	2-I	2-B	2-O	3-T	3-I	3-B	3-O
0	0	0	0	0	0	0	0	0	0	0	0	0
1	10	0	0	10	10	10	-10	5	15	10	-10	0
2	20	0	-10	10	20	15	-15	5	30	10	-20	0
3	25	0	-20	10	25	20	-20	5	40	10	-30	0
4	30	0	-25	10	30	20	-25	5	50	15	-40	0
5	40	5	-30	10	35	25	-30	10	55	15	-50	0
6	45	5	-30	10	40	30	-35	10	60	15	-60	0
7	50	10	-35	10	45	35	-35	10	70	20	-60	0
8*	50	15	-35	10	45	40	-35	10	75	20	-65	0
9	55	20	-40	10	50	50	-40	10	80	60	-15	- 5
10	60	50	-40	10	55	50	-40	10	90	150	-30	- 5
11	65	130	-45	30	60	55	-40	10	100	300	-30	- 5
12	75	180	-45	10	65	80	-40	20	120	510	760	30
13	80	260	-30	30	80	330	-20	30	140	640	850	190
14	85	700	0	0	105	710	360	160	170	780	935	335
15	100	925	310	30	125	890	675	275	305	880	1010	535
16	110	1115	670	30	145	965	850	390	230	940	1080	665
17	130	1320	775	70	170	1050	995	490	300	990	1080	765
18	135	1380	860	105	190	1095	1090	560	335	1035	1130	835
19	140	1440	915	135	200	1105	1165	610	365	1075	1160	865
20	150	1540	965	180	215	1130	1235	675	415	1090	1205	885
21	160	1600	1020	210	230	1155	1310	725	475	1060	1285	900
22	180	1670	1070	250	245	1180	1375	770	535	1070	1435	975
23**	-	-	-	-	-	-	-	-	-	-	-	-

* First Crack ** Ultimate

TABLE B-54

PRESTRESSING STEEL STRAINS (MICRO INCHES PER INCH), BEAM CB-4

Load Stage	Strain Gauge Location				
	a	b	c	d	e
0	-	0	0	0	0
1	-	-15	-20	-30	20
2	-	-30	-30	-55	10
3	-	-40	-40	-80	- 5
4	-	-55	-55	-130	-30
5*	-	-70	-75	-130	-25
6	-	-80	-90	-155	-50
7	-	-85	-95	-175	-40
8	-	-95	-110	-180	-70
9	-	-110	-130	-190	-55
10	-	-120	-140	-200	-50
11	-	-125	-135	-205	-40
12	-	-120	-130	-205	-30
13	-	-105	-110	-200	5
14	-	-55	-105	-205	65
15**	-	20	-25	-210	35

* First Crack ** Ultimate

TABLE B-55

STIRRUP STRAINS (MICRO INCHES PER INCH), BEAM CB-4

Load Stage	Strain Gauge Location											
	1-T	1-S	1-B	1-N	2-T	2-S	2-B	2-N	3-T	3-S	3-B	3-N
0	0	0	0	0	0	0	0	0	0	0	0	0
1	5	5	0	0	0	10	0	0	5	5	0	10
2	10	10	0	0	5	15	-10	0	5	10	0	10
3	15	15	-10	0	10	25	-10	0	10	15	0	10
4	25	35	-15	0	15	40	-15	0	10	30	- 5	10
5*	30	50	-25	0	20	80	-25	0	10	160	-15	10
6	35	85	-30	0	25	145	-35	0	15	305	-20	10
7	55	145	-40	0	30	240	-40	0	20	480	-20	10
8	65	185	-50	0	35	340	-45	0	20	660	-25	10
9	75	260	-55	0	40	490	-45	0	20	720	-20	25
10	80	315	-55	0	40	600	-45	0	25	760	-25	60
11	95	350	-55	0	45	675	-35	0	25	835	-25	110
12	110	365	-45	5	50	730	-30	0	30	875	-30	210
13	125	400	25	10	50	830	-35	0	40	930	-10	360
14	185	450	80	90	75	1075	-45	0	70	985	70	580
15**	630	510	155	605	170	1175	170	45	485	1030	210	735

* First Crack ** Ultimate

TABLE B-56

PRESTRESSING STEEL STRAINS (MICRO INCHES PER INCH), BEAM CB-5

Load Stage	Strain Gauge Location				
	a	b	c	d	e
0	0	0	0	0	0
1	0	0	0	0	10
2	- 5	- 5	-10	10	10
3	- 5	- 5	-10	20	5
4	-10	-10	-15	25	- 5
5	-10	-10	-20	30	0
6	-15	-15	-20	35	0
7	-25	-15	-20	35	-10
8	-30	-20	-25	40	-10
9	-30	-20	-25	45	-10
10	-45	-25	-30	50	-20
11	-95	-40	-30	55	-20
12*	-135	-65	-35	60	-25
13	-500	-455	-215	75	-30
14	-530	-730	-315	90	-35
15	-475	-860	-480	130	-30
16	-390	-875	-590	210	-20
17	-335	-550	-540	310	-35
18	-190	-340	-540	345	-80
19	-75	-400	-510	375	-40
20**	-	-	-	-	-

*First Crack ** Ultimate

TABLE B-57

STIRRUP STRAINS (MICRO INCHES PER INCH), BEAM CB-5

Load Stage	Strain Gauge Location											
	1-T	1-S	1-B	1-N	2-T	2-S	2-B	2-N	3-T	3-S	3-B	3-N
0	0	0	0	0	0	0	0	0	0	0	0	0
1	0	0	0	0	0	0	0	0	0	0	0	0
2	0	5	5	0	5	0	0	0	5	10	0	5
3	0	5	5	- 5	5	5	0	0	10	10	- 5	0
4	0	10	5	- 5	5	10	0	0	10	15	-10	0
5	0	15	10	- 5	5	10	0	0	10	20	-10	0
6	0	20	10	- 5	5	10	0	0	15	20	-10	0
7	0	35	10	0	10	15	0	0	20	20	-10	0
8	0	45	10	0	10	20	0	0	20	25	-10	0
9	5	70	10	0	10	25	0	0	25	30	-15	5
10	10	90	10	0	10	30	0	5	25	35	-15	5
11	10	120	10	5	10	35	0	5	30	40	-15	5
12*	40	135	10	10	10	60	- 5	10	30	50	-20	5
13	585	175	5	-10	35	190	-10	195	50	85	-20	10
14	625	190	5	-15	40	220	-15	205	50	90	-25	15
15	720	230	10	-15	45	295	-20	210	60	100	-30	35
16	820	465	35	- 5	60	380	-15	240	65	125	-35	45
17	890	650	750	65	375	735	55	275	105	125	-40	60
18	1080	1020	1040	510	840	940	480	385	130	125	-30	60
19	1380	1360	1310	730	1405	1330	1115	535	195	465	-50	75
20**	-	-	-	-	-	-	-	-	-	-	-	-

* First Crack ** Ultimate

TABLE B-58

PRESTRESSING STEEL STRAINS (MICRO INCHES PER INCH), BEAM CB-6

Load Stage	Strain Gauge Location				
	a	b	c	d	e
0	0	0	0	0	0
1	- 5	- 5	0	0	20
2	- 5	- 5	0	- 5	20
3	- 5	- 5	0	- 5	-20
4	- 5	-10	0	-10	- 5
5	0	-10	0	-15	0
6	0	-15	- 5	-15	0
7	0	-20	- 5	-15	10
8	5	-25	- 5	-20	15
9	10	-40	-10	-20	15
10*	10	-80	-20	-25	20
11	10	-105	-40	-30	20
12	5	-125	-50	-30	20
13	- 5	-160	-80	-40	25
14	-10	-185	-105	-45	30
15	-45	-245	-145	-80	45
16	-165	-355	-275	-105	125
17	-135	-370	-420	-250	175
18	-130	-350	-450	-275	210
19	-120	-335	-450	-295	215
20	1920	-420	-450	-280	225
21	1920	-440	-430	-255	250
22**	1930	-435	-415	-250	250
23	1950	-70	-425	-370	95

* First Crack ** Ultimate

TABLE B-59

STIRRUP STRAINS (MICRO INCHES PER INCH), BEAM CB-6

Load Stage	Strain Gauge Location											
	1-T	1-S	1-B	1-E	2-T	2-S	2-B	2-E	3-T	3-S	3-B	3-E
0	0	0	0	0	0	0	0	0	0	0	0	0
1	0	0	0	0	0	0	0	0	0	0	0	0
2	0	0	0	0	0	0	0	0	0	0	0	0
3	0	0	0	0	0	0	0	0	0	0	0	0
4	0	5	- 5	0	0	0	0	0	10	0	0	0
5	5	10	0	0	5	0	0	0	10	5	0	5
6	15	10	- 5	5	5	5	0	0	10	5	0	5
7	25	15	- 5	5	10	5	0	5	15	5	0	5
8	50	15	- 5	5	25	5	0	5	15	5	0	5
9	70	15	- 5	5	35	5	0	10	20	10	0	10
10*	90	20	-10	5	60	0	0	10	20	10	0	10
11	90	20	-10	5	70	0	0	10	20	10	- 5	5
12	95	30	-10	5	85	5	0	10	25	15	0	10
13	105	40	-10	5	110	5	- 5	10	30	20	- 5	10
14	120	50	-10	20	140	10	- 5	10	40	30	- 5	10
15	180	80	-10	40	230	10	0	15	65	40	- 5	10
16	315	115	-15	110	370	5	- 5	15	105	80	- 5	10
17	430	120	-20	170	595	5	- 5	15	195	70	-20	115
18	865	190	-25	220	650	-10	-15	120	240	60	-20	165
19	980	315	-20	235	1205	-30	-10	270	295	60	0	240
20	1080	720	30	270	1370	-40	-10	390	340	60	20	280
21	1210	910	135	450	1580	-35	10	350	400	75	215	325
22**	1370	1065	410	790	1995	-	650	820	460	85	390	385
23	1440	1240	910	920	-	940	1320	1375	550	140	790	630

* First Crack ** Ultimate

APPENDIX C

PHOTOGRAPHS OF TESTED BEAMS

Photographs of the tested beams are presented in Figures C-1 through C-31 of this appendix. Each figure is composed of four views representing the south, north, top and bottom face of a beam. Continuity of cracks on three sides can be observed; it was not possible to match them since photographs of the different sides were taken at variable distances and angles.

In addition to crack patterns, the following details are also marked: projection of longitudinal and transverse steel on all four faces, location and designation of strain gauges, and projection of an opening in a hollow beam. This appendix, together with the preceding two, gives a complete picture of experimental data required for the study of beam behavior under combined loading throughout the entire loading history.

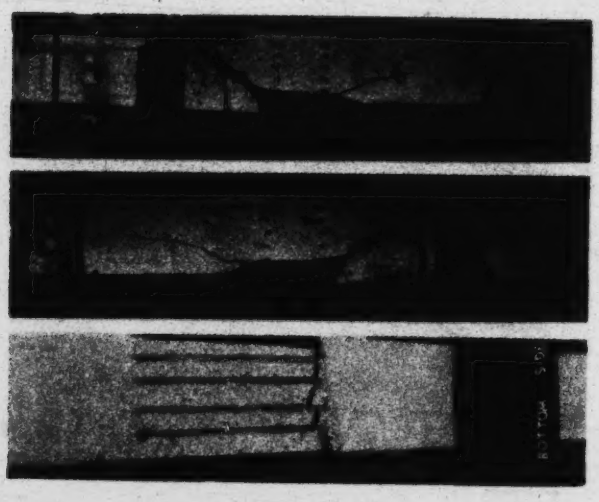

FIG. C-1 CRACK PATTERN AT FAILURE, BEAM BS-1

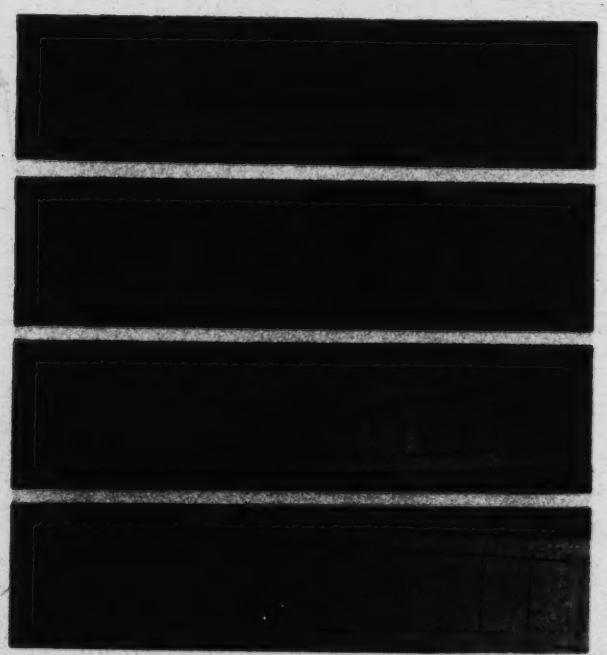

FIG. C-2 CRACK PATTERN AT FAILURE, BEAM BS-1S

FIG. C-3 CRACK PATTERN AT FAILURE, BEAM BS-2

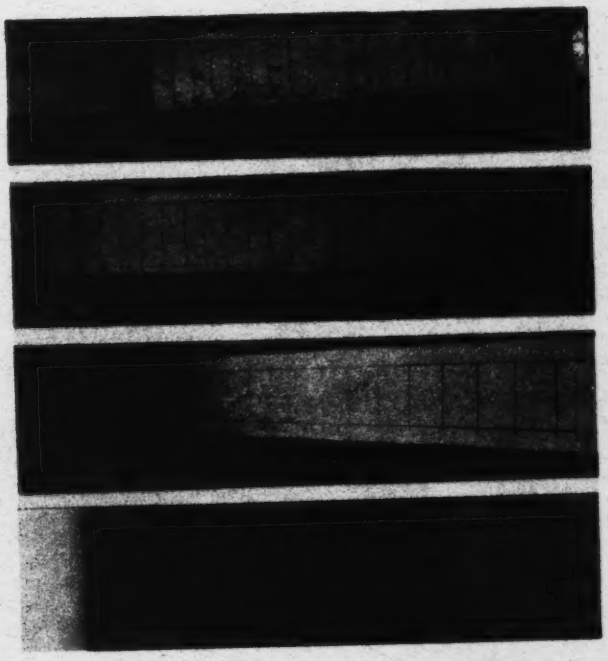

FIG. C-4 CRACK PATTERN AT FAILURE, BEAM BS-2S

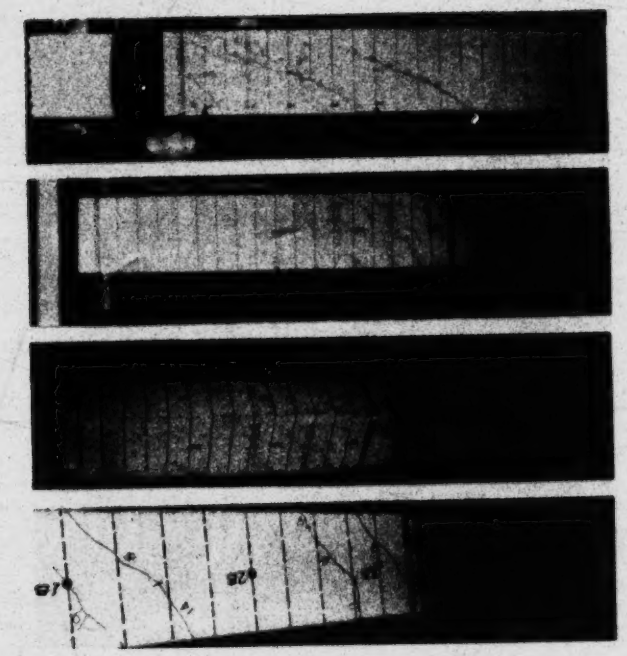

FIG. C-5 CRACK PATTERN AT FAILURE, BEAM BS-3

FIG. C-6 CRACK PATTERN AT FAILURE, BEAM BS-4

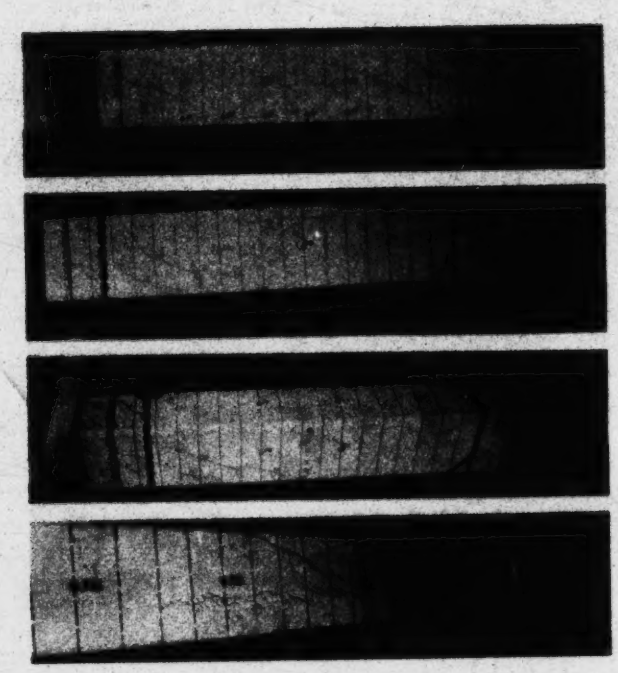

FIG. C-7 CRACK PATTERN AT FAILURE, BEAM BS-5

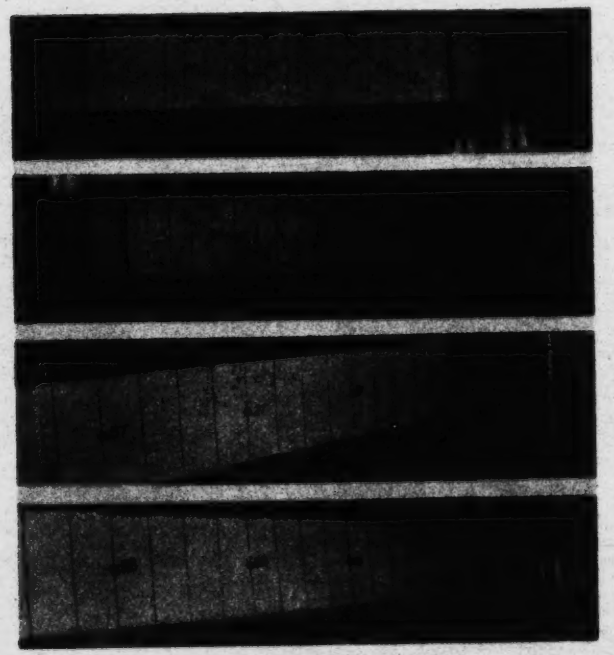

FIG. C-8 CRACK PATTERN AT FAILURE, BEAM BS-6

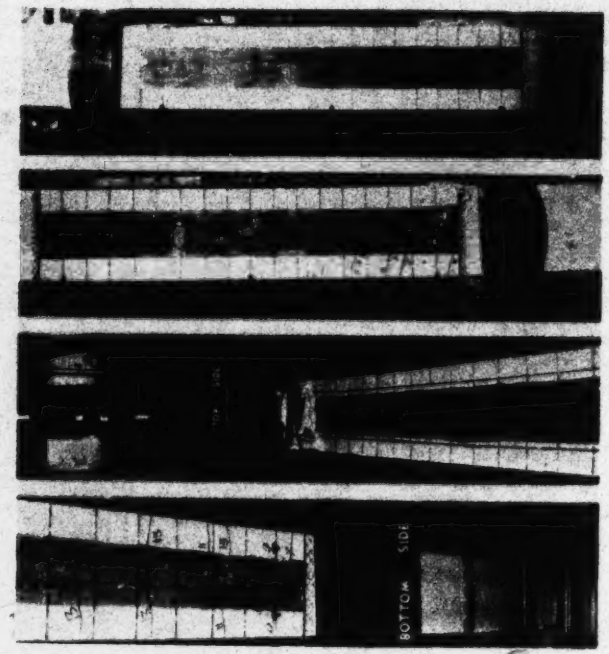

FIG. C-9 CRACK PATTERN AT FAILURE, BEAM BH-1

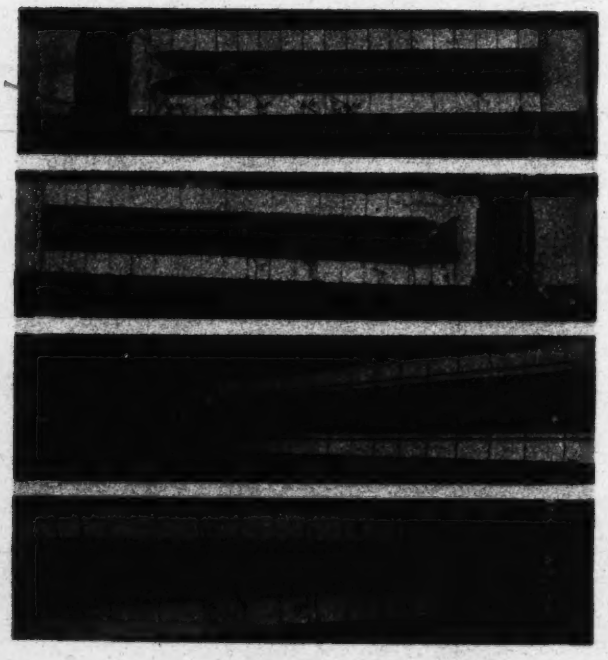

FIG. C-10 CRACK PATTERN AT FAILURE, BEAM BH-2

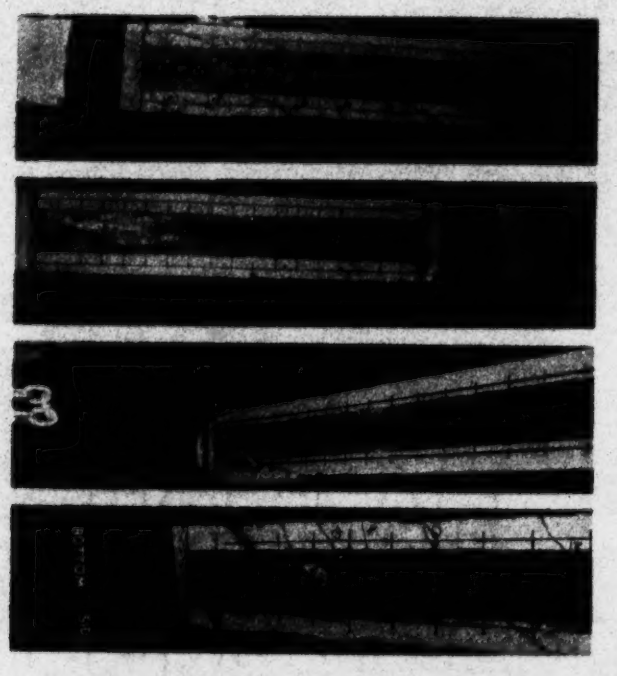

FIG. C-11 CRACK PATTERN AT FAILURE, BEAM BH-3

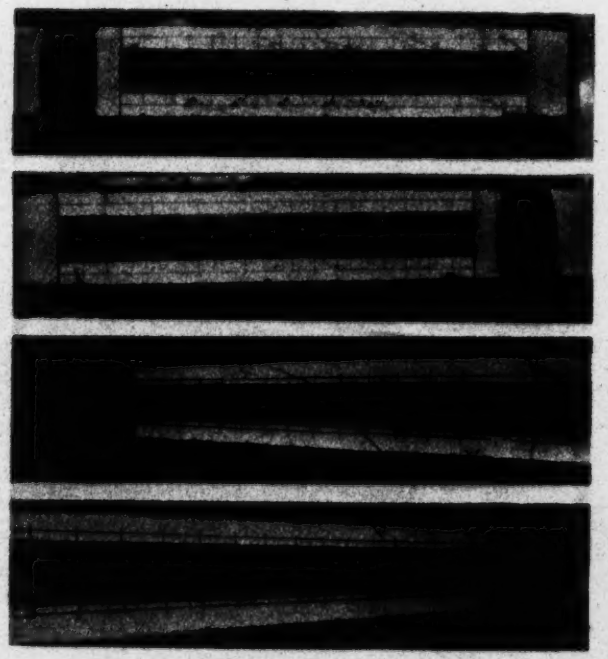

FIG. C-12 CRACK PATTERN AT FAILURE, BEAM BH-4

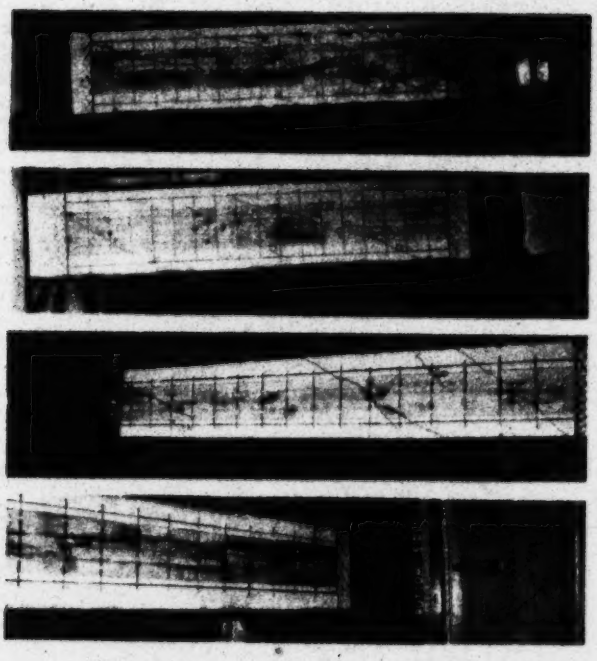

FIG. C-13 CRACK PATTERN AT FAILURE, BEAM BH-5

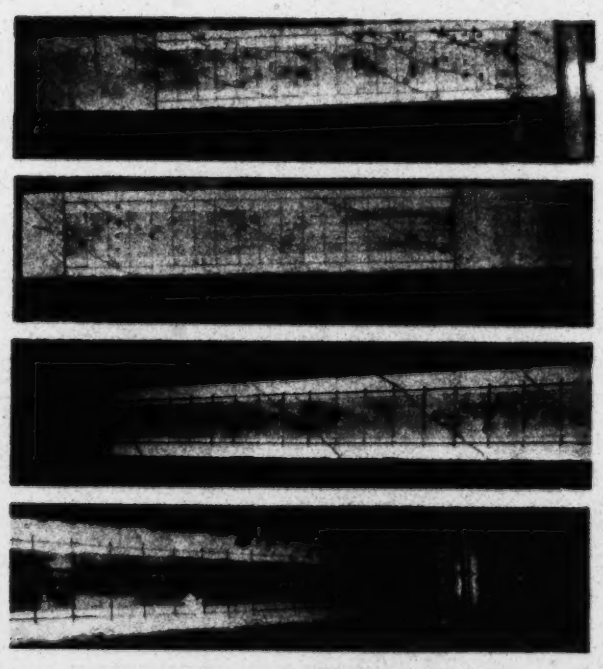

FIG. C-14 CRACK PATTERN AT FAILURE, BEAM BH-6

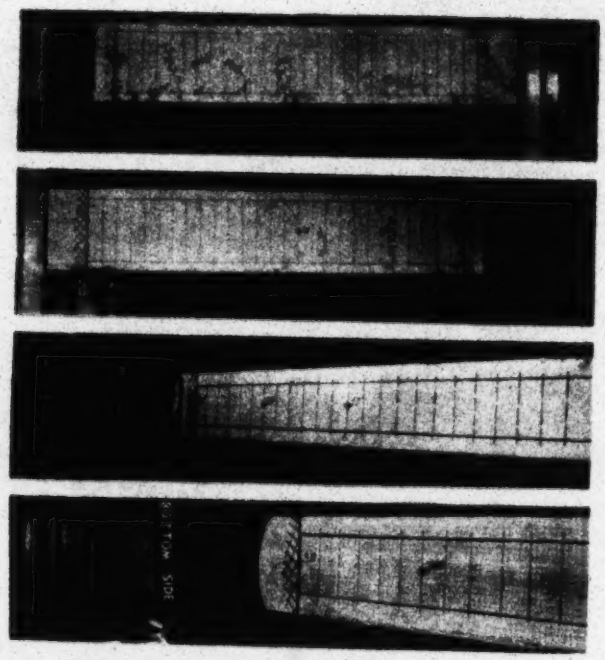

FIG. C-15 CRACK PATTERN AT FAILURE, BEAM B1S-2b

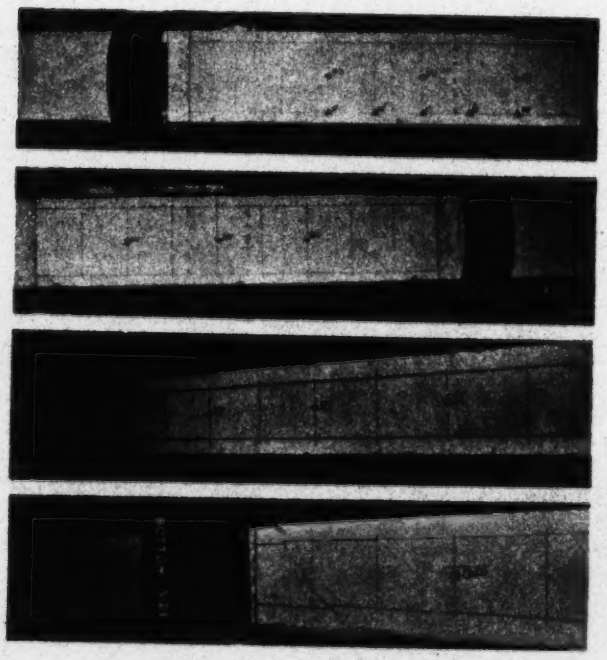

FIG. C-16 CRACK PATTERN AT FAILURE, BEAM B1S-4a

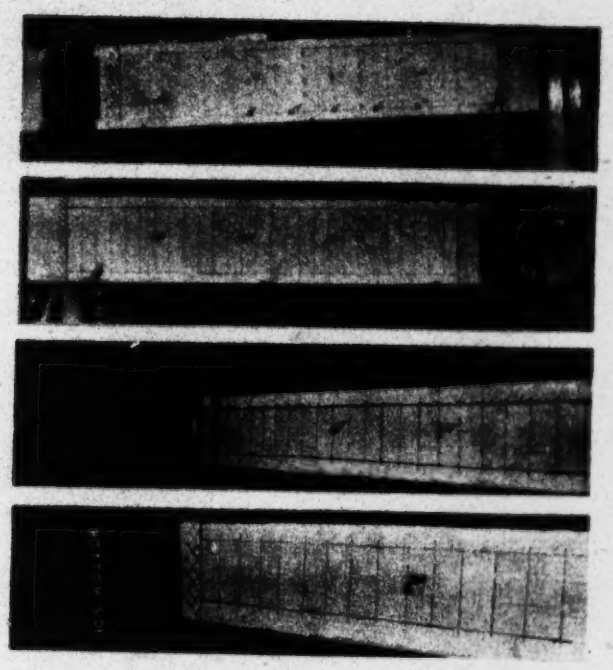

FIG. C-17 CRACK PATTERN AT FAILURE, BEAM B1S-4b

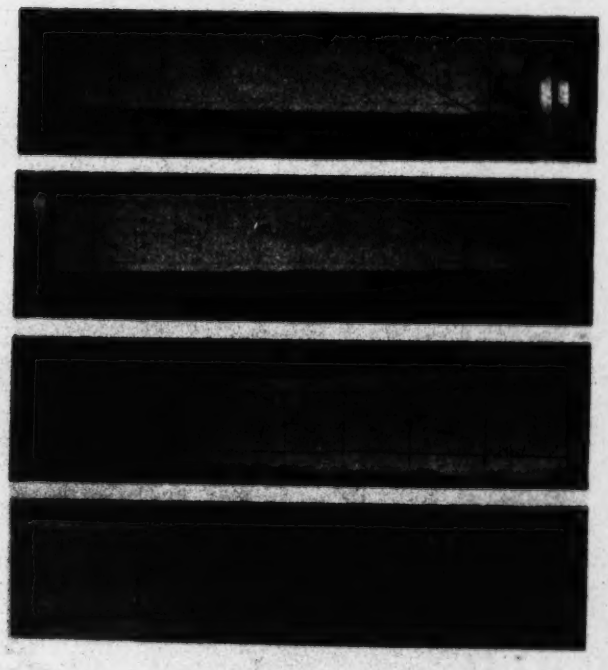

FIG. C-18 CRACK PATTERN AT FAILURE, BEAM B1S-6a

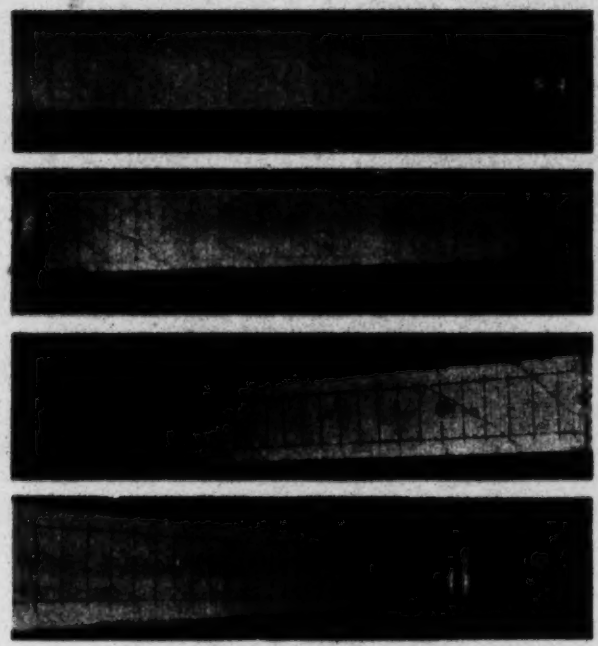

FIG. C-19 CRACK PATTERN AT FAILURE, BEAM B1S-6b

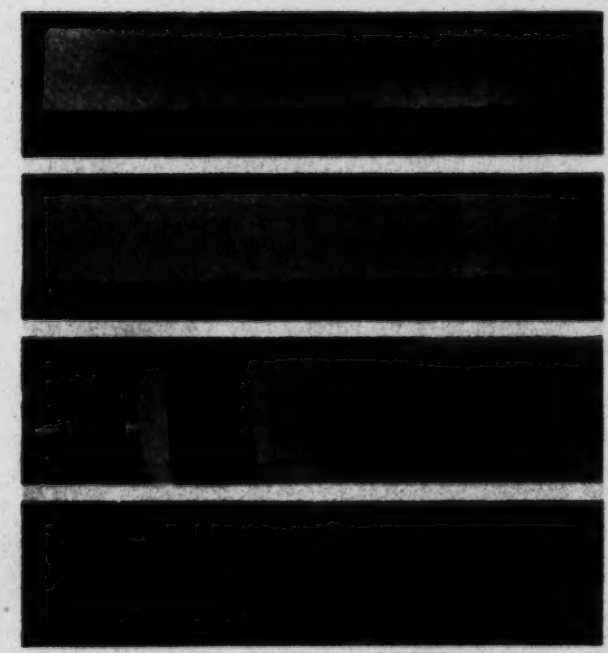

FIG. C-20 CRACK PATTERN AT FAILURE, BEAM CS-1

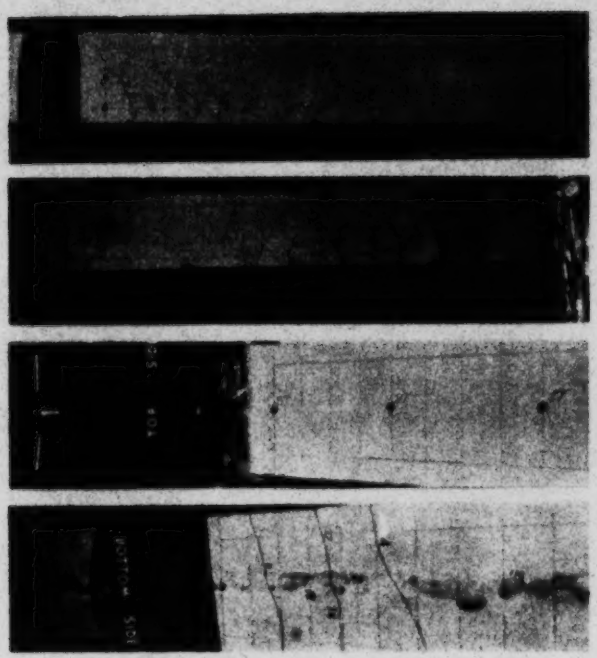

FIG. C-21 CRACK PATTERN AT FAILURE, BEAM CS-2

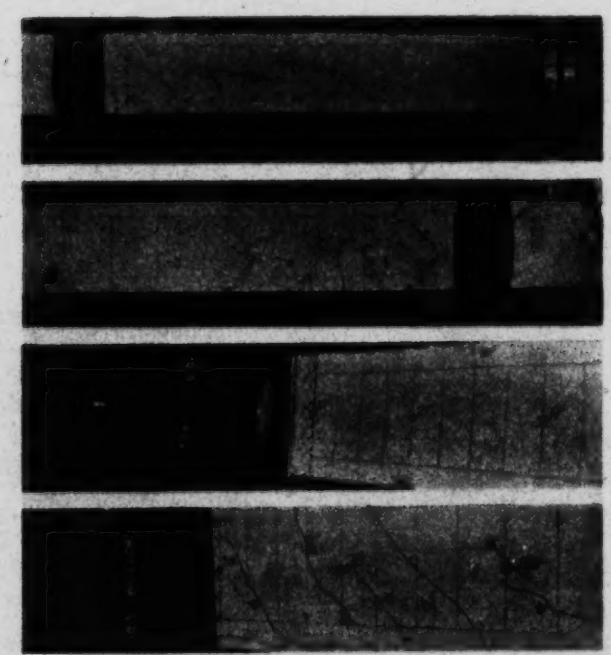

FIG. C-22 CRACK PATTERN AT FAILURE, BEAM CS-3

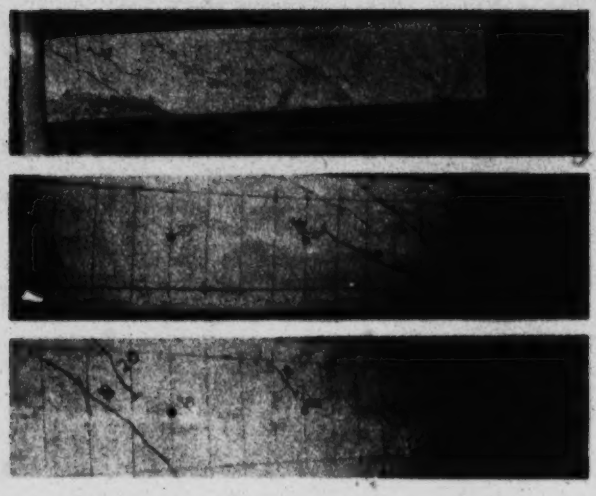

FIG. C-23 CRACK PATTERN AT FAILURE, BEAM CS-4

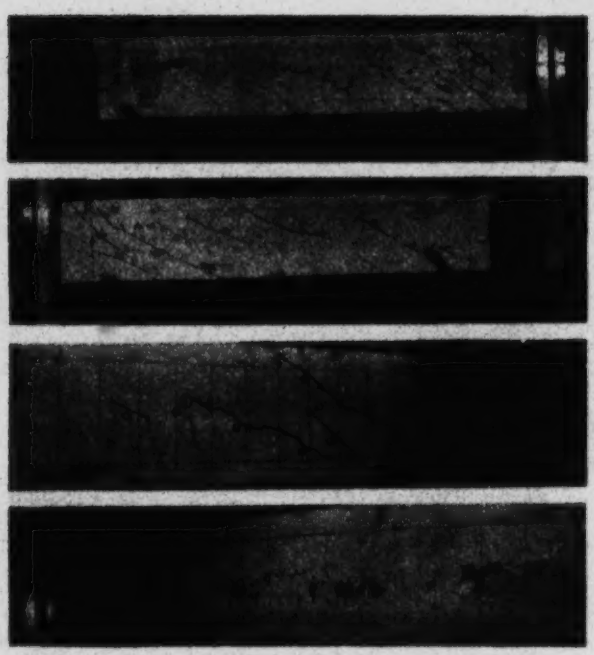

FIG. C-24 CRACK PATTERN AT FAILURE, BEAM CS-5

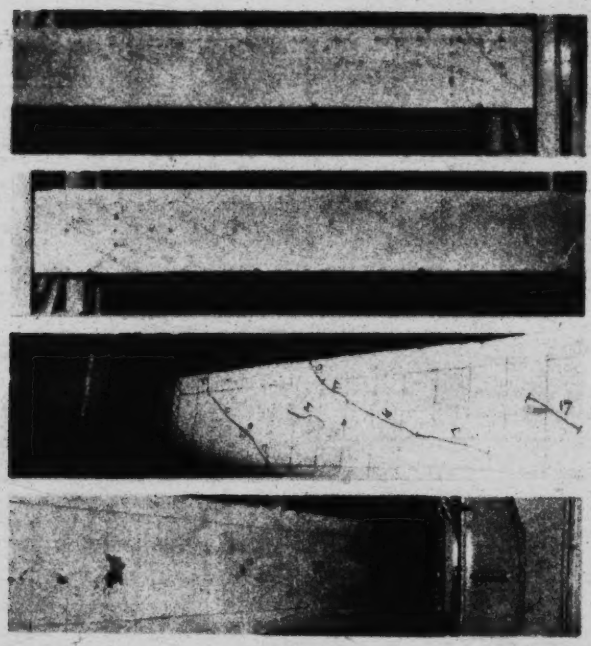

FIG. C-25 CRACK PATTERN AT FAILURE, BEAM CS-6

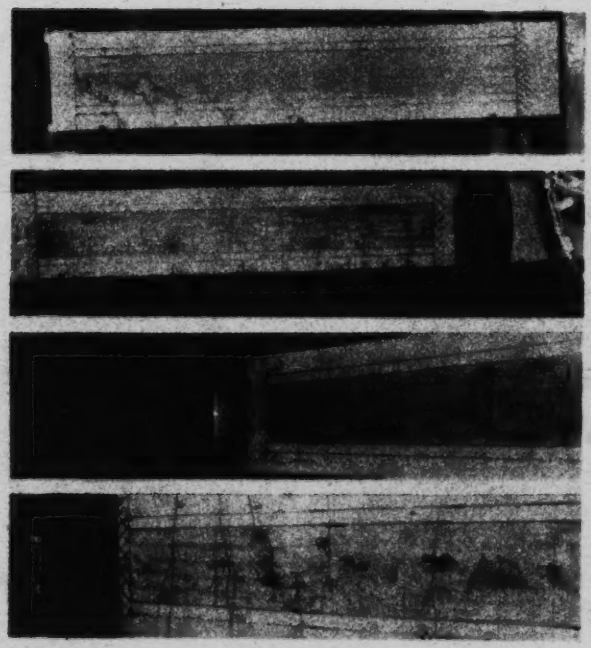

FIG. C-26 CRACK PATTERN AT FAILURE, BEAM CH-1

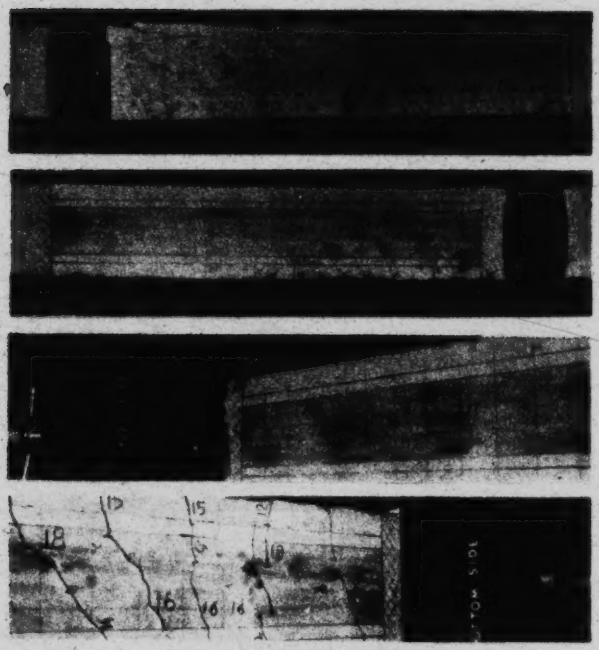

FIG. C-27 CRACK PATTERN AT FAILURE, BEAM CH-2

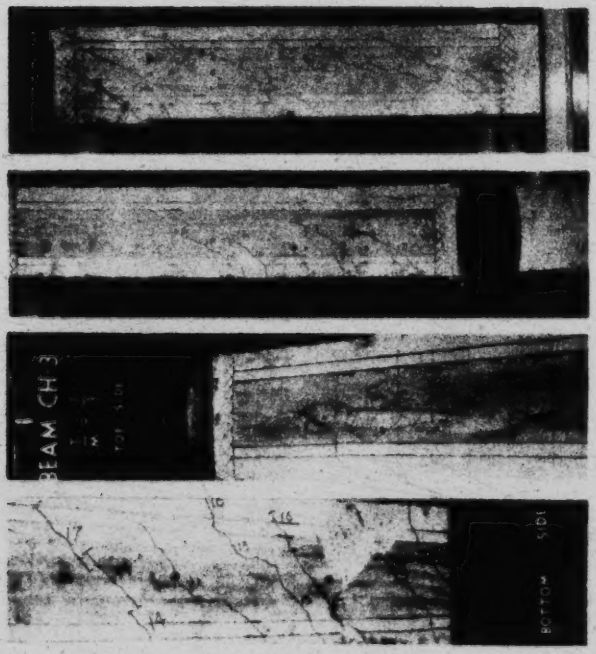

FIG. C-28 CRACK PATTERN AT FAILURE, BEAM CH-3

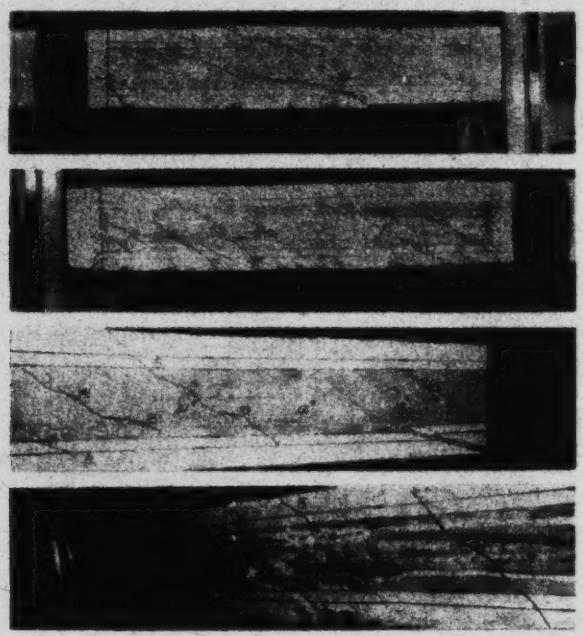

FIG. C-29 CRACK PATTERN AT FAILURE, BEAM CH-4

FIG. C-30 CRACK PATTERN AT FAILURE, BEAM CH-5

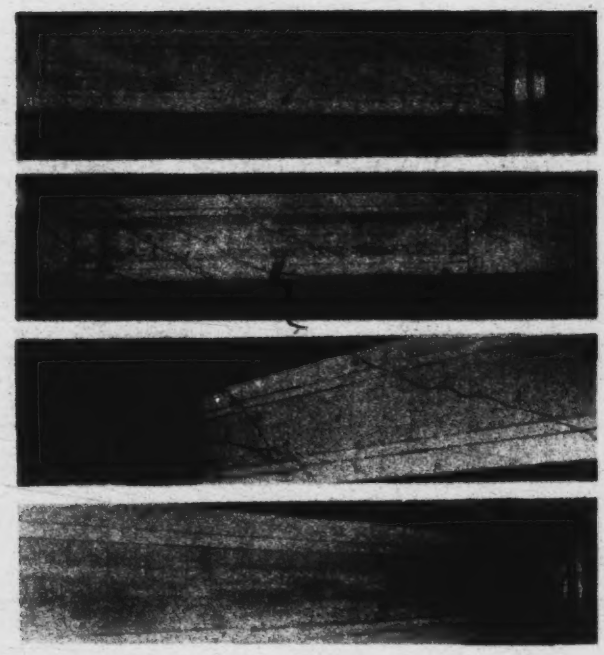

FIG. C-31 CRACK PATTERN AT FAILURE, BEAM CH-6

APPENDIX D

COMPUTER PROGRAM

In this appendix a complete listing of the computer program with examples of output for each mode is presented. Nomenclature used in the program is given in Section D.1. Figure D.1 presents a general flow chart and identifies subroutines. Within the program numerous comment cards are included to describe subroutines and major statements; therefore no detailed flow chart is presented.

******

The author and the University of Alberta disclaim responsibility for missuse of the following program, nor will they be responsible for errors in the listing.

D.1 NOMENCLATURE FOR COMPUTER PROGRAM

A	DEPTH OF NEUTRAL AXIS
A1,A2,A3,A4	CONCRETE COVER ON EACH OF FOUR STIRRUP LEGS
ALFAE1	TORSION FACTOR IN ST. VENANT THEORY
ALFAE2	TORSION FACTOR IN ST. VENANT THEORY
AP	AREA OF A PRESTRESSING STRAND
ARCCOM	AREA OF AN ELEMENT IN COMPRESSION ZONE
AST	AREA OF A STIRRUP LEG
B	WIDTH OF A BEAM CROSS-SECTION
BETA	INCLINATION OF COMPRESSION ZONE W.R.T. LONGITUDINAL BEAM AXIS
BH	WIDTH OF AN OPENING IN A HOLLOW BEAM
BM	BENDING MOMENT
C	TOTAL COMPRESSIVE FORCE
D	DISTANCES FROM THE BOTTOM FACE OF A BEAM TO PRESTRESSING STRAND
DELTA	LOADING RATIO
DFMOD1	DISTANCE FROM EAST SUPPORT TO THE FAILURE CROSS-SECTION FOR MODE 1
DFMOD2	DISTANCE FROM EAST SUPPORT TO THE FAILURE CROSS-SECTION FOR MODE 2
DFMOD3	DISTANCE FROM EAST SUPPORT TO THE FAILURE CROSS-SECTION FOR MODE 3
DS	LOCATION OF PRESTRESSING STRANDS W.R.T. SIDE FACE OF A BEAM
DST1	DISTANCE FROM TOP FACE OF A BEAM TO THE UPPER STIRRUP LEG
DST2	DISTANCE FROM THE TOP FACE OF A BEAM TO THE LOWER STIRRUP LEG

DST3	DISTANCE FROM THE SIDE FACE OF A BEAM TO STIRRUP LEG LOCATED ADJACENT TO THAT FACE
DST4	DISTANCE FROM THE SIDE FACE OF A BEAM TO THE STIRRUP LEG LOCATED FURTHEST FROM THAT FACE
ECCN	ECCENTRICITY OF PRESTRESSING FORCE
ECON	MODULUS OF ELASTICITY OF CONCRETE
EPSCOM	COMPRESSIVE STRAIN IN STIRRUPS
EPSCE	STRAIN AT THE LEVEL OF THE REINFORCEMENT DUE TO EFFECTIVE PRESTRESS
EPSCU	CONCRETE STRAIN AT FAILURE
EPSSA	INCREASE IN STRAIN IN THE PRESTRESSING REINFORCEMENT BETWEEN PRESTRESS AND FAILURE
EPSSE	EFFECTIVE PRESTRAIN CORRESPONDING TO EFFECTIVE PRESTRESS
EPSSU	STRAIN IN THE PRESTRESSING REINFORCEMENT AT FAILURE
EPSTEN	TENSILE STRAIN IN STIRRUPS
ER	ERROR IN SUM OF FORCES PERPENDICULAR TO A CROSS-SECTION
ES	MODULUS OF ELASTICITY OF PRESTRESSING STEEL
ESTIR	MODULUS OF ELASTICITY OF TRANSVERSE REINFORCEMENT
FC	CYLINDER STRENGTH OF CONCRETE
FCELEM	ELEMENT STRESS IN COMPRESSION ZONE
FCOM	COMPRESSIVE STRESS IN STIRRUPS
FPULT	ULTIMATE STRENGTH OF PRESTRESSING STEEL
FSU	STRESS IN PRESTRESSING STEEL AT ULTIMATE
FTEN	TENSILE STRESS IN STIRRUPS
FYSTIR	ULTIMATE STRENGTH OF STIRRUPS

H	HEIGHT OF A BEAM CROSS-SECTION
HH	HEIGHT OF AN OPENING IN A HOLLOW BEAM
PHI	CURVATURE
S	STIRRUP SPACING
SIGMA	PRESTRESSING FORCE PER UNIT AREA
SMAXB	CONCRETE MAXIMUM PRINCIPAL STRESS (CRACK LOCATED ON BOTTOM FACE)
SMINB	CONCRETE MINIMUM PRINCIPAL STRESS (CRACK LOCATED ON BOTTOM FACE)
SMAXS	CONCRETE MAXIMUM PRINCIPAL STRESS (CRACK LOCATED ON SIDE FACE)
SMINS	CONCRETE MINIMUM PRINCIPAL STRESS (CRACK LOCATED ON SIDE FACE)
SMAXT	CONCRETE MAXIMUM PRINCIPAL STRESS (CRACK LOCATED ON TOP FACE)
SMINT	CONCRETE MINIMUM PRINCIPAL STRESS (CRACK LOCATED ON TOP FACE)
T	TOTAL TENSILE FORCE
TC	TENSILE FORCE DUE TO CONCRETE UNCRACKED ZONE
TCOM	TOTAL COMPRESSIVE FORCE DUE TO STIRRUPS
TCR	CRACKING TORQUE
TF	FLANGE THICKNESS IN A HOLLOW BEAM
THETA	ANGLE OF INITIAL CRACK
TTEN	TOTAL TENSILE FORCE DUE TO STIRRUPS
TW	DOUBLE WALL THICKNESS IN A HOLLOW BEAM
V	SHEAR FORCE
XCR	DEPTH OF THE TENSILE UNCRACKED ZONE
XINC	INCREMENT OF DEPTH OF NEUTRAL AXIS

XIX	MOMENT OF INERTIA ABOUT X-AXIS
XIY	MOMENT OF INERTIA ABOUT Y-AXIS
XKSI	LOADING RATIO
XKSIBT	TORSION TO BENDING RATIO ON BETA PLANE
XL	TOTAL LENGTH OF A BEAM
XMODR	MODULUS OF RUPTURE OF CONCRETE
XNCOM	NUMBER OF STIRRUPS INTERSECTED IN COMPRESSION ZONE
XNTEN	NUMBER OF STIRRUPS INTERSECTED IN TENSION ZONE
YC	DISTANCES FROM NEUTRAL AXIS TO CENTROIDS OF ELEMENTS IN COMPRESSION ZONE

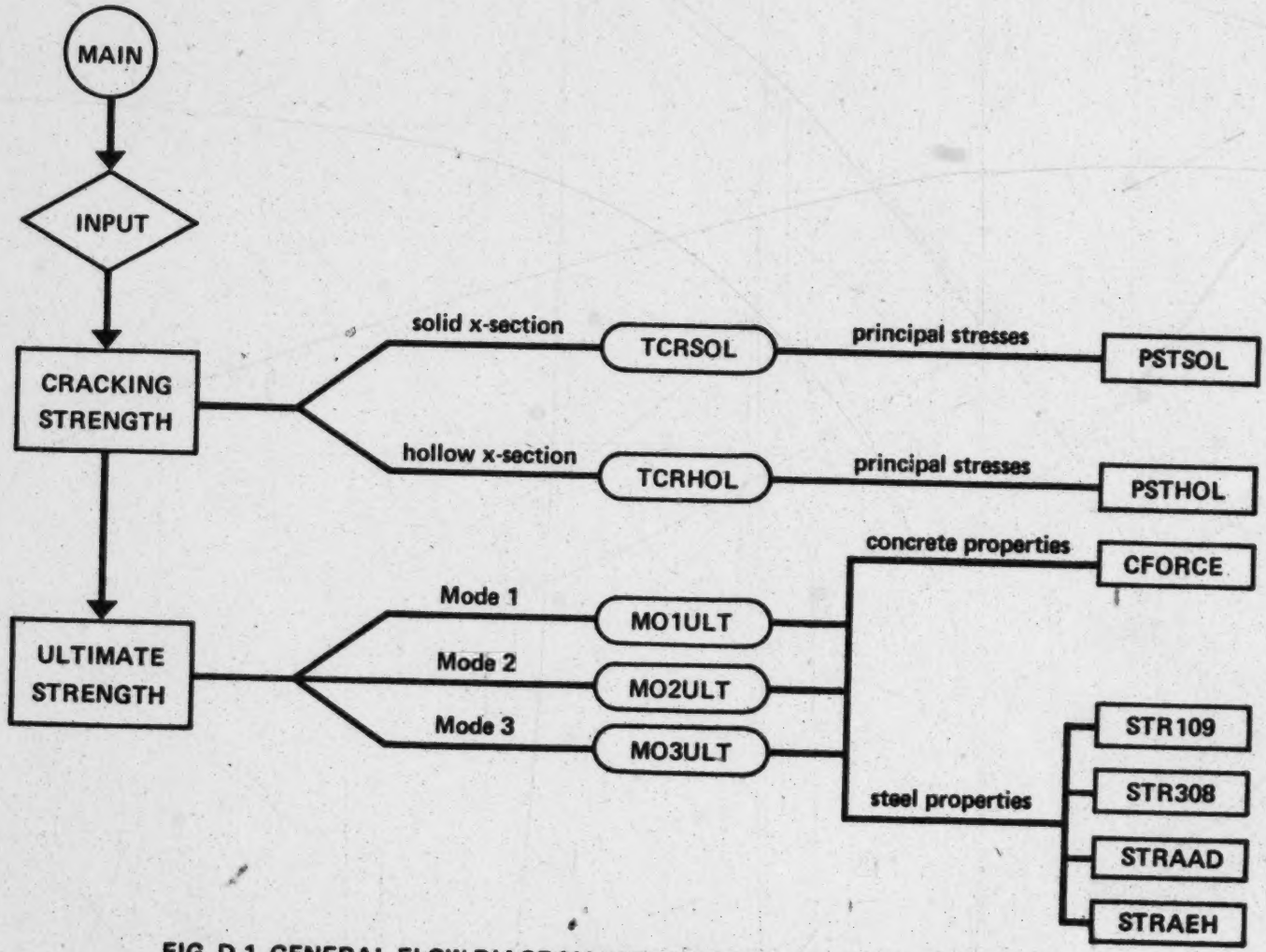

FIG. D-1 GENERAL FLOW DIAGRAM AND SUBROUTINE IDENTIFICATION

```
C     MAIN LINK
C
      IMPLICIT REAL*8(A-H,O-Z)
C
      COMMON AP,AST,B,FE,FSH,TSH,ES,ESTIP,EPSCF,EPSSE,EPSSA,EPSSH,H,N,
     2NH,NV,NI,PC,ENCRP,EPSCH,ECON,CCCH,A,SINC,T,C,KB,KEST,DELTA,
     3DST1,DST2,DST3,DST4,S,SIGMA,TANH,FPULT,FYSTR
     4,DFROD1,DFROD2,DFROD3,DS,KE1,TC,ECH,BETA,THETA,TH,TF,
     5EPSCON,EPSTEN,FCOMP,FYES,ENCON,ENYEN,TCON,TYES,A1,A2,A3,A4
     6,TCP,NR,Y,IBASE,ANING,SHAFT,SAINT,SHARE,SHIED,KIE,KIY,SI,SY,OS,OY
     7,ALPAR1,ALPAR2,THPRB,THPRS,THPRT
     8,AS,YS,APEA,YC,X,Y,DEPTH,ABIALL,FSUBC,SUAREA,YROD,EYIELD,ESH,
     9PULT,FFELD,FULT,FSH,PHIFAC,KELEN,TOTALF,TOTALP,
     1 TOTALH,EAS,FS,SUAF,SUAFP,SUAFH,CONST,PHI,DIP,ABCCOH,FCELEN
     2,HCOH,HCURP,FCOHP,ACOHP,ELFORC,FCCC,RESIST,FCEL
     3,THETA9,THETA8,THETTH
C
      COMMON N,H,NODE,NELLAS,NSTEEL,NADEEP,NRCOHP
C
      DIMENSION AP(10),B(10),FE(10),FSH(10),TSH(10),ES(10),
     1 EPSCF(10),EPSSE(10),FPSSA(10),EPSSH(10),DS(10),FPULT(10)
     2,AS(20),YS(20),APEA(500),YC(500),X(500),Y(500),KELEN(500),EAS(20),
     3 FCEL(500),FS(20),FCELEN(500),ABCCOH(500),ELFORC(500)
C
  10  CALL INPUT
C
      IF(BH.LT.1.0)CALL TCH001
      IF(BH.GE.1.0)CALL TCH002
C
C     CHANGE FOLLOWING CARD FOR NODE 2 (CALL H02ULT) AND FOR NODE 3 (CAL
C    L H03ULT)
      CALL H01ULT
      GO TO 10
      END
```

```
      SUBROUTINE INPUT
C
      IMPLICIT REAL*8(A-H,O-Z)
C
      COMMON AP,AST,B,FE,FSH,TSH,ES,ESTIP,EPSCF,EPSSE,EPSSA,EPSSH,H,N,
     2NH,NV,NI,PC,ENCRP,EPSCH,ECON,CCCH,A,SINC,T,C,KB,KEST,DELTA,
     3DST1,DST2,DST3,DST4,S,SIGMA,TANH,FPULT,FYSTR
     4,DFROD1,DFROD2,DFROD3,DS,KE1,TC,ECH,BETA,THETA,TH,TF,
     5EPSCON,FPSTEN,FCOMP,FYES,ENCON,ENYEN,TCON,TYES,A1,A2,A3,A4
     6,TCP,NR,Y,IBASE,ANING,SHAFT,SAINT,SHARE,SHIED,KIE,KIY,SI,SY,OS,OY
     7,ALPAR1,ALPAR2,THPRB,THPRS,THPRT
     8,AS,YS,APEA,YC,X,Y,DEPTH,ABIALL,FSUBC,SUAREA,YROD,EYIELD,ESH,
     9PULT,FFELD,FULT,FSH,PHIFAC,KELEN,TOTALF,TOTALP,
     1 TOTALH,EAS,FS,SUAF,SUAFP,SUAFH,CONST,PHI,DIP,ABCCOH,FCELEN
     2,HCOH,HCURP,FCOHP,ACOHP,ELFORC,FCCC,RESIST,FCEL
     3,THETA9,THETA8,THETTH
C
      COMMON N,H,NODE,NELLAS,NSTEEL,NADEEP,NRCOHP
C
      DIMENSION AP(10),B(10),FE(10),FSH(10),TSH(10),ES(10),
     1 EPSCF(10),EPSSE(10),EPSSA(10),EPSSH(10),DS(10),FPULT(10)
     2,AS(20),YS(20),APEA(500),YC(500),X(500),Y(500),KELEN(500),EAS(20),
     3 FCEL(500),FS(20),FCELEN(500),ABCCOH(500),ELFORC(500)
      DIMENSION TITLE(5),STAR(6)
C
      DATA STAR/6H******/
C     TITLE (BEAM NUMBER ,ETC.)
      READ(5,16,END=1000)TITLE
C     BEAM DIMENSIONS (IN)
      READ(5,30)B,H,BH,NH,NI
C     H = NO. OF PRESTRESSING STRANDS AND NODE = STRESS-STRAIN CHARACTER
C     ISTICS NODE=1 CORRESPONDS TO 1/2 INCH STRAND AND NODE=2 TO 1/8 INC
C     H STRAND, NODE=3 GROUPS AA-AD, NODE=4 GROUPS AE-AH
      READ(5,40)N,NODE
C     PRESTRESSING STEEL AREAS (SQ.INS)
      READ(5,30)(AP(I),I=1,N)
C     TRIANGULAR STEEL (ONE LEG) AREA
      READ(5,30)AST
C     STEEL LOCATIONS (DISTANCES FROM THE BOTTOM IN INCHES)
      READ(5,30)(B(I),I=1,N)
C     STEEL LOCATIONS (DISTANCES FROM THE SIDE IN INCHES)
      READ(5,30)(BC(I),I=1,N)
C     TRANSVERSE STEEL LOCATIONS (DISTANCES FROM THE TOP AND SIDES)
      READ(5,30)DST1,DST2,DST3,DST4
C     STIRRUP SPACING (IN.)
      READ(5,30)S
C     ULTIMATE STRESS IN PRESTRESSING STEEL - KSI
C     YIELD STRESS OF MILD STEEL - KSI
      READ(5,30)(FPULT(I),I=1,N)
      READ(5,30)FYSTR
C     MODULI OF ELASTICITY OF PRESTRESSING STEEL - KSI
      READ(5,30)(ES(I),I=1,N)
C     MODULI OF ELASTICITY OF MILD STEEL - KSI
      READ(5,30)ESTIP
C     EFFECTIVE PRESTRESSING FORCES (KIPS)
```

```
      READ(5,10)(FE(I),I=1,N)
C     CONCRETE COMPRESSIVE STRENGTH (PSI),MODULUS OF RUPTURE AND
C     ULTIMATE COMPRESSIVE STRAIN
      READ(5,10)FC,RMODR,EPSCU
C     LOADING PATTERN INCR AND DELTA
      READ(5,10)XINCR,DELTA
C     LOCATION OF FAILURE SURFACE MEASURED FROM EAST SUPPORT (IN.)
      READ(5,35)DFMOD1,DFMOD2,DFMOD3
   10 FORMAT(5F10)
   25 FORMAT(12I,4A4,/ 5X,'* ',5A4,' *'/ 6X,4A4////)
   30 FORMAT(8F10.4)
   40 FORMAT(8I10)
C     MODULUS OF ELASTICITY OF CONCRETE (A C I FORMULA) - PSI
      EC=6.5*SQRT(FC)
C     COEFFICIENT OF THE DEPTH OF N.A.
      IF(FC.LT.4000.0)XK1=0.85
      IF(FC.GT.4000.0)XK1=0.85-0.05*(FC-4000.00)/1000.00
C     EFFECTIVE PRESTRAIN CORRESPONDING TO EFFECTIVE PRESTRESS
C     FLANGE AND WEB THICKNESSES OF THE BOLLOM I-SECTION
      TW=B-LR
      TF=(H-HR)/2.00
      GO TO 56 I=1,N
   56 EPSE(I)=(FE(I)/AP(I))/EE(I)
C     INITIAL ECCENTRICITY (ECCN)
      SUMF=0.00
      DO 60 I=1,N
   60 SUMF=SUMF+FE(I)
      A=SUMF*1000.00/(B*B-BR*HR)
      SMOF=0.00
      DO 70 I=1,N
   70 SMOF=SMOF+FE(I)*D(I)
      ECCN=SMOF/SUMF
      ECCN=H/2.00-ECCN
C     INITIAL STRAINS AT THE TOP,BOTTOM AND STEEL LEVELS
      XI=(B**3-BR**3)/12.00
      XN=XI/(H/2.)
      STPBST=-SUMF/(B*H-BR*HR)+SUMF*ECCN/XI
      STPBSB=-SUMF/(B*H-BR*HR)-SUMF*ECCN/XI
      EPSCBT=STPBST/(EC0K/1000.0)
      EPSCBB=STPBSB/(EC0K/1000.0)
      TANA=(APSCBB-EPSCBT)/H
      DO 80 I=1,N
   80 EPSCE(I)=EPSCBB-TANA*D(I)
      WRITE(6,340)
C     WRITE INPUT DATA
      WRITE(5,20)STAB,TITLE,STAB
      WRITE(6,90)
      WRITE(6,100)
      WRITE(6,110)B,BR,H,HR,EE
      WRITE(6,120)R,RODE
      WRITE(6,130)(AP(I),I=1,N)
      WRITE(6,350)
      WRITE(6,140)ART
      WRITE(6,150)(D(I),I=1,N)
      WRITE(6,350)
      WRITE(6,160)(FE(I),I=1,N)
      WRITE(6,350)
      WRITE(6,170)DST1,DST2,DST3,DST4
      WRITE(6,180)S
      WRITE(6,190)(FE(I),I=1,N)
      WRITE(6,350)
      WRITE(6,200)(ES(I),I=1,N)
      WRITE(6,360)
      WRITE(6,210)FSTIR
      WRITE(6,350)
      WRITE(6,220)(FFULT(I),I=1,N)
      WRITE(6,350)
      WRITE(6,230)FYSTIR
      WRITE(6,350)
      WRITE(6,240)FC
      WRITE(6,250)RMODR
      WRITE(6,260)EPSCU
      WRITE(6,270)ART
      WRITE(6,280)RART
      WRITE(6,290)DELTA
      WRITE(6,300)DFMOD1,DFMOD2,DFMOD3
      WRITE(6,310)FCCN
      WRITE(6,320)ASIGMA
      WRITE(6,330)(EPSSE(I),I=1,N)
      WRITE(6,340)
      WRITE(6,345)EPSCET,(EPSCE(I),I=1,N)
      WRITE(6,340)EPSCTB
      WRITE(6,360)
   90 FORMAT(5X,'INPUT VARIABLES')
  100 FORMAT(5X'*****************',///)
  110 FORMAT(5X,'BEAM DIMENSIONS',/5X,'OUTSIDE:',25X'HOLLOW:',/5X,
     2'WIDTH (IN.)  =',F7.2,10X,F7.2,/5X,'HEIGHT (IN.) =',F7.2,
     3/5X,'LENGTH (IN.) =',F7.2//)
  120 FORMAT(5X,'NO. OF PRESTRESSING STRANDS PROVIDED (N) , AND THEIR SI
     ZE (NUMB) :',/5X,'N     =',I10,/5X,'NUMB =',I10//)
  130 FORMAT(5X,'AREAS OF PRESTRESSING STRANDS (SQ.IN.):',/5X,8F9.4,//)
  140 FORMAT('5X,'AREA OF TRANSVERSE STEEL - ONE LEG (SQ.IN.):',F10.4,
     2 //)
  150 FORMAT(5X,'PRESTRESSING STEEL LOCATIONS (DISTANCES FROM THE BOTTOM
     2 IN INCHES) :'/,5X,8F10.2,//)
  160 FORMAT('5X,'PRESTRESSING STEEL LOCATIONS (DISTANCES FROM THE SIDE I
     2N INCHES) :'/5X,8F10.2,//)
  170 FORMAT(5X,'STIRRUP LOCATION IN CROSS-SECTION:',/5X'DIST.',12,2F10.
     2,/5X,'NUMB.', 2F10.4,//)
  180 FORMAT(5X,'STIRRUP SPACING (IN.), S=',F10.3,//)
  190 FORMAT(5X,'EFFECTIVE PRESTRESSING FORCES (KIPS) :',/5X,8F10.2,//)
  200 FORMAT(5X,'MODULI OF ELASTICITY OF PRESTRESSING STEEL (ES):'/
     2X,8F10.2,//)
  210 FORMAT(5X,'MODULI OF ELASTICITY OF MILD STEEL :'/5X,8F10.2,//)
  220 FORMAT(5X,'ULTIMATE STRESSES OF PRESTRESSING STEEL :'/5X,8F10.3,//
     2)
  230 FORMAT(5X,'ULTIMATE STRESS OF MILD STEEL :',/5X,8F10.3,//)
  240 FORMAT(5X,'CONCRETE COMPRESSIVE STRENGTH (PSI):'/5X'FC=',F10.2,//)
  250 FORMAT(5X,'MODULUS OF RUPTURE (PSI):'/5X,'RMODR=',F10.2,//)
  260 FORMAT(5X,'CONCRETE ULTIMATE COMPRESSIVE STRAIN :'/5X,'EPSCU =',
```

```
     3F10.5,//)
 270 FORMAT(5X,'COEFFICIENT OF DEPTH OF NEUTRAL AXIS ( A C I FORMULA)
     2 =',F5.3,//)
 280 FORMAT(5X,'TORSION TO BENDING RATIO , T/B     =',F10.3,//)
 290 FORMAT(5X'TORSION TO SHEAR RATIO (2*T/(D*V))  =',F13.6,//)
 300 FORMAT(5X,'LOCATION OF FAILURE SURFACE (IN.) FROM LEFT SUPPORT 1'
     1,/5X,'DFROD1 =',F9.1,/5X,'DFROD2 =',F9.1,/5X,'DFROD3 =',F9.1//)
 310 FORMAT(5X,'INITIAL ECCENTRICITY (IN.), ECCN  =',F10.6,//)
 311 FORMAT(5X,'ANCHAGE PRESTRESS (PSI) F/A       =',F10.0,//)
 320 FORMAT(5X'INITIAL STRAIN IN PRESTRESSING STEEL 1',/5X,8F13.6,//)
 330 FORMAT(5X,'INITIAL STRAINS IN CONCRETE (TOP, STEEL LAYERS AND BOTT
     2OM)',/5X,F10.6/5X,8F10.6)
 340 FORMAT(5X,8F10.6,//)
 350 FORMAT( //)
 360 FORMAT( 1H1)
C    CHANGE FOLLOWING CARD TO SELECT DESIRED ACCURACY
C    ( 'STEP' DENOTES THICKNESS OF THE ELEMENT IN INCHES)
     STEP=0.625
C    CHANGE FOLLOWING CARDS FOR MODES 2 & 3
     NELEM=1.6001+H/STEP
     IF(NN.GT.0.5)GO TO 440
     DO 430 I=1,NELEMS
 430 AREA(I)=B*STEP
     GO TO 450
 440 NSHOT=(B-BN)*1.5001/2.88/STEP
     DO 430 I=1,NSHOT
 420 AREA(I)=B*STEP
     NUEN=NN*1.001 /STEP
     NSH=NSHOT+1
     NMEN=NSHOT+NMEN
     DO 430 I=NSH,NMEN
 430 AREA(I)=(B-BN)*STEP
     NTOP=(H-BN)*1.5001/2.88
     NSH=NSHOT+NUEN+1
     DO 440 I=NSH,NELEMS
 440 AREA(I)=B*STEP
 450 CONTINUE
C    CALCULATE DISTANCES TO THE CENTROIDS OF THE ELEMENT
     YC(1)=STEP/2.00
     DO 445 I=1,NELEMS
     J=I-1
 445 YC(I)=YC(J)+STEP
     RETURN
1000 STOP
     END
```

```
     SUBROUTINE STR102
C    THIS SUBROUTINE SOLVES FOR STRESSES AND FORCES IN PRESTRESSING
C    STRANDS CONSIDERING ALSO NONLINEAR PORTION OF STRESS-STRAIN CURVE
C    FOR 1/2 IN. DIA. STRAND
C
     IMPLICIT REAL*8(A-H,O-Z)
C
     COMMON AP,AST,D,FE,FSU,TSU,ES,ESTIN,EPSCE,FPSSE,EPSSA,EPSSU,B,H,
    2BN,HN,XL,YC,XNODE,EPSCU,ICON,ICCN,A,XINC,T,C,ES,XASI,DELTA,
    3DST1,DST2,DST3,DST4,S,SIGMA,TANB,FPULT,FYSTIN
    4,DFROD1,DFROD2,DFROD3,D1,XN1,TC,XCR,BETA,THETB,TV,TF,
    5EPSCON,FYSTIN,FCON,FTEN,XNCON,XNTEN,TCON,TTEN,A1,A2,A3,A4
    6,TCR,RR,V,SHARS,SHINS,SHANT,SHINT,SHARB,SHINB,XII,XIY,S1,S7,S8,S9
    7,ALFAE1,ALFAE2,TWPRB,TWPRS,TWPST
    8,AS,YS,AREA,YC,X,Y,DEPTH,AXIALL,FSUPC,XNAREA,YMOD,XYIELD,ESH,
    9FPULT,FYTLP,FULT,YSH,PHIFAC,EELEM,TOTALP,TOTALP,
    1 TOTALM,TAS,FS,SUMF,SUMFP,SUM79,CGUPT,FHI,DEP,ABCCON,FCELEM
    3,NCON,ACONF,FCONF,ACCEP,ELFOSC,FCCC,ERRINT,FCEL
    3,TWISH,TWISB,TWSTH
C
     COMMON N,M,NODE,NELEMS,NSTEEL,NADEEP,NECONF
C
     DIMENSION AP(10),D(10),FE(10),FSU(10),TSU(10),ES(10),
    1 FPSCE(10),FPSSE(10),EPSSA(10),EPSSU(10),DS(10),FPULT(10)
    2,AS(20),YS(20),AREA(500),YC(500),X(500),Y(500),EELEM(500),BAS(30),
    3 FCEL(50C),FS(20),FCELEM(500),ABCCON(500),ELFOSC(500)
C
C    NOTE: ALL STRESSES IN KSI - FORCES IN KIPS
     DO 5C I=1,N
     IF(EPSSU(I).GT.0.00 .AND.EPSSU(I). LT.0.0070)GO TO 20
     IF(EPSSU(I).GT.0.0070 .AND.EPSSU(I). LT.0.014)GO TO 30
     IF(EPSSU(I).GT.0.014)GO TO 40
  20 FSU(I)=ES(I)*EPSSU(I)
     GO TO 50
  3C FSU(I)=-1020700.00*(EPSSU(I))**2+58403.0*EPSSU(I)-56.70
     GO TO 50
  40 FSU(I)=440.00*EPSSU(I)+256.3
  5C CONTINUE
C    CHECK WHETHER STRESSES EXCEED ULT. STRESS
     DO 72 I=1,N
  7C IF(FSU(I).GT.FPULT(I))FSU(I)=FPULT(I)
C    FORCES IN PRESTRESSING STRANDS
     DO 8C I=1,N
  8C TSU(I)=FSU(I)*AP(I)
     RETURN
     END
```

```
      SUBROUTINE STRESS
C     THIS SUBROUTINE SOLVES FOR STRESSES AND FORCES IN PRESTRESSING
C     STRANDS CONSIDERING ALSO NONLINEAR PORTION OF STRESS-STRAIN CURVE
C     FOR 1/4 IN. DIA. STRAND
C
      IMPLICIT REAL*8(A-H,O-Z)
C
      COMMON AP,AST,B,FE,FSH,TSH,ES,ESTIR,EPSCE,EPSSE,EPSSA,EPSSU,N,M,
     2DD,HH,HL,PC,XMPP,EPSCU,ECUR,ECCR,A,SIMC,T,C,ED,EASI,DELTA,
     3DST1,DST2,DST3,DST4,S,SIGMA,TANB,PPULT,PYSTIR
     4,DFROM1,DFROM2,DFROM3,DS,YA1,TC,RCA,PETA,THETA,TW,TF,
     5EPJCOR,EPSIRE,ECOR,FYER,EPCOR,EPTER,TCOR,TTAR,A1,A2,A3,A4
     6,TCB,BW,Y,BMARR,BMINS,BMART,BMINT,BPARR,BMINR,EII,EIY,EX,EY,GX,GY
     7,ALFAR1,ALFAR2,TWPPR,TWPPS,TWPRT
     8,AS,YS,APYA,YC,X,Y,DEPTH,ASTALL,FSUBC,EMARFA,YBOT,EYIELD,EBR,
     9RULT,FYIELD,FULT,YBR,PNIFAC,EXLES,TOTALF,TOTALP,
     1 TOTALR,YAS,FS,SUMF,SUMFP,SUMFR,COUNT,PNT,DEP,ARCCOR,FCELBR
     2,ECOR,ECCRP,FCCRP,ACCRP,ELFORC,FCCC,ESSINT,FCEL
     3,THETAP,THETAR,THETTR
      COMMON N,M,NOBE,NELTRS,NSTEEL,NADEEP,NECORP
      DIMENSION AP(16),D(10),FE(10),FSH(10),TSH(10),ES(10),
     1 EPSCE(10),EPSSE(10),EPSSA(10),EPSSU(10),DS(10),FPULT(10)
     2,AS(20),YS(20),APYA(500),YC(500),X(500),Y(500),EXLES(500),EAS(20),
     3 FCPL(500),FS(20),FCELBR(500),ARCCOR(500),ELFORC(500)
C
C     NOTE: ALL STRESSES IN KSI - FORCES IN KIPS
      DO 50 I=1,N
      IF(AP(I).GT.0.00 .AND.EPSSU(I). LT.0.0070)GO TO 30
      IF(EPSSU(I).GT.0.0070 .AND.EPSSU(I). LT.0.014)GO TO 30
      IF(EPSSU(I).GT.0.014)GO TO 40
   20 FSH(I)=ES(I)*EPSSU(I)
      GO TO 50
   30 FSH(I)=-17656475.00*(EPSSU(I))**2+65496.00*EPSSU(I)-29.7
      GO TO 50
   40 FSH(I)=444.00*EPSSU(I)+254.70
   50 CONTINUE
C     CHECK WHETHER STRESSES EXCEED ULT. STRESS
      DO 70 I=1,N
   70 IF(FSH(I).GT.FPULT(I))FSH(I)=FPULT(I)
C     FORCES IN PRESTRESSING STRANDS
      DO 80 I=1,N
   80 TSH(I)=FSH(I)*AP(I)
      RETURN
      END
```

```
      SUBROUTINE STRAND
C     THIS SUBROUTINE SOLVES FOR STRESSES AND FORCES IN PRESTRESSING
C     STRANDS CONSIDERING ALSO NONLINEAR PORTION OF STRESS-STRAIN CURVE
C     FOR THE FOLLOWING GROUPS OF STRANDS AS, AB, AC, AD
      IMPLICIT REAL*8(A-H,O-Z)
      COMMON AP,AST,F,FE,FSH,TSH,ES,ESTIR,EPSCE,EPSSE,EPSSA,EPSSU,N,M,
     2DD,HH,HL,PC,XMPP,EPSCU,ECUR,ECCR,A,SIMC,T,C,ED,EASI,DELTA,
     3DST1,DST2,DST3,DST4,S,SIGMA,TANB,PPULT,PYSTIR
     4,DFROM1,DFROM2,DFROM3,DS,YA1,TC,RCA,PETA,THETA,TW,TF,
     5EPJCOR,EPSIRE,ECOR,FYER,EPCOR,EPTER,TCOR,TTAR,A1,A2,A3,A4
     6,TCB,BW,Y,BMARR,BMINS,BMART,BMINT,BPARR,BMINR,EII,EIY,EX,EY,GX,GY
     7,ALFAR1,ALFAR2,TWPPR,TWPPS,TWPRT
     8,AS,YS,APYA,YC,X,Y,DEPTH,ASTALL,FSUBC,EMARFA,YBOT,EYIELD,EBR,
     9RULT,FYIELD,FULT,YBR,PNIFAC,EXLES,TOTALF,TOTALP,
     1 TOTALR,YAS,FS,SUMF,SUMFP,SUMFR,COUNT,PNT,DEP,ARCCOR,FCELBR
     2,ECOR,ECCRP,FCCRP,ACCRP,ELFORC,FCCC,ESSINT,FCEL
     3,THETAP,THETAR,THETTR
      COMMON N,M,NOBE,NELTRS,NSTEEL,NADEEP,NECORP
      DIMENSION AP(10),D(10),FE(10),FSH(10),TSH(10),ES(10),
     1 EPSCE(10),EPSSE(10),EPSSA(10),EPSSU(10),DS(10),FPULT(10)
     2,AS(20),YS(20),APYA(500),YC(500),X(500),Y(500),EXLES(500),EAS(20),
     3 FCPL(500),FS(20),FCELBR(500),ARCCOR(500),ELFORC(500)
C     NOTE: ALL STRESSES IN KSI - FORCES IN KIPS
      DO 50 I=1,N
      IF(I.EQ.1.OR.I.EQ.4)GO TO 45
C     1/2 INCH STRAND
      IF(EPSSU(I).GT.0.00 .AND.EPSSU(I). LT.0.0070)GO TO 20
      IF(EPSSU(I).GT.0.0070 .AND.EPSSU(I). LT.0.014)GO TO 30
      IF(EPSSU(I).GT.0.014)GO TO 40
   20 FSH(I)=FE(I)*EPSSU(I)
      GO TO 50
   30 FSH(I)=-19128700.00*(EPSSU(I))**2+48403.0*EPSSU(I)-36.75
      GO TO 50
   40 FSH(I)=448.00*EPSSU(I)+256.3
      GO TO 50
C     3/8 INCH STRAND
   45 IF(EPSSU(I).GT.0.00 .AND.EPSSU(I). LT.0.0070)GO TO 120
      IF(EPSSU(I).GT.0.0070 .AND.EPSSU(I). LT.0.014)GO TO 130
      IF(EPSSU(I).GT.0.014)GO TO 140
  120 FSH(I)=FE(I)*EPSSU(I)
      GO TO 50
  130 FSH(I)=-17656475.00*(EPSSU(I))**2+65496.00*EPSSU(I)-29.7
      GO TO 50
  140 FSH(I)=444.00*EPSSU(I)+254.70
   50 CONTINUE
C     CHECK WHETHER STRESSES EXCEED ULT. STRESS
      DO 70 I=1,N
   70 IF(FSH(I).GT.FPULT(I))FSH(I)=FPULT(I)
C     FORCES IN PRESTRESSING STRANDS
      DO 80 I=1,N
   80 TSH(I)=FSH(I)*AP(I)
      RETURN
      END
```

```
      SUBROUTINE STRAPS
C     THIS SUBROUTINE  COMPUTES THE STRESSES AND FORCES IN PRESTRESSING
C     STRANDS CONSIDERING ALSO SHALLOWAR PORTION OF STRESS-STRAIN CURVE
C     FOR THE FOLLOWING GROUPS OF BEAMS A1, A2, A3, A4
      IMPLICIT REAL*8(A-H,O-Z)
      COMMON AP,AST,D,PE,PSH,TSH,ES,ESTIF,EPSCE,EPSSE,EPSSA,EPSSH,H,H,
     2PH,PR,YL,YC,EMODP,FPSTH,FCOM,ECCH,A,EINC,T,C,FB,ESSI,DELTA,
     3DST1,DST2,DST3,DST4,S,SIGMA,YASH,FPULT,FYSTIF
     4,DFSC01,DFS002,DFP003,DS,XX1,TC,ICH,BETA,THETA,TU,TF,
     5EFSCOM,FFSTFH,FCON,FTEH,EMCON,ESTEH,TCON,TTEH,A1,A2,A3,A4
     6,TCP,ES,Y,SHAIS,SRINS,SHAXT,SRINT,SHAXH,SHISH,XII,XIY,SX,SY,QX,QY
     7,ALPAE1,ALPAE2,THFPS,THPRS,THPST
     8,AS,FS,AREA,YC,X,Y,DEPTH,ARIALL,FSHDC,ESHDEA,FHOD,ETIELD,ESH,
     9RULT,FYILD,FULT,YSH,PHIPAC,EELEH,TOTALP,TOTALP,
     1 TOTALH,LAS,FS,SUMF,SUMFP,SUMFH,CONST,PHI,DEP,ARCCON,PCELEH
     2,HCOM,ECOMP,FCOMP,ACOMP,ELFONC,FCCC,ESSIOT,FCEL
     3,THETPH,THETSP,THETTH
      COMMON H,H,EOPE,YELEAH,HSTEEL,HADEEP,HECOMP
      DIMENSION AP(10),D(10),PE(10),PSH(10),TSH(10),ES(10),
     1 EPSCE(10),EPSSI(10),EPSSA(10),EPSSH(10),DE(10),FPULT(10)
     2,AS(20),YS(20),AREA(500),YC(500),X(500),Y(500),EELEH(500),EAS(20),
     3 PCEL(500),FS(20),PCELEH(500),ARCCOH(500),ELFONC(500)
C     NOTE: ALL STRESSES IN KSI - FORCES IN KIPS
      DO 99 I=1,H
      IF(I.EQ.1.OR.I.EQ.T.OR.I.EQ.4)GO TO 45
C     1/2 INCH STRAND
      IF(EPSSH(I).GT.0.00 .AND.EPSSH(I). LT.0.0070)GO TO 30
      IF(EPSSH(I).GT.0.0070 .AND.EPSSH(I). LT.0.014)GO TO 30
      IF(EPSSH(I).GT.0.014)GO TO 40
   30 PSH(I)=ES(I)*EPSSH(I)
      GO TO 50
   30 PSH(I)=-1820700.00*(EPSSH(I))**3+48403.0*EPSSH(I)-66.70
      GO TO 50
   40 PSH(I)=400.00*EPSSH(I)+256.2
      GO TO 50
C     3/8 INCH STRAND
   45 IF(EPSSH(I).GT.0.00 .AND.EPSSH(I). LT.0.0070)GO TO 120
      IF(EPSSH(I).GT.0.0070 .AND.EPSSH(I). LT.0.014)GO TO 130
      IF(EPSSH(I).GT.0.014)GO TO 140
  120 PSH(I)=ES(I)*EPSSH(I)
      GO TO 50
  130 PSH(I)=-17654?5.00*(EPSSH(I))**2+45496.00*EPSSH(I)-34.7
      GO TO 50
  140 PSH(I)=400.00*EPSSH(I)+294.70
   50 CONTINUE
C     CHECK WHETHER STRESSES EXCEED ULT. STRESS
      DO 70 I=1,H
   70 IF(PSH(I).GT.FPULT(I)) PSH(I)=FPULT(I)
C     FORCES IN PRESTRESSING STRANDS
      DO 80 I=1,H
   80 TSH(I)=PSH(I)*AP(I)
      RETURN
      END




      SUBROUTINE TCPSOL
C     THIS SUBROUTINE SOLVES FOR CRACKING TORQUE AND ANGLE OF INCLINATIO
C     N OF FIRST CRACK W.R.T. LONGITUDINAL AXIS OF BEAM - SOLID R-SECT.
C
      IMPLICIT REAL*8(A-H,O-Z)
C
      COMMON AP,AST,D,PE,PSH,TSH,ES,ESTIF,EPSCE,EPSSE,EPSSA,EPSSH,H,H,
     2PH,PR,YL,YC,EMODP,EPSCU,ECON,FCCH,A,EINC,T,C,FB,ESSI,DELTA,
     3DST1,DST2,DST3,DST4,S,SIGMA,YASH,FPULT,FYSTIF
     4,DFSC01,DFS002,DFP003,DS,XX1,TC,ICH,BETA,THETA,TU,TF,
     5EFSCOM,FFSTFH,FCON,FTEH,EMCON,ESTEH,TCON,TTEH,A1,A2,A3,A4
     6,TCP,ES,Y,SHAIS,SRINS,SHAXT,SRINT,SHAXH,SHISH,XII,XIY,SX,SY,QX,QY
     7,ALPAE1,ALPAE2,THFPS,THPRS,THPST
     8,AS,FS,AREA,YC,X,Y,DEPTH,ARIALL,FSHDC,ESHDEA,FHOD,ETIELD,ESH,
     9RULT,FYILD,FULT,YSH,PHIPAC,EELEH,TOTALP,TOTALP,
     1 TOTALH,LAS,FS,SUMF,SUMFP,SUMFH,CONST,PHI,DEP,ARCCON,PCELEH
     2,HCOM,ECOMP,FCOMP,ACOMP,ELFONC,FCCC,ESSIOT,FCEL
     3,THETPH,THETSP,THETTH
C
      COMMON H,H,EOPE,YELEAH,HSTEEL,HADEEP,HECOMP
C
      DIMENSION AP(10),D(10),PE(10),PSH(10),TSH(10),ES(10),
     1 EPSCE(10),EPSSE(10),EPSSA(10),EPSSH(10),DE(10),FPULT(10)
     2,AS(20),YS(20),AREA(500),YC(500),X(500),Y(500),EELEH(500),EAS(20),
     3 PCEL(500),FS(20),PCELEH(500),ARCCOH(500),ELFONC(500)
C
C     CHECK FOR PURE BENDING CASE
      IF(ABSZ.LT.0.005)RETURN
      SIGMA=SIGMA/1000.00
      COEFB=180.00/3.14159
      AX=2*H*H**2/3.00
      AY=H**2*H/3.00
      FT=ERDTH/1000.00
      FC=FC/1000.00
      RCIEX3=0.00010
      AR=H/D
      IF(AR.LT.1.05.AND.AR.GT.0.95)ALPAE1=0.215
      IF(AR.LT.1.05.AND.AR.GT.0.95)ALPAE2=0.215
      IF(AR.LT.1.55.AND.AR.GT.1.45)ALPAE1=0.260
      IF(AR.LT.1.55.AND.AR.GT.1.45)ALPAE2=0.230
      IF(AR.LT.2.05.AND.AR.GT.1.95)ALPAE1=0.305
      IF(A .LT.2.05.AND.AR.GT.1.95)ALPAE2=0.245
C     CRACK STARTS AT THE BOTTOM
      ND=1
      CK=0.00/3.00*(FT/FC)**2
      S*AX=2.00*FT/DSQRT(3.0000)
      EINC=SHAXH/10.00
      SHAIH=SHAXH+EINC
  100 SHAIH=SHAIH-EINC
      TCPH=6.00*ALPAF2*SHAXH*SX*(-3.00*ALPAE2/EXSI*DSQRT((3.00*ALPAE2/EX
     2SI) **2+SIGMA/SHAIH*(1.00+6.00*ECCH/H)+1.00))
      TAN2TH=1.00/(3.00*ALPAE2) *2CRH*EXSI/(-SIGMA*EXSI*SX*(1.00+6.00*
     2ECCH/H)*TCRH)
      THETAH=DATAN(TAN2TH)/2.00
      THETSH=THETAH
```

```
      THETP3=3.14159/4.00-THETA0
C     CHECK ORIENT OF PRINCIPAL STRESS
      IF(SIN(2TH.LT.6.03)THETA0=THETA3-3.14159/2.00
      THETA1=THETA0+COEFB
      TCP=TCA3
      BA=TCP/BP SI
      V=2.00*TCP/(B*DELTA)
      CALL PSTCOL
      NO=NO+1
      IF(PO.GT.200) WRITE(6,70)
      IF(NO.GT.250)GO TO 110
      SNIN1Q=(1.00-(SNAIA/PC)**2/CE)*PC
      EB=(SNAIB/PC)**2-CE*(1.00-SNIN1/PC)
      IF(ABS(ABS(SNIN1)-SNINEQ).LT.0.001)GO TO 110
      IF(SIGN(1.0,B)).GT.SNINEQ)GO TO 100
      SNAIB=SNIN1+DINC
      DINC=DINC/10.00
      GO TO 105
  110 CONTINUE
      TCP33=ESTIP*AST*ECTERS*DCOS(THETA3)*A/(DTAN(THETA3)+E)*(E+E)*0.43
      TCPPTO=TCP3+TCP33
      WRITE(6,10)
      WRITE(6,20)
      WRITE(6,30)
      WRITE(6,40)TCP3,THETA3,THETA3,TCP33,TCPSTO,SNAIB,SNIN3,TAP33,ES,NO
C     CRACK STARTS AT THE SIDE
      NO=1
      SNAIC=2.00*FT/SQRT(3.0000)
      DINC=SPAIC/10.00
      SNAIB=SNAIB+DINC
  200 SNAIC=SNAIC-DINC
      TCP3=SNAIB**6.0*EY/(1.00/ALPAE1+3.00/DELTA)*DSQRT(1.00+SIGMA1/SNAIB)
      TAN2TH=2.67*DSQRT(1.00+SIGMA1/SNAIB)/(SIGMA1/SNAIB)
      THETA3=DATAN(TAN2TH)/2.00
      THETA3=THETA3
      THETA3=THETA3+COEFB
      TCP=TCP3
      BA=TCP/BSI
      V=2.00*TCP/(B*DELTA)
      CALL PSTCOL
      NO=NO+1
      IF(NO.GT.250) WRITE(6,70)
      IF(NO.GT.200)GO TO 210
      SNINEQ=(1.00-(SNAIS/PC)**2/CE)*PC
      EB=(SNAIS/PC)**2-CE*(1.00-SNIN1/PC)
      IF(DABS(DABS(SNIN1)-SNINEQ).LT.0.001)GO TO 210
      IF(DABS(SNIN1).GT.SNINEQ)GO TO 200
      SNAIS=SNAIS+DINC
      DINC=DINC/10.00
      GO TO 205
  210 CONTINUE
      TCP33=ESTIP*AST*ECTERS*DCOS(THETA3)*A/(DTAN(THETA3)+E)*(E+E)*0.43
      TCPSTO=TCP3+TCP33
      WRITE(6,50)TCP3,THETA3,THETA3,TCP33,TCPSTO,SNAIS,SNIN3,TAP33,ES,NO
C     CRACK STARTS AT THE TOP
      NO=1
      SNAIT=2.00*FT/SQRT(3.0000)
      DINC=SPAIT/10.00
      SNAIT=SNAIT-DINC
  300 SPAIT=SNAIT-DINC
      IF(SNAIT.LT.0.00)GO TO 310
      TCP3=0.00*ALPAE2*SNAIT*SI*(+).00*ALPAE2/ZESI*DSQRT((3.0*ALPAE2/ZES
     21)**2*SIGMA/SNAIT*(1.00-6.00*ECCN/N)+1.00))
      TAN2TH=1.00/(3.00*ALPAE2)*TCP3*ZESI/(+SIGMA*ZESI*SI*(1.00-6.00*
     2ECCN/N)+TCP3)
      THETA3=DATAN(TAN2TH)/2.00
      THETA3=THETA3
      THETA3=THETA3+COEFB
      TCP=TCP3
      V=2.00*TCP/(B*DELTA)
      BA=TCP/BSI
      CALL PSTCOL
      NO=NO+1
      IF(PO.GT.200) WRITE(6,70)
      IF(PO.GT.200)GO TO 310
      SNINEQ=(1.00-(SPAIT/PC)**2/CE)*PC
      EB=(SNAIT/PC)**2-CE*(1.00-SNIN1/PC)
      IF(DABS(DABS(SNIN3)-DABS(SNINEQ)).LT.0.001)GO TO 310
      IF(DABS(SNINT).GT.SNINEQ)GO TO 300
      SNAIT=SNAIT+DINC
      DINC=DINC/10.00
      GO TO 305
  310 CONTINUE
      TCP33=ESTIP*AST*ECTERS*DCOS(THETA3)*A/(DTAN(THETA3)+E)*(E+E)*0.43
      TCPTTO=TCP3+TCP33
C     SELECT GOVERNING ANGLE ( RADIANS )
      WRITE(6,60)TCP3,THETA3,THETA3,TCP33,TCPTTO,SNAIT,SNINT,TAP3T,ES,NO
   10 FORMAT(/,5X,'CRACKING STATUS')
   20 FORMAT(59,'*********************',/)
   30 FORMAT(12X,'TCP3OR CONC   TH.(RD)   TH.(DEG)   TOT STIR  TOT.TORQ.
     2   SPRINCPAL  SPRINCAIN THETA(RES)    ERROR    NO.ITER',/)
   40 FORMAT(4X,'BOTTOM',9F11.5,I6)
   50 FORMAT(4X,'SIDE  ',9F11.5,I6)
   60 FORMAT(4X,'TOP   ',9F11.5,I6)
   70 FORMAT(5X,'SPECIFIED NO. OF ITERATIONS WAS EXCEEDED')
      PC=PC*1000.00
      SIGMA=SIGMA*1000.00
      RETURN
      END
```

```
      SUBROUTINE PRINCI
C     THIS SUBROUTINE SOLVES FOR PRINCIPAL STRESSES UNDER COMB. LOADING
C
      IMPLICIT REAL*8(A-H,O-Z)
C     FOR BALID E-SELTION
      COMMON AP,AST,B,FE,FSB,TSB,EC,ESTIP,EPSCR,EPSSE,EPSSA,EPSSB,B,B,
     2BB,HH,EL,DC,SH BP,EPSCB,FCHR,FCFR,A,SIMC,T,C,EB,SMBI,DELTA,
     3DST1,DST2,DST3,BETB,B,SIGRA,TABS,FPOLT,FPSTIB
     8,BPPSB1,PPSHB2,BEAM-B1,BC,BE1,TC,SCR,BETA,THETA,TH,TF,
     5FP.CGA,IPSTFB,ICOR,FTFB,EBCHR,ENTAB,TCHR,TTEB,A1,A2,A3,AB
     6,TCB,SR,V,SHEAB,SAINI,SHANT,SHINT,SHEBB,SHIBB,XIE,XII,SE,SI,QE,QI
     7,ALFAE1,ALFAI2,TPPBE,TBPBI,TBPBI
     8,AS,TS,ASTA,TC,E,V,DEPTH,AXIALL,PSUBC,ISAFEA,IXBB,CYIELD,ESE,
     9EBLT,FFIELD,FBLT,TSB,FAIFAC,EXLEN,TOTALP,TOTALP,
     T TOTALE,FAS,IE,ISHF,SUBFP,SHAFB,COUNT,PHI,DEP,ABCCBA,PCELBB
     2,NCSB,ECOMP,FCOMP,ACOMP,ELMOBC,PCCC,ESSIBC,PCEL
     3,TNFIBB,TNETSB,TNETSB
C
      COMMON B,A,KOBE,BELEAS,WSTEEL,BABEEP,NECOAP
C
      DIMENSION AP(10),B(10),FE(10),FSB(10),TSB(10),ES(10),
     1 EPSCA(10),EPSSE(10),EPSSA(10),EPSSB(10),BS(10),FFBLT(10)
     2,AS(23),TS(20),AREA(500),TC(500),E(500),T(500),EELEA(500),BAS(20),
     3 PCEL(500),FS(20),PCELLB(500),ABCCBA(500),ELFOBC(500)
C
C     SHEAR STRESSES DUE TO TORSION
      TAUVT=TCP/(ALFAE1*B**2)
      TAUBT=TCP/(ALFAE2*B**2)
      TAUIT=TAUBT
C     SHEAR STRESSES DUE TO FLEXURAL SHEAR
      TAUBV=3.00*V/(2.00*B*H)
      TAUEV=0.0E
      TAUIV=0.0E
C     NORMAL STRESSES DUE TO FLEXURAL MOMENT
      SIGMB=0.00
      SIGMIB=-MB/SE
      SIGMBB=MB/SE
C     NORMAL STRESSES DUE TO PRESTRESS
      SIGPBP=-SIGMA
      SIGPIP=SIGMBP*(1.00-6.00*ECCB/H)
      SIGMIP=SIGMBP*(1.00+6.00*ECCB/H)
C     COMBINED STRESSES
      SI.MAT=SIGMIP+SIGMIP
      TAUT=TAUTT+TAUTV
      BADT=DSQRT((SIGMAT/2.00)**2+TAUT**2)
      SMAXT=SIGMAT/2.00+BADT
      SMINT=SIGMAT/2.00-BADT
      SIGMAB=SIGMBP+SIGMVP
      TAUB=TAUBT+TAUBV
      BADB=DSQRT((SIGMAB/2.00)**2+TAUB**2)
      SMAXB=SIGMAB/2.00+BADB
      SMINB=SIGMAB/2.00-BADB
      SIGMAB=SIGMBB+SIGMBP
      TAUB=TAUBT+TAUBV
      BADB=DSQRT((SIGMAB/2.00)**2+TAUB**2)
      SMAXB=SIGMAB/2.00+BADB
      SMINB=SIGMAB/2.00-BADB
      COEFB=180.0E/3.14159
      THEAB=DATAN(TAUB/(-SIGMAB/2.00))*COEFB/2.00
      THFBS=DATAN(TAUS/(-SIGMAS/2.00))*COEFB/2.00
      THFBT=DATAN(TAUT/(-SIGMAT/2.00))*COEFB/2.00
      RETURN
      END
```

```
      SUBROUTINE TCRKCL
C     THIS SUBROUTINE SOLVES FOR CRACKING TOUGHS AND ANGLE OF INCLINATION
C     M OF FIRST CRACK W.R.T. LONGITUDINAL AXIS OF BEAM - HOLLOW B-SECT.
C
      IMPLICIT REAL*8(A-H,O-Z)
C
      COMMON AP,AST,B,FE,FYB,TSB,RS,ESTIB,EPSCE,EPSSE,EPSSA,EPSBB,B,B,
     2BB,HB,EL,PC,RMODB,EPSCB,TCOB,FCCB,A,AINC,T,C,ES,ANGI,DELTA,
     3SST1,SST2,SST3,SSTB,S,SIGMA,TANB,FFULT,FYSTIB
     4,DFROB1,DFROB2,DBROB1,BS,RE1,TC,RCB,BETA,THETA,TH,YY,
     5EPSCOB,EPSCAB,FCOB,FCBB,EBCOB,EMTAB,TCOB,FTLB,A1,A2,A3,A4
     6,TCB,BB,Y,SNAXE,SNIPS,SNAXF,SAINT,SNAXB,SNIPB,EIE,EIF,SX,SY,SX,SY
     7,ALPAE1,ALPAE2,TWPBE,TWPPS,TWPST
     8,AS,YS,APTA,YC,X,Y,EPSTA,ANIALL,FBUBC,EMABEA,TWOB,EIFLB,EBB,
     9EULT,FFULB,FULT,YSB,EPSC,EPSAC,EELEA,TOTALP,TOTALP,
     1 TOTALS,EAS,FS,SUMF,SUMFF,SUMFS,COUNT,PHI,DEP,EBCCOB,FCELBB
     2,MCOB,ECOMP,TCCAP,ACOMP,ELPOBC,FCCC,SHEINT,FCEL
     3,THETBB,THETSP,THETTB
C
      COMMON N,A,MODE,NFLEAS,NSYZEL,NADDIP,NECOAP
C
      DIMENSION AP(10),B(10),FE(10),FBB(10),TSB(10),ES(10),
     1 EPSCE(10),EPSSE(10),EPSSA(10),EPSBB(10),BB(10),FFULF(10)
     2,AS(23),YS(20),AREA(500),TC(500),I(500),F(500),.EELEA(500),BAS(20),
     3 FCEL(500),FS(20),FCELEA(500),ABCCOB(500),ELPOBC(500)
C
C     CHECK FOR PURE BENDING CASE
      IF(BM2I.LT.0.00%) RETURN
      SIGMA=SIGMA/1000.00
      COEFB=180.00/3.14159
      XII=(B**3*D-BB**3*DD)/12.00
      XIF=(B**3*H-BB**3*HH)/12.00
      SX=XII/(D/2.00)
      SF=XIF/(H/2.00)
      XIS=/*H**3/12.00
      SS=XIS/(H/2.00)
      SS=SX/SS
      QI=(B*D**2-BB*DD**2)/8.00
      QT=(B**2*H-BB**2*HH)/8.00
      .WFT=B*H-BB*DD
      XE1=BB/B
      XE2=HH/H
      XE=XE1
      IF(XE2.LE.XE1) XE=XE2
      XC=1.00-XE**B
      FC=ABOCB/1000.00
      ICYES=0.00C15
C     CRACK STARTS AT THE BOTTOM
      TCBB=2.00/3.00+3.14159*XC*FT*SX*(-3.00*3.14159*XC/(16.0*EXSI)+DSQR
     2T((3.00*3.14159*XC/16.00/EXSI)**2+(SIGMA/FT*(1.00-ICCB*ABST/SI)*1.
     3)*PS**2))/PS**2
      TANTB=(3.00/3.00+3.14159*XC)*TCBB*SX*EXSI/(-SIGMA*EXSI*SX*(1.00+
     2ICCB*ABST/SI)*TCBB)
      THETAB=DATAN(TANTB)/2.00
      THETBB=THETAB
      THETBB=THETBB/2.00-THETOB
C     CHECK FOR LAST OF PRINCIPAL STRESS
      IF(TANTB.LT.0.00) THETBB=THETBB-3.14159/2.00
      THETBB=THETBB*COEFB
      TCB=TCPB
      BM=TCB/EXSI
      V=2.00*TCB/(B*DELTA)
      CALL PSTROL
      TCBBS=ESTIB*AST*ECTEPS*DCOS(THETBB)*A/(DTAN(THETBB)*S)*(B+B)*0.43
      WRITE(6,10)
      WRITE(6,20)
      WRITE(6,40)TCBB,THETBB,THETBB,TCBBS,TCBSTO,SHAXB,SHINB,TWPBB
      WRITE(6,*00)
      TCPBCC=TCBB+TCBBS
C     CRACK STARTS AT THE SIDE
      TCBS=FC*DSQRT(1.00+SIGMA/FT)/(16.00/(3.14159*B*B**2*EC)*2.00*QI/
     2(B*AIB*EW*DELTA))
      TANSTB=2.00*DSQRT(1.00+SIGMA/FT)/(SIGMA/FT)
      THETAS=DATAN(TANSTB)/2.00
      THETSB=SPEIAS
      THETSB=THETAS*COEFB
      TCB=TCBS
      BM=TCB/EXSI
      V=2.00*TCB/(B*DELTA)
      CALL PSTROL
      TCBSS=ESTIB*AST*ECTEPS*DCOS(THETSB)*A/(DTAN(THETSB)*S)*(B+B)*0.43
      TCBSTC=TCBS+TCBSS
      WRITE(6,50)TCBS,THETSB,THETSB,TCBSS,TCBSTO,SHAXB,SHINB,TWPBB
C     CRACK STARTS AT THE TOP
      TCBT=3.00/4.00*3.14159*XC*FT*SX*(+3.00*3.14159*XC/(16.0*EXSI)+DSQR
     2T((3.00*3.14159*XC/16.00/EXSI)**2+(SIGMA/FT*(1.00-ICCB*ABST/SI)*1.
     3)*PS**2))/PS**2
      TANTB=(3.00/4.00*3.14159*XC)*TCBT*SX*EXSI/(+SIGMA*EXSI*SX*(1.00+
     2ICCB*ABST/SI)*TCBT)
      THETAT=DATAN(TANTTB)/2.00
      THETTB=THETAT
      THETTB=THETTB*COEFB
      TCB=TCBT
      BM=TCB/EXSI
      V=2.00*TCB/(B*DELTA)
      CALL PSTROL
      TCBTS=ESTIB*AST*ECTEPS*DCOS(THETTB)*A/(DTAN(THETTB)*S)*(B+B)*0.43
      TCBTTC=TCBT+TCBTS
      WRITE(6,60)TCBT,THETTB,THETTB,TCBTS,TCBTTO,SHAXT,SHINT,TWPBT
 10   FORMAT(///,51,'CRACKING STRENGTH')
 20   FORMAT('1',*******************',///)
 30   FORMAT(121,'TCBOMI CONC   TR. (DB)    TR. (DEG)    TOB STEE  TWT.TOBO.
     2   SPRINCMAX   SPRINCMIN THETA(DEG)',/)
 40   FORMAT(41,'BOTTOM=',9F11.5,I6)
 50   FORMAT(41,'SIDE   =',9F11.5,I6)
 60   FORMAT(41,'TOP    =',9F11.5,I6)
      SIGMA=SIGMA*1000.00
      RETURN
      END
```

```
      SUBROUTINE PSTROL
C     THIS SUBROUTINE SOLVES FOR PRINCIPAL STRESSES UNDER COMB. LOADING
C     FOR HOLLOW R-SECTION
C
      IMPLICIT REAL*8(A-H,O-Z)
C
      COMMON AP,ACT,D,PE,PSH,TSH,ES,ESTEN,EPSCE,EPSSE,EPSSA,EPSSU,B,H,
     2BH,HH,EL,PC,PMODB,EPSCH,ECOM,PCOM,A,XINC,T,C,TH,EAST,DELTA,
     3DST1,DST2,DST3,DST4,S,SIGMA,TANB,PPULT,PESTEN
     4,DFB1D1,DFB2D2,DFB0D2,DS,XN1,TC,RCS,BETA,THETA,TW,TF,
     5EPSCOM,FPSTPE,PCOM,PTEN,ZNCOM,ENTEN,TCOM,TTEN,A1,A2,A3,A4
     6,TCP,BH,V,SMALL,SMINS,SMALT,SMIAT,SMAXB,SMINB,SIE,SII,SS,ST,SS,ST
     7,ALPHE1,ALPAE2,TEPNB,TMPSS,TMPST
     8,AS,TS,APEA,TC,X,Y,SMPTd,ARIALL,PBUSC,XNAPEA,THOD,EYIELD,ESH,
     9EULT,FYIELD,PULT,YSH,PNIPAC,EELEN,TOTALF,TCTALF,
     1 TOTALH,EAS,PS,SUMF,SUMFP,SUMFB,COUNT,PSI,DEP,ABCCOS,FCELSH
     2,RCOS,TCOMP,FCOMP,ACOMP,ELFORC,FCCC,EASINT,FCEL
     3,THETAm,THETSH,THETH
C
C
      COMMON H,M,KODE,HELENS,HSTEEL,HADDED,HECOMP
      DIMENSION AP(10),E(10),PE(10),PSH(10),TSH(10),ES(10),
     1 EPSCH(10),EPSSE(10),EPSSA(10),EPSSU(10),BS(10),PPULT(10)
     2,AS(20),TS(20),AREA(500),TC(500),X(500),Y(500),EELEN(500),EAS(20),
     3 FCEL(50C),PS(20),FCELEH(500),ABCCOS(500),ELFORC(500)
C
      COEFD=180.00/3.14159
      XII=(B*H**3)-BH*HH**3)/12.00
      XIY=(B**3*H-BH**3*HH)/12.00
      SX=XII/(H/2.00)
      SY=XIY/(B/2.00)
      QI=(B*H**2-BH*HH**2)/8.00
      QY=(H**2*B-BH**2*HH)/8.00
      ANIT=B*H-BH*HH
      XN1=BH/B
      XN2=HH/H
      XN=XN1
      IF(XN2.LT.XN1)XN=XN2
      XC=1.00-XN**4
C     SHEAR STRESSES DUE TO TORSION
      TAUVT=16.00*TCH/(3.14159*H**2*B*XC)
      TAUHT=16.00*TCA/(3.14159*H**2*B*XC)
      TAUTT=TAUHT
C     SHEAR STRESSES DUE TO FLEXURAL SHEAR
      TAUVV=1*QI/(XII*TW)
      TAUTV=0.CO
      TAUHV=0.00
C     NORMAL STRESSES DUE TO FLEXURAL MOMENT
      SIGMVB=0.CO
      SIGMTB=-BM/SX
      SIGMHB=BM/SX
C     NORMAL STRESSES DUE TO PRESTRESS
      SIGMVP=-SIGMA
      SIGMTP=SIGMVP*(1.00-ECCH*ANET/SX)
      SIGMHP=SIGMVP*(1.00+ECCH*ANET/SX)
C     COMBINED STRESSES
      SIGMTT=SIGMTB+SIGMTP
      TAUT=TAUTT+TAUTV
      RADT=DSQRT((SIGMTT/2.00)**2+TAUT**2)
      S*1T=SIGMTT/2.00+RADT
      S2TT=SIGMTT/2.00-RADT
      SIGMHS=SIGMVB+SIGMVP
      TAUHS=TAUVT+TAUHV
      RADH=DSQRT((SIGMHS/2.00)**2+TAUH**2)
      S*1H=SIGMHS/2.00+RADH
      S2TH=SIGMHS/2.00-RADH
      SIGMAT=SIGMB+SIGMBP
      TAUH=TH PHT+TAUHV
      RADB=DSQRT((SIGMHB/2.00)**2+TAUB**2)
      S*1HB=SIGMHB/2.00+RADB
      S2THB=SIGMHB/2.00-RADB
      COEFD=180.00/3.14159
      THTBT=DATAN(TAUB/(-SIGMHB/2.00))*COEFD/2.00
      THTHS=DATAN(TAUH/(-SIGMHS/2.00))*COEFD/2.00
      THTTT=DATAN(TAUT/(-SIGMTT/2.00))*COEFD/2.00
      RETURN
      END
```

```
      SUBROUTINE CPWPCH
C
C     THIS SUBROUTINE SOLVES FOR STRESSES OF THE CONCRETE ELEMENTS
C     WHICH ARE SUBJECTED TO COMPRESSION USING HOGNESTAD'S STRESS-STRAIN
C     CURVE AND CALCULATES TOTAL COMPRESSIVE FORCE
C
      IMPLICIT REAL*8(A-H,O-Z)
C
      COMMON AP,AST,B,FE,FSU,TSU,ES,ESTID,EPSCE,EPSSE,EPSSA,EPSSU,A,B,
     2RR,NR,EL,FC,EMODS,EPSCO,ACON,ECCN,A,RINC,T,C,EP,REST,DELTA,
     3DST1,DST2,DST3,DST4,S,SIGAA,TABB,FPULT,FYSTIR
     8,EPMOD1,EPMOD2,EPMOD),BS,EF1,TC,ECE,BETA,THETA,TH,TF,
     5EPSCCN,EPSTEN,FCON,FTEN,RNCON,ENTEN,TCON,TTEN,A1,A2,A3,A4
     6,TCP,BR,W,SMAIS,SMINS,SMAXT,SMINT,SMAXB,SMINB,EIE,EIF,EI,ET,OI,OE
     7,ALPAE1,ALPAE2,THPRB,THPBE,THPBT
     8,AS,YS,APAA,YC,X,Y,DEPTH,AXIALL,PSUBC,EPABPA,YBOB,EYIELD,ESB,
     9EULT,FYYLD,FULT,YSH,PHIPAC,EELEM,TOTALF,TOTALP,
     1 TOTALM,LAS,P2,SUMP,SUMFP,SUMFM,COUNT,PHI,REP,ABCCOB,FCELEB
     2,NCCR,ECONP,FCONP,ACONP,ELFOBC,FCCC,EESIBT,FCEL
     3,THETBF,THETIB,THETTB
C
      COMMON N,M,NODE,NELEAS,NSTEEL,NABEEP,NECONP
C
      DIMENSION AP(10),B(10),FE(10),FSU(10),TSU(10),ES(10),
     1 EPSCE(10),EPSSE(10),EPSSA(10),EPSSU(10),ES(10),FPULT(10)
     2,AS(20),YS(20),AREA(500),YC(500),X(500),Y(500),EELEM(500),EAS(30),
     3 FCEL(500),BS(20),FCELEM(500),ABCCON(500),ELFOBC(500)
C
C     HEIGHT OF THE ELEMENT
      NELEM=N/NELEMS
C     NUMBER OF THE WHOLE ELEMENTS THAT ARE IN COMPRESSION
      A=1.00001*A
      NECONP=A/NELEM
      A=A/1.0001
C     HEIGHT OF THE PORTION OF THE ELEMENT WHICH IS SUBJECTED TO COMPR.
C     AND IS BOUNDED BY NEUTRAL AXIS
      HCOP=A-NECONP*NELEM
C     DISTANCES FROM N. A. TO CENTROIDS OF COMPRESSION ELEMENTS
      IF(NECONP.LT.1)GO TO 111
      DO 100 I=1,NECONP
  100 FCEL(I)=HCON+NELEM*(2.00*I-1.00)/2.00
C     STRAINS AT THE CENTROIDS OF THE ELEMENTS
      DO 110 I=1,NECONP
  110 EELEM(I)=FCEL(I)*PHI
  111 CONTINUE
C     STRAIN AT THE TOP OF THE PORTION OF ELEMENT BOUNDED BY N. A.
      ECONP=PHI*HCON
C     ELEMENT STRESSES
      FCPP=0.85*FC
      EC=1850000.00+500.00*FCPP
      EO=2.00*FCPP/EC
      EU=0.0038
      IF(NECONP.LT.1)GO TO 121
      DO 120 I=1,NECONP
      IF(EELEM(I).GE.0.00.AND.EELEM(I).LT.EO)GO TO 130
      IF(EELEM(I).GE.EO.AND.EELEM(I).LT.EU)GO TO 140
      IF(EELEM(I).GE.EU)GO TO 150
  130 FCELEM(I)=(2.00*EELEM(I)/EO-(EELEM(I)/EO)**2)*FCPP
      GO TO 120
  140 FCELEM(I)=FCPP-0.15*FCPP/(EU-EO)*(EELEM(I)-EO)
      GO TO 120
  150 FCELEM(I)=FCPP-0.15*FCPP
  120 CONTINUE
C     STRESS IN THE PORTION OF THE ELEMENT NEXT TO N. A.
  121 IF(ECONP.GT.0.00.AND.ECONP.LT.EO)GO TO 155
      IF(ECONP.GE.EO.AND.ECONP.LT.EU)GO TO 156
      IF(ECONP.GE.EU)GO TO 157
  155 FCONP=(2.00*ECONP/EO-(ECONP/EO)**2)*FCPP
      GO TO 158
  156 FCONP=FCPP-0.15*FCPP/(EU-EO)*(ECONP-EO)
      GO TO 158
  157 FCONP=FCPP-0.15*FCPP
  158 CONTINUE
C     AREAS OF THE ELEMENTS WHICH ARE IN COMPRESSION COUNTING FROM N.A.
C     UPWARDS
      IF(NECONP.LT.1)GO TO 180
      DO 160 I=1,NECONP
      IXX=NELEMS-NECONP
  160 ABCCON(I)=AREA(IXX)*HCOP/NELEM/DSIN(BETA)
C     ELEMENT COMPRESSIVE FORCES
      DO 170 I=1,NICONP
  170 ELFOBC(I)=ABCCON(I)*FCELEM(I)
C     TOTAL COMPRESSIVE FORCE
      FCTOT=0.00
      DO 180 I=1,NECONP
  180 FCTOT=FCTOT+ELFOBC(I)
  181 IF(NECONP.LT.1)FCTOT=0.00
C     AREA OF THE PORTION OF THE ELEMENT NEXT TO N. A.
      IXX=NELEMS-NECONP
      ACONP=AREA(IXX)*HCOP/NELEM/DSIN(BETA)
C     AND FORCE IN THE PORTION OF THE ELEMENT NEXT TO N. A.
      FCCC=ACONP*FCCPP/2.00
C     TOTAL FORCE IN THE COMPRESSION ZONE (POUNDS)
      C=FCTOT+FCCC
C     TOTAL FORCE IN THE COMPRESSION ZONE (KIPS)
      C=C/1000.00
      RETURN
      END
```

```
      SUBROUTINE MOMULT
C
C     THIS SUBROUTINE SOLVES FOR ULTIMATE CAPACITIES TAKING INTO
C     ACCOUNT TORSIONAL COMPONENT ON THE INCLINED PLANE
C
      IMPLICIT REAL*8(A-H,O-Z)
C
      COMMON AP,ASP,D,FP,FCM,FSU,ES,EPSTA,EPSCE,EPSSE,EPSSA,EPSSD,B,H,
     2BW,HW,XL,FC,XW,DB,EPSCB,ECOS,ESIN,A,SINC,T,C,EB,AESI,DELTA,
     3DST1,DST2,DST3,DST4,S,SIGMA,YABB,FPULT,FYSTIR
     4,DFPOB1,DFPOB2,DFPOB3,BZ,AAI,TC,ACB,BETA,THETA,TU,FF,
     5EPSCON,EPSTEA,FCON,FTEA,ENCON,XATER,YCON,YTER,A1,A2,A3,A4
     6,TCP,PT,V,SHARS,SHIRS,SHART,SHIRT,SHARB,SHIRB,AIR,AIV,SE,ST,QZ,QT
     7,ALPAE1,ALPAE2,THPPB,THPBS,THPBT
     8,AS,YS,APTA,TC,X,Y,DLPTH,AVEALL,PSUEC,ESAREA,YMOD,EYIELD,ESH,
     9EPSP,FYTLD,FULT,YSH,PHIFAC,ZELEM,TOTALP,TOTALP,
     1 TOTALH,EAC,PS,SECP,SUMFP,SUMPW,COUNT,PHI,SEP,ARCCOS,PCELEM
     2,MCCH,ECCRP,FCCRP,ACCRP,ELFORC,FCCC,RESIST,PCEL
     3,THETAB,THETAA,THETIB
C
      COMMON P,H,MODE,NELEMS,NSTEEL,NADEEP,NSCOND
C
      DIMENSION AP(10),B(10),FE(10),FSU(10),TSU(10),ES(10),
     1 EPSCE(10),EPSEE(10),EPSSA(10),EPSSE(10),DS(10),FPULT(10)
     2,AS(20),YS(20),AREA(500),TC(500),X(500),Y(500),ESTRA(500),EAS(20),
     3 PCEL(500),PS(20),PCELEM(500),ARCCOS(500),ELFORC(500)
C
      REAL PHITAC,MBETAP,MBETAN,MBETAV,MBETAT
 10 FORMAT(///,5X,'FIRST  MODE - ULTIMATE CAPACITY,STRAINS AND EQUILIB
     2RIUM CHECK')
 20 FORMAT(5X,'*****************************************************
     2*******'//)
C     CHECK FOR PURE BENDING CASE
      IF(YBSE.LT.0.005)THETA=1.570595
      IF(YBSE.LT.0.005)GO TO 21
      THETA=THETAD
 21 CONTINUE
      THETAC=THETA*180.00/3.14159
      WRITE(6,10)
      WRITE(6,20)
      WRITE(6,30)THETA,THETAD
 30 FORMAT(5X,'INCLINATION OF INITIAL CRACK: THETA(RAD.) =',F8.4/
     2 )X,'  THETA(DEG.) =',F8.4//)
      ITERNA=0
C     ASSUME COMPRESSION STRAIN IN BETA PLANE AND ITS INCREMENT
      EPSCAS=0.004
      EPSINC=0.0002
 40 EPSCAS=EPSCAS-EPSINC
C     ASSUME DEPTH OF NEUTRAL AXIS AND ITS INCREMENT
      AINC=H/NELEMS
C     ITERATION FOR POSITION OF NEUTRAL AXIS STARTS
      N=0
      A=AINC
 50 A=A+AINC
C     FIND INCLINATION OF COMPRESSION ZONE, BETA
      TANBET=B/(B+2.0*(H-A))*DTAN(THETA)
      BETA=DATAN(TANBET)
C     CALCULATE CURVATURE
      HELPS=H/NELEMS
      PHI=EPSCAS/(A-HELPS/2.0)
C     PRESTRESSING STEEL STRAINS
      DO 60 I=1,N
 60 EPSSA(I)=((H-A)-D(I))*PHI*DSIN(BETA)
C     TOTAL STRAINS IN STEEL IN LONGITUDINAL DIRECTION
      DO 70 I=1,N
 70 EPSSD(I)=EPSSE(I)-EPSCE(I)+EPSSA(I)
C     CALCULATE STRESSES AND FORCES IN PRESTRESSING STRANDS FROM STRESS-
C     STRAIN DIAGRAMS
      IF(NODE.EQ.1)CALL STR102
      IF(NODE.EQ.2)CALL STR300
      IF(NODE.EQ.3)CALL STRAAD
      IF(NODE.EQ.4)CALL STRAER
C     TENSILE FORCE OF PRESTRESSING STEEL IN ORIGINAL DIRECTION
      TS=0.00
      DO 90 I=1,N
 90 TS=TS+TSU(I)
C     TOTAL TENSILE FORCE IN PRESTRESSING STEEL PERP. TO BETA PLANE
      TS=TS*DSIN(BETA)
C     TENSILE FORCE IN CONCRETE
      FPSCB=1000./FCOB
      ECB=EPSCB/PHI
      IF(ECB.GT.(H-A))ECB=H-A
      TC=ESADD*BCP/2.00*P/DSIN(BETA)/1000.00
C     CONTRIBUTION OF TRANSVERSE STEEL (STIRRUPS - HORIZONTAL LEGS ONLY)
      EPSTOP=PHI*(DST1-A)
      EPSBOT=PHI*(DST2-A)
C     STRAIN IN THE DIRECTION OF TRANSVERSE STEEL
      EPSTOP=EPSTOP*DCOS(BETA)
      EPSBOT=EPSBOT*DCOS(BETA)
C     STRESSES IN THE DIRECTION OF TRANSVERSE STEEL
      FTOP=EPSTOP*ESTIR
      FBOT=EPSBOT*ESTIR
C     CHECK WHETHER STRESSES EXCEED FY
      IF(FTOP.GT.FYSTIR)FTOP=FYSTIR
      IF(FTOP.LT.(-FYSTIR))FTOP=-FYSTIR
      IF(FBOT.GT.FYSTIR)FBOT=FYSTIR
C     FORCES IN STIRRUPS
      TTOP=FTOP*ASE
      TBOT= BOT*AST
C     NO. OF STIRRUPS INTERCEPTED BY BETA  AND THETA PLANE
      A3=DST3
      A4=P-ESTR
      ERBOT=(P-A3-A4)/DTAN(THETA)/S
      ETTOP=(H-A3-A4)/DTAN(BETA)/S
C     TOTAL FORCE IN STIRRUPS (BOTTOM AND TOP)
      TTOP=TTOP*ERTOP
      TBOT=TBOT*ERBOT
C     NEGLECT CONTRIBUTION OF STIRRUPS IN COMPRESSION
      TTOP=0.00
C     TOTAL FORCE IN STIRRUPS PERP. TO BETA PLANE
```

```
      TOTTR=(TTOP+TBOT)*BCOS(BETA)
C
C     TOTAL TENSILE FORCE IN X-SECTION PERP. TO BETA PLANE (KIPS)
      T=TS+TC+TSTIP
C
C     COMPRESSIVE FORCE IN CONCRETE (KIPS)
C
      CALL CFORCE
C
C     ERROR IN SUM OF HORIZONTAL FORCES (IN PERCENTAGES)
C
      EA=T-C
C     NUMBER OF ITERATIONS
C
      N=N+1
      WRITE(N,*)ERROR
      IF(N.GT.300)RETURN
      IF(ABS(ERROR).LE.1.50)GO TO 110
      IF(ERROR.GT.0.00)GO TO 50
      A=A-AINC
      AINC=AINC/10.00
      GO TO 50
  110 CONTINUE
      BETA1=BETA*180.00/3.14159
C     TORSION TO BENDING RATIO ON THE INCLINED (BETA) PLANE
      RATIOT=(EKSI*DTAN(BETA)-1.00)/(EKSI+DTAN(BETA))
C
C     CALCULATE BENDING MOMENT ON THE INCLINED (BETA) PLANE
C     MOMENTS ARE TAKEN ABOUT N. A.
C
C     CONCRETE COMPRESSION ZONE CONTRIBUTION
      MBETAC=0.00
      IF(NECOMP.LT.1)GO TO 121
      DO 120 I=1,NECOMP
  120 MBETAC=MBETAC+FCEL(I)*ELPDBC(I)
  121 IF(NECOMP.LT.1)MBETAC=0.00
      MBETAC=MBETAC*FCCC*2.00/3.00*BCOS
      MBETAC=MBETAC/1000.00
C     COMPRESSION ZONE STEEL CONTRIBUTION
      MBETAP=0.00
      DO 130 I=1,N
  130 MBETAP=MBETAP+TSN(I)*DSIN(BETA)*(D-A-D(I))
C     CONCRETE TENSION ZONE CONTRIBUTION
      CMONTE=TC*2.00/3.00*BCS
C     NEGLECT CONTRIBUTION OF TENSION ZONE
      CMCRTE=0.00
C     STIRRUP CONTRIBUTION - HORIZONTAL LEGS
      MBETAH=(TTOP*DABS(A-DST1)+TBOT*DABS(A-DST2))
C     STIRRUP CONTRIBUTION - VERTICAL LEGS
C     NUMBER OF STIRRUPS INTERCEPTED
      XNVERT=(DST2-A)/DTAN(ZBETA)/S
C     AVERAGE STRAIN IN VERTICAL STIRRUPS
      EPSAVV=PHI*(DST2-A)/2.00*BCOS(BETA)
C     AVERAGE STRESS IN VERTICAL LEGS
      SVERT=EPSAVV*ESTIR
      IF(SVERT.GT.FYSTIR)SVERT=FYSTIR
C     TOTAL FORCE IN VERTICAL STIRRUPS
      FVERT=SVERT*AST*XNVERT
C     FLEXURAL AND TORSIONAL MOMENT ON BETA PLANE DUE TO VERT. STIRRUPS
      XMOMV=FVERT*(B-A3-AA)
      MBETAV=XMCSV*BCOS(BETA)
      TBETAV=XMOMV*DSIN(BETA)
C     TOTAL BENDING MOMENT ON INCLINED PLANE
      MBETAT=MBETAC+MBETAP+MBETAH+MBETAV+CMONTE
C     TOTAL TORQUE ON INCLINED PLANE
      TBETAT=(RATIOT)*MBETAT
C     TORQUE TAKEN BY COMPRESSION ZONE AND DOWEL FORCES IN BOTTOM LAYER
C     OF LONGITUDINAL STEEL
      TBETAC=TBETAT-TBTAV
C     TORQUE TAKEN BY COMPONENTS OF LONGITUDINAL STEEL AND DOWEL FORCES
      TLONG=0.00
      DO 135 I=1,N
  135 TLONG=TLONG+TSN(I)*(D(I)-D(1))*BCOS(BETA)
C     SHEAR FORCE (KIPS) IN COMPRESSION ZONE
      VBETAC=(TBETAT-TLONG)/(N-D(1)-A/2.00)
C     CHECK FOR THE CASE OF HOLLOW X-SECTION (N.A. BELOW FLANGE DEPTH)
      TW2=TW/2.00
      IF(YN.GT.1.00.AND.TF.LT.A)VBETAC=(TBETAT-TLONG)/(N-D(1)-TF/2.00)
      VBETAC=DABS(VBETAC)
C     SHEAR STRESSES IN COMPRESSION ZONE (KSI)
      TAUC=VBETAC/(A*B/DSIN(BETA))
C     CHECK FOR THE CASE OF HOLLOW X-SECTION (N.A. BELOW FLANGE DEPTH)
      IF(YN.GT.1.00.AND.TF.LT.A)TAUC=VBETAC/(TF*B/DSIN(BETA)+
     2(A-TF)*TW/DSIN(BETA))
C     SHEAR STRESS IN COMPRESSION ZONE (PSI)
      TAUC=TAUC*1000.00
C     CONFINED CAPACITIES AT ULTIMATE
      TORQUE=MBETAT/(FCOS(BETA)*DSIN(BETA)/ZEXI)
      RATIO=TORQUE/EKSI
      SHEAR=BRCH/BFHCBI
      ITERNA=ITERNA+1
      IF(ITERNA.GT.65)RETURN
C     SPECIFIED CONSTANTS:
C
C     POISSON'S RATIO
      PR=0.16
C     MODULUS OF ELASTICITY AS PER A.C.I. CODE
      ELMOD=470C0.00*RSQRT(FC)
C     SHEAR MODULUS
      G=ELMOD/(2.00*(1.00+PR))
C     SHEAR STRAIN
      GAMAXY=TAUC/G
C     MAXIMUM COMPRESSIVE STRAIN
      EPSCPR=0.0035
C     MAXIMUM TENSILE STRAIN
      EPSTPR=0.00015
C     SPECIFIED ERROR IN STRAIN INTERACTION EQUATION (TENSILE STRAIN)
      EPSCPR=0.00001
      IF(NECOMP.LT.1)GO TO 105
      COEFEL=ECLEN(NECOMP)/2.00
```

```
  105 IF(DFCC*0.LT.1)CORFEL=SCORP/2.00
      COFFSA=CAPART/2.00
      PARAPS=SQRT(CORFEL**2+COEFSA**2)
      EPSC=CORFEL*PARAPS
      EPST=PARA*(CORFEL-PARAPS)
      EPSCEC=EPSCPP*(1.00-(EPST/EPSTPP)**2)
      ERRA=EPSCEC-EPSC
      IF(ABS(EPRA).LT.SPECER)GO TO 132
      IF(EPRA.LT.0.00)GO TO 40
      EPSCAS=EPSCAS+EPSINC
      EPSINC=EPSINC/10.00
      GO TO 40
  132 CONTINUE
C     CALCULATE PRINCIPAL STRESSES
C     COMPRESSIVE STRESS
      FCPP=0.85*FC
      EC=1420000.00+500.00*FCPP
      EO=2.85*FCPP/EC
      EO=0.0038
      IF(EPSC.GE.0.00.AND.EPSC.LT.EO)STRESC=(1.00*EPSC/EO-(EPSC/EO)**2)*
     2FCPP
      IF(EPSC.GT.EO)STRESC=FCPP-0.15*FCPP/(EU-EO)*(EPSC-EO)
C     TENSILE STRESS
      FT1=2.00/SQRT(3.0000)*RMODR
      IF(EPST.GE.0.00.AND.EPST.LT.0.0001)STREST=FT1/0.0001*EPST
      IF(EPST.GE.0.0001)STREST=FT1
C
C     WRITE INCLINATION OF COMPRESSION ZONE W.R.T. LONGITUDINAL AXIS
      WRITE(6,299)BETA,BETAI
C     WRITE INCREASE IN STRAINS IN PRESTRESSING STEEL BETWEEN INITIAL
C     AND ULTIMATE LOAD
      WRITE(6,310)
      WRITE(6,225)(I,EPSSA(I),I=1,N)
C     WRITE ULTIMATE STRAIN IN PRESTRESSING STEEL
      WRITE(6,296)
      WRITE(6,229)(I,EPSSB(I),I=1,N)
C     WRITE NO. OF ITERATIONS REQUIRED (CURVATURE)
      WRITE(6,246)M
C     WRITE THE DEPTH OF COMPRESSIVE BLOCK (N.A. LOCATION)
      WRITE(6,255)A
C     WRITE CURVATURE
      WRITE(6,260)PHI
C     WRITE STRESSES IN STEEL
      WRITE(6,270)
      WRITE(6,226)(I,FSU(I),I=1,N)
C     WRITE FORCES IN PRESTRESSING STEEL
      WRITE(6,280)
      WRITE(6,220)(I,TSU(I),I=1,N)
C     WRITE STRAINS IN TRANSVERSE STEEL
      WRITE(6,290)
      WRITE(6,305)EPSTOP,EPSBOT
C     WRITE STRESSES IN TRANSVERSE STEEL
      WRITE(6,310)FTOP,FBOT
C     WRITE NO. OF STIRRUPS INTERCEPTED
      WRITE(6,320)NTOP,NBOT
C     WRITE EQUILIBRIUM CHECK (TOTAL TENSILE AND COMPRESSIVE FORCE)
      WRITE(6,330)
      WRITE(6,340)T
      WRITE(6,350)C
      WRITE(6,360)ER
C     WRITE MOMENT TO BENDING RATIO ON THE INCLINED (BETA) PLANE
      WRITE(6,361)RATIOT
C     WRITE NUMBER OF THE ELEMENTS IN COMPRESSION
      WRITE(6,370)NECOMP
C     WRITE STRAINS IN THE CENTROIDS OF THE COMPRESSION ELEMENTS
      IF(NFCOMP.LT.1)GO TO 399
      WRITE(6,390)
      WRITE(6,220)(I,EELEM(I),I=1,NECOMP)
C     WRITE DISTANCES FROM N.A. TO CENTROIDS OF THE COMPRESSION ELEMENTS
      WRITE(6,440)
      WRITE(6,220)(I,FCEL(I),I=1,NECOMP)
  399 CONTINUE
C     WRITE HEIGHT OF THE PORTION OF THE ELEMENT IN COMPRESSION BOUNDED
C     BY N. A.
      WRITE(6,480)HCON
C     WRITE STRAIN AT THE TOP OF THE PORTION OF ELEMENT BOUNDED BY N. A.
      WRITE(6,410)FCONP
C     WRITE ELEMENT STRESSES
      IF(NFCOMP.LT.1)GO TO 421
      WRITE(6,420)
      WRITE(6,226)(I,FCELEM(I),I=1,NECOMP)
  421 CONTINUE
C     WRITE STRESS IN THE PORTION OF THE ELEMENT BOUNDED BY N.A.
      WRITE(6,430)FCCNP
C     WRITE AREAS OF THE COMPRESSION ELEMENTS
      IF(NECOMP.LT.1)GO TO 441
      WRITE(6,446)
      WRITE(6,226)(I,ARCCOM(I),I=1,NECOMP)
  441 CONTINUE
C     UPDATE AREA OF THE PORTION OF THE COMPRESSION ELEM. BOUNDED BY N.A.
      WRITE(6,456)ACONP
      WRITE(6,471)EPVERT,EPSAVT,SVERT
      WRITE(6,480)
      WRITE(6,492)RBETAC
      WRITE(6,494)CMONTE
      WRITE(6,500)RBETAP
      WRITE(6,510)RBETAB
      WRITE(6,520)RBTTAV
      WRITE(6,530)PBETAB
      WRITE(6,540)TBETAT
      WRITE(6,550)TBETAV
      WRITE(6,560)TBETAC
      WRITE(6,570)VBETAC
      WRITE(6,580)TABC
      IF(NECOMP.LT.1)GO TO 462
      WRITE(6,590)FCELEM(NECOMP)
  462 CONTINUE
      WRITE(6,591)ITERNA
      WRITE(6,592)STRESS
      WRITE(6,595)EPST
```

```
      WRITE(6,593)STRESC
      WRITE(6,596)EPSC
      WRITE(6,594)EPSA
      WRITE(6,600)TORQUE,AMOM,SHEAR
      WRITE(6,610)
200   FORMAT(///,5X,'INCLINATION OF COMPRESSION SCALE',5X'BETA(RAD) =',F6
     2.3,/,42X,'BETA(DEG) =',F6.2,///)
213   FORMAT(5X,'INCREASE IN STRAIN IN STEEL BETWEEN INITIAL AND ULTIMAT
     2E LOADS',/)
220   FORMAT(8(5X,I4,4X,F12.6,10X,I4,4X,F12.6,/) )
230   FORMAT(5X,'ULTIMATE STRAIN IN STEEL (IN PERCENT) =',/)
240   FORMAT(5X,'NUMBER OF ITERATIONS REQD. FOR CURVATURE =',I4///)
250   FORMAT(5X,'NEUTRAL AXIS LOCATION (IN INCHES, FROM THE TOP)',A=',
     2F10.4///)
260   FORMAT(5X,'CURVATURE (RADIANS/IN), PHI=',F10.7,///)
270   FORMAT(5X,'STRESSES IN PRESTRESSING STRANDS AT ULTIMATE (KSI) ='/)
280   FORMAT(5X,'FORCES IN PRESTRESSING STRANDS AT ULTIMATE(KIPS) =')
290   FORMAT(1H1,///,5X,'STRAINS AND STRESSES IN HORIZONTAL LEGS OF STIRR
     2UPS AT ULTIMATE =',/)
300   FORMAT(5X,'STRAIN IN TOP    LEG =',F10.6,/5X,'STRAIN IN BOTTOM LEG
     2 =',F10.6,//)
310   FORMAT(5X,'STRESS IN TOP    LEG =',F10.2,/5X,'STRESS IN BOTTOM LEG
     2 =',F10.2,//)
320   FORMAT(5X,'NO. OF STIRRUPS INTERCEPTED :',/5X'AT THE TOP    =',
     2F5.2,/5X,'AT THE BOTTOM =',F5.2,//)
330   FORMAT(5X,'EQUILIBRIUM CHECKS')
340   FORMAT(5X,'TENSILE FORCE (KIPS),     T =',F10.3)
350   FORMAT(5X,'COMPRESSIVE FORCE (KIPS), C =',F10.3,/)
360   FORMAT(5X,'ERROR IN PERCENTAGE (T-C)/T*100 =',F10.5,///)
361   FORMAT(5X,'TORSION TO BENDING RATIO ON THE INCLINED (BETA) PLANE ,
     2 KSI=',A =',F10.5,///)
370   FORMAT(5X,'NUMBER OF THE ELEMENTS IN COMPRESSION =',I4,///)
380   FORMAT(5X,'STRAINS IN THE CENTROIDS OF COMPRESSION ELEMENTS :',/)
390   FORMAT(//,5X,'DISTANCES FROM N.A. TO CENTROIDS OF THE COMPRESSION
     2ELEMENTS :',/)
400   FORMAT(//,5X,'HEIGHT OF THE PORTION OF ELEMENT IN COMPRESSION
     2BOUNDED BY N. A. (INCHES) =',F8.5,///)
410   FORMAT(5X,'STRAIN AT THE TOP OF THE PORTION OF ELEMENT BOUNDED BY
     2N.A. =',F12.6,///)
420   FORMAT(1H1,//,5X,'COMPRESSION ELEMENT STRESSES :',/)
430   FORMAT(//,5X,'STRESS AT THE TOP OF PORTION OF THE COMPRESSION ELEM
     2ENT BOUNDED BY N. A.   (F S I )=',F12.5,///)
440   FORMAT(5X,'AREAS OF THE ELEMENTS IN COMPRESSION :',/)
450   FORMAT(//,5X,'AREA OF THE PORTION OF COMPRESSION ELEMENT BOUNDED B
     2Y N. A.   (SQ. INS.) =',F12.5,///)
471   FORMAT(    4X,'NUMBER OF STIRRUPS(VERT. LEGS ON ONE SIDE) INTERCE
     2PTED:',F10.5/5X,'AVERAGE STRAIN IN VERTICAL LEGS OF STIRRUPS
     3       :',F10.5/5X,'AVERAGE STRESS IN VERTICAL LEGS OF STIRRUPS
     4       :',F10.5///)
480   FORMAT(5X,'BENDING MOMENTS (IN.KIPS.) ON INCLINED (BETA) PLANE :'/
     2)
490   FORMAT(5X,'DUE TO CONCRETE COMPRESSION ZONE :',F10.4)
491   FORMAT(5X,'                        TENSION ZONE :',F10.4)
500   FORMAT(5X,'                  PRESTRESSING STEEL :',F10.4)
510   FORMAT(5X,'      STIRRUPS (HORIZONTAL LEGS) :',F10.4)
520   FORMAT(5X,'       STIRRUPS (VERTICAL LEGS) :',F10.4/)
530   FORMAT(5X,'TOTAL BENDING MOMENT ON BETA PLANE :',F10.4//)
540   FORMAT(5X,'TOTAL TORQUE (IN.KIPS) ON BETA PLANE :',F10.4//)
550   FORMAT(5X,'TORQUE TAKEN BY STIRRUPS (VERT. LEGS) :',F10.4//)
560   FORMAT(5X,'TORQUE TAKEN BY CONCR. COMPR. ZONE AND DOWELS :',F10.4/
     2/)
570   FORMAT(5X,'SHEAR FORCE (KIPS) IN COMPR. ZONE :',F10.4//)
580   FORMAT(5X,'SHEAR STRESS (PSI) IN COMPR. ZONE :',F10.4//)
590   FORMAT(5X,'NORMAL STRESS (PSI) IN COMPRESSION ZONE :',F10.4//)
591   FORMAT(5X,'NUMBER OF ITERATIONS FOR N.A. POSITIO :',I3//)
592   FORMAT(5X,'MAXIMUM (TENSILE) PRINCIPAL STRESS (PSI) ON BETA PLANE
     2 :',F10.2//)
593   FORMAT(5X,'MINIMUM (COMPRESSIVE) PRINCIPAL STRESS (PSI) ON BETA PL
     2ANE :',F10.2//)
594   FORMAT(5X,'ERROR IN STRESS INTERACTION EQUATION :',F10.4//)
595   FORMAT(5X,'MAXIMUM (TENSILE) PRINCIPAL STRAIN (IN/IN) ON BETA PLAN
     2E :',F12.8//)
596   FORMAT(5X,'MINIMUM (COMPRESSIVE) PRINCIPAL STRAIN (IN/IN) ON BETA
     2PLANE :',F12.8//)
600   FORMAT(/5X,'COMBINED CAPACITIES AT ULTIMATE (IN.KIPS AND KIPS) :',
     2//5X,'TORSION :',F8.2/5X,'BENDING :',F8.2,/5X,'SHEAR   :',F8.2//)
610   FORMAT(1H1)
      RETURN
      END
```

```
      SUBROUTINE ANALYS
C
C     THIS SUBROUTINE SOLVES FOR ULTIMATE CAPACITIES TAKING INTO
C     ACCOUNT TORSIONAL COMPONENT ON THE INCLINED PLANE
C
      IMPLICIT REAL*8(A-H,O-Z)
C
      COMMON AP,AST,B,FE,FSH,FSH,ES,FSTIR,EPSCE,FPSSE,EPSSA,EPSSB,H,N,
     2SH,NH,IL,IC,ERROR,IPSCH,ECON,ICCH,A,ZITC,T,C,EP,ZEZI,DELTA,
     3DST1,DST2,DST3,DST4,S,SIGEA,TANB,FPULT,FYSTIR
     4,DFNODE,DFSCH2,DFNLDI,ES,IH1,TC,ECP,BETA,THETA,TH,TF,
     5EPSCCH,EPSTEH,ICCH,FTEH,EHCCH,EATEH,TCOH,TTEH,A1,A2,A3,A4
     6,TCH,BP,Y,SHAPE,SHIFT,SMART,SMINT,SHARH,SHINH,ZIH,ZIY,SI,SY,QE,QY
     7,ALPAE1,ALPAE2,TAPPH,THPRS,THPHT
     8,AS,YS,AFEA,YC,H,T,DEPTH,ARTALL,PSUBC,APAREA,YNOH,ZYZELH,ESH,
     9ZULT,FFALH,FULT,YSH,PHIFAC,ZELEH,TOTALF,TOTALP,
     1 TOTALH,FAS,FH,SUMF,SUMPP,SHEFH,COUNT,PHI,DEP,ABCCOH,FCELEH
     2,MOCP,FCOMP,FCOMP,ACOMP,ELFOPC,FCCC,ZESIST,FCEL
     3,TWIEH,TMATCH,THITH
C
      COMMON N,H,NODE,ZELEH,ZSTEEL,HARZEP,ZECOMP
C
      DIMENSION AP(10),B(10),FE(10),FSH(10),TSH(10),ES(10),
     1 EPSCE(10),EPSSE(10),EPSSA(10),EPSSH(10),AS(10),FFULT(10)
     2,AS(20),YS(20),AREA(500),YC(500),Z(502),Y(500),ZELEH(500),EAS(20),
     3 FCEL(500),FS(20),FCALEH(500),ABCCOH(500),ELFOPC(500)
C
      REAL NDTTAC,NDTTAP,NDTTAH,NDTTAY,NDTTAT
      WRITE(6,16)
   16 FORMAT(///,5X,'SECOND NODE - ULTIMATE CAPACITY,STRAINS AND NODELIN
     2EISH CHECK')
      WRITE(6,20)
   20 FORMAT(5X,'**********************************************************
     2*******'//)
C     CHECK FOR POOR BENDING CASE
      IF(ZNSI.LT.0.06%) THETA=1.566031
      IF(ZNSI.LT.0.005) RETURN
      THETA=THETAH
   21 CONTINUE
      THETAD=THETA*180.00/3.14159
      WRITE(6,36) THETA,THETAD
   36 FORMAT(5X,'INCLINATION OF INITIAL CRACK: THETA(RAD.) =',F8.4,/
     2 33X,'  THETA(DEG.) =',F8.4//)
C     ASSUME DEPTH OF NEUTRAL AXIS AND ITS INCREMENT
      AINC=H/ZELEH
      ITERNA=0
C     ITERATION FOR POSITION OF NEUTRAL AXIS STARTS
      A=H
      A=0.8*H
   46 A=A-AINC
C     CHECK THAT DEPTH OF N. A. IS NOT EQUAL ZERO
      IF(A.LT.0.01)GO TO 180
C     FIND INCLINATION OF COMPRESSION ZONE, BETA
      TANBET=H/(H*2.0*(B-A))*DTAN(THETA)
      BETA=DATAN(TANBET)
C     ASSUME CURVATURE AND ITS INCREMENT
      PHI=0.0000
      CINC=0.0001
C     ITERATION FOR CURVATURE STARTS
      N=0
   50 PHI=PHI+CINC
C     PRESTRESSING STEEL STRAINS
      DO 60 I=1,N
   60 EPSSA(I)=(DS(I)-A)*PHI*DSIN(BETA)
C     TOTAL STRAINS IN STEEL IN LONGITUDINAL DIRECTION
      DO 70 I=1,N
   70 EPSSB(I)=EPSSE(I)+EPSSA(I)
C     CALCULATE STRESSES AND FORCES IN PRESTRESSING STRANDS FROM STRESS-
C     STRAIN DIAGRAMS
      IF(NODE.EQ.1)CALL STR102
      IF(NODE.EQ.2)CALL STR300
      IF(NODE.EQ.3)CALL STRAAD
      IF(NODE.EQ.4)CALL STRAEN
C     TENSILE FORCE OF PRESTRESSING STEEL IN ORIGINAL DIRECTION
      TS=0.00
      DO 90 I=1,N
   90 TS=TS+TAB(I)
C     TOTAL TENSILE FORCE IN PRESTRESSING STEEL PERP. TO BETA PLANE
      TS=TS*DSIN(BETA)
C     TENSILE FORCE IN CONCRETE
      EPACP=EMODP/ECON
      ECP=EPSCE/PHI
      IF(ECP.GT.(H-A))ECP=H-A
      TC=EMODP*ECP/2.00*H/DSIN(BETA)/1000.00
C     CONTRIBUTION OF TRANSVERSE STEEL (STIRRUPS - VERTICAL LEGS ONLY)
      EPSCCH=PHI*(DST2-A)
      EPSTEH=PHI*(DST3-A)
C     STRAIN IN THE DIRECTION OF TRANSVERSE STEEL
      EPSCCH=EPSCCH*DCOS(BETA)
      EPSTEH=EPSTEH*DCOS(BETA)
C     STRESSES IN THE DIRECTION OF TRANSVERSE STEEL
      FCOH=EPSCCH*FSTIR
      FTEH=EPSTEH*ESTIR
C     CHECK ULTIMATE STRESSES EXCEED FY
      IF(FCOH.GT.FYSTIR)FCOH=FYSTIR
      IF(FCOH.LT.(-FYSTIR))FCOH=-FYSTIR
      IF(FTEH.GT.FYSTIR)FTEH=FYSTIR
C     FORCES IN STIRRUPS
      TCOH=FCOH*AST
      TTEH=FTEH*AST
C     NO. OF STIRRUPS INTERCEPTED BY BETA  AND THETA PLANE
      A1=DSTI
      A2=H-DST2
      A3=DST3
      A4=P-DST4
      ENCOH=(H-A1-A3)/DTAN(BETA)/S
      ENTEH=(H-A1-A2)/DTAN(THETA)/S
C     TOTAL FORCE IN STIRRUPS (BOTTOM AND TOP)
      TCOH=TCOH*ENCOH
      TTEH=TTEH*ENTEH
```

```
C     SELECT CONTRIBUTION OF STIRRUPS IN COMPRESSION
      TCON=0.0
C     TOTAL FORCE IN STIRRUPS PERP. TO BETA PLANE
      TSTIR=(TCON+TYLD)*DCOS(BETA)
C     TOTAL TENSILE FORCE IN X-SECTION PERP. TO BETA PLANE (KIPS)
      T=TS+TC+TSTIR
C
C     COMPRESSIVE FORCE IN CONCRETE (KIPS)
C
      CALL CFORCE
C
C     ERROR IN SUM OF HORIZONTAL FORCES (IN PERCENTAGES)
C
      ER=T-C
C
C     NUMBER OF ITERATIONS
C
      N=N+1
      IF(N.GE.500)GO TO 100
      GO TO 102
  100 WRITE(6,101)N
      IF(N.GE.503)PETURN
  101 FORMAT(5X,'SPECIFIED NUMBER OF ITERATIONS FOR CURVATURE HAS EXCEED
     2ED N=',I4////)
      GO TO 136
  102 CONTINUE
      IF(ABS(ER).LE.0.05)GO TO 110
      IF(ER.GT.0.00)GO TO 50
      P.AI=PHI-CINC
      CIAC=CINC/10.0
      GO TO 90
  110 CONTINUE
      BETA1=BETA*180.00/3.14159
C     TOPSICK TO BENDING RATIO ON THE INCLINED (BETA) PLANE
      RESIBT=BTAR(BETA)
C
C     CALCULATE BENDING MOMENT ON THE INCLINED (BETA) PLANE
C     MOMENTS ARE TAKEN ABOUT N. A.
C
C     CONCRETE COMPRESSION ZONE CONTRIBUTION
      RBETAC=0.00
      IF(NECOMP.LT.1)GO TO 121
      DO 120 I=1,NECOMP
  120 RBETAC=RBETAC+FCEL(I)*ELFORC(I)
  121 IF(NECOMP.LT.1)RBETAC=0.00
      RBETAC=RBETAC*FCCC*2.00/3.00*DCOS
      RBETAC=RBETAC/1000.00
C     PRESTRESSING STEEL CONTRIBUTION
      RBETAP=0.00
      DO 130 I=1,N
  130 RBETAP=RBETAP+TEN(I)*ESIN(BETA)*(DS(I)-A)
C     CONCRETE TENSION ZONE CONTRIBUTION
      CRONTE=TC*2.00/3.00*ICR
C     NEGLECT CONTRIBUTION OF TENSION ZONE
      CRONTE=0.00
C     STIRRUP CONTRIBUTION - VERTICAL LEGS
      PBETAV=(TCON*PABS(A-DST))*TYLD*DABS(A-DST))
C     STIRRUP CONTRIBUTION - HORIZONTAL LEGS
C     NUMBER OF STIRRUPS INTERCEPTED
      XNUMB=(DST0-A)/DTAN(ZBETA)/S
C     AVERAGE STRAIN IN HORIZONTAL LEGS
      EPSAVH=PHI*(DST0-A)/2.00*DCOS(BETA)
C     AVERAGE STRESS IN HORIZONTAL LEGS
      SHOP=EPSAVH*ESTIR
      IF(SHOP.GT.FYSTIR)SHOP=FYSTIR
C     TOTAL FORCE IN HORIZONTAL STIRRUPS
      FHOR=SHOP*ASI*XNUMB
C     FLEXURAL AND TORSIONAL MOMENT ON BETA PLANE DUE TO HOR. STIRRUPS
      RMOMH=FHOR*(H-A1-A2)
      RBETAH=RMOMH*DCOS(BETA)
      TBETAH=RMOMH*ESIN(BETA)
C     TOTAL BENDING MOMENT ON INCLINED PLANE
      PBETAT=PBETAC+RBETAP+RBETAH+RBETAV+CRONTE
C     TOTAL TORQUE ON INCLINED PLANE
      TBETAT=(RESIBT)*RBETAT
C     TORQUE TAKEN BY COMPRESSION ZONE AND DOWEL FORCES IN BOTTOM LAYER
C     OF LONGITUDINAL STEEL
      TBETAC=TBETAT-TBTAH
C     TORQUE TAKEN BY COMPONENTS OF LONGITUDINAL STEEL AND DOWEL FORCES
      TLONG=0.00
      DO 135 I=1,N
  135 TLONG=TLONG+TEN(I)*(DS(I)-DS(I))*DCOS(BETA)
C     SHEAR FORCE (KIPS) IN COMPRESSION ZONE
      VBETAC=(TBETAT+TLONG)/(DS(1)-A/2.00)
C     CHECK FOR THE CASE OF HOLLOW X-SECTION (N.A. BELOW FLANGE DEPTH)
      TW12=TW/2.00
      IF(BM.GT.T.00.AND.TW12.LT.A)VBETAC=(TBETAT+TLONG)/(DS(1)-TW12/2.0)
C     SHEAR STRESS IN COMPRESSION ZONE (KSI)
      TAUC=VBETAC/(A*M/ESIN(BETA))
C     CHECK FOR THE CASE OF HOLLOW X-SECTION (N.A. BELOW FLANGE DEPTH)
      IF(BM.GT.1.00.AND.TW12.LT.A)TAUC=VBETAC/(TW12*M/BSIN(BETA)+
     2(A-TW12)*TF*2.00/BSIN(BETA))
C     SHEAR STRESS IN COMPRESSION ZONE (PSI)
      TAUC=TAUC*1000.00
C     COMBINED CAPACITIES AT ULTIMATE
      TORQUE=BETAT/(DCOS(BETA)*(1.00+1.00/DELTA*A/(B*DELTA)))
      BSHR=TORQUE/ESIN
      SHEAR=BCOS/DCOS1
      ITERBA=ITERBA+1
      IF(ITERBA.GT.500)WRITE(6,131)
      IF(ITERBA.GT.500)GO TO 132
  131 FORMAT(5X,'NUMBER OF SPECIFIED ITERATIONS (FOR N.A.) EXCEEDED')
C     SPECIFIED CONSTANTS:
C
C     POISSON'S RATIO
      PR=0.15
C     MODULUS OF ELASTICITY AS PER A.C.I. CODE
      ELCOD=57000.00*SQRT(FC)
C     SHEAR MODULUS
      G=ELACD/(2.00*(1.00+PR))
```

```
C     STRAIN STRAIN
      GAPASS=TANC/H
C     MAXIMUM COMPRESSIVE STRAIN
      EPSCPP=0.0019
C     MAXIMUM TENSILE STRAIN
      EPSTPP=0.00015
C     SPECIFIED EPSPP IN STRAIN INTERACTION EQUATION (TENSILE STRAIN)
      SPECEP=0.000102
      IF(NECOMP.LT.1)GO TO 185
      COEPEL=EALEN(NECOMP)/2.00
  185 IF(NECOMP.LT.1)COEPEL=BCOMP/2.00
      COEPGA=GAPASS/2.00
      RADEPS=DSQRT(COEPEL**2+COEPGA**2)
      EPSC=COEPEL*RADEPS
      EPST=EABS(COEPEL-RADEPS)
      EPSTEQ=DSQRT(EPSTPP**2/EPSCPP*BABS(EPSCPP-EPSC))
      ISSA=IPSTEQ-EPST
      IF(DABS(ASPA).LT.SPECEP)GO TO 132
      IF(ASPA.GT.0.66)GO TO 48
  180 A=A+AINC
      AINC=AINC/10.00
      GO TO 48
  132 CONTINUE
C     CALCULATE PRINCIPAL STRESSES
C     COMPRESSIVE STRESS
      FCPP=0.85*FC
      EC=1405000.00+500.00*FCPP
      EO=2.00*FCPP/EC
      EU=0.0038
      IF(EPSC.GE.0.00.AND.EPSC.LT.EO)STRESC=(2.00*EPSC/EO-(EPSC/EO)**2)*
     1FCPP
      IF(EPSC.GE.EO.AND.EPSC.LT.EU)STRESC=FCPP-0.15*FCPP/(EU-EO)*(EPSC-
     1EO)
C     TENSILE STRESS
      FT1=2.00/DSQRT(3.000)*RMODR
      IF(EPST.GE.0.00.AND.EPST.LT.0.0001)STRST=FT1/0.0001*EPST
      IF(EPST.GE.0.0001)STRST=FT1
C     WRITE INCLINATION OF COMPRESSION ZONE W.R.T. LONGITUDINAL AXIS
      WRITE(6,206)BETA,BETA1
C     WRITE INCREASE IN STRAINS IN PRESTRESSING STEEL BETWEEN INITIAL
C     AND ULTIMATE LOAD
      WRITE(6,210)
      WRITE(6,220)(I,EPSSA(I),I=1,N)
C     WRITE ULTIMATE STRAIN IN PRESTRESSING STEEL
      WRITE(6,230)
      WRITE(6,220)(I,EPSSB(I),I=1,N)
C     WRITE NO. OF ITERATIONS REQUIRED (CURVATURE)
      WRITE(6,240)N
C     WRITE THE DEPTH OF COMPRESSIVE BLOCK (N.A. LOCATION)
      WRITE(6,250)A
C     WRITE CURVATURE
      WRITE(6,260)PHI
C     WRITE STRESSES IN STEEL
      WRITE(6,270)
      WRITE(6,220)(I,FSS(I),I=1,N)
C     WRITE FORCES IN PRESTRESSING STEEL
      WRITE(6,280)
      WRITE(6,220)(I,TSS(I),I=1,N)
C     WRITE STRAINS IN TRANSVERSE STEEL
      WRITE(6,290)
      WRITE(6,300)EPSCON,EPSTEN
C     WRITE STRESSES IN TRANSVERSE STEEL
      WRITE(6,310)FCON,FTEN
C     WRITE NO. OF STIRRUPS INTERCEPTED
      WRITE(6,320)NNCPR,NNTPR
C     WRITE EQUIBRILIUM CHECK (TOTAL TENSILE AND COMPRESSIVE FORCE)
      WRITE(6,330)
      WRITE(6,340)T
      WRITE(6,350)C
      WRITE(6,360)ER
C     WRITE TENSION TO BENDING RATIO ON THE INCLINED (BETA) PLANE
      WRITE(6,361)RESIST
C     WRITE LENGTH OF THE ELEMENTS IN COMPRESSION
      WRITE(6,370)BECOMP
C     WRITE STRAINS IN THE CENTROIDS OF THE COMPRESSION ELEMENTS
      IF(NECOMP.LT.1)GO TO 399
      WRITE(6,380)
      WRITE(6,220)(I,EPLEN(I),I=1,NECOMP)
C     WRITE DISTANCES FROM N.A. TO CENTROIDS OF THE COMPRESSION ELEMENTS
      WRITE(6,390)
      WRITE(6,220)(I,FCEL(I),I=1,NECOMP)
  399 CONTINUE
C     WRITE HEIGHT OF THE PORTION OF THE ELEMENT IN COMPRESSION BOUNDED
C     BY N. A.
      WRITE(6,400)HCOR
C     WRITE STRAIN AT THE TOP OF THE PORTION OF ELEMENT BOUNDED BY N. A.
      WRITE(6,413)ECCAP
C     WRITE ELEMENT STRESSES
      IF(NECOMP.LT.1)GO TO 421
      WRITE(6,420)
      WRITE(6,220)(I,FCELEM(I),I=1,NECOMP)
  421 CONTINUE
C     WRITE STRESS IN THE PORTION OF THE ELEMENT BOUNDED BY N.A.
      WRITE(6,430)FCOMP
C     WRITE AREAS OF THE COMPRESSION ELEMENTS
      IF(NECOMP.LT.1)GO TO 441
      WRITE(6,440)
      WRITE(6,220)(I,ARCCOR(I),I=1,NECOMP)
  441 CONTINUE
C     WRITE AREA OF THE PORTION OF THE COMPRESSION ELEM. BOUNDED BY N.A.
      WRITE(6,450)ACOMP
C     WRITE FORCES IN THE ELEMENTS IN COMPRESSION
      WRITE(6,471)RSHOR,EPSAVR,SHOR
      WRITE(6,480)
      WRITE(6,490)RBETAC
      WRITE(6,491)CMONTR
      WRITE(6,500)RBETAP
      WRITE(6,510)RBETAR
      WRITE(6,520)RBETAV
      WRITE(6,530)RBETAT
```

```
      WRITE(6,*40)TBETAI
      WRITE(6,*45)TBETAD
      WRITE(6,*70)TBETAC
      WRITE(6,*03)TAUC
      IF(*ECOMP.LT.1)GO TO 663
      WRITE(6,*50)PCBEAM(RECOMP)
663 CONTINUE
      WRITE(6,*91)ITAPOA
      WRITE(6,*92)APST
      WRITE(6,*95)STRESP
      WRITE(6,*93)RPSC
      WRITE(6,*94)STRESC
      WRITE(6,*90)EPOA
      WRITE(6,*CC)TCPOOF,BAOA,SHEAR
      WRITE(6,*10)
200 FORMAT(5X,'INCLINATION OF COMPRESSION ZONE=',5X'BETA(RAD) =',F6.2
   2,/,2X,'BETA(DEG) =',F6.2,//)
210 FORMAT(5X,'INCREASE IN STRAIN IN STEEL BETWEEN INITIAL AND ULTIMAT
   2E LOAD:',/)
220 FORMAT(8(5X,I6,4X,F12.6,10X,I4,4X,F12.6,/) )
230 FORMAT(5X,'ULTIMATE STRAIN IN STEEL (IN PERCENT) =',/)
240 FORMAT(5X,'NUMBER OF ITERATIONS NEED. FOR CURVATURE =',I4//)
250 FORMAT(5X,'NEUTRAL AXIS LOCATION (IN INCHES,FROM THE SIDE),B=',
   2F10.4///)
260 FORMAT(5X,'CURVATURE (RADIANS/IN), PHI=',F10.7,//)
270 FORMAT(5X,'STRESSES IN PRESTRESSING STRANDS AT ULTIMATE (KSI) :'/)
280 FORMAT(5X,'FORCES IN PRESTRESSING STRANDS AT ULTIMATE(KIPS) :')
290 FORMAT(1H1,//,5X,'STRAINS AND STRESSES IN VERTICAL  LEGS OF STIRR
   2UPS AT ULTIMATE :'/)
300 FORMAT(5X,'STRAIN IN COMPR. LEG =',F10.6,/5X,'STRAIN IN TENSN. LEG
   2 =',F10.6,//)
310 FORMAT(5X,'STRESS IN COMPR. LEG =',F10.2,/5X,'STRESS IN TENSN. LEG
   2 =',F10.2,//)
320 FORMAT(5X,'NO. OF STIRRUPS INTERCEPTED :',/5X'AT THE C. SIDE=',
   2F5.2,/5X,'AT THE T. SIDE=',F5.2,//)
330 FORMAT(5X,'EQUILIBRIUM CHECKS')
340 FORMAT(5X,'TENSILE FORCE (KIPS),    T =',F10.5)
350 FORMAT(5X,'COMPRESSIVE FORCE (KIPS), C =',F10.5,/)
360 FORMAT(5X,'ERROR IN PERCENTAGE (T-C)/T*100 =',F10.5,///)
361 FORMAT(5X,'TORSION TO BENDING RATIO ON THE INCLINED (BETA) PLANE ,
   2 RSI=BETA =',F10.5,///)
370 FORMAT(5X,'NUMBER OF THE ELEMENTS IN COMPRESSION =',I4,///)
380 FORMAT(5X,'STRAINS IN THE CENTROIDS OF COMPRESSION ELEMENTS :',/)
390 FORMAT(//,5X,'DISTANCES FROM N.A. TO CENTROIDS OF THE COMPRESSION
   2ELEMENTS :',/)
400 FORMAT(//,5X,'HEIGHT OF THE PORTION OF ELEMENT IN COMPRESSION
   2BOUNDED BY N. A.(INCHES) =',F8.5,///)
410 FORMAT(5X,'STRAIN AT THE TOP OF THE PORTION OF ELEMENT BOUNDED BY
   2N.A. =',F12.6,///)
420 FORMAT(1H1,//,5X,'COMPRESSION ELEMENT STRESSES :',/)
430 FORMAT(//,5X,'STRESS AT THE TOP OF PORTION OF THE COMPRESSION ELEM
   2ENT BOUNDED BY N. A.   (P E I )=',F12.5,///)
440 FORMAT(5X,'AREAS OF THE ELEMENTS IN COMPRESSION :',/)
450 FORMAT(//,5X,'AREA OF THE PORTION OF COMPRESSION ELEMENT BOUNDED B
   2Y N. A.   (SQ. INS.) =',F12.5,///)
460 FORMAT(    4X,'NUMBER OF STIRRUPS(NOS.  LEGS ON ONE SIDE) INTERCE
   2PTED=',F10.5/5X,'AVERAGE STRAIN IN HORIZON. LEGS OF STIRRUPS
   3      :',F10.5/5X,'AVERAGE STRESS IN HORIZON. LEGS OF STIRRUPS
   4      :',F10.5///)
480 FORMAT(5X,'BENDING MOMENTS (IN.KIPS.) ON INCLINED (BETA) PLANE :'/
   2)
490 FORMAT(5X,'DUE TO CONCRETE COMPRESSION ZONE :',F10.4)
491 FORMAT(5X,'                                 TENSION ZONE :',F10.4)
500 FORMAT(5X,'                 PRESTRESSING STEEL :',F10.4)
510 FORMAT(5X,'       STIRRUPS (HORIZONTAL LEGS) :',F10.4)
520 FORMAT(5X,'         STIRRUPS (VERTICAL LEGS) :',F10.4//)
530 FORMAT(5X,'TOTAL BENDING MOMENT ON BETA PLANE :',F10.4//)
540 FORMAT(5X,'TOTAL TORQUE (IN.KIPS) ON BETA PLANE :',F10.4//)
550 FORMAT(5X,'TORQUE TAKEN BY STIRRUPS (VERT. LEGS) :',F10.4//)
570 FORMAT(5X,'SHEAR FORCE (KIPS) IN COMPR. ZONE :',F10.4//)
580 FORMAT(5X,'SHEAR STRESS (PSI) IN COMPR. ZONE :',F10.4//)
590 FORMAT(5X,'NORMAL STRESS (PSI) IN COMPRESSION ZONE :',F10.4//)
591 FORMAT(5X,'NUMBER OF ITERATIONS FOR N.A. POSITIO :',I3//)
592 FORMAT(5X,'MAXIMUM (TENSILE) PRINCIPAL STRAIN IN THE COMPRESSION Z
   2ONE :',F12.8//)
593 FORMAT(5X,'MINIMUM (COMPRESSIVE) PRINCIPAL STRAIN IN THE COMPRESS
   2ION ZONE :',F12.8//)
594 FORMAT(5X,'ERROR IN STRESS INTERACTION EQUATION :',F12.8//)
595 FORMAT(5X,'MAXIMUM (TENSILE) PRINCIPAL STRESS IN THE COMPRESSION Z
   2ONE :',F12.8//)
596 FORMAT(5X,'MINIMUM (COMPRESSIVE) PRINCIPAL STRESS IN THE COMPRESS
   2ION ZONE :',F12.8//)
600 FORMAT(/5X,'COMBINED CAPACITIES AT ULTIMATE (IN.KIPS AND KIPS):',
   2//5X,'TORSION :',F8.2/5X,'BENDING :',F8.2,/5X,'SHEAR   :',F8.2//)
610 FORMAT(1H1)
    RETURN
    END
```

```
      SUBROUTINE MODULT
C
C     THIS SUBROUTINE SOLVES FOR ULTIMATE CAPACITIES TAKING INTO
C     ACCOUNT TORSIONAL COMPONENT ON THE INCLINED PLANE
C
      IMPLICIT REAL*8(A-H,O-Z)
C
      COMMON AP,AST,B,FY,FSU,TSU,ES,FSTIP,EPSCP,EPSSE,EPSSA,EPSSU,B,H,
     2DH,HW,HL,PC,EPOSP,EPSCH,ECON,FCCH,A,AINC,T,C,ED,EASI,DELTA,
     3DST1,DST2,DST3,DSTH,S,SIGMA,YARM,FPULT,FSTIP
     4,SPACST,FYHOOP,SPHOOP),DS,KK1,TC,ECP,BETA,THETA,TU,TF,
     5EPSCOM,IFSTEM,FCOT,FTEN,EMODM,EMTEN,TCOM,TTEN,A1,A2,A3,A4
     6,ICP,EM,H,SMAVS,SMINS,SPART,SOINT,SMAXB,SMINB,HIL,HIT,HL,HT,HH,HT
     7,ALPAP1,ALPAE2,TMPRB,TMPAS,TMPBT
     8,AS,TS,APTA,TC,X,Y,DEPTH,AXIALL,FSUMC,IWAREA,TMOD,EYIELD,ESH,
     9FULT,FYILD,FULT,TSH,FNIFAC,CRAKM,TWTALP,TCTALP,
     1 TOTALL,CAS,PS,SUMF,SUMFP,SHEFM,COUNT,PHI,REP,ABCCOS,FCYLSH
     2,HCCH,FCOFP,FCOMP,ACCAP,ELPOSC,FCCC,EASIBS,FCEL
     3,THETAP,TWETSH,THETTH
C
      COMMON H,B,NOBE,NSLINE,NSTEEL,NADDED,NSCOMP
C
      DIMENSION AP(10),B(10),FS(10),FSU(10),TSU(10),ES(10),
     1 EPSCE(10),EPSSE(10),EPSSA(10),EPSSU(10),DS(10),FPULT(10)
     2,AS(20),TS(20),APTA(500),TC(500),X(500),Y(500),CELLH(530),EAS(20),
     3 FCEL(500),FS(20),FCILLH(530),ABCCOS(500),ELPOSC(500)
C
      REAL MBETAC,MBETAP,MBETAN,MBETAV,MBETAT
   16 FORMAT(///,5X,'THIRD  MODE - ULTIMATE CAPACITY,STRAINS AND ROTATIO
     2NSUM C=RCH')
   20 FORMAT(5X,'0*****************************************************
     2******'//)
C     CHECK FOR PURE BENDING CASE
      IF(EASI.LT.0.005)THETA=1.570595
      IF(EASI.LT.0.005)GO TO 21
      THETA=THETTH
   21 CONTINUE
      THETAD=THETA*180.00/3.141593
      WRITE(6,16)
      WRITE(6,20)
      WRITE(6,30)THETA,THETAD
   30 FORMAT(5X,'INCLINATION OF INITIAL CRACK: THETA(RAD.) =',F8.4,/
     2 5X,'  THETA(DEG.)  =',F8.4//)
      ITZERA=0
C     ASSUME COMPRESSION STRAIN IN BETA PLANE AND ITS INCREMENT
      EPSCAS=0.004
      EPSINC=0.0002
      GO TO 32
   31 EPSCAS=0.0062
      EPSINC=0.00001
   32 CONTINUE
   40 EPSCAS=EPSCAS-EPSINC
C     CHECK THAT ASSUMED STRAIN IS NOT ZERO
      IF(EPSCAS.GT.(-0.00001).AND.EPSCAS.LT.0.00301)GO TO 31
C     ASSUME DEPTH OF NEUTRAL AXIS AND ITS INCREMENT
      AINC=H/HELFHS
C     ITERATION FOR POSITION OF NEUTRAL AXIS STARTS
      N=0
      A=AINC
   50 A=A+AINC
C     FIND INCLINATION OF COMPRESSION ZONE, BETA
      TARGET=B/(B+2.0*(H-A))*DTAN(THETA)
      BETA=DATAN(TARGET)
C     CALCULATE CURVATURE
      HELFHS=A/HELFHS
      PHI=EPSCAS/(A-HELFA/2.00)
C     PRESTRESSING STEEL STRAINS
      DO 60 I=1,N
   60 EPSSA(I)=(P(I)-A)*PHI*DSIN(BETA)
C     TOTAL STRAINS IN STEEL IN LONGITUDINAL DIRECTION
      DO 70 I=1,N
   70 EPSSU(I)=EPSSE(I)-EPSCE(I)+EPSSA(I)
C     CALCULATE STRESSES AND FORCES IN PRESTRESSING STRANDS FROM STRESS-
C     STRAIN DIAGRAMS
      IF(MODP.EQ.1)CALL STP302
      IF(MODP.EQ.2)CALL STR308
      IF(MODP.EQ.3)CALL STRAAB
      IF(MODE.EQ.4)CALL STRAKH
C     TENSILE FORCE OF PRESTRESSING STEEL IN ORIGINAL DIRECTION
      TS=0.00
      DO 90 I=1,N
   90 TS=TS+TSU(I)
C     TOTAL TENSILE FORCE IN PRESTRESSING STEEL PERP. TO BETA PLANE
      TS=TS*DSIN(BETA)
C     TENSILE FORCE IN CONCRETE
      EPSCH=EMODM/ECON
      ECH=EPSCH/PHI
      IF(ECH.GT.(H-A))ECH=H-A
      TC=EMODM*ECH/2.00*B/DSIN(BETA)/1000.00
C     CONTRIBUTION OF TRANSVERSE STEEL (STIRRUPS - HORIZONTAL LEGS ONLY)
      EPSTOT=PHI*(DST1-A)
      EPSTOP=PHI*(DST2-A)
C     STRAIN IN THE DIRECTION OF TRANSVERSE STEEL
      EPSTOP=EPSTOP*DCOS(BETA)
      EPSBOT=EPSBOT*DCOS(BETA)
C     STRESSES IN THE DIRECTION OF TRANSVERSE STEEL
      FTOP=EPSTOP*ESTIR
      FBOT=EPSBOT*ESTIR
C     CHECK WHETHER STRESSES EXCEED FY
      IF(FTOP.GT.FYSTIR)FTOP=FYSTIR
      IF(FTOP.LT.(-FYSTIR))FTOP=-FYSTIR
      IF(FBOT.GT.FYSTIR)FBOT=FYSTIR
      IF(FBOT.LT.(-FYSTIR))FBOT=-FYSTIR
C     FORCES IN STIRRUPS
      TTOP=FTOP*AST
      TBOT=FBOT*AST
C     NO. OF STIRRUPS INTERCEPTED BY BETA  AND THETA PLANE
      A3=DETI
      A4=B-DETB
      NSTOP=(A3-A4)/DTAN(THETA)/S
```

```
      XMOMT=(B-A1-A4)/STAN(BETA)/6.
C     TOTAL FORCE IN STIRRUPS (BOTTOM AND TOP)
      TTOP=TTOP+XMTOP
      TBOT=TBOT+XMBOT
C     NEGLECT CONTRIBUTION OF STIRRUPS IN COMPRESSION
      TBOT=0.00
C     TOTAL FORCE IN STIRRUPS PERP. TO BETA PLANE
      TSTIR=(TTOP+TBOT)*DCOS(BETA)

C     TOTAL TENSILE FORCE IN X-SECTION PERP. TO BETA PLANE (KIPS)
      T=TS+TC+TSTIR

C     COMPRESSIVE FORCE IN CONCRETE (KIPS)

      CALL CFORCE

C     ERROR IN SUM OF HORIZONTAL FORCES (IN PERCENTAGES)

      ER=T-C

C     NUMBER OF ITERATIONS

      N=N+1
      RELFR=R/RILER
      IF(N.GT.100)RETURN
      IF(DABS(AA).LE.0.05)GO TO 110
      IF(AA.GT.0.00)GO TO 50
      A=A-AINC
      AINC=AINC/10.00
      GO TO 50
  110 CONTINUE
      BETA1=BETA*180.00/3.14159
C     TORSION TO BENDING RATIO ON THE INCLINED (BETA) PLANE
      RATIOT=(RESI*STAN(BETA)+1.00)/(RESI-STAN(BETA))

C     CALCULATE BENDING MOMENT ON THE INCLINED (BETA) PLANE
C     MOMENTS ARE TAKEN ABOUT H. A.

C     CONCRETE COMPRESSION ZONE CONTRIBUTION
      RBETAC=0.00
      IF(NICOMP.LT.3)GO TO 121
      DO 120 I=1,NICOMP
  120 RBETAC=RBETAC+FCEL(I)*ELFORC(I)
  121 IF(NICOMP.LT.3)RBETAC=0.00
      RBETAC=RBETAC+FCCC*2.00/3.00*HCON
      RBETAC=RBETAC/1000.00
C     PRESTRESSING STEEL CONTRIBUTION
      RBTAP=0.00
      DO 130 I=1,N
  130 RBETAP=RBETAP+TSD(I)*DSIN(BETA)*(D(I)-A)
C     CONCRETE TENSION ZONE CONTRIBUTION
      CWORTE=TC*2.00/3.00*HCB
C     NEGLECT CONTRIBUTION OF TENSION ZONE
      CWORTE=0.00
C     STIRRUP CONTRIBUTION - HORIZONTAL LEGS
      RBETAH=(TTOP*DABS(A-DST2)+TBOT*DABS(A-DST1))
C     STIRRUP CONTRIBUTION - VERTICAL LEGS
C     NUMBER OF STIRRUPS INTERCEPTED
      XNUMBS=(DST2-A)/DTAN(THETA)/S
C     AVERAGE STRESS IN VERTICAL STIRRUPS
      FSAVV=PHI*(DST2-A)/2.00*DSIN(BETA)
C     AVERAGE STRESS IN VERTICAL LEGS
      AVFPT=FSAVV*ESTIR
      IF(SAFPT.GT.FYSTIR)SVERT=FYSTIR
C     TOTAL FORCE IN VERTICAL STIRRUPS
      FVERT=SVERT*ASI*XNUMBT
C     FLEXURAL AND TORSIONAL MOMENT ON BETA PLANE DUE TO VERT. STIRRUPS
      XMOMT=FVFPT*(F-A1-A4)
      RBETAV=RBCHVE*COS(PITA)
      TBLTAV=RBCVVE*DSIN(BETA)
C     TOTAL FLEXURAL MOMENT ON INCLINED PLANE
      RBETAT=RBETAC+RBETAP+RBETAH+RBETAV+CWORTE
C     TOTAL TORQUE ON INCLINED PLANE
      TBETAT=(RATIOT)*RBETAT
C     TORQUE TAKEN BY COMPRESSION ZONE AND DOWEL FORCES IN BOTTOM LAYER
C     OF LONGITUDINAL STEEL
C     TORQUE TAKEN BY COMPONENTS OF LONGITUDINAL STEEL AND DOWEL FORCES
      TBETAC=TBETAT-TBETAB
      TLONG=0.00
      DO 135 I=1,N
  135 TLONG=TLONG+TSN(I)*(F(I)-D(1))*DCOS(BETA)
C     SHEAR FORCE (KIPS) IN COMPRESSION ZONE
      VBETAC=(TBETAT+TLONG)/(H-D(1)-A/2.00)
C     CHECK FOR THE CASE OF HOLLOW X-SECTION (N.A. BELOW FLANGE DEPTH)
      TS2=TS/2.00
      IF(FA.GT.1.00.AND.TF.LT.A)VBETAC=(TBETAT+TLONG)/(H-D(1)-TF/2.00)
      VBETAC=DABS(VBETAC)
C     SHEAR STRESSES IN COMPRESSION ZONE (PSI)
      TAUC=VBETAC/(A*B/DSIN(BETA))
C     CHECK FOR THE CASE OF HOLLOW X-SECTION (N.A. BELOW FLANGE DEPTH)
      IF(FA.GT.1.00.AND.TF.LT.A)TAUC=VBETAC/(TF*B/DSIN(BETA)+
     2(A-TF)*TW/DSIN(BETA))
C     SHEAR STRESS IN COMPRESSION ZONE (PSI)
      TAUC=TAUC*1000.00
C     COMPUTE CAPACITIES AT ULTIMATE
      TORQUE=RBETAT/(DCOS(PITA)-DSIN(BETA)/RESI)
      RPOR=ICOMP/XNSI
      SNEAP=RNCH/EFMOD1
      ITERNA=ITERNA+1
      IF(ITERNA.GT.45)RETURN
C     SPECIFIED CONSTANTS
C
C     POISSON'S RATIO
      PR=0.16
C     MODULUS OF ELASTICITY AS PER A.C.I. CODE
      ELNOD=57000.00*SQRT(FC)
C     SHEAR MODULUS
      G=ELMOD/(2.00*(1.00+PR))
C     SHEAR STRAIN
      GAMAY=TAUC/G
C     MAXIMUM COMPRESSIVE STRAIN
```

```
      EPSCPP=0.0034
C     MAXIMUM TENSILE STRAIN
      EPSTPP=0.0001
C     SPECIFIED **VPP IN STRAIN INTERACTION EQUATION (TENSILE STRAIN)
      SPECXP=0.65*FC
      IF(NICONF.LT.1)GO TO 105
      COEFEL=ALLEN(NICONF)/2.00
  105 IF(NICONF.LT.1)COEFEL=XCONF/2.00
      COEFSA=SAFAIL/2.00
      RADEPS=0.5*SQRT(COEFEL**2+COEFSA**2)
      EPSC=COEFEL+RADEPS
      EPST=ABS(COEFEL-RADEPS)
      EPSCY=(EPSCPP*(1.00-(EPST/EPSTPP)**2)
      EPSA=EPSCPP-EPSC
      IF(ABS(EPSA).LT.EPSCER)GO TO 133
      IF(EPSA.LT.0.66)GO TO 40
      EPSCAS=EPSCAS+EPSINC
      EPSINC=EPSINC/10.00
      GO TO 46
  133 CONTINUE
C     CALCULATE PRINCIPAL STRESSES
C     CONFINED STRESS
      FCPP=0.85*FC
      EC=1800000.00*500.00*FCPP
      EO=2.00*FCPP/EC
      EN=6.0034
      IF(EPSC.GE.0.06.AND.EPSC.LT.EO)STRESC=(2.00*EPSC/EO-(EPSC/EO)**2)*
     1FCPP
      IF(EPSC.GT.EO)STRESC=FCPP-0.15*FCPP/(EU-EO)*(EPSC-EO)
C     TENSILE STRESS
      FT1=2.00/SQRT(1.0000)*XMODB
      IF(EPST.GE.0.00.AND.EPST.LT.0.0001)STREST=FT1/0.0001*EPST
      IF(EPST.GE.0.0001)STREST=FT1
C
C     WRITE INCLINATION OF COMPRESSION ZONE W.R.T. LONGITUDINAL AXIS
      WRITE(6,100)BETA,BETA1
C     WRITE INCREASE IN STRAINS IN PRESTRESSING STEEL BETWEEN INITIAL
C     AND ULTIMATE LOAD
      WRITE(6,200)
      WRITE(6,220)(I,EPSSA(I),I=1,N)
C     WRITE ULTIMATE STRAIN IN PRESTRESSING STEEL
      WRITE(6,230)
      WRITE(6,220)(I,EPSSU(I),I=1,N)
C     WRITE NO. OF ITERATIONS REQUIRED (CURVATURE)
      WRITE(6,240)N
C     WRITE THE DEPTH OF COMPRESSIVE BLOCK (N.A. LOCATION)
      WRITE(6,250)A
C     WRITE CURVATURE
      WRITE(6,260)PHI
C     WRITE STRESSES IN STEEL
      WRITE(6,270)
      WRITE(6,220)(I,FSS(I),I=1,N)
C     WRITE FORCES IN PRESTRESSING STEEL
      WRITE(6,280)
      WRITE(6,220)(I,TSS(I),I=1,N)
C     WRITE STRAINS IN TRANSVERSE STEEL
      WRITE(6,290)
      WRITE(6,300)EPSCCP,EPSSOT
C     WRITE STRESSES IN TRANSVERSE STEEL
      WRITE(6,310)FTCP,FSOT
C     WRITE NO. OF STIRRUPS INTERCEPTED
      WRITE(6,320)NTOP,NBOT
C     WRITE EQUILIBRIUM CHECK (TOTAL TENSILE AND COMPRESSIVE FORCE)
      WRITE(6,330)
      WRITE(6,340)T
      WRITE(6,350)C
      WRITE(6,360)TB
C     WRITE INCLINATION TO BENDING AXIS ON THE INCLINED (BETA) PLANE
      WRITE(6,361)XBEND
C     WRITE NUMBER OF THE ELEMENTS IN COMPRESSION
      WRITE(6,370)NECOMP
C     WRITE STRAINS IN THE CENTROIDS OF THE COMPRESSION ELEMENTS
      IF(NICONF.LT.1)GO TO 399
      WRITE(6,380)
      WRITE(6,220)(I,ECELE(I),I=1,NECOMP)
  399 CONTINUE
C     WRITE STRAIN AT THE TOP OF THE PORTION OF ELEMENT BOUNDED BY N. A.
      WRITE(6,410)ICOMP
C     WRITE ELEMENT STRESSES
      IF(NICONF.LT.1)GO TO 421
      WRITE(6,420)
      WRITE(6,220)(I,FCELE(I),I=1,NECOMP)
  421 CONTINUE
C     WRITE STRESS IN THE PORTION OF THE ELEMENT BOUNDED BY N.A.
      WRITE(6,430)FCCOMP
C     WRITE AREAS OF THE COMPRESSION ELEMENTS
      IF(NICONF.LT.1)GO TO 441
      WRITE(6,440)
      WRITE(6,220)(I,ABCCON(I),I=1,NECOMP)
  441 CONTINUE
C     WRITE AREA OF THE PORTION OF THE COMPRESSION ELEM. BOUNDED BY N.A.
      WRITE(6,450)ACOMP
      WRITE(6,451)EVERST,EPSAVV,EVERT
      WRITE(6,460)
      WRITE(6,470)*PPTAC
      WRITE(6,471)CMONTE
      WRITE(6,500)MBETAP
      WRITE(6,510)MPPTAP
      WRITE(6,520)MPETAP
      WRITE(6,530)MBETAT
      WRITE(6,540)TBETAT
      WRITE(6,542)TPPTAT
      WRITE(6,560)TPETAC
      WRITE(6,570)TBETAC
      WRITE(6,580)TACC
      IF(NICONF.LT.1)GO TO 443
      WRITE(6,590)FCELE(NECOMP)
  443 CONTINUE
      WRITE(6,591)ITERBA
      WRITE(6,592)NIBEST
```

```
      WRITE(6,595)BPSF
      WRITE(6,596)STRFSC
      WRITE(6,597)STRSC
      WRITE(6,598)FPSA
      WRITE(6,70)TOPSUB,PHSB,SHEAB
      WRITE(6,612)
      WRITE(6,619)
200 FORMAT(//,5X,'INCLINATION OF COMPRESSION ZONE:',5X'BETA(RAD) =',F6
     2.3,/5X,'BETA(DEG) =',F6.3,//)
210 FORMAT(5X,'INCREASE IN STRAIN IN STEEL BETWEEN INITIAL AND ULTIMAT
     2E LOADS',/)
220 FORMAT(4('5X,I3,4X,F12.6,3CX,I3,4X,F12.4,/) )
230 FORMAT(5X,'ULTIMATE STRAIN IN STEEL (IN PERCENT) =',/)
240 FORMAT(5X,'NUMBER OF ITERATIONS REQD. FOR CURVATURE =',I3//)
250 FORMAT(5X,'NEUTRAL AXIS LOCATION (IN INCHES, FROM THE TOP)=',
     2F12.4///)
260 FORMAT(5X,'CURVATURE (RADIANS/IN), PHI=',F10.7,///)
270 FORMAT(5X,'STRESSES IN PRESTRESSING STRANDS AT ULTIMATE (KSI) =')
280 FORMAT(5X,'FORCES IN PRESTRESSING STRANDS AT ULTIMATE(KIPS) =')
290 FORMAT(    //,5X,'STRAINS AND STRESSES IN HORIZONTAL LEGS OF STIRR
     2UPS AT ULTIMATE :')
300 FORMAT(5X,'STRAIN IN TOP    LEG =',F10.6,/5X,'STRAIN IN BOTTOM LEG
     2 =',F10.6,//)
310 FORMAT(5X,'STRESS IN TOP    LEG =',F10.2,/5X,'STRESS IN BOTTOM LEG
     2 =',F10.2,//)
320 FORMAT(5X,'NO. OF STIRRUPS INTERCEPTED :',/5X'AT THE TOP    =',
     2F5.2,/5X,'AT THE BOTTOM =',F5.2,//)
330 FORMAT(5X,'EQUILIBRIUM CHECKS')
340 FORMAT(5X,'TENSILE FORCE (KIPS),      T =',F10.5)
350 FORMAT(5X,'COMPRESSIVE FORCE (KIPS), C =',F10.5,/)
360 FORMAT(5X,'ERROR IN PERCENTAGE (T-C)/T*100 =',F10.5,///)
361 FORMAT(5X,'TORSION TO BENDING RATIO ON THE INCLINED (BETA) PLANE ,
     2 BETA =',F10.5,///)
370 FORMAT(5X,'NUMBER OF THE ELEMENTS IN COMPRESSION =',I3,///)
380 FORMAT(5X,'STRAINS IN THE CENTROIDS OF COMPRESSION ELEMENTS :',/)
410 FORMAT(5X,'STRAIN AT THE TOP OF THE PORTION OF ELEMENT BOUNDED BY
     2N.A. =',F12.6,///)
420 FORMAT(//,5X,'COMPRESSION ELEMENT STRESSES :',/)
430 FORMAT(//,5X,'STRESS AT THE TOP OF PORTION OF THE COMPRESSION ELEM
     2ENT BOUNDED BY N. A.   (P S I )=',F12.5,///)
440 FORMAT(5X,'AREAS OF THE ELEMENTS IN COMPRESSION :',/)
450 FORMAT(//,5X,'AREA OF THE PORTION OF COMPRESSION ELEMENT BOUNDED B
     2Y N. A.   (SQ. INS.) =',F12.5,///)
471 FORMAT(    4X,'NUMBER OF STIRRUPS(VERT. LEGS OR ONE SIDE) INTERCE
     2PTED',F10.5/5X,'AVERAGE STRAIN IN VERTICAL LEGS OF STIRRUPS
     3       :',F10.5/5X,'AVERAGE STRESS IN VERTICAL LEGS OF STIRRUPS
     4       :',F10.5///)
480 FORMAT(5X,'BENDING MOMENTS (IN.KIPS.) ON INCLINED (BETA) PLANE :'/
     2)
490 FORMAT(5X,'DUE TO CONCRETE COMPRESSION ZONE :',F10.4)
491 FORMAT(5X,'                                 TENSION ZONE :',F10.4)
502 FORMAT(5X,'                    PRESTRESSING STEEL :',F10.4)
510 FORMAT(5X,'          STIRRUPS (HORIZONTAL LEGS) :',F10.4)
520 FORMAT(5X,'                   STIRRUPS (VERTICAL LEGS) :',F10.4//)
530 FORMAT(5X,'TOTAL BENDING MOMENT ON BETA PLANE :',F10.4//)
540 FORMAT(5X,'TOTAL TORQUE (IN.KIPS) ON BETA PLANE :',F10.4//)
550 FORMAT(5X,'TORQUE TAKEN BY STIRRUPS (VERT. LEGS) :',F10.4//)
560 FORMAT(5X,'TORQUE TAKEN BY CONCR. COMPR. ZONE AND DOWELS :',F10.4/
     2/)
570 FORMAT(5X,'SHEAR FORCE (KIPS) IN COMPR. ZONE :',F10.4//)
580 FORMAT(5X,'SHEAR STRESS (PSI) IN COMPR. ZONE :',F10.4//)
590 FORMAT(5X,'NORMAL STRESS (PSI) IN COMPRESSION ZONE :',F10.4//)
591 FORMAT(5X,'NUMBER OF ITERATIONS FOR N.A. POSITIO :',I3//)
592 FORMAT(5X,'MAXIMUM (TENSILE) PRINCIPAL STRESS (PSI) ON BETA PLANE
     2 :',F10.2//)
593 FORMAT(5X,'MINIMUM (COMPRESSIVE) PRINCIPAL STRESS (PSI) ON BETA PL
     2ANE :',F10.2//)
594 FORMAT(5X,'ERROR IN STRESS INTERACTION EQUATION :',F10.4//)
595 FORMAT(5X,'MAXIMUM (TENSILE) PRINCIPAL STRAIN (IN/IN) ON BETA PLAN
     2E :',F12.9//)
596 FORMAT(5X,'MINIMUM (COMPRESSIVE) PRINCIPAL STRAIN (IN/IN) ON BETA
     2PLANE :',F12.9//)
620 FORMAT(1/'5X,'CORRESPONDING CAPACITIES AT ULTIMATE (IN.KIPS AND KIPS):',
     2/5X,'TORSION :',F9.2/5X,'BENDING :',F9.2,/5X,'SHEAR   :',F9.2//)
612 FORMAT(1H1)
      RETURN
      END
```

```
**************************
*   B E A M - A B - 6    *
**************************


INPUT VARIABLES
***************


MEAN DIMENSIONS
OUTSIDE:                    HOLLOW:
WIDTH (IN.)  =    8.00        0.00
HEIGHT (IN.) =   17.00        0.00
LENGTH (IN.) = 100.00

NO. OF PRESTRESSING STRANDS PROVIDED (N) , AND THEIR SIZE (4000#)
N    =          6
4000 =          3

AREAS OF PRESTRESSING STRANDS (SQ.IN.)=
   0.1440   0.1440   0.0000   0.0000   0.1440   0.1440

AREA OF TRANSVERSE STEEL - ONE LEG (SQ.IN.)=    0.0300

PRESTRESSING STEEL LOCATIONS (DISTANCES FROM THE BOTTOM IN INCHES) =
      1.00     1.00     4.00     6.00    11.00    11.00

PRESTRESSING STEEL LOCATIONS (DISTANCES FROM THE SIDE IN INCHES) =
      5.00     1.00     4.00     3.00     5.00     1.00

STIRRUP LOCATION IN CROSS-SECTION:
VERT.     0.6250   11.3750
HORIZ.    0.6250    6.3750

STIRRUP SPACING (IN.). S=      3.00

EFFECTIVE PRESTRESSING FORCES (KIPS) =
     19.86    19.92    11.86    11.48    19.86    19.48

MODULI OF ELASTICITY OF PRESTRESSING STEEL (KSI)=
  27500.00  27500.00  29000.00  29000.00  27500.00  27500.00

MODULI OF ELASTICITY OF MILD STEEL =
  29520.00

ULTIMATE STRESSES OF PRESTRESSING STEEL =
   270.300   270.300   275.625   275.625   270.300   270.300

ULTIMATE STRESS OF MILD STEEL =
    67.337

CONCRETE COMPRESSIVE STRENGTH (PSI)=
FC=   5820.00

MODULUS OF RUPTURE (PSI)=
RMODR=    649.00

CONCRETE ULTIMATE COMPRESSIVE STRAIN =
EPSCU =  -0.003300

COEFFICIENT OF DEPTH OF NEUTRAL AXIS ( A C I FORMULA)   K1 = 0.70

TORSION TO BENDING RATIO , T/M     =     1.000

TORSION TO SHEAR RATIO (=T/(IP*V)) =     9.7500

LOCATION OF FAILURE SURFACE (IN.) FROM LEFT SUPPORT =
DFMOD1 =     20.0
DFMOD2 =     20.0
DFMOD3 =     20.0

INITIAL ECCENTRICITY (IN.), ECCN  =    0.0215

AVERAGE PRESTRESS (PSI) P/A       = 1421.0000

INITIAL STRAIN IN PRESTRESSING STEEL =
  0.005315  0.005330  0.005130  0.004931  0.005315  0.004919

INITIAL STRAINS IN CONCRETE (TOP, STEEL LEVELS AND BOTTOM)=
 -0.
 -0.  -0.  -0.  -0.  -0.  -0.
 -0.
```

CHECKING STRENGTH
oooooooooooooooo

	TORQUE CENT	FR,(KIPS)	[illegible]	TOR STIF	YIELD,MOM.	SHEAR,MAX	SHEAR,MIN	TWIST,ANGLE(RAD)	CHECK	NO,YIELD
BOTTOM	144.22163	0.42333	[illegible]	3.27188	144.63618	0.44658	-0.02178	35.78803	-0.00250	18
SIDE 1	118.50644	0.44574	24.11196	1.54532	114.04979	0.44965	-1.87168	28.11196	-0.00302	22
TOP 1	252.27479	0.31968	14.31536	5.41294	237.00784	0.30322	-3.31692	14.31536	-0.00000	32

SECOND MODE - ULTIMATE CAPACITY,STRAINS AND EQUILIBRIUM CHECK
oooooooooooooooooooooooooooooooooooooooooooooooooooooooooooooo

INCLINATION OF INITIAL CRACK: THETA(RAD.) = 0.4887
THETA(DEG.) = 28.1180

INCLINATION OF COMPRESSION ZONE: BETA(RAD) = 0.27
BETA(DEG) = 15.37

INCREASE IN STRAIN IN STEEL BETWEEN INITIAL AND ULTIMATE LOADS

1	0.300298	2	-0.000022
3	0.000196	4	0.000651
5	0.000284	6	-0.000022

ULTIMATE STRAIN IN STEEL (IN PERCENT) :

1	0.[illegible]637	2	0.005333
3	0.[illegible]447	4	0.004383
5	0.004681	6	0.005210

NUMBER OF ITERATIONS NEED. FOR CURVATURE = 16

NEUTRAL AXIS LOCATION (IN INCHES.FROM THE SIDE).A= 1.388888

CURVATURE (RADIANS/IN). PHI= 0.0002730

STRESSES IN PRESTRESSING STRANDS AT ULTIMATE (KSI) :

1	154.196643	2	146.650667
3	163.164675	4	153.252969
5	154.838283	6	143.648632

FORCES IN PRESTRESSING STRANDS AT ULTIMATE(KIPS) :

1	22.734794	2	21.118263
3	13.054758	4	12.260290
5	22.161981	6	20.650481

STRAINS AND STRESSES IN VERTICAL LEGS OF STIRRUPS AT ULTIMATE :

STRAIN IN COMP. LEG = -0.000178
STRAIN IN TENSN. LEG = 0.031973

STRESS IN COMP. LEG = -0.36
STRESS IN TENSN. LEG = 31.00

NO. OF STIRRUPS INTERCEPTED :
AT THE C. SIDE=11.17
AT THE T. SIDE= 6.27

EQUILIBRIUM CHECK:
TENSILE FORCE (KIPS). T = 63.27871
COMPRESSIVE FORCE (KIPS). C = 63.29184

ERROR IN PERCENTAGE (T-C)/T*100 = -0.03434

TORSION TO BENDING RATIO ON THE INCLINED (BETA) PLANE . KBIBETA = 0.37[illegible]

NUMBER OF THE ELEMENTS IN COMPRESSION = 6

STRAINS IN THE CENTROIDS OF COMPRESSION ELEMENTS :

1	0.000058	2	0.000189
3	0.000184	4	0.000218
5	0.000273	6	0.000328

DISTANCES FROM N.A. TO CENTROIDS OF THE COMPRESSION ELEMENTS :

1	0.200000	2	0.600000
3	0.600000	4	0.000000
5	1.200000	6	1.200000

HEIGHT OF THE PORTION OF ELEMENT IN COMPRESSION ROUNDED BY N.A.(INCHES) = 0.10000

STRAIN AT THE TOP OF THE PORTION OF ELEMENT BOUNDED BY N.A. = 0.000007

COMPRESSION ELEMENT STRESSES :

1	235.296494	2	665.049218
3	949.214645	4	997.913794
5	1181.199757	6	1329.742895

STRESS AT THE TOP OF PORTION OF THE COMPRESSION ELEMENT BOUNDED BY N. A. (P S I)= 110.34170

AREAS OF THE ELEMENTS IN COMPRESSION :

1	0.044770	2	0.044770
3	0.044770	4	0.044770
5	0.044770	6	0.044770

AREA OF THE PORTION OF COMPRESSION ELEMENT BOUNDED BY N. A. (SQ. INS.) = 0.02700

NUMBER OF STIRRUPS(NO. LEGS ON ONE SIDE) INTERCEPTED : 3.37535
AVERAGE STRAIN IN HORIZON. LEGS OF STIRRUPS : 0.00004
AVERAGE STRESS IN HORIZON. LEGS OF STIRRUPS : 10.03230

BENDING MOMENTS (IN.KIPS.) ON INCLINED (BETA) PLANE :

DUE TO CONCRETE COMPRESSION ZONE : 27.0447
TENSION ZONE : 5.8388
PRESTRESSING STEEL : 91.0100
STIRRUPS (HORIZONTAL LEGS) : 19.4787
STIRRUPS (VERTICAL LEGS) : 48.4021

TOTAL BENDING MOMENT ON BETA PLANE : 148.7044

TOTAL TORQUE (IN.KIPS) ON BETA PLANE : 48.8838

TORSUC TAKEN BY STIRRUPS (VERT. LEGS) : 5.3838

SHEAR FORCE (KIPS) IN COMPR. ZONE : 97.4041

SHEAR STRESS (PSI) IN COMPR. ZONE : 976.9837

NORMAL STRESS (PSI) IN COMPRESSION ZONE : 1329.7039

NUMBER OF ITERATIONS FOR N.A. POSITION : 23

MAXIMUM (TENSILE) PRINCIPAL STRAIN IN THE COMPRESSION ZONE : 0.00014017

MAXIMUM (TENSILE) PRINCIPAL STRESS IN THE COMPRESSION ZONE : 541.5944

MINIMUM (COMPRESSIVE) PRINCIPAL STRAIN IN THE COMPRESSION ZONE : 0.00046777

MINIMUM (COMPRESSIVE) PRINCIPAL STRESS IN THE COMPRESSION ZONE : 1436.4798

ERROR IN STRESS INTERACTION EQUATION : 0.00009829

COMBINED CAPACITIES AT ULTIMATE (IN.KIPS AND KIPS) :

TORSION : 102.78
BENDING : 130.77
SHEAR : 4.00

```
**************************
*   B E A M  NO. - 20    *
**************************


INPUT VARIABLES
***************


BEAM DIMENSIONS
OUTSIDE                          HOLLOW
WIDTH (IN.)  =    8.50           0.00
HEIGHT (IN.) =   12.00           0.00
LENGTH (IN.) = 100.00

NO. OF PRESTRESSING STRANDS PROVIDED (N) , AND THEIR SIZE (NOSE)
N    =         4
NOSE =         8

AREAS OF PRESTRESSING STRANDS (SQ.IN.)
   0.0480   0.0480   0.0480   0.0480

AREA OF TRANSVERSE STEEL - ONE LEG (SQ.IN.)    0.1180

PRESTRESSING STEEL LOCATIONS (DISTANCES FROM THE BOTTOM IN INCHES)
      1.50     1.50    10.50    10.50

PRESTRESSING STEEL LOCATIONS (DISTANCES FROM THE SIDE IN INCHES)
      4.00     1.50     6.50     1.50

STIRRUP LOCATION IN CROSS-SECTION)
VERT.     1.1250   10.8750
HORIZ.    1.1250    6.8750

STIRRUP SPACING (IN.). S=      3.37

EFFECTIVE PRESTRESSING FORCES (KIPS)
     13.18    13.59     9.13     9.09

MODULI OF ELASTICITY OF PRESTRESSING STEEL (KSI)
  28000.00  28000.00  28500.00  28000.00

MODULI OF ELASTICITY OF MILD STEEL
  29000.00

ULTIMATE STRESSES OF PRESTRESSING STEEL
   270.025   270.025   270.025   270.025

ULTIMATE STRESS OF MILD STEEL
    60.000

CONCRETE COMPRESSIVE STRENGTH (PSI)
FC=   5000.00

MODULUS OF RUPTURE (PSI)
SMCRU=   600.00

CONCRETE ULTIMATE COMPRESSIVE STRAIN
EPSCU =  -0.00300

COEFFICIENT OF DEPTH OF NEUTRAL AXIS ( A C I FORMULA)   K1 = 0.70

TORSION TO BENDING RATIO , T/M     =     0.110

TORSION TO SHEAR RATIO (T*S/(2*V)) =     1.9630

LOCATION OF FAILURE SURFACE (IN.) FROM LEFT SUPPORT
DFWRD1 =    87.0
DFWRD2 =    87.0
DFWRD3 =    87.0

INITIAL ECCENTRICITY (IN.), ECCN  =    0.7648

AVERAGE PRESTRESS (PSI) P/A       =  457.0125

INITIAL STRAIN IN PRESTRESSING STEEL
  0.002075  0.002446  0.002054  0.002032

INITIAL STRAINS IN CONCRETE (TOP, STEEL LEVELS AND BOTTOM)
 -0.000707
 -0.002210 -0.002569 -0.003077 -0.003077
 -0.002192
```

CRACKING STRENGTH
****

	TOPCON CONC	TP.(KSI)	TM.(DEG)	TMO STIN	TOT.TORQ.	SHEAR(KIPS)	SHEAR(KIPS)	THETA(DEG)	CRACK	NP.ITER
BOTTOM	20.24574	1.45177	79.67796	0.78477	20.67614	6.71157	-0.03178	-10.16795	-0.05334	11
SIDE 1	93.42148	0.61789	35.40253	7.59700	101.01917	0.46731	-0.42513	35.40253	-0.08200	20
TOP 1	174.27634	0.07770	0.09702	44.73619	219.00853	-0.68098	-0.43928	0.09702	-0.06231	11

FIRST MODE - ULTIMATE CAPACITY,STRAINS AND EQUILIBRIUM CHECK
****

INCLINATION OF INITIAL CRACK: THETA(RAD.) = 1.3938
THETA(DEG.) = 79.8571

INCLINATION OF COMPRESSION ZONE: BETA(RAD) = 1.60
BETA(DEG) = 97.00

INCREASE IN STRAIN IN STEEL BETWEEN INITIAL AND ULTIMATE LOADS

1	0.014287	2	0.010007
3	0.008056	4	0.000000

ULTIMATE STRAIN IN STEEL (IN PERCENT) :

1	0.024082	2	0.020072
3	0.014835	4	0.006000

NUMBER OF ITERATIONS REQD. FOR CURVATURE = 20

NEUTRAL AXIS LOCATION (IN INCHES, FROM THE TOP).= 1.000000

CURVATURE (RADIANS/IN). PHI= 0.0026277

STRESSES IN PRESTRESSING STRANDS AT ULTIMATE (KSI) :

1	204.240356	2	200.140520
3	110.616526	4	110.000520

FORCES IN PRESTRESSING STRANDS AT ULTIMATE(KIPS) :

1	21.300382	2	21.201042
3	9.329168	4	9.209168

STRAINS AND STRESSES IN HORIZONTAL LEGS OF STIRRUPS AT ULTIMATE :

STRAIN IN TOP LEG = -0.000516
STRAIN IN BOTTOM LEG = 0.012996

STRESS IN TOP LEG = -15.32
STRESS IN BOTTOM LEG = 43.33

NO. OF STIRRUPS INTERCEPTED :
AT THE TOP = 1.11
AT THE BOTTOM = 0.31

EQUILIBRIUM CHECK:
TENSILE FORCE (KIPS). T = 52.81967
COMPRESSIVE FORCE (KIPS). C = 51.26034

ERROR IN PERCENTAGE (T-C)/T*100 = 0.95016

TORSION TO BENDING RATIO ON THE INCLINED (DELTA) PLANE . RSIBETA = -0.00019

NUMBER OF THE ELEMENTS IN COMPRESSION = 60

STRAINS IN THE CENTROIDS OF COMPRESSION ELEMENTS :

1	0.000032	2	0.000008
3	0.000158	4	0.000221
5	0.000246	6	0.000268
7	0.000411	8	0.000476
9	0.000537	10	0.000600
11	0.000666	12	0.000727
13	0.000790	14	0.000853
15	0.000910	16	0.000970
17	0.001043	18	0.001108
19	0.001166	20	0.001232
21	0.001298	22	0.001360
23	0.001422	24	0.001484
25	0.001548	26	0.001611
27	0.001674	28	0.001736
29	0.001801	30	0.001864
31	0.001927	32	0.001991
33	0.002054	34	0.002117
35	0.002180	36	0.002243
37	0.002307	38	0.002370
39	0.002433	40	0.002496
41	0.002559	42	0.002623
43	0.002686	44	0.002749
45	0.002812	46	0.002875

97	0.[illegible]	98	0.[illegible]
99	0.[illegible]	50	0.[illegible]
91	0.[illegible]	92	0.[illegible]
93	0.[illegible]	94	0.[illegible]
95	0.[illegible]	96	0.[illegible]
97	0.[illegible]	98	0.[illegible]
99	0.[illegible]	60	0.[illegible]

DISTANCES FROM N.A. TO CENTROIDS OF THE COMPRESSION ELEMENTS :

1	0.012500	2	0.037500
3	0.062500	4	0.087500
5	0.112500	6	0.137500
7	0.162500	8	0.187500
9	0.212500	10	0.237500
11	0.262500	12	0.287500
13	0.312500	14	0.337500
15	0.362500	16	0.387500
17	0.412500	18	0.437500
19	0.462500	20	0.487500
21	0.512500	22	0.537500
23	0.562500	24	0.587500
25	0.612500	26	0.637500
27	0.662500	28	0.687500
29	0.712500	30	0.737500
31	0.762500	32	0.787500
33	0.812500	34	0.837500
35	0.862500	36	0.887500
37	0.912500	38	0.937500
39	0.962500	40	0.987500
41	1.012500	42	1.037500
43	1.062500	44	1.087500
45	1.112500	46	1.137500
47	1.162500	48	1.187500
49	1.212500	50	1.237500
51	1.262500	52	1.287500
53	1.312500	54	1.337500
55	1.362500	56	1.387500
57	1.412500	58	1.437500
59	1.462500	60	1.487500

HEIGHT OF THE PORTION OF ELEMENT IN COMPRESSION BOUNDED BY N. A.(INCHES) =-0.00000

STRAIN AT THE TOP OF THE PORTION OF ELEMENT BOUNDED BY N.A. = -0.000000

COMPRESSION ELEMENT STRESSES :

1	170.324831	2	388.524950
3	629.479250	4	866.990010
5	1099.260635	6	1322.231314
7	1539.860653	8	1748.252652
9	1950.369312	10	2145.852632
11	2332.690612	12	2512.671252
13	2689.682593	14	2850.990514
15	3004.259135	16	3140.126416
17	3303.734358	18	3448.839960
19	3584.979722	20	3698.732104
21	3804.120727	22	3913.284878
23	4011.491673	24	4104.454617
25	4184.871660	26	4247.443344
27	4289.860598	28	4401.291293
29	4457.297197	30	4505.877942
31	4547.212967	32	4581.842712
33	4607.997210	34	4627.384384
35	4639.508713	36	4644.130698
37	4622.439239	38	4591.076779
39	4543.512349	40	4435.949029
41	4304.901498	42	4170.119841
43	4040.852431	44	4021.198281
45	4348.777977	46	4346.259342
47	4339.704913	48	4307.339483
49	4278.888853	50	4250.481824
51	4221.997104	52	4193.472784
53	4165.868135	54	4138.343995
55	4109.879478	56	4079.619046
57	4041.129010	58	4027.048167
59	3944.221757	60	3965.737327

STRESS AT THE TOP OF PORTION OF THE COMPRESSION ELEMENT BOUNDED BY N. A. (F S I)= -0.00000

AREAS OF THE ELEMENTS IN COMPRESSION :

1	0.229376	2	0.230376
3	0.229376	4	0.230376
5	0.229376	6	0.230376
7	0.229376	8	0.230376
9	0.229376	10	0.230376
11	0.229376	12	0.230376
13	0.229376	14	0.230376
15	0.229376	16	0.230376
17	0.229376	18	0.230376
19	0.229376	20	0.230376
21	0.229376	22	0.230376
23	0.229376	24	0.230376
25	0.229376	26	0.230376

27	0.230196	28	0.230196
29	0.230196	30	0.230196
31	0.230196	32	0.230196
33	0.230196	34	0.230196
35	0.230196	36	0.230196
37	0.230196	38	0.230196
39	0.230196	40	0.230196
41	0.230196	42	0.230196
43	0.230196	44	0.230196
45	0.230196	46	0.230196
47	0.230196	48	0.230196
49	0.230196	50	0.230196
51	0.230196	52	0.230196
53	0.230196	54	0.230196
55	0.230196	56	0.230196
57	0.230196	58	0.230196
59	0.230196	60	0.230196

AREA OF THE PORTION OF COMPRESSION ELEMENT BOUNDED BY N. A. (SQ. INS.) = -0.00000

NUMBER OF STIRRUPS(VERT. LEGS ON ONE SIDE) INTERCEPTED: 8.00700
AVERAGE STRAIN IN VERTICAL LEGS OF STIRRUPS : 0.00045
AVERAGE STRESS IN VERTICAL LEGS OF STIRRUPS : 43.33330

BENDING MOMENTS (IN.-KIPS.) ON INCLINED (BETA) PLANE :

DUE TO CONCRETE COMPRESSION ZONE : 44.3703
TENSION ZONE : 0.0000
PRESTRESSING STEEL : 331.6179
STIRRUPS' (HORIZONTAL LEGS) : 13.0497
STIRRUPS (VERTICAL LEGS) : 7.4331

TOTAL BENDING MOMENT ON BETA PLANE : 396.9697

TOTAL TORQUE (IN.-KIPS) ON BETA PLANE : -193.5525

TORQUE TAKEN BY STIRRUPS (VERT. LEGS) : 11.4447

TORQUE TAKEN BY CONCR. COMPR. ZONE AND DOWELS : -204.9972

SHEAR FORCE (KIPS) IN COMPR. ZONE : 10.5104

SHEAR STRESS (PSI) IN COMPR. ZONE : 734.8868

NORMAL STRESS (PSI) IN COMPRESSION ZONE : 3948.7573

NUMBER OF ITERATIONS FOR N.A. POSITION : 4

MAXIMUM (TENSILE) PRINCIPAL STRESS (PSI) ON BETA PLANE : 99.69

MAXIMUM (TENSILE) PRINCIPAL STRAIN (IN/IN) ON BETA PLANE : 0.00001005

MINIMUM (COMPRESSIVE) PRINCIPAL STRESS (PSI) ON BETA PLANE : 3968.97

MINIMUM (COMPRESSIVE) PRINCIPAL STRAIN (IN/IN) ON BETA PLANE : 0.00377886

ERROR IN STRESS INTERACTION EQUATION : 0.000009

COMBINED CAPACITIES AT ULTIMATE (IN.-KIPS AND KIPS):

TENSION : 69.10
BENDING : 420.90
SHEAR : 0.42

```
**************************
*   B E A M  C B - 6   *
**************************


INPUT VARIABLES
***************


BEAM DIMENSIONS
OUTSIDE:                    HOLLOW:
WIDTH (IN.)  =  12.00         6.00
HEIGHT (IN.) =  12.00         6.00
LENGTH (IN.) = 100.00

NO. OF PRESTRESSING STRANDS PROVIDED (N) , AND THEIR SIZE (NSIZE):
N   =        7
NSIZ =       1

AREA OF PRESTRESSING STRANDS (SQ.IN.):
  0.1440   0.1440   0.1440   0.1440   0.1440   0.1440   0.1440

AREA OF TRANSVERSE STEEL - ONE LEG (SQ.IN.):    0.0500

PRESTRESSING STEEL LOCATIONS (DISTANCES FROM THE BOTTOM IN INCHES) :
     2.00     2.00     2.00     2.00     2.00    10.00    10.00

PRESTRESSING STEEL LOCATIONS (DISTANCES FROM THE SIDE IN INCHES) :
    10.00     6.00     6.00     6.00     2.00    10.00     2.00

STIRRUP LOCATION IN CROSS-SECTION:
VERT.     1.5625   10.4375
HORIZ.    1.5625   10.4375

STIRRUP SPACING (IN.), S=      3.00

EFFECTIVE PRESTRESSING FORCES (KIPS) :
    16.06    15.99    15.43    15.25    15.77    19.12    19.69

MODULI OF ELASTICITY OF PRESTRESSING STEEL (KSI):
 27500.00 27500.00 27500.00 27500.00 27500.00 27500.00 27500.00
MODULI OF ELASTICITY OF MILD STEEL :
 29000.00

ULTIMATE STRESSES OF PRESTRESSING STEEL :
  276.389  276.389  276.389  276.389  276.389  276.389  276.389

ULTIMATE STRESS OF MILD STEEL :
   53.333

CONCRETE COMPRESSIVE STRENGTH (PSI):
FC=  5476.00

MODULUS OF RUPTURE (PSI):
RMOPS=    329.00

CONCRETE ULTIMATE COMPRESSIVE STRAIN :
EPSCU =  -0.00300

COEFFICIENT OF DEPTH OF NEUTRAL AXIS ( A C I FORMULA)   B1 = 0.78

TORSION TO BENDING RATIO , T/M    =    31.044

TORSION TO SHEAR RATIO (2*T/(D*V)) =    152.1510

LOCATION OF FAILURE SURFACE (IN.) FROM LEFT SUPPORT :
DFROM1 =     12.0
DFROM2 =     12.0
DFROM3 =     12.0

INITIAL ECCENTRICITY (IN.), ECCP  =    1.3333

AVERAGE PRESTRESS (PSI) P/A       =  1006.2037

INITIAL STRAIN IN PRESTRESSING STEEL :
 0.004956 0.004938 0.003896 0.003851 0.003982 0.004829 0.004972

INITIAL STRAINS IN CONCRETE (TOP, STEEL LEVELS AND BOTTOM):
 -0.000118
 -0.000358 -0.000350 -0.000350 -0.000350 -0.000350 -0.000350 -0.000165
 -0.000199
```

CRACKING STRENGTH
****

	TOPSOIL CONC	TH.(IN)	TH.(MM)	TOP STIR	TOT.TOPO.	SPRINCRAK	SPRINCRAK	THETA(DEG)
BOTTOM:	250.66868	0.30588	22.10946	19.76949	270.23817	0.32500	-1.96923	22.10946
SIDE 1	313.96750	0.44794	25.63617	16.20571	330.25361	0.32500	-1.81120	25.63617
TOP 1	166.47594	0.55570	31.83938	11.85938	178.33534	0.32500	-0.84281	31.83938

THIRD MODE - ULTIMATE CAPACITY,STRAINS AND EQUILIBRIUM CHECK
****

INCLINATION OF INITIAL CRACK: THETA(RAD.) = 0.5557
THETA(DEG.) = 31.8398

INCLINATION OF COMPRESSION ZONE: BETA(RAD) = 0.21
BETA(DEG) = 12.33

INCREASE IN STRAIN IN STEEL BETWEEN INITIAL AND ULTIMATE LOADS

1	0.000155	2	0.000155
3	0.000155	4	0.000155
5	0.000155	6	0.000193
7	0.000193		

ULTIMATE STRAIN IN STEEL (IN PERCENT) :

1	0.004561	2	0.004569
3	0.004482	4	0.004357
5	0.004048	6	0.004186
7	0.004330		

NUMBER OF ITERATIONS REQD. FOR CURVATURE = 33

NEUTRAL AXIS LOCATION (IN INCHES, FROM THE TOP),A= 0.662560

CURVATURE (RADIANS/IN), PHI= 0.0006127

STRESSES IN PRESTRESSING STRANDS AT ULTIMATE (KSI) :

1	125.437165	2	126.951058
3	121.062165	4	119.812165
5	123.402276	6	170.115031
7	176.073366		

FORCES IN PRESTRESSING STRANDS AT ULTIMATE(KIPS) :

1	16.242952	2	17.992952
3	17.432952	4	17.252952
5	17.772952	6	24.496569
7	25.366569		

STRAINS AND STRESSES IN HORIZONTAL LEGS OF STIRRUPS AT ULTIMATE :

STRAIN IN TOP LEG = 0.005769
STRAIN IN BOTTOM LEG = 0.000455

STRESS IN TOP LEG = 53.33
STRESS IN BOTTOM LEG = 13.76

NO. OF STIRRUPS INTERCEPTED :
AT THE TOP = 6.76
AT THE BOTTOM =13.05

EQUILIBRIUM CHECK:
TENSILE FORCE (KIPS), T = 82.81866
COMPRESSIVE FORCE (KIPS), C = 82.79291

ERROR IN PERCENTAGE (T-C)/T*100 = 0.01775

TORSION TO BENDING RATIO ON THE INCLINED (BETA) PLANE , RBETA = 0.25010

NUMBER OF THE ELEMENTS IN COMPRESSION = 32

STRAINS IN THE CENTROIDS OF COMPRESSION ELEMENTS :

1	0.000009	2	0.000025
3	0.000043	4	0.000055
5	0.000078	6	0.000096
7	0.000101	8	0.000116
9	0.000132	10	0.000147
11	0.000162	12	0.000178
13	0.000193	14	0.000208
15	0.000224	16	0.000239
17	0.000254	18	0.000270
19	0.000285	20	0.000300
21	0.000316	22	0.000331
23	0.000346	24	0.000361
25	0.000377	26	0.000392
27	0.000407	28	0.000423
29	0.000438	30	0.000453
31	0.000469	32	0.000489

STRAIN AT THE TOP OF THE PORTION OF ELEMENT BOUNDED BY N.A. = 0.000003

COMPRESSION ELEMENT STRESSES :

1	37.872156	2	150.594655
3	742.909939	4	220.799826
5	296.258896	6	367.276849
7	657.874236	8	448.681885
9	527.760487	10	587.089692
11	645.969709	12	700.425932
13	762.961886	14	820.010863
15	877.196964	16	933.930587
17	990.230933	18	1046.110002
19	1151.[illegible]	20	1156.572338
21	1211.159548	22	1265.217510
23	1319.946196	24	1372.345632
25	1425.215732	26	1477.656585
27	1529.648162	28	1581.250461
29	1632.983484	30	1683.127229
31	1733.021697	32	1783.286809

STRESS AT THE TOP OF PORTION OF THE COMPRESSION ELEMENT BOUNDED BY N. A. (F & I)= 6.31942

AREAS OF THE ELEMENTS IN COMPRESSION :

1	1.016036	2	1.016036
3	1.016036	4	1.016036
5	1.016036	6	1.016036
7	1.016036	8	1.016036
9	1.016036	10	1.016036
11	1.016036	12	1.016036
13	1.016036	14	1.016036
15	1.016036	16	1.016036
17	1.016036	18	1.016036
19	1.016036	20	1.016036
21	1.016036	22	1.016036
23	1.016036	24	1.016036
25	1.016036	26	1.016036
27	1.016036	28	1.016036
29	1.016036	30	1.016036
31	1.016036	32	1.016036

AREA OF THE PORTION OF COMPRESSION ELEMENT BOUNDED BY N. A. (SQ. INS.) = 0.14168

NUMBER OF STIRRUPS(VERT. LEGS ON ONE SIDE:) INTERCEPTED: 5.17195
AVERAGE STRAIN IN VERTICAL LEGS OF STIRRUPS : 0.00063

BENDING MOMENTS (IN.KIPS.) ON INCLINED (BETA) PLANE :

DUE TO CONCRETE COMPRESSION ZONE : 22.6845
TENSION ZONE : 0.0000
PRESTRESSING STEEL : 118.9660
STIRRUPS (HORIZONTAL LEGS) : 122.4827
STIRRUPS (VERTICAL LEGS) : 39.2093

TOTAL BENDING MOMENT ON BETA PLANE : 303.3830

TOTAL TORQUE (IN.KIPS) ON BETA PLANE : 75.8767

TORQUE TAKEN BY STIRRUPS (VERT. LEGS) : 8.3834

TORQUE TAKEN BY CONCR. COMPR. ZONE AND DOWELS : 67.5713

SHEAR FORCE (KIPS) IN COMPR. ZONE : 48.2760

SHEAR STRESS (PSI) IN COMPR. ZONE : 1881.4877

NORMAL STRESS (PSI) IN COMPRESSION ZONE : 1783.2869

NUMBER OF ITERATIONS FOR N.A. POSITION : 32

MAXIMUM (TENSILE) PRINCIPAL STRESS (PSI) ON BETA PLANE : 375.28

MAXIMUM (TENSILE) PRINCIPAL STRAIN (IN/IN) ON BETA PLANE : 0.00013718

MINIMUM (COMPRESSIVE) PRINCIPAL STRESS (PSI) ON BETA PLANE : 2298.76

MINIMUM (COMPRESSIVE) PRINCIPAL STRAIN (IN/IN) ON BETA PLANE : 0.00082118

ERROR IN STRESS INTERACTION EQUATION : 0.000001

COMBINED CAPACITIES AT ULTIMATE (IN.KIPS AND KIPS):

TORSION : 392.47
BENDING : 9.96
SHEAR : 0.03